AD NUMBER

AD908657

LIMITATION CHANGES

TO:

Approved for public release; distribution is unlimited.

FROM:

Distribution authorized to U.S. Gov't. agencies only; Test and Evaluation; DEC 1972. Other requests shall be referred to Army Aviation Systems Test Activity, Edwards AFB, CA.

AUTHORITY

USAAVSCOM Itr, 12 Nov 1973

AD_____
RDTE PROJECT NO.
AVSCOM PROJECT NO. 70-24
USAASTA PROJECT NO. 70-24

AUTOROTATIONAL ENTRY IMPROVEMENT PROGRAM TH-55A HELICOPTER

FINAL REPORT

BARCLAY H. BOIRUN
PROJECT OFFICER/ENGINEER

WILLIAM R. BENOIT
LTC, TC
US ARMY
PROJECT PILOT

DECEMBER 1972

UNITED STATES ARMY AVIATION SYSTEMS TEST ACTIVITY
EDWARDS AIR FORCE BASE, CALIFORNIA 93523

DISCLAIMER NOTICE

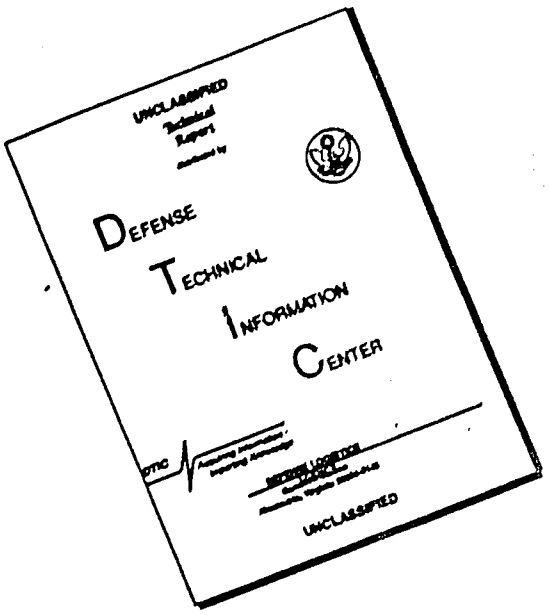

THIS DOCUMENT IS BEST QUALITY AVAILABLE. THE COPY FURNISHED TO DTIC CONTAINED A SIGNIFICANT NUMBER OF PAGES WHICH DO NOT REPRODUCE LEGIBLY.

DISCLAIMER NOTICE

The findings of this report are not to be construed as an official Department of the Army position unless so designated by other authorized documents.

REPRODUCTION LIMITATIONS

Reproduction of this document in whole or in part is prohibited except with permission obtained through the Commander, United States Army Aviation Systems Command, Attention: AMSAV-EF, Post Office Box 209, St. Louis, Missouri 63166. The Defense Documentation Center, Cameron Station, Alexandria, Virginia 22314, is authorized to reproduce the document for United States Government purposes.

DISPOSITION INSTRUCTIONS

Destroy this report when it is no longer needed. Do not return it to the originator.

TRADE NAMES

The use of trade names in this report does not constitute an official endorsement or approval of the use of the commercial hardware and software.

ERRATA SHEET

1. Page 21, para 57, 4th line.....Change "3.4" to "3.0"
2. Page 24, para 64, 2nd line.....Change "light" to "right"
3. Page 47, para 121, 3rd line....Scratch out "by dividing the local velocity"
4. Page 67, equation (12).....Change the term "AS_z^2" to "$AS\ z_t^2$"
5. Page 70, Figure 5, left margin....Change "$\Delta q_o/q_o$" to "$\Delta q/q_o$"

RDTE PROJECT NO.
AVSCOM PROJECT NO. 70-24
USAASTA PROJECT NO. 70-24

AUTOROTATIONAL ENTRY IMPROVEMENT PROGRAM

TH-55A HELICOPTER

FINAL REPORT

BARCLAY H. BOIRUN
PROJECT OFFICER/ENGINEER

WILLIAM R. BENOIT
LTC, TC
US ARMY
PROJECT PILOT

DECEMBER 1972

UNITED STATES ARMY AVIATION SYSTEMS TEST ACTIVITY
EDWARDS AIR FORCE BASE, CALIFORNIA 93523

ABSTRACT

The TH-55A helicopter was tested by the United States Army Aviation Systems Test Activity from October 1970 to May 1972 as part of a development program to improve the autorotational entry characteristics. Previous United States Army Aviation Systems Test Activity tests and operational experience at the United States Army Primary Helicopter School, Fort Wolters, Texas, indicated that the TH-55A exhibited excessive nose-down pitching and left rolling motions following simulated power failures. The United States Army Aviation Systems Command directed the United States Army Aviation Systems Test Activity to investigate the autorotational entry characteristics of the standard helicopter and to evaluate the characteristics with a reduced-chord horizontal stabilizer configuration developed by the Hughes Tool Company. The data from these tests indicated that other minor stabilizer configuration changes could also improve the autorotational entry characteristics. An experimental development program was conducted to determine an optimum stabilizer configuration. This program resulted in the development of a reduced-span stabilizer with an upper-leading-edge spoiler which improved the nose-down pitching characteristics without seriously degrading other handling qualities. A second phase of the test program was conducted to verify the structural adequacy and basic airworthiness of the new stabilizer for the entire flight envelope contained in the 1967 Hughes TH-55A owner's manual. Testing was successfully concluded, but a reduction of dynamic directional stability of the helicopter was observed. However, the decrease in dynamic directional stability was significantly outweighed by the improvement that was achieved in the autorotational entry characteristics and other flying qualities. As a result of this test program, the active fleet of TH-55A helicopters was converted to the horizontal stabilizer configuration developed by the United States Army Aviation Systems Test Activity.

TABLE OF CONTENTS

INTRODUCTION

BACKGROUND

1. In 1967, the procurement of the Hughes Tool Company (HTC) TH-55A helicopter was initiated by the United States Army to obtain a low-cost primary training helicopter. During the final phases of delivery in April and May of 1968, one aircraft was tested by the United States Army Aviation Systems Test Activity (USAASTA) to determine compliance with contractual performance guarantees. During the test program, a qualitative evaluation of handling qualities was also performed. The aircraft exhibited an undesirable pitch-down characteristic after simulated engine failures, a deficiency requiring mandatory correction (ref 1, app A). Subsequent reports from the Army Primary Helicopter School at Fort Wolters, Texas, described this characteristic as "nose tuck" and indicated that it may have contributed to unsuccessful forced landings following an engine failure.

2. The HTC proposed to correct this characteristic with a two-step horizontal stabilizer modification program. The reduced-chord horizontal stabilizer on the HTC Model 269C helicopter, which exhibits better autorotational entry characteristics, is interchangeable with the standard TH-55A stabilizer. Therefore, the first step was intended to provide an interim solution by installing the Model 269C stabilizer. In the event that this stabilizer was inadequate, the second step was a major redesign of the tail section. The United States Army Aviation Systems Command (AVSCOM) directed USAASTA to conduct a quantitative flight test program of both the standard stabilizer (for base-line data) and the reduced-chord stabilizer configuration (ref 2, app A). Following the initial flight tests and discussions with HTC, the test plan was expanded to include measurement of stabilizer loads and local flow data which could be used in the proposed redesign effort.

3. Analysis of the initial test data indicated that an in-house modification of the horizontal stabilizer might improve the "nose tuck" characteristic and provide a cost savings over the contractor's proposal. A proposal was submitted by USAASTA to AVSCOM (ref 3, app A) to develop and test various stabilizer configurations until an "optimum" configuration for an interim configuration was determined. In this report, the discussion of the development of the optimum stabilizer configuration was designated Phase I.

4. Following the development of the optimum configuration, an additional test request was received from AVSCOM (ref 4, app A) for substantiation of the airworthiness and Army qualification of the TH-55A with the USAASTA modified stabilizer. Phase II of this report presents results of the qualification testing of the recommended final configuration.

TEST OBJECTIVES

Stabilizer Development (Phase I)

5. The original objectives of this test were to establish base-line handling qualities of the standard TH-55A and to evaluate the effects of the HTC reduced-chord stabilizer on autorotational entry characteristics. The explicit objectives are detailed as follows:

a. Quantitatively determine autorotational entry characteristics of the basic TH-55A.

b. Establish base-line data with the basic TH-55A relative to longitudinal and lateral-directional characteristics in hover and forward flight.

c. Quantitatively determine autorotational entry characteristics of the TH-55A with the reduced-chord stabilizer under the same flight conditions as the basic aircraft.

d. Evaluate longitudinal and lateral-directional characteristics of the modified aircraft in hover and forward flight to ensure no degradation from the basic aircraft.

e. Qualitatively assess low-speed flight characteristics of the basic and modified aircraft, and if substantial differences were noted, quantitatively identify them.

f. Quantitatively evaluate the effect of removing the canopy slat to determine if the aircraft can be safely flown in this configuration.

6. During the test, the additional objective of acquiring engineering data on which to base further design efforts was established in the event that the reduced-chord stabilizer did not provide an adequate improvement. Analysis of these data established the requirement to develop an optimum stabilizer for the interim configuration which would improve the autorotational entry characteristics without degradation of the overall handling qualities.

Stabilizer Qualification (Phase II)

7. The Phase II test objective was to evaluate the airworthiness of the TH-55A helicopter with the USAASTA-developed (optimum configuration) horizontal stabilizer. A secondary objective was to provide sufficient data for possible Federal Aviation Agency (FAA) certification.

DESCRIPTION

8. The test TH-55A helicopter is a two-place helicopter with side-by-side seating manufactured by the Hughes Tool Company and is used by the United States Army as a primary trainer. It incorporates a single, three-bladed, fully articulated, main rotor and a two-bladed, teetering, antitorque tail rotor. It is equipped with a Lycoming H10-360-B1A reciprocating engine, with a standard-day, sea-level rating of 180 shaft horsepower (shp) at 2900 rpm. The helicopter weight empty is 1006 pounds, and the design gross weight is 1670 pounds. A complete listing of pertinent engineering data may be found in the FAA Type Certificate Data Sheet (ref 5, app A).

Horizontal Stabilizer

9. The standard TH-55A horizontal stabilizer has a rectangular planform, symmetrical NACA 0012 airfoil of 28 inches, span, and 16.8 inches, chord. It is constructed by forming a corrugated aluminum skin over an S-shaped main spar and capping the ends. The structure is held together with rivets and weighs approximately 3 pounds. The stabilizer is mounted on the aft right side of the tail boom with a positive dihedral angle of 35 degrees and a positive incidence of 4.5 degrees to the longitudinal axis of the fuselage.

10. During Phase I, a total of 11 horizontal stabilizer configurations were tested. The airfoil and geometric characteristics are shown in table 1, and the individual configurations are listed in detail as follows:

a. Standard stabilizer (base-line data).

b. Reduced-chord stabilizer (HTC 269C).

c. Reduced-chord stabilizer with full-span upper-leading-edge spoiler.

d. Standard stabilizer with full-span upper-leading-edge spoiler combined with either a 0-, 3-, 6-, 9-, or 12-inch lower-leading-edge spoiler.

e. Reduced-span stabilizer (4.5, 7, and 9 inches removed spanwise) with full-span upper-leading-edge spoiler.

11. The HTC reduced-chord stabilizer consisted of a standard stabilizer with the aft 25 percent of the stabilizer chord removed and the trailing edge capped. This modification changed the cross-sectional area, the aspect ratio, the effective thickness, and blunted the trailing edge to a thickness of 1.1 inches.

12. The reduced-span configurations were constructed by cutting the standard stabilizer spanwise and reinstalling the end cap. The locations for cutting were restricted by the corrugated surface beads since the end cap could not be riveted at these locations. This modification changed only the planform area and aspect ratio.

Table 1. Geometry of Horizontal Stabilizers.

Stabilizer Configuration[1]	Span (in.)	Chord (in.)	Aspect Ratio	Planform Area (ft^2)	Planform Area Reduction (%)
Standard	28.0	16.8	1.67	3.27	Zero
Reduced chord[2]	28.0	12.7	2.21	2.47	24
Reduced span	23.5	16.8	1.39	2.74	16
Reduced span	21.0	16.8	1.25	2.45	25
Reduced span	19.0	16.8	1.13	2.22	32

[1]All stabilizers were developed from the standard stabilizer which has a NACA 0012 cross section and is 1.75 inches thick.
[2]In the reduced-chord configuration, the airfoil cross section had a blunt trailing edge 1.1 inches thick.

13; A spoiler for the various stabilizers was made from a strip of angle aluminum and was attached by end clips so that it could be easily removed and reinstalled with no structural modification to the basic stabilizer. The spoiler was 3/4 inch in height and was located 3/4 inch aft of the leading edge on the upper surface. This location was used primarily for convenience, and no attempts were made to optimize the spoiler height or location.

14. The canopy slat was added to the original TH-55A helicopter to improve the handling qualities characteristics. It is located about 5 inches above the canopy bubble directly overhead the pilot. It has an airfoil cross section with a chord of 5 inches and extends over the full width of the canopy in span. The canopy slat is attached on both sides of the canopy above the doors, and the center is supported by a pylon. The canopy slat was only removed from the standard stabilizer configuration during a portion of the base-line tests.

SCOPE OF TEST

Stabilizer Development (Phase I)

15. The horizontal stabilizer development program was limited to relatively simple modifications to the standard or reduced-chord stabilizers of the type that could be made in the field at low cost to the Army. For this reason and to limit the scope of the program to provide an effective interim configuration, no investigation

of the effects of the stabilizer's dihedral or incidence angle was conducted. Standard dihedral and incidence angles were determined from HTC test programs.

16. The TH-55A training profile at the United States Army Primary Helicopter School, Fort Wolters, Texas, requires normal climb, cruise, and steady-state autorotational flight at 50 knots indicated airspeed (KIAS). Climb-out from confined areas requires high-power climbing flight below 50 KIAS until barriers have been cleared. High-speed cruise (cross-country) is 60 KIAS. The total flight profile is within 500 feet of the ground, with the exception of the two cross-country flights flown by the students in primary training. This profile was the basis for selection of the airspeeds for the stabilizer development program.

17. During the documentation of the basic aircraft handling qualities (development of base-line data), several autorotational entries were made in level flight within the airspeed range of hover to 65 KIAS at rotor speeds of 483 rpm (standard) and 450 rpm. Tests were performed at the forward and aft center-of-gravity (cg) locations to determine cg effects. Full-power-climb autorotational entries at 483 rpm were performed between 30 and 47 knots calibrated airspeed (KCAS) to determine the "worst-case" autorotational entry. Entries were accomplished with all controls fixed and were terminated at the maximum-allowable delay time. The base-line test conditions are summarized in table 2. Tests with the canopy slat removed were only conducted at an aft cg.

18. The effectiveness of each new configuration was determined during the configuration development portion of Phase I. To economize time and funds, only the 38- to 56-KCAS range was used to check changes in trim shifts, pitching with sideslip, and longitudinal stability until the final configuration was determined. The autorotational entry and other handling quality characteristics were compared against the base-line configurations to determine the effects of the stabilizer and canopy slat configuration changes. Approximately 33 hours of productive flight test time at Edwards Air Force Base, California, was required for Phase I. The tests were conducted from November 1970 to June 1971.

Table 2. Base-Line Handling Qualities Test Conditions for Phase I.[1],[2]

Test	Flight Condition	Calibrated Airspeed (kt)
Control positions in trimmed forward flight	Climb	30 to 56
	Level	30 to 68
	Autorotation	28 to 68
Static lateral-directional stability	Level	32, 47, and 61
	Autorotation	32, 47, and 61
Collective-fixed static longitudinal stability	Level	30, 37, 47, 56, and 68
Controllability	Level	47
Maneuvering stability	Level	47 and 56
Autorotational entries	Level	Hover, 30, 37, 47, 56, and 61
	Climb	34, 42, and 50

[1]Standard stabilizer.
[2]Rotor speed: 483 and 450 rpm.
Center of gravity: aft and forward.
Density altitude: 4000 feet.
Gross weight: 1620 pounds.

Stabilizer Qualification (Phase II)

19. In Phase II, emphasis was placed on handling qualities and structural demonstration tests. The stabilizer qualification handling qualities test conditions are summarized in table 3. The handling qualities tests were conducted in the most critical aircraft configuration, and the structural demonstrations were conducted at the most critical flight conditions. Approximately 10 hours of productive flight test time in the area of Edwards Air Force Base were required to achieve the test objectives. The tests were conducted from October 1971 to May 1972.

Table 3. Handling Qualities Test Conditions for Phase II.[1]

Test	Flight Condition	Airspeed Required[2]	Tested Calibrated Airspeed (kt)
Control positions in trimmed forward flight	Climb	Zero to $1.11V_{NE}$	34 to 56
	Level	Zero to $1.11\ V_{NE}$	22 to 78
	Autorotation	Zero to $1.11V_{NE}$	28 to 72
Hover and low-speed flight	Level[4]	20 knots, forward and rearward	22 KTAS[3], forward and rearward
		25 knots, sideward	22 KTAS, left and right
Collective-fixed static longitudinal stability	Climb	$V_{max\ R/C}$	44 and 50
	Level	V_{max}, $0.8V_H$, $1.11V_{NE}$	40, 56, 67, and 78
	Autorotation	$V_{min\ R/D}$, $0.8V_H$	38 and 56
Static lateral-directional stability	Climb	$V_{max\ R/C}$	44
	Level	$V_{max\ R/C}$, $0.8V_H$, V_H, $1.11V_{NE}$	40, 49, and 56
	Autorotation	$V_{min\ R/D}$, $0.8V_H$	38 and 56
Dynamic longitudinal and lateral-directional stability	Climb	$V_{max\ R/C}$	44
	Level	$V_{max\ R/C}$, $0.8V_H$, V_H	40, 56, and 67
	Autorotation	$V_{min\ R/D}$, $0.8V_H$	38 and 56
Maneuvering stability	Pull-up	$V_{max\ R/C}$, V_{NE}	40 and 70

[1]Final reduced-span stabilizer. Rotor speed: 483 rpm, power ON; 530 rpm, power OFF. Center of gravity: aft (FS 99.2). Density altitude: 4000 feet. Gross weight: 1650 pounds.
[2]Reference 4, appendix A.
[3]Knots true airspeed.
[4]In ground effect.

METHODS OF TEST

Stabilizer Development (Phase I)

20. Established engineering stability and control flight test techniques were employed during the conduct of the handling qualities tests. The test methods used are outlined in the test plan (ref 6, app A). The trim points were established using a turn-and-sideslip indicator which placed the aircraft in conditions normally experienced by service pilots.

21. During the experimental development of the optimum stabilizer, each new configuration was first flown through the handling qualities tests and then through the autorotational entry tests. A control fixture was used to aid in holding the cyclic control position fixed to eliminate any control feedback input. The aircraft attitudes, angular rates, and pilot comments were used to compare each configuration with other configurations and with the base-line data. A forward-looking cockpit camera was also used to obtain pictures for a visual comparison of the motion of the aircraft. The data analysis following each flight was used to determine the configuration of the next stabilizer modification and to compare the handling qualities with previous configurations. This procedure was followed until the optimum configuration was determined.

Stabilizer Qualification (Phase II)

22. The qualification tests were conducted using the methods discussed in the test request (ref 4, app A). In the handling qualities tests, the aircraft was trimmed at near-zero sideslip instead of with the sideslip ball centered. When applicable, the test methods required for MIL-H-8501A (ref 7) compliance were employed.

23. Special ground and flight tests were conducted to determine the natural frequency and vibration characteristics and critical flight loads of both the standard and final reduced-span horizontal stabilizers.

CHRONOLOGY

Stabilizer Development (Phase I)

24. The chronology of events in the stabilizer investigation program is as follows:

Test directive received	31	July	1970
Test plan approved	17	September	1970
Test helicopter received	8	October	1970
Test plan expanded	20	October	1970
Instrumentation completed	9	November	1970
First test flight	16	November	1970
Proposal submitted for experimental tests	23	March	1971
Safety-of-flight release for configuration development	16	April	1971
Reduced-chord testing completed	11	May	1971
Configuration testing completed	28	June	1971
Letter report completed	1	August	1971

Stabilizer Qualification (Phase II)

25. The chronology of the stabilizer substantiation/qualification program is as follows:

Test directive received	10	August	1971
Instrumentation and recalibration completed	28	October	1971
Initiated qualification tests	17	November	1971
Flight testing completed	26	May	1972

RESULTS AND DISCUSSION

STABILIZER INVESTIGATION (PHASE I)

General

26. Base-line data for the standard TH-55A configuration were obtained from handling qualities and autorotational entry flight tests before the modified horizontal stabilizer configurations were tested. The HTC reduced-chord configuration was then installed and tested. When little improvement was noted in the autorotational entry characteristics, the experimental development tests were initiated. Following each configuration change, the data were investigated both quantitatively and qualitatively for an improvement. No improvement resulted in discontinuance of further testing with the particular configuration, and an investigation was conducted to determine a more promising modification. This procedure culminated with a configuration that reduced the undesirable aircraft pitch response during autorotational entries and provided information to define the cause of the excessive motions.

27. The only reduced-chord configuration tested was provided by HTC. Although this configuration provided a significant improvement in the static flying qualities (the static trim shift required to go from maximum-power climb to steady autorotation at a given airspeed was reduced by more than 1 inch), the pitch and roll during autorotational entry was only slightly reduced. Therefore, the primary objective of adequately improving the autorotational entry was not achieved by this configuration.

28. The effect of the upper-leading-edge spoiler on the autorotational entry characteristics was insignificant on the standard and reduced-chord stabilizers. However, a significant improvement in the longitudinal cyclic trim shift required to change from full-power climbs to autorotation at a given airspeed was noted. The low-speed flying qualities were also improved, including a reduction of a divergent 3-axis oscillation encountered in crosswind hover conditions. The upper-leading-edge spoiler was incorporated on all of the reduced-span configurations.

29. The lower-leading-edge spoilers were used to simulate the effect of cutting the stabilizer spanwise. A qualitative investigation was conducted where the lower spoiler length was increased 3 inches between each test flight on the standard stabilizer with the full-span upper spoiler. The results were that the 3- to 6-inch spoiler provided a modest improvement while the 9-inch spoiler provided a significant improvement in the autorotational entry characteristics. A 12-inch spoiler did not show any further improvement.

30. A small end plate was attached to the spar cap on several of the configurations to spoil any flow over the end of the stabilizer during sideslip. The end plate

tended to reduce the initial aircraft motions following a sudden power reduction. However, the aircraft reactions between 1 or 2 seconds after power reduction were more abrupt. Since the data showed that at the time of recovery the contribution of the end plate was insignificant, the end plate was dropped from consideration.

31. Recognizing that reducing the span would be more effective than the lower surface spoilers, the first cut was made 4.5 inches from the outboard end. This resulted in a small improvement in aircraft motions during autorotational entries. With 7 inches removed, there was more improvement in the entry motions, but the aircraft dynamic stability was slightly reduced. A 9-inch span reduction was then tested, and only a minor improvement in the entry characteristics was attained over the 7-inch reduction, while the dynamic stability was further degraded. On the basis of the experimental development effort, the 21-inch span stabilizer (7-inch cut) with a full-span upper-leading-edge spoiler was determined to be the optimum stabilizer configuration for the Army's training mission. Although this configuration could be less desirable for cross-country flying due to its reduced dynamic stability characteristics, it was selected because the primary test objective of improving the nose-down pitching during autorotational entry was achieved.

HANDLING QUALITIES

32. The TH-55A was tested for the basic stability and control characteristics that were expected to be significantly influenced by the horizontal stabilizer configuration. The results for the 21-inch-span and the HTC reduced-chord stabilizer configurations are compared with the base-line standard stabilizer configuration. The results indicate where the modified stabilizers either improved or degraded the base-line data.

Control System Characteristics

33. The flight controls of the TH-55A are a cyclic stick, a collective stick, directional pedals, and a twist grip throttle. The control systems are not boosted. The cyclic stick is equipped with a spring-loaded device for trimming forces during flight. It is actuated by an electrical servo that is engaged by a thumb switch on the cyclic grip. A friction lock is incorporated on the collective stick to hold the stick in any desired position. Throttle control is accomplished by a twist grip on the collective stick. The pedals are equipped with a spring bungee to trim out steady pedal forces. The pedals can be positioned on the pedal shafts to accommodate individual pilots. Full travel of the longitudinal cyclic, lateral cyclic, collective stick, and pedal controls was 13, 11.5, 10.2, and 8.5 inches, respectively.

34. The TH-55A cyclic control position data were significantly affected by the control linkage rigging. For this reason, the cyclic control position data in this report may differ from other sources because there is a range of allowable blade angles for any particular stick position. The gradients of the data presented were unaffected, although the control margins were affected. Within the allowable blade movement range, the longitudinal and lateral cyclic stick can have a maximum

variation of 1.5 and 1.1 inches, respectively. Rigging the controls to provide the maximum aft stick movement would be desirable for recovery following the autorotational entries. The TH-55A cyclic rigging specifications are provided in the FAA Type Certificate Data Sheet (ref 5, app A) and have been partially reproduced in table 4. The blade movement was calculated by the difference of the blade angle at neutral cyclic stick position and the blade angle at full-throw position. The cyclic rigging used on the test aircraft is shown in table 5. The individual blades, identified as red, blue, and yellow, had slightly different settings after rotor tracking because of differences in twist or condition of the blades. The control system characteristics were unchanged by the horizontal stabilizer configuration, and the control rigging in table 5 was maintained throughout all of the test program.

Table 4. Cyclic Control Rigging Specification.[1]

Cyclic Control Displacement From Neutral	Allowable Blade Movement[2] (deg)	Blade Azimuth Position (deg)
Full forward	7.5 to 9.4	90
Full aft	6.0 to 7.5	90
Full left	6.5 to 7.5	180
Full right	5.3 to 6.3	180

[1]FAA Type Certificate Data Sheet No. 4H12.
[2]Collective in full-down position.

Table 5. Cyclic Control Rigging During Test.

Cyclic Control	Blade Movement[1] (deg)		
	Red	Blue	Yellow
Full forward	8.8	9.1	9.1
Full aft	6.4	6.5	6.5
Full left	6.5	6.6	6.6
Full right	5.2	5.2	5.2

[1]Collective in full-down position.

Controllability

35. The controllability characteristics in forward flight were determined by measuring the control power, sensitivity, and response. The control power is defined as the maximum aircraft attitude displacement attained in a specified time interval following a control step input. Control sensitivity is defined as the maximum angular acceleration attained per inch of control step input, and control response is defined as the maximum angular rate attained per inch of a control step input. The controllability characteristics were determined for the standard stabilizer configuration at maximum gross weight at both forward and aft cg locations. The modified-stabilizer or canopy-slat-removed configurations were not tested because they were not expected to significantly affect the controllability. Tests were conducted at a 47-KCAS cruise speed in level forward flight at an average density altitude of 4000 feet by introducing various-sized longitudinal, lateral, and directional control step inputs. The test results are shown in figures 1 through 3, appendix D. A summary of the forward cg data is shown in table 6.

Table 6. Controllability in Level Forward Flight.[1]

Control Applied	Control Power[2] (deg/in.)	Control Response (deg/sec/in.)	Control Sensitivity (deg/sec^2/in.)
Longitudinal	2.0	9.5	16.0
Lateral	2.0	23.0	31.0
Directional (right)	5.0	20.0	42.0
Directional (left)	5.0	13.0	24.0

[1]Average flight conditions:
Entry airspeed: 47 KCAS.
Center-of-gravity location: FS 96.0 (fwd).
Gross weight: 1670 pounds.

[2]Control power determined at 1 second for longitudinal and directional control inputs and at 1/2 second for lateral control inputs.

36. The longitudinal controllability and control power characteristics were generally satisfactory for the conditions tested. The response and sensitivity to forward and aft step inputs were linear and nearly identical. The maximum acceleration occurred within 0.75 second, and the maximum rate occurred within 1.5 seconds following the control step input.

37. The lateral controllability and control power characteristics were generally satisfactory. The sensitivity and response to both left and right step inputs were

nearly linear and identical. The maximum acceleration occurred within 0.75 second, and the maximum rate generally occurred within 1.5 seconds after the control step input.

38. The overall directional controllability and control power characteristics were also satisfactory. The response was dependent on both the step input direction and cg location. For right pedal step inputs, the response was linear and slightly reduced at the forward cg location. With left pedal step inputs, the sensitivity and response were slightly reduced from the right pedal input at the aft cg location, and were significantly reduced at forward cg locations. The maximum acceleration usually occurred within 1.0 second, and the maximum rate occurred within 1.5 seconds after the control step input.

Hover and Low-Speed Flight

39. The TH-55A was qualitatively tested in hovering flight with wind conditions of 20 knots or greater. The test was conducted at maximum gross weight and forward cg and at an average skid height of 8 feet. The aircraft was aligned with the relative wind and slowly yawed 360 degrees about a point. When the standard and reduced-chord stabilizers were installed, a 3-axis oscillatory instability was present at relative wind angles near 82 and 225 degrees from the nose. The aircraft began to oscillate about the yaw, roll, and pitch axes and rapidly diverged until the relative wind angle was changed by directional control application. The pilot could not maintain the aircraft at these critical azimuth angles for more than a short time (3 or 4 seconds) with maximum pilot effort to do so.

40. Installation of the full-span upper-leading-edge spoiler to either the standard or reduced-chord stabilizer resulted in a significant reduction of this dynamic instability. Oscillations still occurred at the critical relative wind angles, but they were controllable by the pilot while maintaining the critical angles. The reduced-span stabilizer configurations further reduced this hovering instability characteristic. The final reduced-span stabilizer was a considerable improvement over the standard configuration while hovering in winds.

Control Positions in Trimmed Forward Flight

41. Control trim characteristics were evaluated by trimming the helicopter in steady-heading, coordinated, forward flight conditions listed in table 2. The tests were flown at a pressure altitude of 4000 feet, maximum gross weight, and at both forward and aft cg locations. Figures 4 through 8, appendix D, present the basic control position data for the standard and reduced-chord stabilizer, and figures 33 through 34 present the data for the final reduced-span stabilizer. A comparison of the longitudinal cyclic trim position with forward flight speed for the principle stabilizer configurations is shown in figure A. In level flight, the control position requirements were similar for all three stabilizers. Above 35 KCAS, forward control displacement was required for increased airspeed. Essentially no change in control position was required in the low-speed range between 20 and 30 KCAS on the final stabilizer. The standard configuration was not tested in this regime.

SYMBOL	STABILIZER CONFIGURATION	AVG DENSITY ALTITUDE (FEET)	AVG GROSS WEIGHT (POUNDS)	AVG CG LOCATION (INCHES)
———	STANDARD	4100	1670	95.2 (FWD)
— - —	REDUCED CHORD	4400	1640	95.7 (FWD)
———	FINAL REDUCED SPAN	4100	1670	95.2 (FWD)

LEVEL

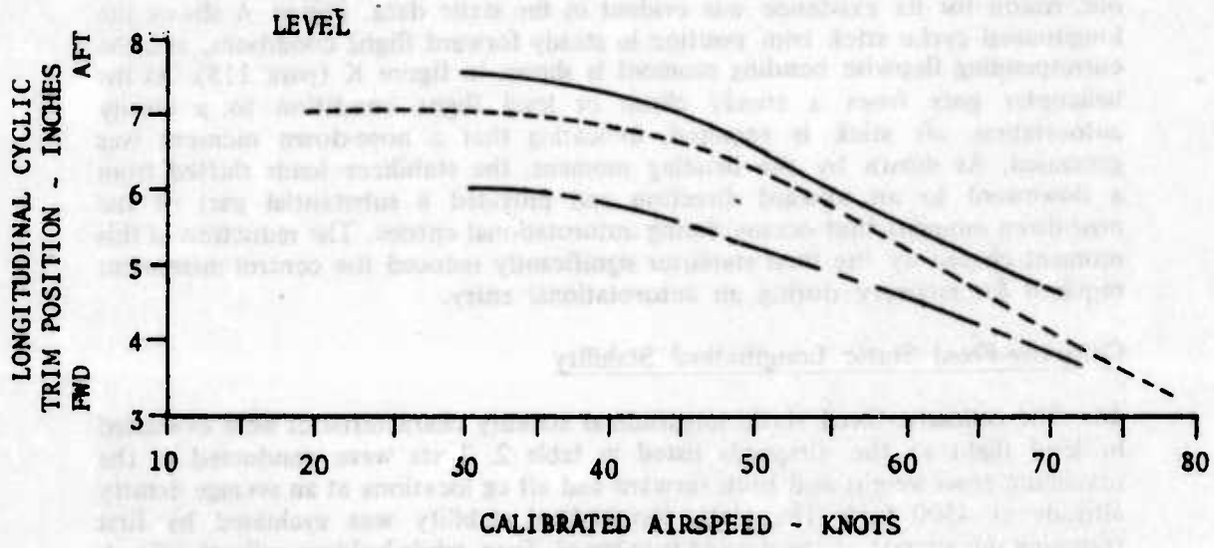

Figure A. Comparison of the Longitudinal Cyclic Trim Control Positions in Forward Flight.

42. The control position requirements during climb and autorotation were similar to those obtained during level flight testing. However, the maximum longitudinal control trim change with power was found to be greatly reduced by both the reduced-chord and final reduced-span stabilizer. The maximum longitudinal cyclic trim position shift required to go from a maximum-power climb to full autorotation exceeded the MIL-H-8501A limit of 3 inches with the standard configuration at both forward and aft cg locations. Figures 9 and 10, appendix D, show a summary of the maximum aft trim shift required in the standard, reduced-chord, and final reduced-span configuration. Both the reduced-span and reduced-chord configurations reduced the trim shift to within the required 3-inch limit at all cg locations. Removal of the canopy slat did not significantly affect the trim characteristics, except that the maximum longitudinal trim shift was slightly increased.

43. For the standard stabilizer in autorotation, an average of 0.72-inch forward longitudinal cyclic control was required per inch of aft cg travel. In climb, the variation was 0.6 inch of forward cyclic per inch of aft cg travel. This difference

in slope caused the curves to converge, and thus the longitudinal cyclic trim shift was lower at the aft cg. This trend was generally true for all stabilizer configurations tested.

44. In forward flight, all the stabilizer configurations tested provided adequate control margins for the flight envelope contained in the 1967 Hughes Model 269A owner's manual (ref 8, app A).

45. Although the "nose tuck" problem occurred during a dynamic flight condition, one reason for its existence was evident in the static data. Figure A shows the longitudinal cyclic stick trim position in steady forward flight conditions, and the corresponding flapwise bending moment is shown in figure K (para 115). As the helicopter goes from a steady climb or level flight condition to a steady autorotation, aft stick is required, indicating that a nose-down moment was generated. As shown by the bending moment, the stabilizer loads shifted from a downward to an upward direction and provided a substantial part of the nose-down moment that occurs during autorotational entries. The reduction of this moment change by the final stabilizer significantly reduced the control movement required for recovery during an autorotational entry.

Collective-Fixed Static Longitudinal Stability

46. The collective-fixed static longitudinal stability characteristics were evaluated in level flight at the airspeeds listed in table 2. Tests were conducted at the maximum gross weight and both forward and aft cg locations at an average density altitude of 4500 feet. The static longitudinal stability was evaluated by first trimming the aircraft at the desired trim speed. Then, while holding collective fixed, the helicopter was displaced from the trim speed and again stabilized at incremental speeds greater and less than the trim speed. Data recorded at each stabilized airspeed are presented in figures 11 through 15, appendix D. In general, the static longitudinal stability, as indicated by the variation of control position with airspeed, was weak but stable and nearly linear about the trim points for all configurations tested. The longitudinal stability was generally weakest at low speeds and improved with increasing airspeed.

47. A summary of the control position gradient with airspeed is shown in figure 16, appendix D, for the standard, reduced-chord, and final reduced-span stabilizer configurations. The control position gradients for forward cg locations were generally stronger than those for the aft cg locations. The longitudinal static stability with the reduced-chord stabilizer was generally weaker than the standard configuration. The longitudinal stability of the final reduced-span stabilizer was less at airspeeds below 40 KCAS, but was better than the standard configuration at higher speeds. Basically, the stabilizer configurations tested had only minor effects on the static longitudinal stability, but the final reduced-span configuration provided some improvement at cruising and higher flight speeds.

48. Figure 16, appendix D, also shows that the static longitudinal stability of the standard TH-55A with the canopy slat removed was essentially neutral at the aft cg. This characteristic is undesirable, but the aircraft was controllable in this configuration and can be safely flown.

Static Lateral-Directional Stability

49. The static lateral-directional stability characteristics were measured by recording data during stabilized flight at various sideslip angles while maintaining a constant heading at selected trim airspeeds in level flight. The tests were conducted at maximum gross weight, an average density altitude of 4000 feet, and at both forward and aft cg locations. The detailed test results for the standard and reduced-chord stabilizers are presented in figures 17 through 21, appendix D. The test results for the final reduced-span configuration are presented in figures 38 and 39.

50. For all stabilizer configurations tested, the static directional stability was determined to be positive (increasing left pedal required for increasing right sideslip, and vice versa). The pedal gradient was slightly stronger as airspeed was increased. Only minor variations resulted from cg location or rotor speed changes.

51. The longitudinal cyclic trim changes with sideslip provided an indication of the pitching moment generated by sideslip. As right sideslip was increased, more aft stick was required, which indicated that a nose-down pitching moment was generated. Figure B is a comparison of the longitudinal control requirements associated with the standard, reduced-chord, and final reduced-span configurations. To provide a direct comparison, the longitudinal control is presented in terms of the trim shift from zero sideslip. The reduced-span configuration reduced the aft stick requirement for a given increase in right sideslip. The reduced-chord configuration is also shown to have provided some improvement between 20 and 30 degrees of right sideslip, but then required more aft stick than the standard configuration at higher angles. The canopy slat did not appear to have any effect on this characteristic.

SYMBOL	STABILIZER CONFIGURATION	CALIBRATED AIRSPEED (KNOTS)	AVG GROSS WEIGHT (POUNDS)	AVG CG LOCATION (INCHES)
———	STANDARD	47	1680	96.3
—·—	REDUCED CHORD	47	1690	96.2
- - -	FINAL REDUCED SPAN	47	1670	95.2

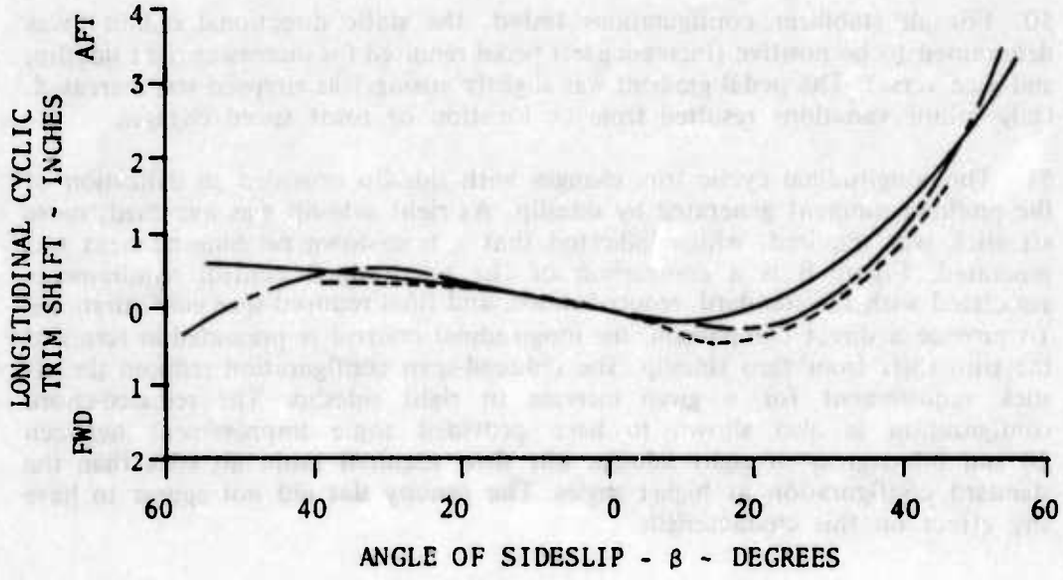

Figure B. Comparison of Longitudinal Characteristics in Steady Sideslip.

52. Dihedral effect, as indicated by the variation of lateral control position with sideslip, is compared for the three primary stabilizers in figure C. The TH-55A has a strong positive dihedral effect. This effect grew stronger with increasing airspeed and varied slightly with cg location, rotor speed, and stabilizer configuration. The variation of the dihedral effect due to the stabilizer configuration is shown to be insignificant. The canopy slat had no effect on the dihedral characteristics.

SYMBOL	STABILIZER CONFIGURATION	CALIBRATED AIRSPEED (KNOTS)	AVG GROSS WEIGHT (POUNDS)	AVG CG LOCATION (INCHES)
———	STANDARD	47	1680	96.3
— - —	REDUCED CHORD	47	1690	96.2
- - -	FINAL REDUCED SPAN	47	1670	95.2

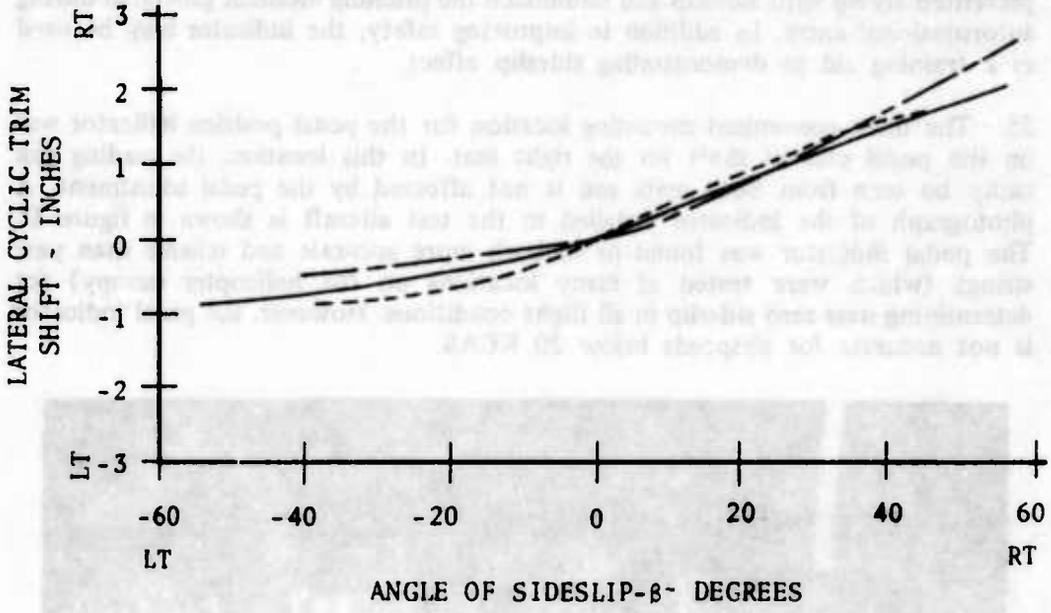

Figure C. Comparison of Dihedral Effect.

53. The side-force characteristics, as indicated by the variation of bank angle with steady-heading sideslip, were basically positive for all stabilizer configurations tested. However, the gradient (degree-of-bank/degree-of-sideslip) was very weak and sometimes became neutral at high sideslip angles. For the standard stabilizer, the gradient varied from 0.1 at 35 KCAS to 0.3 at 61 KCAS. The variation with cg location appeared to be insignificant. Only minor variations were generated by the stabilizer modification, although the reduced-chord configuration appeared to have the weakest gradient for conditions tested. Due to the weak side-force characteristics, sideslip was found to be difficult to detect in flight. Trim conditions established with the aid of a turn-and-bank indicator which was added for these tests sometimes produced very high inherent sideslip angles. This was particularly noticeable in climbs. An investigation revealed that the sideslip angle could vary as much as 10 degrees at 47 KCAS with the ball essentially remaining centered due to the weak side-force characteristic. The effect of initial sideslip on the aircraft response during autorotational entry was discussed in paragraph 51.

54. The pedal position required for zero sideslip was found to be approximately constant with airspeed during climb, level flight, or autorotation. Thus, it was possible to construct a simple pedal position indicator that was calibrated to the correct position for zero sideslip in 47-KCAS level flight. The indicator was sufficiently accurate at all other airspeeds above translation speed. Similarly, a position was marked for climb and autorotation. These positions were color-coded: red for climb, yellow for level flight, and green for autorotation. This indicator prevented flying with sideslip and minimized the pitching moment generated during autorotational entry. In addition to improving safety, the indicator may be used as a training aid in demonstrating sideslip effect.

55. The most convenient mounting location for the pedal position indicator was on the pedal control shaft for the right seat. In this location, the reading can easily be seen from both seats and is not affected by the pedal adjustment. A photograph of the indicator installed in the test aircraft is shown in figure D. The pedal indicator was found to be both more accurate and reliable than yaw strings (which were tested at many locations on the helicopter canopy) for determining near-zero sideslip in all flight conditions. However, the pedal indicator is not accurate for airspeeds below 20 KCAS.

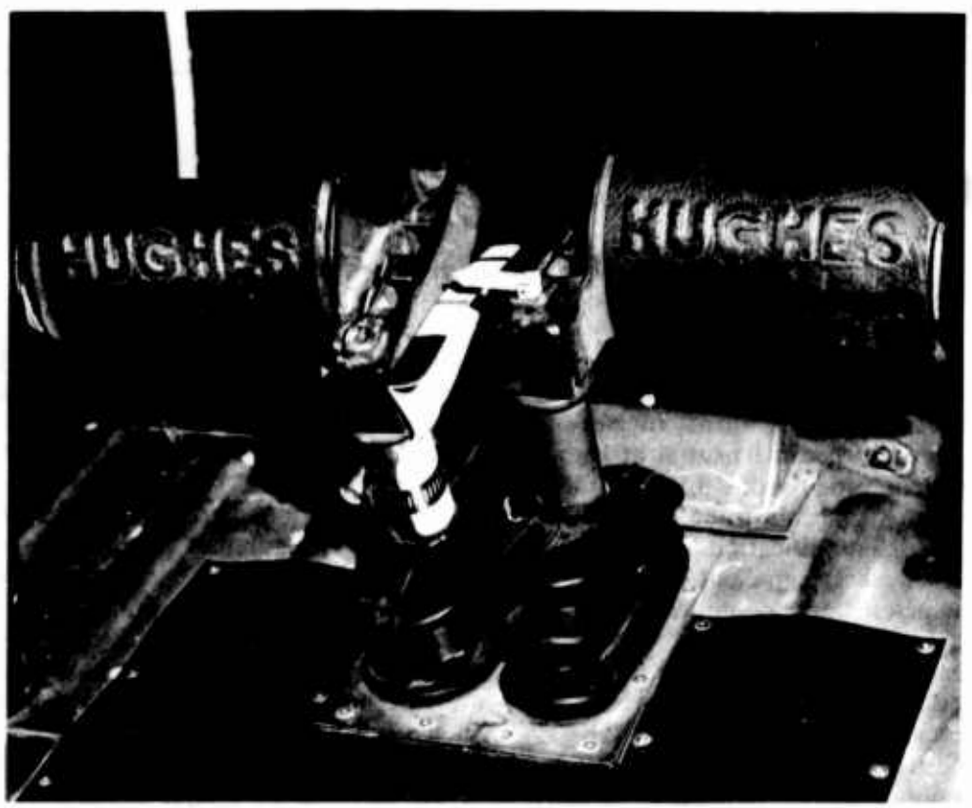

Figure D. Photograph of TH-55A Pedal Position Indicator.

Dynamic Longitudinal Stability

56. Short-period dynamic longitudinal stability characteristics were evaluated at 47 KCAS in level forward flight and an average density altitude of 4500 feet. Tests were conducted at maximum gross weight with both forward and aft cg locations. The dynamic stability was determined from the response of the aircraft following a gust disturbance which was simulated by applying a 1/2- to 1-inch longitudinal control pulse of 1/2-second duration. Following the pulse, the control was held fixed until the aircraft oscillations were damped or pilot corrective action was required. The aircraft motions following the control inputs were analyzed by determining the period and damping ratio using methods discussed in Cornell Aeronautical Laboratory Report No. 177 (ref 9, app A). The long-period dynamic stability characteristics were not determined.

57. A comparison of dynamic longitudinal stability characteristics for the standard, reduced-chord, and final reduced-span configurations is shown in table 7. With the standard stabilizer, the longitudinal oscillation was usually highly damped and had an average period of oscillation of 3.4 seconds. The damping was greatest at the forward cg and decreased with aft cg movement. The response of the reduced-chord configuration was similar to the standard configuration, while some degradation was observed with the final reduced-span configuration. At the aft cg location and at airspeeds below 56 KCAS, the lateral-directional mode was also excited by the longitudinal pulse and was undamped with the final reduced-chord configuration.

Table 7. Comparison of Dynamic Longitudinal Stability Characteristics in Level Flight.[1]

Stabilizer Configuration	Period of Oscillation (sec)	Damping Characteristics		Center-of-Gravity Location (in.)
		Ratio	Description	
Standard	3.0	0.32	Moderate	96.0 (fwd)
Reduced chord	3.0	0.50	Strong	96.0 (fwd)
Reduced span	3.4	0.34	Moderate	95.2 (fwd)
Standard	3.0	0.26	Moderate	99.0 (aft)
Reduced chord	2.8	0.39	Moderate	99.0 (aft)
Reduced span	3.4	0.28	Moderate	99.2 (aft)

[1]Flight conditions:
Rotor speed: 483 rpm.
Airspeed: 47 KCAS.
Average gross weight: 1650 pounds.
Average density altitude: 4400 feet.

58. When the standard stabilizer configuration was tested with the canopy slat removed, the longitudinal damping was neutral for the aft cg location. The period of the undamped oscillation remained about 3.4 seconds, which was controllable, and recovery was easily accomplished.

Dynamic Lateral-Directional Stability

59. Short-period dynamic lateral-directional stability tests were conducted similarly to the longitudinal dynamic stability tests, except that lateral and directional pulses were applied. The test conditions were identical to the longitudinal test conditions. The lateral-directional dynamic stability characteristics are summarized in table 8. The aircraft response to either lateral or directional pulses was oscillatory about all three axes. The predominant oscillation was yaw, which was coupled with both roll and pitch. Due to the unsymmetrical static lateral-directional characteristics, the response was most severe when left pedal pulses were applied.

60. The oscillations were lightly damped at all conditions tested with the standard stabilizer installed. The period of oscillation ranged from 3.2 to 3.4 seconds. The damping was weakest at aft cg conditions. The lateral-directional stability characteristics were not significantly changed by the reduced-chord stabilizer configuration. With the final reduced-span stabilizer installed, the period of the oscillation was unchanged but the damping was noticeably reduced. In level flight below 56 KCAS, the damping became neutral when the cg was aft of fuselage station (FS) 98.0 and became slightly negative at the furthest aft cg location. Although the neutral and negative short-period damping is undesirable, the nature of the oscillatory motion was improved, in that less pitch was generated by the yaw. The motion could be easily stopped or controlled by the pilot. When the canopy slat was removed from the standard configuration, the aircraft response was similar to the final reduced-chord configuration for the aft cg location.

Maneuvering Stability

61. During the stabilizer development, maneuvering stability was qualitatively determined by making windup turns from 47-KCAS level forward flight conditions. As the normal load factor increased, forward longitudinal stick force was required to maintain airspeed, which is considered to be negative maneuvering stability. The push force was highest at the aft cg location. This characteristic is the primary reason that control feedback during autorotational entries opposed the aircraft motion. The importance of this control force on the feedback autorotational entry characteristics will be further discussed in paragraph 62. Qualitatively, the stabilizer or canopy-slat-removed configurations did not significantly affect the maneuvering stability characteristics.

Table 8. Comparison of Dynamic Lateral-Directional Stability Characteristics in Level Flight.[1]

Stabilizer Configuration	Mode of Response	Period of Oscillation (sec)	Damping Characteristics		Center-of-Gravity Location (in.)
			Ratio	Description	
Standard	Lateral	3.2	0.35	Moderate	96.2 (fwd)
	Directional	2.9	0.12	Weak	
Reduced chord	Lateral	3.4	0.35	Moderate	
	Directional	3.1	0.11	Weak	
Reduced span	Lateral	3.2	0.22	Weak	95.2 (fwd)
	Directional	3.1	0.06	Weak	
Standard	Lateral	3.3	0.17	Weak	99.0 (aft)
	Directional	3.3	0.16	Weak	
Reduced chord	Lateral	3.3	0.13	Weak	
	Directional	3.2	0.03	Neutral	
Reduced span	Lateral	3.3	0.14	Weak	
	Directional	3.2	-0.01	Negative	

[1]Flight conditions:
Rotor speed: 483 rpm.
Airspeed: 47 KCAS.
Average density altitude: 4400 feet.
Average gross weight: 1650 pounds.

Autorotational Entry Characteristics

62. Prior to initiating the autorotational entries, the aircraft was stabilized in unaccelerated, level, ball-centered flight with the controls fixed. A fixture was used to hold the cyclic control fixed, while the collective control was held fixed with the standard friction device. The pedals were manually held fixed by the pilot. This procedure removed feedback from the control loop and ensured that the pilot and control entry response was purely the result of aircraft characteristics. The cyclic control feedback during a stick-free entry was corrective, in that the longitudinal stick moved aft and the lateral stick moved to the right. Even when the pilot manually tried to prevent the cyclic stick from moving, the aircraft motions were reduced from the stick-fixed entries. If the pilot deliberately input incorrect control movement (*ie*, forward or left cyclic control, or left pedal to simulate a student error), the aircraft rolling and pitching motions were considerably worse.

63. The base-line data for the standard stabilizer were observed at maximum gross weight and both forward and aft cg locations. Entries were made from level flight at rotor speeds of both 450 and 483 rpm and indicated airspeeds of 40, 50, 60, and 65 knots. Entries were also made from maximum-power climbs at a rotor speed of 483 rpm and indicated entry airspeeds of 30, 35, 40, and 50 knots. Time histories of the critical parameters measured during the entries for the standard and reduced-span stabilizers are shown in figures 22 through 27, appendix D. The reduced-chord stabilizer data were nearly identical to the standard stabilizer data and were omitted to simplify the figures. A direct comparison of the stabilizer configuration effects on the aircraft response can only be made when the entry airspeed, flight condition, rotor speed, and sideslip angle are identical. Although the data for the standard and final stabilizer configurations are presented at similar airspeeds and flight conditions, a variation of sideslip or rotor speed was often obtained. A higher right sideslip or lower rotor speed (higher torque) increases the helicopter response. For example, in figure 22, the entry was made at lower rotor speed with the final stabilizer, which resulted in generating more sideslip during the maneuver. In this condition, the resulting helicopter motions were nearly the same as the standard configuration. In general, the data presented indicate a significant improvement in control required for recovery, delay time, and helicopter pitch response with the final reduced-span configuration.

64. Regardless of configuration or entry condition, the characteristic aircraft motion following a power reduction was a light yaw followed by left roll and then pitch down. The maximum yaw, roll, and pitch rates occurred between 0.5 to 0.75 second, 1.25 to 1.5 seconds, and 1.5 to 1.75 seconds, respectively, for all entries flown. If the delay time for corrective control input was less than these values, the rates achieved were reduced. Therefore, the FAA requirement to hold only the collective control fixed for 1.0 second while allowing cyclic or directional control inputs would greatly reduce the nose-down pitch rate encountered during the maneuver.

65. Typical maximum values of the angular rates attained during a stick-fixed autorotational entry with the standard stabilizer were determined. The maximum yaw rates attained during the entries varied from 28 to 32 degrees per second (deg/sec). The yaw rate increased with increasing power required. The roll rate varied slightly from 32 to 34 deg/sec and primarily increased with increasing entry airspeed. The pitch rate showed the widest variation and ranged from 18 to 25 deg/sec. The rate increased with both increasing power and airspeed. When a 1-inch left pedal input (opposite direction for recovery) was made following a simulated power failure, the pitch rate would exceed 30 deg/sec. The worst conditions for nose-down pitch were in low-speed maximum-power climbs and at maximum speed in level flight.

66. The delay time (time from point of power reduction to recovery control input) ranged from 1.0 to 2.25 seconds for the standard stabilizer. The delay time decreased as power required or airspeed increased and was usually determined by recovery from undesirable rates or attitudes. With the final reduced-span stabilizer installed, the delay times ranged from 1.5 to 2.8 seconds, and the determining factor was the low rotor speed. In low-power conditions, the aircraft stabilized in a descending left turn at the time of recovery.

67. The sideslip angle prior to entry was also found to affect the pitch rate. During the entries, the sideslip was found to increase by 25 to 30 degrees. A higher entry sideslip caused higher pitch rates to occur, as discussed in paragraph 51. Figures 22 through 29, appendix D, show the effects of varying initial sideslip angle on entry autorotational characteristics. Generally, the trim sideslip angle decreased with increasing airspeed in level flight, and for any given airspeed, it was usually greatest during climb and lowest during autorotation.

68. An example of the improvement in autorotational entry motions achieved by the final reduced-span stabilizer is shown in figure E. The low-sideslip entry condition shown for the final reduced-span stabilizer was obtained using the pedal position indicator (para 54). The higher entry sideslip angles for the standard configuration are representative for those encountered without the pedal position indicator. Autorotational entry data for the standard, reduced-chord, and final reduced-span stabilizers are shown for a 47-KCAS level flight entry. The reduced-chord configuration is shown to be similar to the standard configuration, which was the case for all entry conditions tested. The final reduced-span stabilizer is shown to have considerably reduced the pitching motion and the aft longitudinal cyclic movement required for recovery. Additionally, the maximum-allowable delay time before recovery was increased from 1.5 seconds to nearly 2.8 seconds, where the critical parameter was rotor speed rather than excessive rates or attitudes. The roll rate was only slightly influenced by the stabilizer configuration.

69. The rotor speed decay rates with the collective fixed following descending, level, and climbing flight throttle chops are included in figure 30, appendix D. These data are shown as a function of the manifold pressure (engine power) required to maintain the steady flight condition prior to the throttle chop. With the exception of slightly higher decay rates in hover, definite trends with airspeed or flight condition were not apparent.

SYMBOL	STABILIZER CONFIGURATION	ENTRY AIRSPEED (KCAS)	AVG GROSS WEIGHT (POUNDS)	AVG CG LOCATION (INCHES)	ANGLE OF SIDESLIP (DEGREES)
———	STANDARD	47	1670	99.3	12
— — —	REDUCED CHORD	47	1650	99.2	15
- - - - -	FINAL REDUCED SPAN	47	1670	99.3	4

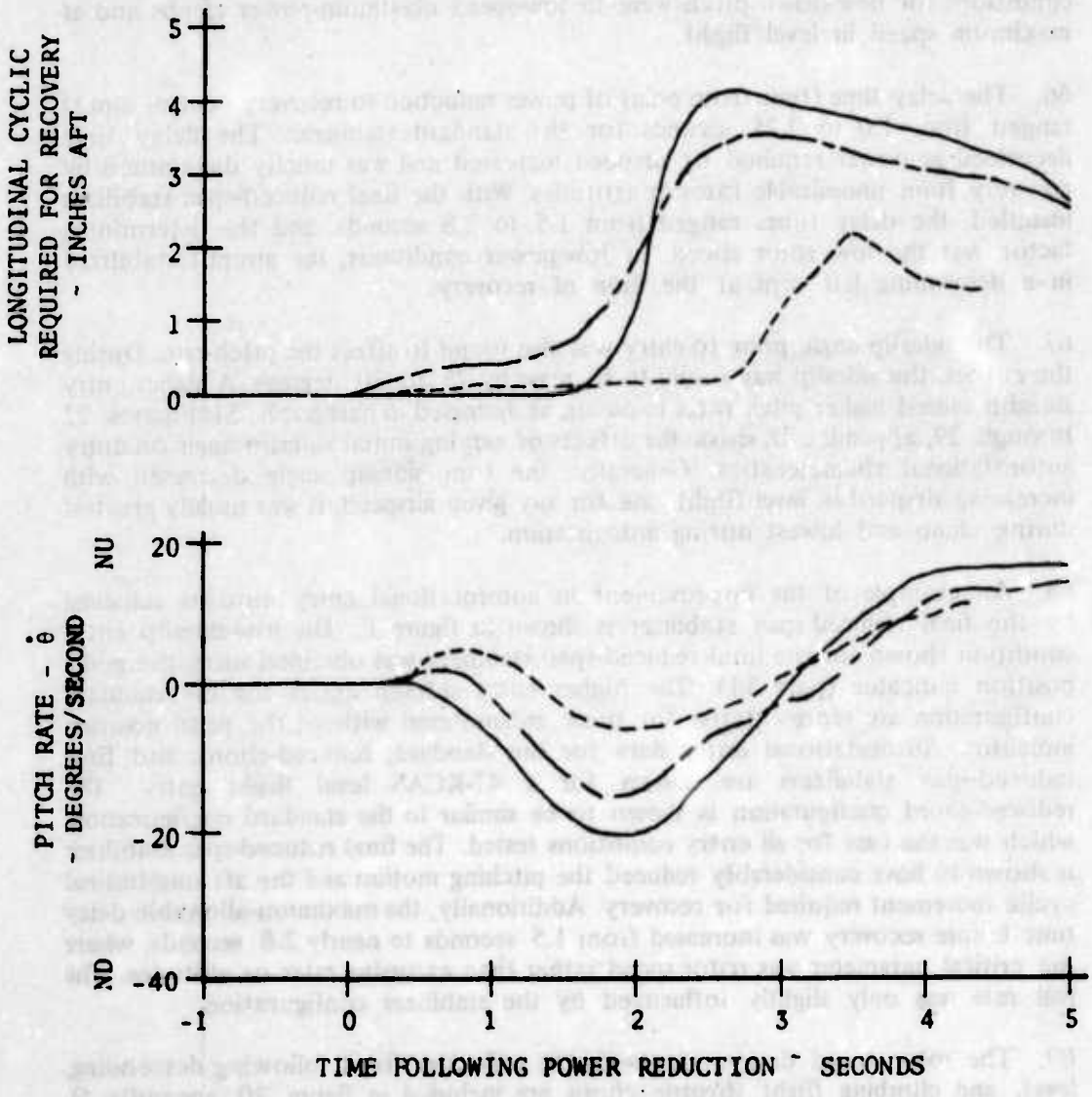

Figure E. Comparison of Longitudinal Characteristics During an Autorotational Entry.

70. The rotor speed decay rates were very high because of the low inertia rotor. The maximum observed decay rate over the first second was 72 rpm/sec, (15 percent/sec) at 23.3 inches of manifold pressure. As shown in figures 22 through 27, appendix D, the initial rotor speed decay rate rapidly diminished with time and was near zero at 3 seconds. A pronounced aircraft vibration was observed as the rotor speed dropped below 340 rpm.

71. When entries were initiated at a rotor speed of 450 rpm, the decay rate was increased over that for the same flight condition at 483 rpm. The rotor speed decreased to 350 rpm approximately 0.5 second earlier because of the higher decay rate and lower initial rotor speed. Operating at a rotor speed of 483 rpm provides the pilot with the longest delay time in the event of a power failure.

STABILIZER QUALIFICATION (PHASE II)

General

72. Following the determination that the 21-inch-span stabilizer with a full-length upper-leading-edge spoiler was the optimum interim configuration for the TH-55A, an Army qualification program was developed by AVSCOM (ref 4, app A). The purpose of the program was to qualify the new stabilizer throughout the flight envelope contained in the 1967 Hughes TH-55A owner's manual from both a handling qualities and structural viewpoint. The same types of stability and control tests conducted in Phase I were continued in Phase II, except that the emphasis was placed on most critical flight conditions and a broader airspeed range. The airspeeds investigated ranged from hover to 1.11V_{NE} (never-exceed airspeed) and included the specific conditions shown in table 3. Although the TH-55A is not required to meet military specifications, the applicable stability and control requirements of MIL-H-8501A (ref 7) were compared with the test results. In most cases, the modified TH-55A met or exceeded these requirements.

73. Structural integrity of the horizontal stabilizer was demonstrated by measuring stabilizer bending loads during maximum load factor maneuvers and by conducting special flutter and vibration tests. The natural frequency of the stabilizer was determined and evaluated relative to the airframe. The final reduced-span stabilizer was structurally acceptable since the measured loads were generally less than the standard configuration loads. However, the natural frequency of the stabilizer structure was slightly increased, which could cause a reduction in fatigue life since it was found to be nearer the primary forcing frequency.

HANDLING QUALITIES

Controllability

74. During Phase II, only hover controllability tests were conducted. These tests were to determine control power and rate damping characteristics in accordance with MIL-H-8501A requirements. The tests were conducted at maximum gross weight, both forward and aft cg locations, a density altitude of 2200 feet, and a skid height of 15 to 20 feet.

75. The longitudinal and directional control power was defined by the attitude attained in 1 second following a 1-inch control step input. The lateral control power was determined by the roll attitude attained in 1/2 second following a 1-inch control step input. The visual-flight-rules (VFR) requirements of MIL-H-8501A, used for comparison, are based on the maximum gross weight of the helicopter. The results obtained for both the forward and aft cg locations are shown in table 9. The TH-55A with the modified stabilizer exceeded the hovering control power requirements about each axis.

76. The rate damping characteristics were determined by calculating the damping moment by the time constant method (ref 10, app A). The test data were compared with MIL-H-8501A requirements, which are based on the principal axis moments of inertia. The moments of inertia for the test configuration were calculated by methods discussed in USAASTA Technical Note No. 24 (ref 11) and are included with the test results in table 9. Following a 1-inch longitudinal control step input, the pitch rate damping moment was found to exceed the requirement. The roll rate damping was slightly less than required. The yaw rate damping was positive, although considerably below the requirement. Weak yaw rate damping is a common characteristic of single-rotor helicopters, and failure to meet this requirement is not a serious shortcoming.

77. The longitudinal control response in hover was generally satisfactory and was nearly twice that for the standard stabilizer at 47-KCAS forward speed. The lateral control response in hover was satisfactory and was nearly the same as for the 47-KCAS level flight condition with the standard stabilizer. The directional control response in hover was satisfactory and was approximately four times greater than the value at 47 KCAS in level flight. Qualitatively, the stabilizer modification did not significantly degrade the controllability characteristics.

Hover and Low-Speed Flight

78. The objectives of these tests were to evaluate the handling qualities and determine control margins in crosswind or downwind hovering conditions. The tests were conducted at maximum gross weight, a density altitude of 2100 feet, and both forward and aft cg locations. The skid height ranged from 10 to 15 feet. A calibrated ground pace vehicle was used to establish airspeeds from zero to 25 knots in increments of 5 knots in sideward and rearward flight.

Table 9. Controllability in Hover.[1]

Center-of-Gravity Location (in.)	Control Axis	Moment of Inertia (slug/ft^2)	Control Power[2] (deg/in.)		Rate Damping (in.-lb/sec^2)		Control Response (deg/sec/in.)
			TH-55A	MIL-H-8501A	TH-55A	MIL-H-8501A	
99.0 (aft)	Longitudinal	540	6	3.3	920	654	18
	Lateral	245	6	2.0	790	847	20
	Directional	417	27	8.0	470	1843	83
95.2 (fwd)	Longitudinal	503	7	3.3	745	622	18
	Lateral	252	5	2.0	840	865	19
	Directional	385	22	8.0	385	1744	85

[1]Average flight conditions:
Density altitude: 2200 feet.
Gross weight: 1670 pounds.

[2]Control power determined at 1 second for longitudinal and directional control inputs and at 1/2 second for lateral control inputs.

79. The test results are graphically presented in figures 31 and 32, appendix D. The cyclic control deflection required was in the direction of increasing airspeed. The collective position was maximum at hover and decreased with increasing airspeeds in all directions. Control margins were adequate for the airspeed range tested, but the longitudinal control was within 10 percent of the aft limit at 18 knots true airspeed (KTAS) in rearward and left sideward flight at the aft cg location. This indicates that the longitudinal control would be near the aft stop in these conditions if the aircraft rigging were set for maximum forward stick movement as discussed in the portion of this report concerning control systems characteristics (para 33).

80. The directional stability was generally weak in sideward flight, and the aircraft was dynamically unstable when translating to the left in the 10- to 25-knot range. Despite this instability, the pilot considered the sideward flight handling qualities to be better than the standard stabilizer in this flight condition.

Control Positions in Trimmed Forward Flight

81. During Phase II tests, control positions were determined in climb, autorotation, and level flight using only the maximum normal rotor speed of 483 rpm. The tests were conducted at maximum gross weight, both forward and aft cg locations, and at an average density altitude of 4150 feet. Control positions were recorded at various stabilized zero-sideslip flight conditions at forward flight speeds ranging from 20 KCAS to $1.11V_{NE}$ and are presented in figures 33 and 34, appendix D.

82. The most critical forward longitudinal control margin of 1.2 inches (9.2 percent) occurred at $1.11V_{NE}$ at the aft cg location. Conversely, the most critical aft longitudinal control margin of 3.1 inches (31.4 percent) occurred in hover at the forward cg location (fig. 31, app D). From approximately 30 to 76 knots, forward longitudinal cyclic control was required with increasing speed, and the trim control position characteristics were generally satisfactory. Qualitatively, a slight discontinuity existed during transitional flight (zero to 30 knots); however, this characteristic was not objectionable to the pilot, and the requirements of MIL-H-8501A were generally met.

Collective-Fixed Static Longitudinal Stability

83. The Phase I test methods were used during the collective-fixed static longitudinal stability qualification tests, except the aircraft was trimmed at near-zero sideslip. The aircraft was tested in climb, autorotation, and level flight conditions. The conditions tested are shown in table 3. Tests were conducted at both forward and aft cg locations, an average density altitude of 4200 feet, and at maximum gross weight. The detailed results of these tests are shown in figures 35 through 37, appendix D.

84. A summary of the static longitudinal stability in level flight is shown in figure 16, appendix D. The aircraft was stable at all forward airspeeds tested and increased as airspeed increased. The level flight static longitudinal stability characteristics were not appreciably changed in either climb or autorotational flight conditions.

Static Lateral-Directional Stability

85. The lateral-directional stability test procedures conformed to those discussed in the Phase I results for level flight conditions. However, in climb and autorotation, the dynamic test technique was used. The data were read at 5-degree increments as sideslip increased from the trim position in each direction. Tests at airspeeds of V_{NE} and $1.11V_{NE}$, requested by AVSCOM (ref 4, app A), were not conducted because of the unavailability of an approved sideslip envelope. The test conditions shown in table 3 were flown at maximum gross weight, both forward and aft cg locations, and an average density altitude of 4200 feet. The detailed test results are presented in figures 38 and 39, appendix D.

86. The static directional stability was positive. The directional control gradient was slightly stronger at higher airspeed and was nearly identical to the standard configuration discussed in the Phase I results.

87. The modified TH-55A was determined to have a positive dihedral effect. The dihedral effect increased slightly at higher airspeed and was similar to the standard configuration.

88. The change in the aft longitudinal cyclic trim as a function of right sideslip was shown to be improved when compared to the standard stabilizer shown in figure B of the Phase I results. The Phase II lateral-directional data indicate that airspeed or cg location do not significantly change the longitudinal trim shift with sideslip. In autorotation, a large aft cyclic movement is required with either left or right sideslip about the trim condition.

Dynamic Longitudinal Stability

89. The short-period dynamic longitudinal stability test methods were the same as in Phase I, except that the aircraft was initially trimmed at zero sideslip. The flight conditions requested by AVSCOM (ref 4, app A) were flown and are listed in table 3. Tests were flown at the maximum gross weight and aft cg configuration, which is normally the worst condition for dynamic stability. The short-period results are summarized in table 10. The long-period dynamic stability characteristics were briefly investigated and were qualitatively determined to be similar to the standard helicopter.

90. In the aft cg configuration, adequate longitudinal stability was exhibited in the level and autorotational flight conditions. Following a longitudinal pulse in low-speed flight, the resulting pitch oscillation would initially damp out, but the lateral-directional mode was excited and became divergent. The resulting roll and

yaw oscillations increased and then coupled with the pitch axis to become an undamped 3-axis oscillation. This situation existed at airspeeds below 60 knots at the aft cg location (FS 99.1).

Table 10. Dynamic Longitudinal Stability Summary.[1]

Flight Condition	Center-of-Gravity Location (in.)	Calibrated Trim Airspeed (kt)	Period of Oscillation (sec)	Damping Characteristics	
				Ratio	Description
Level	95.2 (fwd)	40	3.4	0.24	Weak
		47	3.4	0.34	Moderate
		56	3.0	0.39	Moderate
Level	99.1 (aft)	40	3.0	0.20	Weak
		47	3.4	0.28	Weak
		56	3.3	0.29	Weak
		70	2.9	0.33	Moderate
Climb	99.1 (aft)	44	---	--	Divergent[2]
		50	---	--	Divergent[2]
Auto-rotation	99.1 (aft)	38	[illegible].2	0.48	Strong
		56	3.2	0.42	Strong

[1]Average flight conditions:
Rotor speed: 483 rpm.
Gross weight: 1650 pounds.
Density altitude: 4400 feet.

[2]The short-period response to an aft pulse appeared to be deadbeat, but the long-period response was divergent.

Dynamic Lateral-Directional Stability

91. The short-period dynamic lateral-directional stability characteristics were evaluated using the same techniques as in Phase I testing, except that the aircraft was initially trimmed at zero sideslip. The aircraft was tested at the maximum gross weight and both forward and aft cg locations. The flight conditions and test

results are summarized in table 11. At the aft cg location, lateral-directional oscillations were found to be neutral or negatively damped in low-speed (below 47 KCAS) level flight and climb. An example of the aircraft response to a left lateral control pulse is shown in figure 40, appendix D. This figure corresponds to the 47-KCAS aft cg level flight condition in table 11. The roll and yaw traces show the initial positive lateral damping and the slightly negative directional damping characteristics. The resulting motion becomes a lightly diverging lateral-directional motion where the time to double amplitude exceeds 30 seconds. At airspeed above 56 KCAS, the lateral-directional damping became slightly positive. The damping was positive at all speeds in autorotation.

92. At a mid cg location of FS 98.1 and an airspeed of 40 KCAS, the lateral-directional mode was found to be lightly damped. This appeared to be the cg location beyond which the neutral-to-negative damping occurs. Since the negative lateral-directional dynamic stability increases pilot workload, the maximum aft cg location should be limited to FS 98.1 for normal operation. The period of undamped oscillations (3.2 to 3.4 seconds) was such that they were easily controlled by the pilot and will not be seen by operational pilots. The undamped directional stability at cg locations aft of FS 98.1 is a shortcoming, with no correction required.

Maneuvering Stability

93. The maneuvering stability characteristics were evaluated by conducting steady turns, symmetrical pull-ups, and aft longitudinal control step inputs. For all techniques, the aircraft was stabilized at a trim airspeed in level flight with the collective and trim settings being maintained throughout the maneuver. Stick forces were estimated by the pilot during the steady turns. The tests were conducted at an average density altitude of 4000 feet, maximum gross weight, and an aft cg location.

94. Both the pitch rate and normal acceleration curve became concave downward within 2 seconds of the aft control step inputs. This is in compliance with paragraph 3.2.11.1 of MIL-H-8501A, and was true for all airspeeds tested. The initial minor discontinuity shown in the normal acceleration data was caused by the normal accelerometer being offset from the aircraft cg.

95. The steady-turn tests indicated that the maneuvering stability characteristics were nearly identical to the standard configuration. The cyclic stick feedback forces moved the cyclic control aft, which indicates negative stick-force stability; however, the stick position stability was positive. The feedback forces increased as the cg was moved aft. Symmetrical pull-up data are shown in figure 41, appendix D. Positive stick position maneuvering stability was also evident. The maneuvering characteristics are acceptable for a VFR helicopter trainer.

Table 11. Lateral-Directional Stability Summary.[1]

Flight Condition	Center-of-Gravity Location (in.)	Calibrated Trim Airspeed (kt)	Mode of Response	Period of Oscillation (sec)	Damping Characteristics	
					Ratio	Description
Level	95.2 (fwd)	40	Lateral Directional	3.2 3.0	0.18 0.06	Weak Weak
		47	Lateral Directional	3.2 3.1	0.22 0.06	Weak Weak
		56	Lateral Directional	3.1 2.8	0.28 0.09	Moderate Weak
Level	99.2 (aft)	40	Lateral Directional	3.8 3.7	0.06 -0.01	Weak Negative[2]
		47	Lateral Directional	3.3 3.2	0.14 -0.01	Weak Negative[2]
		56	Lateral Directional	3.2 2.9	0.22 0.00	Weak Neutral[2]
		70	Lateral Directional	2.8 2.7	0.20 0.08	Weak Weak
Climb	99.2 (aft)	44	Lateral Directional	3.8 3.7	0.19 0.00	Weak Neutral[2]
		50	Lateral Directional	3.6 3.3	0.16 0.00	Weak Neutral[2]
Autorotation	99.2 (aft)	38	Lateral Directional	3.4 2.9	0.39 0.18	Strong Weak
		56	Lateral Directional	3.2 3.4	0.46 0.26	Strong Moderate

[1]Flight conditions:
Rotor speed: 483 rpm.
Average gross weight: 1660 pounds.
Average density altitude: 4400 feet.

[2]When the directional stability is neutral or negative, a disturbance results in an undamped Dutch roll regardless of direction of control pulse.

Structural Demonstrations

96. The critical maneuvering flight conditions requested by AVSCOM (ref 4, app A) were flown to demonstrate the structural integrity of the new stabilizer configuration. The tests were conducted at a 4000-foot pressure altitude, maximum gross weight, and a forward cg location (FS 95.2).

97. The results for each maneuver are shown in table 12. The tabulated data are for maximum load factor or the maximum flapwise bending load. The maximum load factor attained during any maneuver was 1.6g. At the maximum-g loading, excessive airframe and cyclic control vibrations indicated blade stall.

98. The maximum flapwise bending load recorded during these maneuvers was 264 inch-pounds (in.-lb) in the directional control reversal maneuver. This load was primarily caused by the high right sideslip angle generated during the maneuver. A high flapwise bending moment of 230 in.-lb on the final reduced-span stabilizer was also observed during the static lateral-directional stability tests (fig. 55, app D). Both values were significantly lower than the maximum load of 650 in.-lb recorded with the standard stabilizer during the Phase I static lateral-directional stability tests (fig. 50). Since the reduced-span stabilizer and standard stabilizer have essentially the same structure, the reduced airloads should provide a greater safety margin.

FLUTTER AND VIBRATION

Ground Tests

99. One of the primary concerns involved when modifying the structural size or stiffness of rotorcraft components is that the natural frequency of the component should not approach the forcing frequency of any rotating components. When this occurs, the stress magnification factor is dramatically increased, and structural failure or reduced fatigue life may occur. The overall stiffness of the new TH-55A horizontal stabilizer was increased because of the reduction in span and the addition of the spoiler. Since greater stiffness usually increases the natural frequency of the structure, tests were conducted to determine the natural frequency of both the standard and final stabilizer configurations. These tests were performed by striking the stabilizer, which was mounted on the aircraft, and recording the resulting free vibration response.

100. The standard stabilizer had a primary flapwise natural frequency of 25 to 26 hertz (Hz) and a chordwise natural frequency of 65 to 70 Hz. These values were increased to 26 to 29 Hz, flapwise, and 90 to 110 Hz, chordwise, on the reduced-chord stabilizer. The free vibration damping ratio on the reduced-span stabilizer was approximately 0.08, flapwise, and 0.16, chordwise.

Table 12. Results of Structural Demonstrations.[1]

Flight Maneuver	Calibrated Airspeed		Normal Load Factor (g)	Rotor Speed (rpm)	Roll Attitude[3] (deg)	Pitch Attitude[4] (deg)	Roll Rate (deg/sec)	Pitch Rate (deg/sec)	Angle of Sideslip (deg)	Flapwise Bending Moment (in.-lb)	Chordwise Bending Moment (in.-lb)
	Required[2]	Test (kt)									
Maximum level flight acceleration	Zero to V_{NE}	Zero to 72	1.13	483	-1.4	-2.5	-2.6, left	1.3	7.4	109.5, down	20.7
Maximum-g symmetrical pull-up	V_{NE}	72	1.61	483	20.0	3.5	0.8, right	13.8	5.6	87.0, down	34.0
Maximum-g right turn	V_{NE}	72	1.45	483	45.0	-9.8	5.2	12.5	5.6	127.8	18.0
Rolling pullout	V_{NE}	72	1.59	504	35.0	-4.0	9.4	12.0	1.6	105.0	-5.0
Maximum-g right turn, constant altitude	$V_{max\ R/C}$	40	1.51	483	42.0	-0.2	---	--	16.0	122.7	38.9
Directional control reversals	V_{NE}	72	1.06 to 1.18	477 to 488	-3.2 to -5.6	-10.7 to -4.7	-17.0 to -24.0	0.0 to -7.0	28.0 to 60.0	87.0 to 264.0	77.0 to 63.0
Pull-up and pushover	V_{NE}	72	1.38 0.53	509 477	-0.5 -2.0	4.8 -18.8	-- --	-- --	8.7 19.4	71.8 224.5	-8.0 -51.5
Power-OFF symmetrical pull-up	V_{NE}	72	1.34	526	-1.1	-1.1	--	--	-0.3	-101.3	7.6
Steady sideslip	---	60	1.0	483	—	—	--	--	42.0	230.0	—

[1]Average flight conditions:
Density altitude: 4900 feet. Gross weight: 1670 pounds.
[2]AVSCOM test request (ref 4, app A).
[3]Positive right wing down.
[4]Positive nose up.

101. The primary driving frequencies were determined by varying the rotor speed from 200 to 483 rpm with the aircraft on the ground while observing the strain gage data for vibratory response. The results of this test are shown in figure F. During this test, the stabilizer was essentially unloaded.

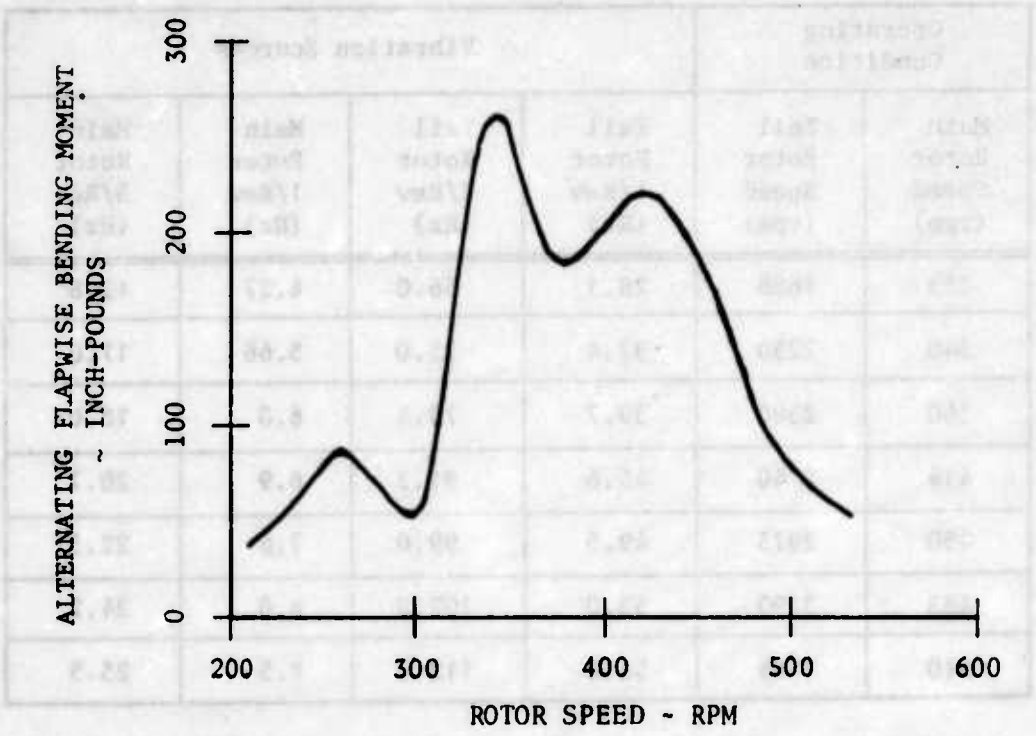

NOTES: 1. Helicopter on ground with collective full down.
2. Peak to peak.

Figure F. Vibratory Response of the Horizontal Stabilizer.

102. The rotor speeds which caused the largest stabilizer vibrations are shown in table 13. The frequencies of the most likely vibration sources are also shown. These sources include a one-per-rotor-revolution (1/rev) and 2/rev of the tail rotor, and a 1/rev and 3/rev of the main rotor. A 1/rev vibration does not occur from rotor aerodynamic sources on either the main or tail rotors; however, it can arise from rotor blade imbalance.

103. The main rotor vibrations are of minor concern because the higher flapwise natural frequency of the modified stabilizer is a favorable improvement. The 2/rev vibrations of the tail rotor are undesirably close to the chordwise natural frequency of the new stabilizer at the normal rotor speed range. This situation could reduce the fatigue life below that of the standard stabilizer. However, the damping ratio

is apparently sufficient to maintain the stress magnification factor at a tolerable value. An improvement could be provided by weighting the stabilizer tip.

Table 13. Vibration Sources at the Horizontal Stabilizer.

Operating Condition		Vibration Sources			
Main Rotor Speed (rpm)	Tail Rotor Speed (rpm)	Tail Rotor 1/Rev (Hz)	Tail Rotor 2/Rev (Hz)	Main Rotor 1/Rev (Hz)	Main Rotor 3/Rev (Hz)
255	1688	28.1	56.0	4.27	12.8
340	2250	37.4	75.0	5.66	17.0
360	2380	39.7	79.5	6.0	18.0
414	2740	45.6	91.2	6.9	20.7
450	2975	49.5	99.0	7.5	22.5
483	3190	53.0	107.0	8.0	24.2
510	3365	56.2	112.0	8.5	25.5

104. The primary problem area appeared to be 1/rev of the tail rotor at low main rotor speeds (330 to 360 rpm). In this range, the driving frequency corresponds to the flapwise natural frequency and provides the worst vibratory response, as shown in figure F. Again, tip weighting would lower the natural frequency and improve this situation. If the tail rotor is in perfect balance, no vibrations will be introduced. However, when more imbalance is present, stronger driving vibrations at these frequencies will occur. Therefore, the tail rotor should be kept as well balanced as possible to reduce structural fatigue.

Flight Tests

105. The flutter and vibration characteristics were observed under the conditions requested by AVSCOM (ref 4, app A). The test conditions were flown at maximum gross weight, an aft cg location (FS 99), and at both 4000- and 9000-foot density altitudes. Vibration data were obtained from the stabilizer flapwise and chordwise bending moments, the aircraft accelerometers, and tail-boom flow-vane oscillograph traces. At the test airspeeds (V_{NE} and $1.11V_{NE}$), blade stall prevented operation at rotor speeds below 400 rpm, and the collective rigging prevented operating above 510 rpm. The test conditions and results are shown in table 14. The vibration frequency shown was the predominant frequency recorded.

Table 14. Vibration and Flutter Test Results.

Density Altitude (ft)	Flight Condition	Rotor Speed (rpm)	Test Calibrated Airspeed (kt)	Aircraft Vibrations[1]						Stabilizer Vibrations[1]			
				Longitudinal		Lateral		Vertical		Flapwise		Chordwise	
				Frequency (Hz)	Amplitude (g)	Frequency (Hz)	Amplitude (g)	Frequency (Hz)	Amplitude (g)	Primary Frequency (Hz)	Amplitude (in.-lb)	Frequency (Hz)	Amplitude (in.-lb)
5,200	Level	450	79	22.5	.06	22.5	.08	22.5	.09	50	105	100	74
		483	79	24.5	.02	—	.07	24.5	.07	54	189	110	62
	Auto-rotation	[2]420	79	43	.08	21	.08	7.5	.06	45	315	20 and 110	136 and 49
		508	79	--	.02	--	.05	--	.17	55	231	55	93
		400	[3]65	20	.13	20	.14	20	.11	45	168	20 and 120	155 and 62
		[4]510	70	8.6	.11	8.6	.09	8.6	.11	8.6 and 57	210 and 210	8.6 and 57	80 and 93
10,100	Level	450	61	22.5	.06	22.5	.08	22.5	.09	50	84	100	74
		483	61	24.5	.035	24.5	.03	24.5	.06	54	189	110	68
	Auto-rotation	450	61	44	.05	—	.02	8.0	.06	50	231	110	37
		507	61	8.6	.10	8.6	.07	8.6	.07	57	252	57	93
		[3]420	55	21	.12	21	.10	21	.09	46	168	130	49
		[4]510	55	8.6	.20	8.6	.11	8.6	.09	52	126	57	93

[1]Amplitudes are peak to peak.
[2]Rotor speed for onset of blade stall.
[3]Airspeed for onset of blade stall.
[4]Rotor speed limited to 510 rpm by test collective rigging.

106. During the level flight tests, the aircraft exhibited a small 3/rev vibration in the longitudinal, lateral, and vertical directions. The predominant response of the new stabilizer was 1/rev of the tail rotor flapwise and 2/rev of the tail rotor chordwise. The level flight conditions appeared to be free of any significant vibration or flutter.

107. During the autorotations at rotor speeds above 483 rpm, the aircraft vibrations increased and were predominately 1/rev in frequency. However, the predominant stabilizer vibrations remained at 1/rev of the tail rotor flapwise and 2/rev of the tail rotor chordwise and were not excessive in amplitude. The predominant stabilizer response generally appeared to be from vibration. However, a flutter condition did appear to exist. Flutter is defined as an aeroelastic, self-excited vibration deriving its energy from the airstream. Therefore, the TH-55A stabilizer is subject to flutter from two sources. First, the stabilizer is located in the nonsteady rotor wake flow conditions; and secondly, it is located on a long tail boom which is subject to vibratory deflection.

108. When operating at the lowest rotor speeds during autorotations, the 3/rev aircraft vibrations increased. These vibrations were also felt in the control system, which indicated the presence of blade stall. During these conditions, the stabilizer flapwise bending frequency remained at 1/rev of the tail rotor; however, at 5200 feet, the chordwise bending exhibited both 2/rev of the tail rotor and 3/rev of the main rotor vibrations. The 3/rev main rotor vibration was the largest vibration recorded by the chordwise gage, but was not considered to be excessive. The vibrations were reduced at 10,100 feet.

109. The flow-field angle-of-attack oscillations were recorded by a flow vane located about 7 inches from the tail boom on a dihedral angle of 35 degrees from the horizontal plane and located about 4 inches forward of the stabilizer. For most level flight and climb conditions, unsteady flow due to the individual blade passage (3/rev) caused less than a ±2-degree angle-of-attack oscillation. However, a flow vane at 1/rev of the main rotor oscillation was much more significant. Although this oscillation appeared to be caused by tail-boom vibration, instrumentation was inadequate to confirm this observation. During autorotation, the stabilizer flow-vane oscillation at 1/rev of the main rotor was as high as ±15 degrees at 510 rotor rpm. However, the lift curve slope of the final reduced-span stabilizer was lowered by the reduced aspect ratio and spoiler configuration, which should reduce the response from that shown by the standard stabilizer. The stabilizer flapwise and chordwise flutter amplitudes were not excessive, and the frequency is safely removed from the natural frequency of the structure.

HORIZONTAL STABILIZER AERODYNAMIC CHARACTERISTICS

General

110. Figure G shows the geometry of the air loads acting in their positive directions on the horizontal stabilizer. The flapwise bending moments (BM_{fw}) were

measured by strain gages located near the stabilizer root. The flapwise gages were located on the upper and lower surfaces of the main spar, and chordwise bending moment (BM_{CW}) gages were located on the upper and lower skin surfaces near the leading edge. These strain gages were calibrated by applying forces at a quarter chord point near the stabilizer tip. The forces were multiplied by the span to obtain the calibration in inch-pounds of moment about the stabilizer root.

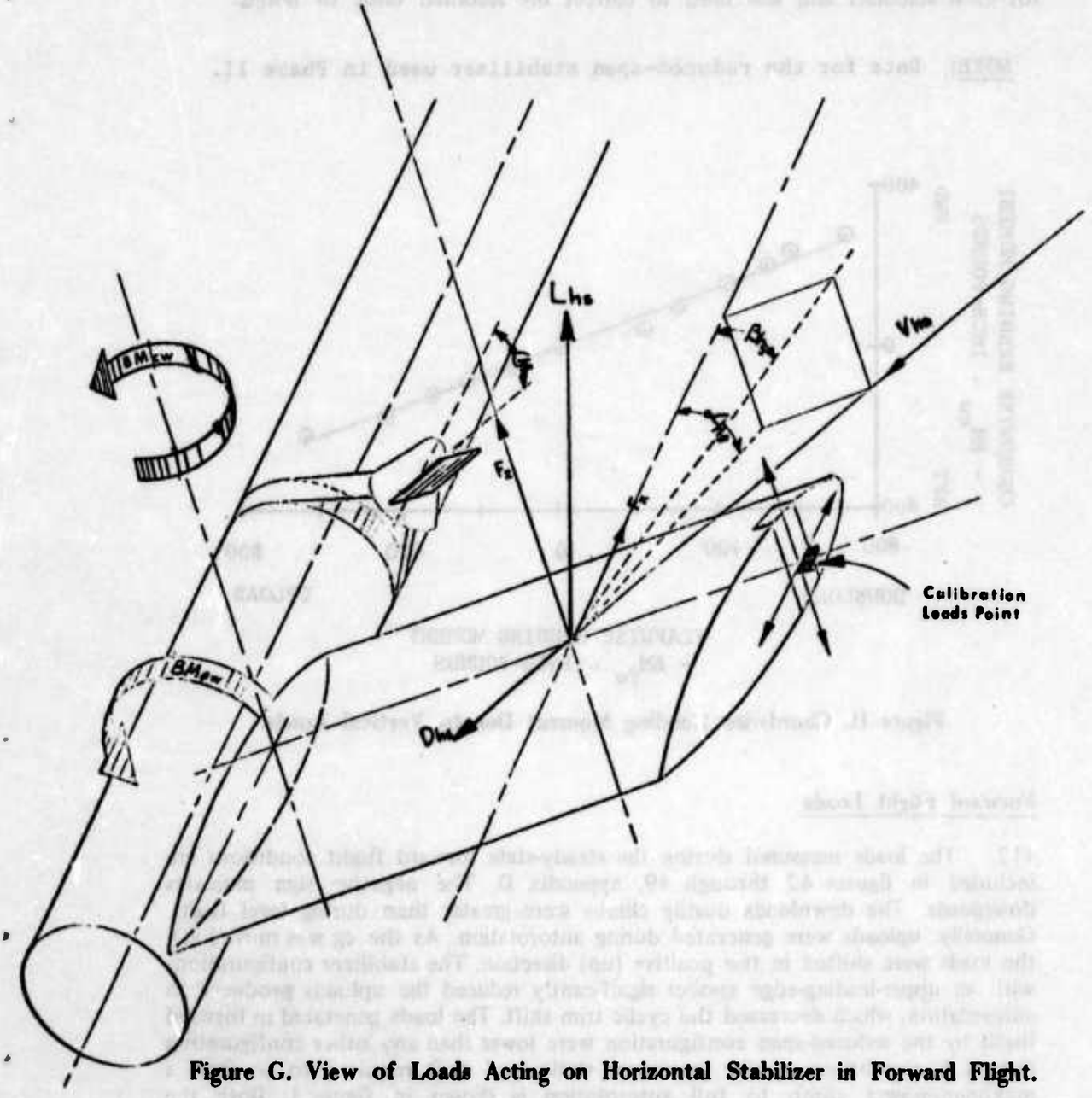

Figure G. View of Loads Acting on Horizontal Stabilizer in Forward Flight.

111. An undesirable feature of the instrumented stabilizer was that the vertical loads were also sensed by the chordwise strain gages. Fortunately, the longitudinal loads were not sensed by the flapwise gages. Thus, the chordwise moments could be determined by first reading the flapwise load and then removing the chordwise bending moment due to vertical loads from the measured value. During the vertical load calibration, a correction curve similar to that shown in figure H was obtained for each stabilizer and was used to correct the recorded value of BM_{cw}.

NOTE: Data for the reduced-span stabilizer used in Phase II.

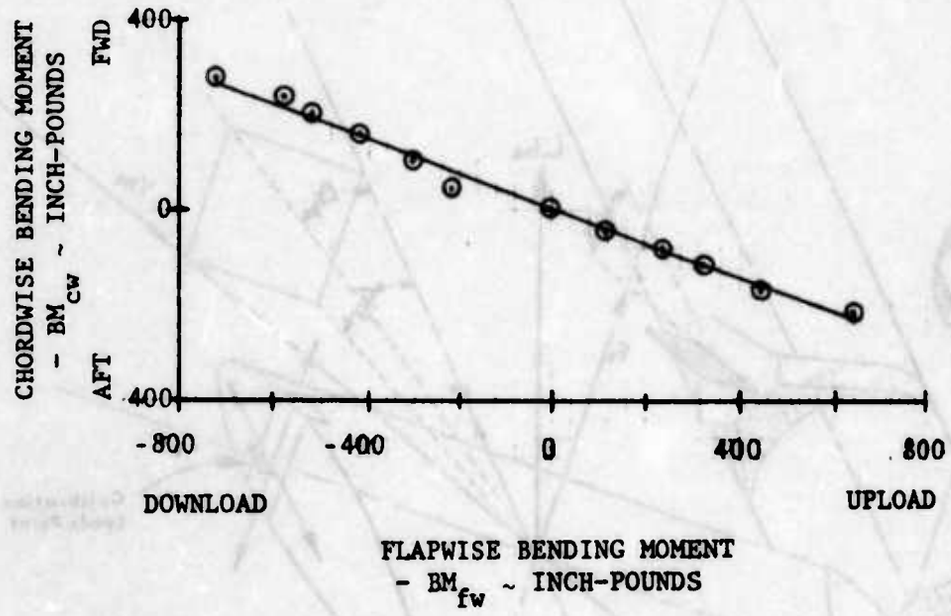

Figure H. Chordwise Bending Moment Due to Vertical Loads.

Forward Flight Loads

112. The loads measured during the steady-state forward flight conditions are included in figures 42 through 49, appendix D. The negative sign indicates downloads. The downloads during climbs were greater than during level flight. Generally, uploads were generated during autorotation. As the cg was moved aft, the loads were shifted in the positive (up) direction. The stabilizer configurations with an upper-leading-edge spoiler significantly reduced the uploads produced in autorotation, which decreased the cyclic trim shift. The loads generated in forward flight by the reduced-span configuration were lower than any other configuration tested. A comparison of the maximum static load shift required to go from a maximum-power climb to full autorotation is shown in figure I. Both the

reduced-chord and final reduced-span configurations significantly lowered the stabilizer load shift, which reduced the longitudinal cyclic trim change, as discussed in paragraph 45.

SYMBOL	STABILIZER CONFIGURATION	AVG DENSITY ALTITUDE (FEET)	AVG GROSS WEIGHT (POUNDS)	AVG CG LOCATION (INCHES)
———	STANDARD	5400	1660	95.1
—·—	REDUCED CHORD	4400	1640	95.7
- - - - -	FINAL REDUCED SPAN	4100	1670	95.2

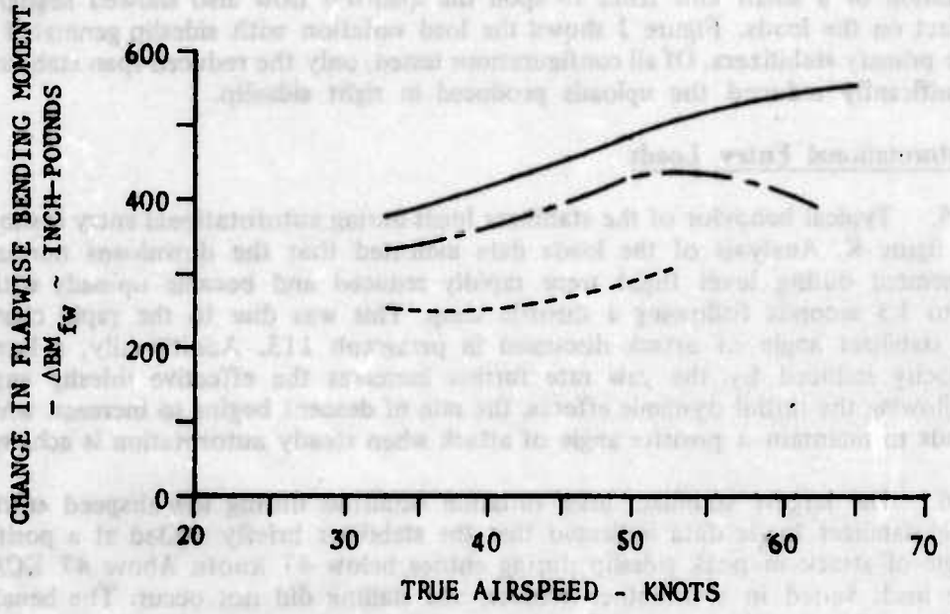

Figure I. Comparison of Stabilizer Load Shift for Maximum-Power Climb to Full Autorotation.

Lateral-Directional Flight Loads

113. The loads data taken in steady-heading sideslips are shown in figures 50 through 55, appendix D. Figure 50 presents the loading on the small vertical fin located just ahead of the stabilizer on the tail boom. These vertical fin loads were determined to be insignificant in comparison to the lateral component of the loads on the horizontal stabilizer and were no longer measured. The largest horizontal stabilizer uploads recorded were at the maximum right sideslip angles tested. The

largest load was on the standard stabilizer, which produced a bending moment of 650 in.-lb at 53 degrees of sideslip at 47 KCAS and an aft cg location. In level flight, right sideslip between 20 and 25 degrees decreased the downloads to zero for all stabilizer configurations tested. Beyond 25 degrees of right sideslip, uploads were produced which caused a nose-down pitching moment on the aircraft. The reduction of download was produced by both the positive dihedral angle of the stabilizer, which couples angle of attack with sideslip, and the outward movement of the stabilizer through the rotor downwash.

114. Figures 50 through 55, appendix D, also show the angle-of-attack correlation with sideslip and stabilizer loads. The upper surface spoiler only slightly reduced these loads, because the stabilizer is in a high three-dimensional flow region, and the drag forces acting on the stabilizer rapidly increased with sideslip. The addition of a small end fence to spoil the spanwise flow also showed negligible effect on the loads. Figure J shows the load variation with sideslip generated by the primary stabilizers. Of all configurations tested, only the reduced-span stabilizers significantly reduced the uploads produced in right sideslip.

Autorotational Entry Loads

115. Typical behavior of the stabilizer loads during autorotational entry is shown in figure K. Analysis of the loads data indicated that the downloads normally generated during level flight were rapidly reduced and became uploads within 1 to 1.5 seconds following a throttle chop. This was due to the rapid change of stabilizer angle of attack discussed in paragraph 113. Additionally, a lateral velocity induced by the yaw rate further increases the effective sideslip angle. Following the initial dynamic effects, the rate of descent begins to increase, which tends to maintain a positive angle of attack when steady autorotation is achieved.

116. The largest stabilizer load variation occurred during low-airspeed entries. The stabilizer loads data indicated that the stabilizer briefly stalled at a positive angle of attack in peak sideslip during entries below 47 knots. Above 47 KCAS, the loads varied in a smoother manner, and stalling did not occur. The benefits from stabilizer stalling were offset because, at the high positive angles of attack, the vertical components of drag became quite large. For this reason, the addition of a spoiler did not significantly lower the load variation encountered during entries.

117. The reduced-chord stabilizer tended to reduce the uploads achieved during the entry, although the overall load variation was not improved. The reduced-span configuration significantly reduced the initial trim loads in all flight conditions, and thereby reduced the overall load variation during the entry. The nose-down pitching during entries was significantly reduced, particularly when initiated from zero sideslip. The loads for the reduced-span stabilizer were lowered by the 25-percent area reduction and the lower lift curve slope.

SYMBOL	STABILIZER CONFIGURATION	CALIBRATED AIRSPEED (KNOTS)	AVG DENSITY ALTITUDE (FEET)	AVG GROSS WEIGHT (POUNDS)	AVG CG LOCATION (INCHES)
———	STANDARD	47	4000	1680	96.3
— — —	REDUCED CHORD	47	4000	1690	96.2
- - - - -	FINAL REDUCED SPAN	47	4150	1670	95.2

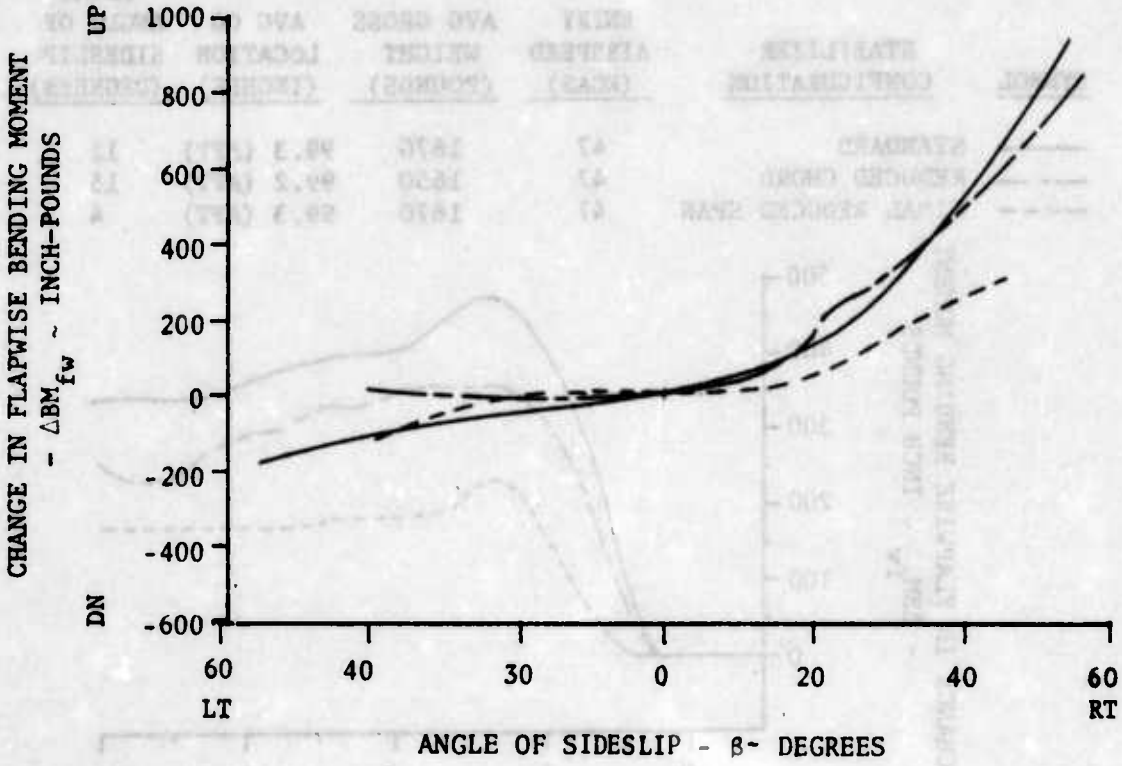

Figure J. Comparison of Horizontal Stabilizer Loading with Sideslip.

Aft Fuselage Tufting

118. The tufting on the aft fuselage and stabilizer was useful in determining the direction and stability of the airflow and the airfoil stalling conditions. The horizontal stabilizer stall was clearly evident from the tuft movement. The tufts were observed from a chase aircraft and were recorded by a movie camera installed on the test helicopter. During steady flight, the flow was generally stable. The standard stabilizer was observed to stall only during entries below 47 KCAS and for a short period of time. In steady-state autorotation, climb, and level flight (above 30 KCAS), the tufts remained attached to the stabilizer. Below 30 KCAS in climb or level flight, the standard stabilizer generally appeared to be stalled. The tufts were not installed on the final stabilizer configuration.

119. In 47-KCAS level flight at high right sideslip, the lateral boundary of the rotor wake appeared to intersect the standard horizontal stabilizer. When this occurred, an aft longitudinal trim change was noted by the pilot. The reduced-span stabilizer configurations delayed this condition by requiring a higher sideslip angle to achieve the same degree of stabilizer penetration out of the rotor wake.

SYMBOL	STABILIZER CONFIGURATION	ENTRY AIRSPEED (KCAS)	AVG GROSS WEIGHT (POUNDS)	AVG CG LOCATION (INCHES)	ENTRY ANGLE OF SIDESLIP (DEGREES)
———	STANDARD	47	1670	99.3 (AFT)	12
—·—	REDUCED CHORD	47	1650	99.2 (AFT)	15
– – –	FINAL REDUCED SPAN	47	1670	99.3 (AFT)	4

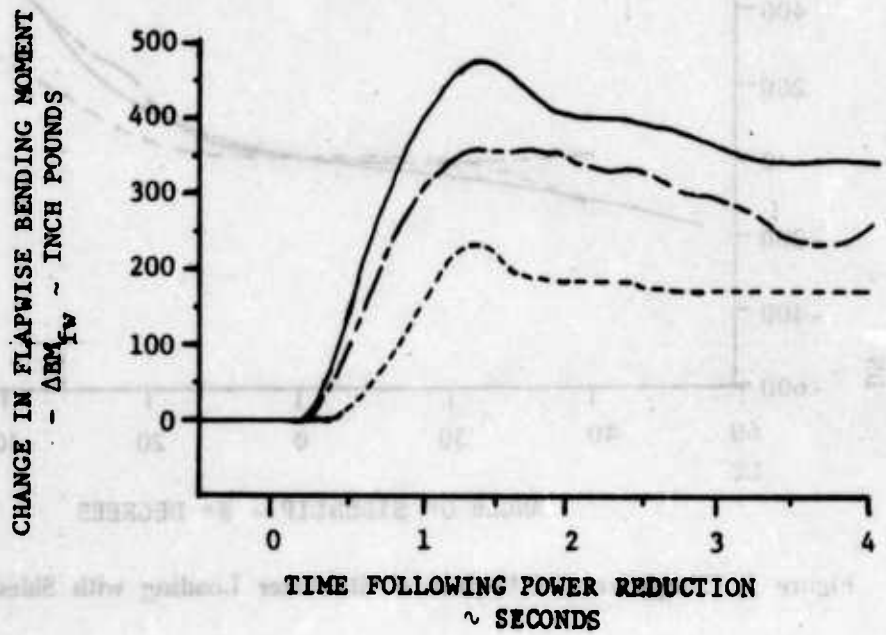

Figure K. Comparison of Horizontal Stabilizer Loads During an Autorotational Entry.

Local Flow Characteristics

120. During the flight tests, the actual wake velocity acting at the flow vane was calculated, as discussed in appendix C. The point at which the local velocity (V_{hs}) was assumed to be acting was at the flow-vane location (approximately 10 inches aft and 28 inches below the rotor disc). In terms of nondimensional distances from the rotor shaft, the flow vane was located at X/R = 1.03, Y/R = 0.053, and Z/R = 0.185.

121. In figure L, the resultant velocity and dynamic pressure ratios are shown in forward flight. The resultant velocity was determined by dividing the measured local velocity by dividing the measured local velocity by the mean value predicted from momentum theory (V'). The dynamic pressure ratio was determined by dividing the local dynamic pressure by the free stream value, as discussed in appendix C. These data were obtained with the reduced-span stabilizer installed, but were nearly the same for all configurations tested. In level flight and climb, both V_{hs}/V' and q/q_o are shown to decrease with increasing airspeed. The resultant velocity ratio indicates that momentum theory becomes more accurate for predicting the local velocity in these flight conditions with increasing advance ratio. In autorotation, the resultant velocity ratio remains near unity for all flight speeds, which indicates that momentum theory is also accurate in autorotation.

122. The trends of the dynamic pressure ratio in level flight agreed well with data from a full-scale model tested in the Ames wind tunnel in 1959 by NACA (ref 8, app A). The wind tunnel data indicated that the dynamic pressure varied considerably with vertical distance from the rotor disc. Assuming flapping and coning were insignificant, the flight test data indicated higher dynamic pressure than the wind tunnel data, when compared at the flow-vane location and the same advance ratio. However, the flight test data were obtained at a higher value of both thrust coefficient (C_T) and disc loading, which are expected to increase the induced velocity. When corrected for disc load variation, at an advance ratio of 0.14, the dynamic pressure ratios were calculated to be very close to the flight test values.

123. The dynamic pressure in autorotation is shown to be reduced from the free stream value. This is caused by the induced velocity opposing the vertical component of airspeed which results in a reduction of the total velocity acting at the stabilizer. This effect is greatest at low speeds where the induced velocity is high.

124. During steady sideslips, a repeatable downwash profile of the rotor wake was obtained along a semicircle behind the rotor disc. In figure M, the sideslip scale was correlated with the equivalent rotor azimuth position on the bottom scale. This profile was not directly comparable with the NACA data (ref 12, app A) because the referenced data were for straight cross sections of the rotor wake. However, the general trend observed was also similar. One significant difference from the wind tunnel data was that the flight measured downwash profile was slightly shifted to the left. The NACA data indicated that the vorticity at the boundary of the rotor wake induces a strong lateral velocity at rotor azimuth positions over 30 degrees. This lateral velocity was not accounted for in the data reduction, and is the primary reason for the divergence of the test results from the wind tunnel data in figure M.

SYMBOL	FLIGHT CONDITION	AVG CG STATION	AVG C_T
○	Level	95.2 (FWD)	.0039
△	Climb	95.2 (FWD)	.0039
□	Autorotation	95.2 (FWD)	.0039
— — —	NACA data corrected for disc loading	--	--

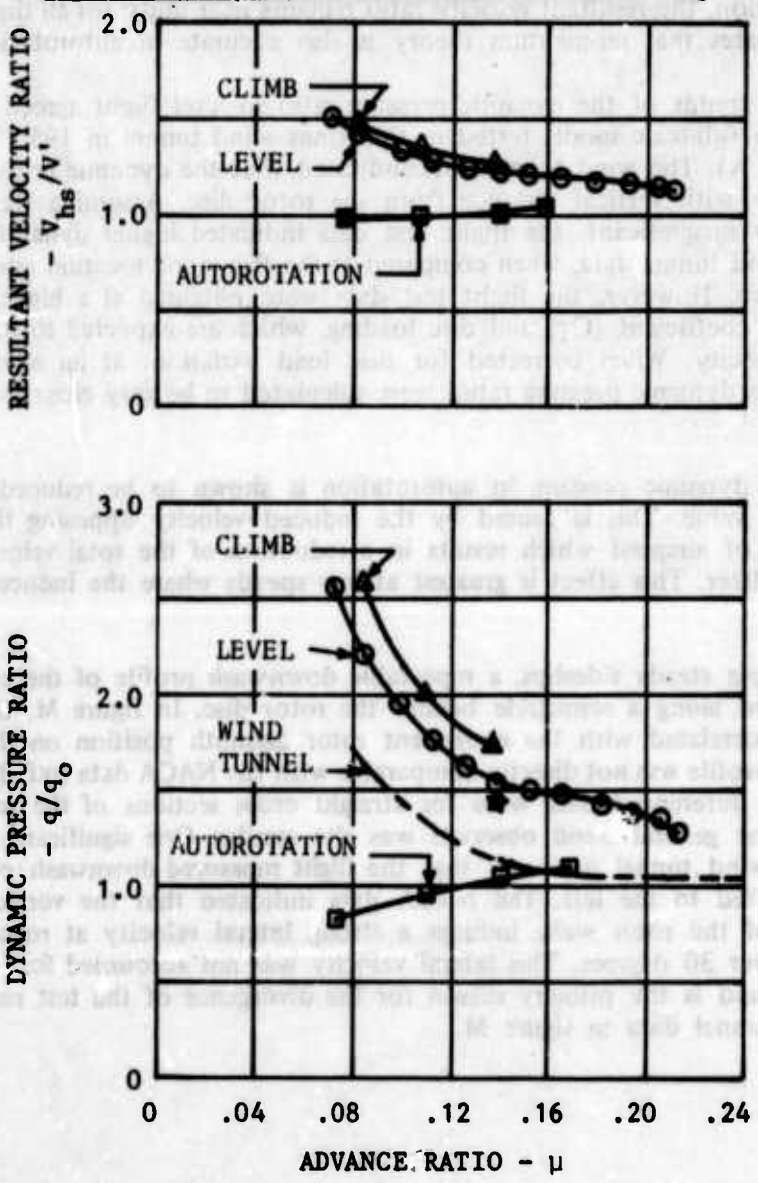

Figure L. Flow Characteristics at the Flow-Vane Location in Forward Flight.

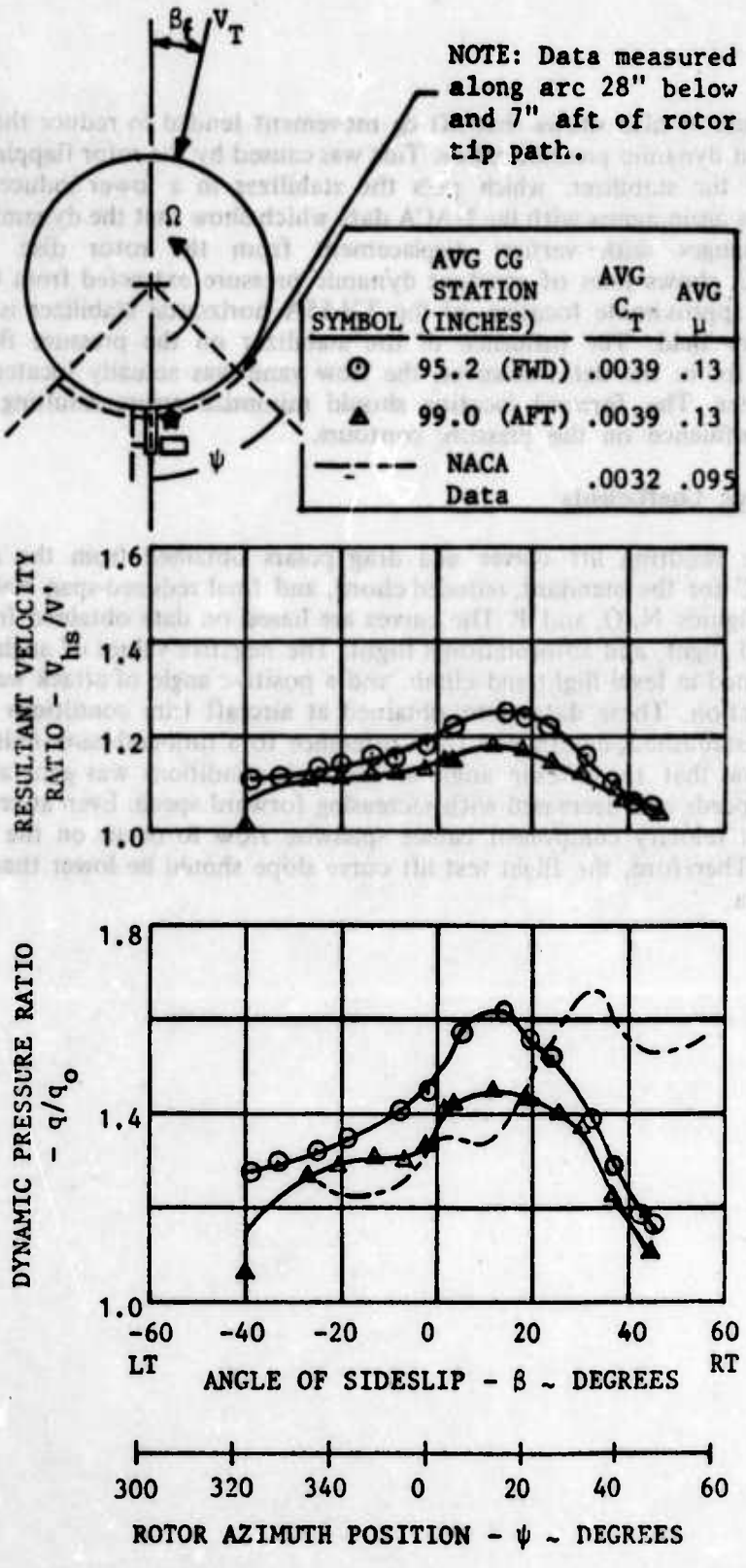

Figure M. Flow Characteristics at the Flow-Vane Location in Steady Sideslip.

125. Figure M also shows that aft cg movement tended to reduce the resultant velocity and dynamic pressure ratios. This was caused by the rotor flapping forward away from the stabilizer, which puts the stabilizer in a lower induced velocity region. This again agrees with the NACA data which show that the dynamic pressure rapidly changes with vertical displacement from the rotor disc. Figure 3, appendix C, shows lines of constant dynamic pressure extracted from the NACA data. The approximate location of the TH-55A horizontal stabilizer is shown in the pressure field. The influence of the stabilizer on the pressure field is not accounted for in the data; however, the flow vane was actually located ahead of the stabilizer. The forward location should minimize errors resulting from the stabilizer influence on the pressure contours.

Aerodynamic Coefficients

126. The resulting lift curves and drag polars obtained from the analysis in appendix C for the standard, reduced-chord, and final reduced-span stabilizers are shown in figures N, O, and P. The curves are based on data obtained from steady climb, level flight, and autorotational flight. The negative values of angle of attack were obtained in level flight and climb, and a positive angle of attack was obtained in autorotation. These data were obtained at aircraft trim conditions which the pilot had established, determined from reference to a turn-and-bank indicator. The results show that the sideslip angle at the trim conditions was generally highest at low airspeeds and decreased with increasing forward speed. Even at zero sideslip, the vertical velocity component causes spanwise flow to occur on the horizontal stabilizer. Therefore, the flight test lift curve slope should be lower than the wind tunnel data.

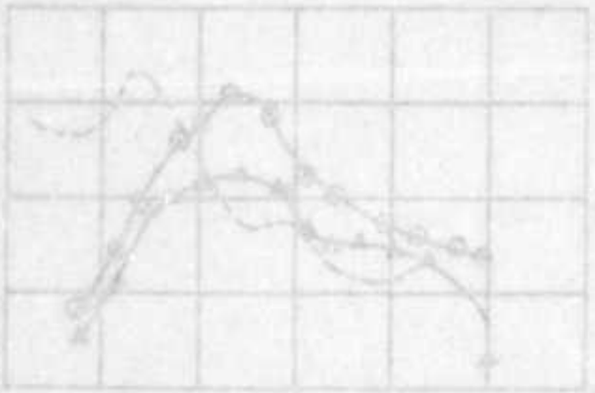

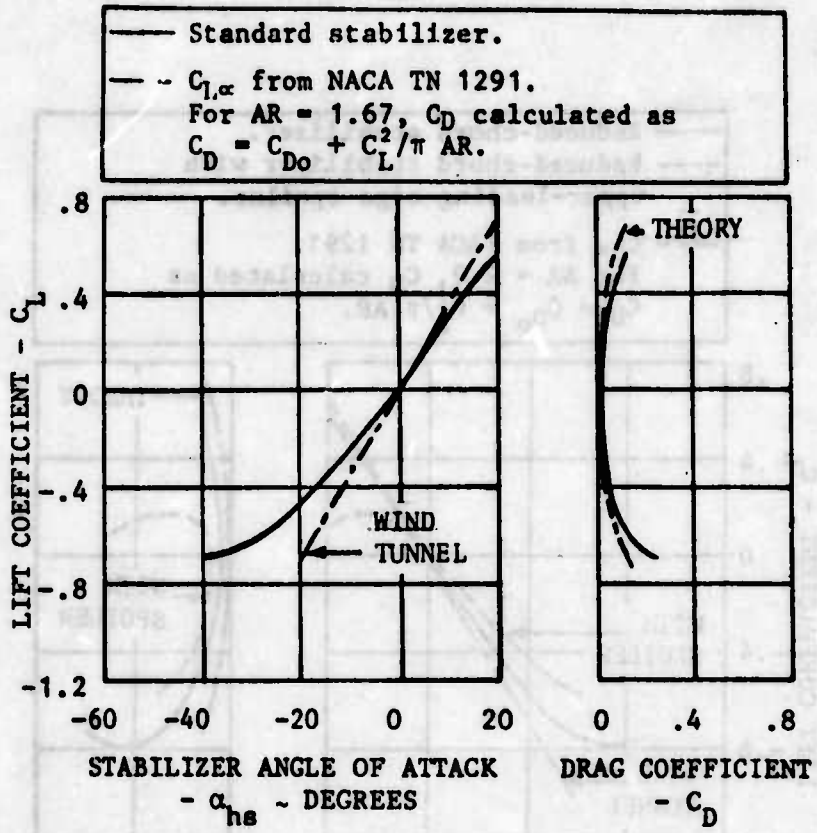

Figure N. Lift Curve and Drag Polar for the Horizontal Stabilizer in Forward Flight.

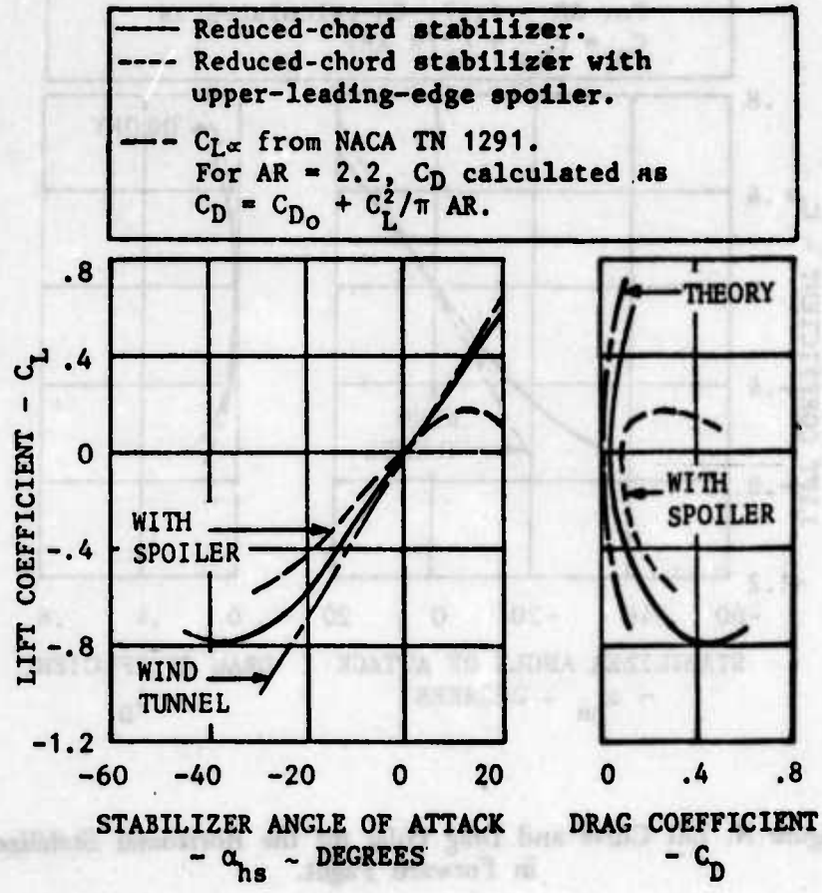

Figure O. Lift Curve and Drag Polar for the Horizontal Stabilizer in Forward Flight.

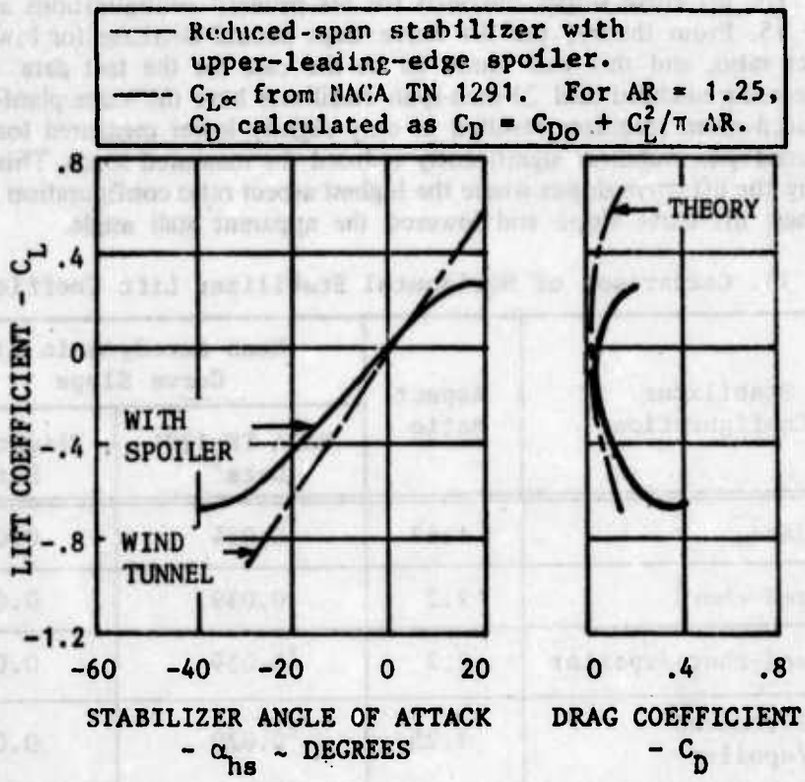

Figure P. Lift Curve and Drag Polar for the Horizontal Stabilizer in Forward Flight.

127. The average lift curve slope calculated from the flight data was normally slightly lower than NACA wind tunnel data for isolated tail surfaces (ref 13, app A). The lift curve slopes obtained for the primary configurations are shown in table 15. From theory, the lift curve slope should decrease for lower values of aspect ratio, and this was found to be the case for the test data. Although both the reduced-chord and 21-inch-span stabilizers have the same planform area, the reduced-chord stabilizer resulted in only slightly lower measured loads, while the reduced-span stabilizer significantly reduced the measured loads. This was also shown by the lift curve slopes where the highest aspect ratio configuration produced the highest lift curve slope and lowered the apparent stall angle.

Table 15. Comparison of Horizontal Stabilizer Lift Coefficients.

Stabilizer Configuration	Aspect Ratio	Mean Aerodynamic Lift Curve Slope	
		NACA TN 1291 Data[1]	Flight Test Data
Standard	1.67	0.034	0.027
Reduced chord	2.2	0.039	0.030
Reduced chord/spoiler	2.2	[2]0.039	0.025
Final reduced span/spoiler	1.25	[2]0.029	0.020

[1]Mean aerodynamic lift curve slope ($\overline{C}_{L_\alpha}$) data based on average of experimental wind tunnel values.
[2]These data do not reflect a spoiler installation.

128. The slope of the lift curve from flight test data appeared to be nonlinear beyond a 20-degree angle of attack. In this region of the curve, the data were collected in low-speed level flight or climb. The measured flow data indicated that under these conditions the largest spanwise flow occurred, and the lift curve slope would be expected to be reduced from sweptwing theory.

129. Figure P shows that the installation of a spoiler on the upper surface significantly lowered the stall angle for positive angles of attack which would reduce the uploads generated in autorotation. At negative angles of attack, it also lowered both the lift curve slope and maximum lift coefficient. This had the effect of reducing the downloads in level flight and climb, which considerably reduced the overall load change over the clean airfoil configuration.

130. The drag coefficient polars are also shown in the lift curve figures. Generally, the results were predictable. The drag coefficient for the reduced-chord configuration (with its thick trailing edge) was nearly twice the value of the standard stabilizer at all values of lift prior to stall. As shown by the dashed line in figure O, the addition of the spoiler further increased the drag coefficient. On the reduced-chord and reduced-span configurations (figs. O and P), the rapid increase in drag due to spoiler-induced stall at positive angle of attack was observed.

131. The two-dimensional drag coefficient for clean airfoils calculated by conventional theory (ref 14, app A) is shown in the drag polar figures. At low values of lift, the drag coefficient was not accurately calculated by the flight test analysis. The profile drag coefficient appeared to be two or three times larger than theory. This was primarily due to the low value of drag loading under these conditions, which was within the accuracy of the measured chordwise bending moment. However, the trends appeared to be valid, and the values calculated from the flight data became more accurate at higher values of lift. It seems reasonable that the drag coefficient would be higher (particularly for the spoiler and blunt-trailing-edge configurations) than the theoretical values determined from steady flow and clean airfoil conditions.

WEIGHT AND BALANCE

132. The weight and balance were determined before and after the instrumentation package was installed. The instrumentation added 276 pounds to the empty weight of the aircraft, and when combined with the other required mission equipment, made testing at other than maximum gross weight impractical. A configuration for both a forward and aft cg location at maximum gross weight was determined. The aft cg limit (FS 100) was attained by locating 35 pounds of lead ballast on the tail-boom saddle point. Weight and balance data for each test condition were calculated from the amount of fuel on board and the basic weight data.

AIRSPEED CALIBRATION

133. The standard TH-55A pitot-static system with a sensitive airspeed indicator was used to obtain the airspeed data. This system was calibrated by a pace aircraft and ground speed course methods. The pace aircraft (OH-58A) was used to obtain data in level, climb, and descending flight conditions; and the ground speed course was used to check the level flight data. The tests were conducted with doors on at maximum gross weight and a forward cg location. The rotor speed was 483 rpm, and the density altitude was 4400 feet for the pace tests and 2400 feet for the ground speed course tests. All tests were conducted out of ground effect.

134. The resulting airspeed calibration is shown in figure 56, appendix D. The position error in level flight in AFFTC-TR-60-2 (ref 15, app A) was found to be similar. Below 60 KCAS, the position error in climb and autorotation varied from the level flight results.

CONCLUSIONS

STABILIZER DEVELOPMENT (PHASE I)

135. The 21-inch-span stabilizer with a full-span upper-leading-edge spoiler was determined to be the optimum interim stabilizer configuration for the Army training mission (para 31).

136. The initial sideslip was determined to significantly affect the nose-down pitching moment generated during an autorotational entry (paras 51 and 67).

137. The use of the pedal position indicator to maintain low sideslip angles in normal flight minimized the nose-down pitching moment generated during autorotational entry (para 54).

138. The final reduced-span stabilizer degraded the dynamic lateral-directional stability characteristics (para 60).

139. Removal of the canopy slat degraded the static and dynamic stability characteristics. However, the aircraft was controllable and can be safely flown (paras 48, 51, 52, 58, 60, and 61).

STABILIZER QUALIFICATION (PHASE II)

140. The TH-55A was determined to have adequate handling qualities characteristics when equipped with the 21-inch-span horizontal stabilizer developed in the Phase I testing (paras 74 through 95).

141. The undamped dynamic directional stability characteristic at airspeeds below 56 KCAS in the aft cg configuration was a shortcoming, with no correction required. However, the pilot workload may be reduced by limiting the aft cg location to FS 98.1 for normal operation (para 92).

142. The final reduced-span stabilizer was structurally acceptable for the full flight envelope contained in the 1967 Hughes TH-55A owner's manual (para 98).

RECOMMENDATIONS

STABILIZER DEVELOPMENT (PHASE I)

143. The standard stabilizer should be reduced by 7 inches and a full-span spoiler added to the upper leading edge. The spoiler location should be the same as for the test and demonstration flights (para 31).

144. The longitudinal cyclic control should be rigged to allow for the maximum-allowable aft displacement (para 34).

145. The pedal position indicator should be installed to prevent flying with any appreciable sideslip (para 54).

STABILIZER QUALIFICATION (PHASE II)

146. The standard TH-55A operational flight envelope may be used for the aircraft equipped with the final reduced-span stabilizer, except that the maximum aft cg location should be limited to 98.1 inches to reduce pilot workload in normal operation.

147. If the new stabilizer exhibits a significantly reduced fatigue life during operational experience, the natural frequency of the stabilizer should be reduced by tip weighting (para 104).

APPENDIX A. REFERENCES

1. Final Report, USAASTA, Project No. 67-22, *Engineering Flight Test of the TH-55A Primary Helicopter Trainer Limited Performance Evaluation*, November 1969.

2. Letter, AVSCOM, AMSAV-E(ER), 27 July 1970, subject: Test Request No. 70-24, TH-55A Autorotational Entry Characteristics.

3. Letter, USAASTA, SAVTE-M, 6 April 1971, subject: Proposal for Additional Modification and Testing of the TH-55A Horizontal Stabilizer.

4. Letter, AVSCOM, AMSAV-EFT, 5 August 1971, subject: TH-55A Horizontal Stabilizer Substantiation/Qualification.

5. Type Certificate Data Sheet, Federal Aviation Administration, No. 4H12, 19 June 1972, subject: Hughes 269 Helicopter.

6. Test Plan, USAASTA, Project No. 70-24, *Autorotational Entry and Flying Quality Characteristics of a TH-55A Helicopter Modified with a Reduced Chord Horizontal Stabilizer*, November 1970.

7. Military Specification, MIL-H-8501A, *Helicopter Flying and Ground Handling Qualities; General Requirements For*, 7 September 1961, Amended 3 April 1962.

8. Owner's Manual, Hughes Tool Company, *US Army TH-55A Primary Trainer*, 8 November 1967.

9. Report, Cornell Aeronautical Laboratory, Inc., Report No. 177, *A Collection of Flight Test Data Reduction Techniques*, 1971.

10. Technical Note, USAASTA, TN No. 42, *The Time Constant Method of Calculating Angular Rate Damping for a Helicopter*, February 1972.

11. Technical Note, USAASTA, TN No. 23, *Methods for Estimating Aircraft Mass Moments of Inertia*, January 1972.

12. Report, NACA, Report No. 1319, *Induced Velocities Near a Lifting Rotor with Non Uniform Disk Loading*, 1957.

13. Technical Note, NACA, TN No. 1291, *Collection and Analysis of Wind Tunnel Data on the Characteristics of Isolated Tail Surface With and Without End Plates*, May 1947.

14. Handbook, Etkin, B., *Dynamics of Flight*, John Wiley and Sons, 1962.

15. Final Report, Air Force Flight Test Center, AFFTC-TR-60-2, *YHO-2HU Air Force Flight Evaluation*, February 1960.

16. Technical Note, USAASTA, TN No. 28, *Calculation of Aircraft Airspeed Components Using Boom Mounted Instrumentation*, March 1972.

APPENDIX B. TEST INSTRUMENTATION

GENERAL

1. The test instrumentation was installed and maintained by the Instrumentation and Calibration Division of USAASTA. The strain gaging on the various stabilizers was provided under contract by the Hughes Tool Company. Due to space limitations, the left seat was removed and the oscillograph and basic instrumentation package were mounted in its position. A movie camera was also mounted above the oscillograph at the pilot's eye level so that it could either take pictures of the instrument panel and horizon, or be reversed to photograph the tail boom and horizon stabilizer.

TEST PARAMETERS

2. The instrumentation was calibrated by standard USAASTA and Air Force calibration laboratory procedures prior to commencing the test program. The primary data sources consisted of sensitive instrumentation on the pilot panel (fig. 1) and the oscillograph parameters. The instrumented stabilizer and flow vane are shown in figure 2. Since only one seat was in the test aircraft, the pilot read the test condition data over the radio, and they were recorded by the engineer in a chase aircraft. The instrumentation was recalibrated prior to the Phase II testing.

3. The following instrumentation was provided:

Pilot Panel

Sensitive airspeed (ship's system)
Sensitive altimeter (ship's system)
Sensitive rotor tachometer
Sensitive manifold pressure gage
Sideslip indicator (boom mounted)
Longitudinal cyclic position
Lateral cyclic position
Collective stick position
Pedal position
Vertical accelerometer

Oscillograph

Longitudinal control position
Lateral control position
Collective control position
Directional control position
Engine manifold pressure

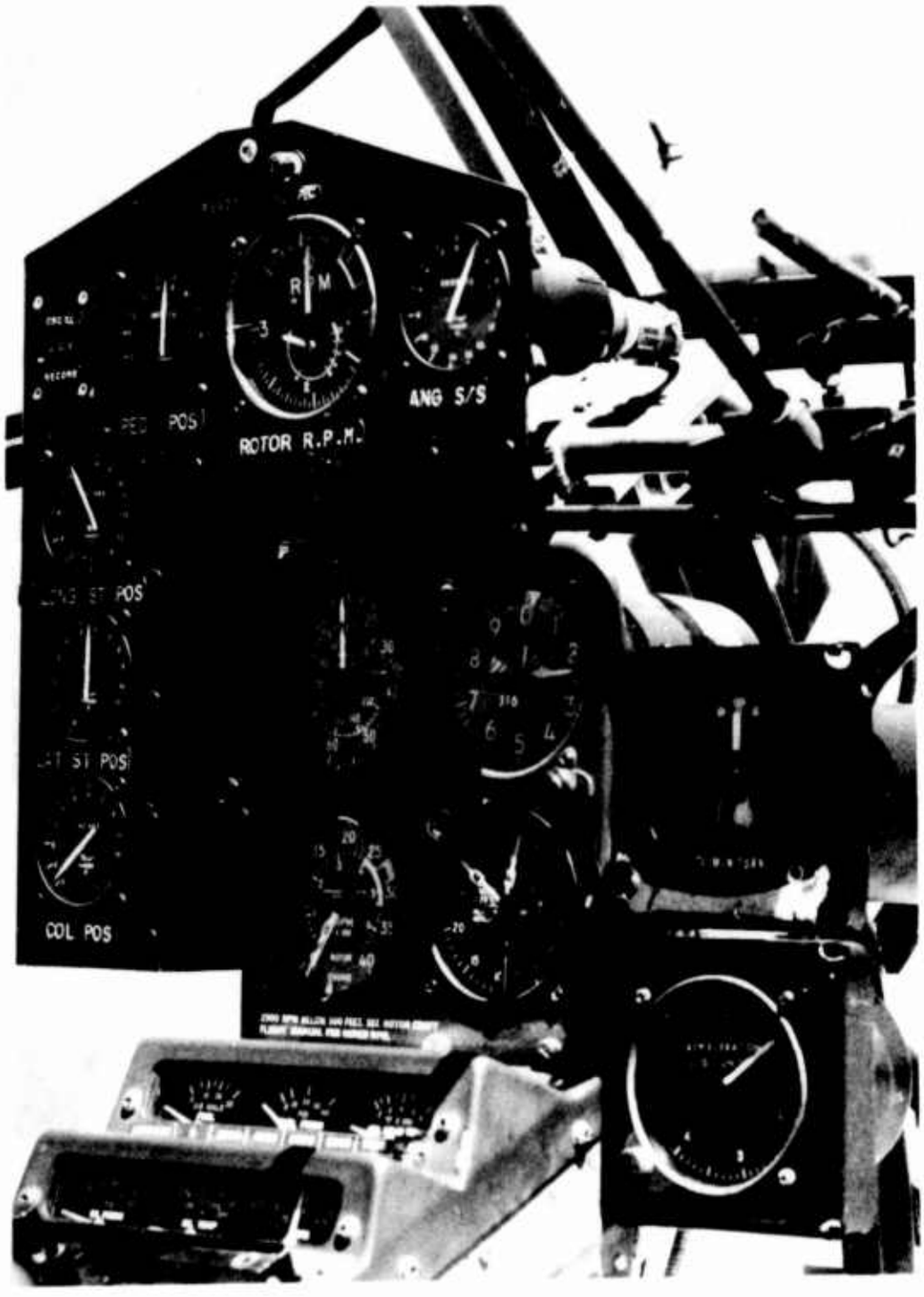

Figure 1. Photograph of Instrumentation on the Pilot Panel.

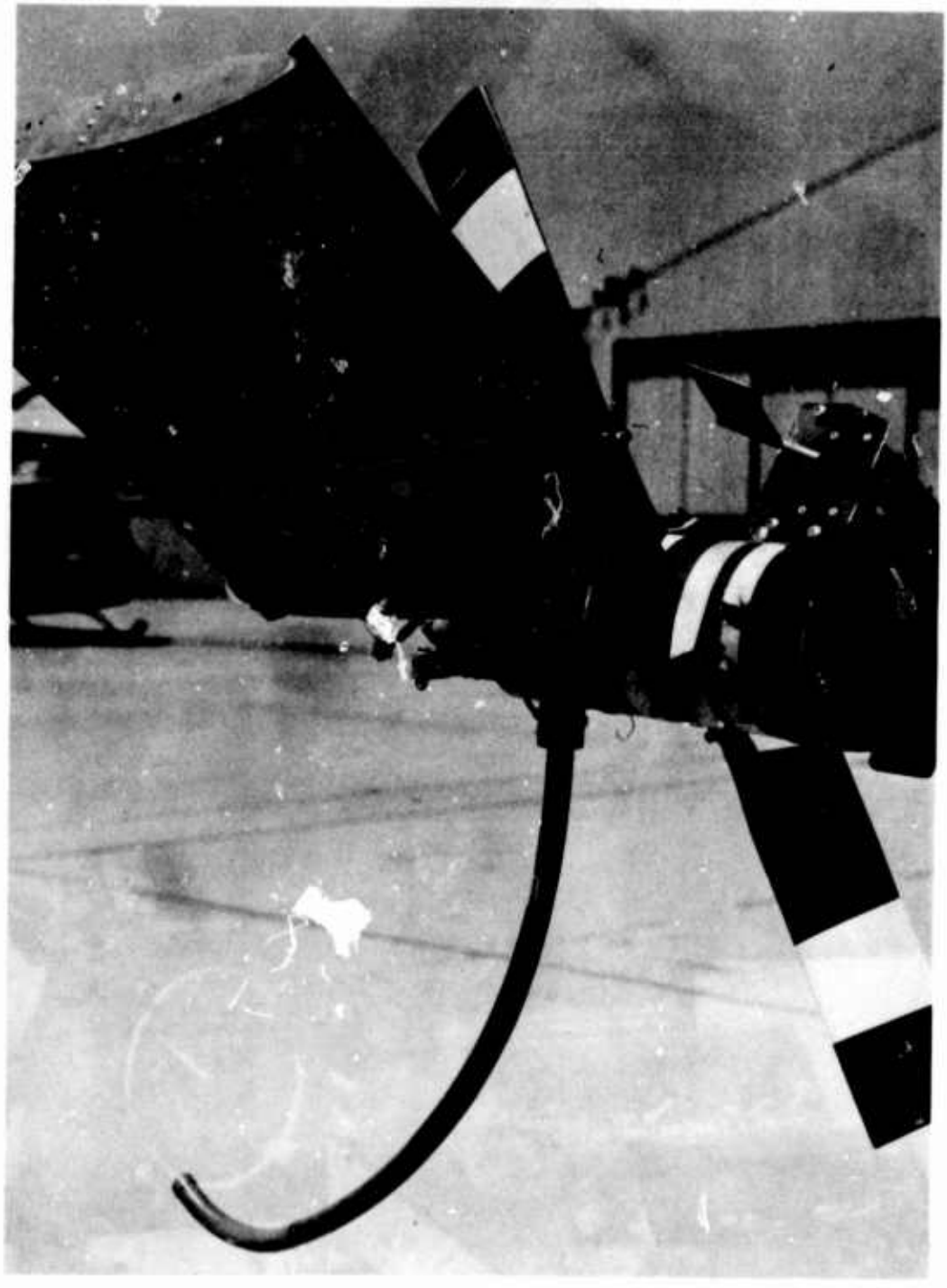

Figure 2. Photograph of Instrumented Stabilizer and Flow Vane.

Rotor speed
Sideslip
Horizontal stabilizer angle of attack
Flapwise bending moment on horizontal stabilizer
Flapwise bending moment on vertical stabilizer
Chordwise bending moment on horizontal stabilizer
Normal acceleration (cg)
Longitudinal acceleration (cg)
Lateral acceleration (cg)
Pitch attitude
Roll attitude
Yaw attitude
Pitch rate
Roll rate
Yaw rate

4. The reference body stations for the TH-55A are shown in figure 3 and the locations of the instrumentation sensors are as follows:

Instrumentation

Sideslip vane: FS -4.0, WL 1.0, BL -26.0
Vertical accelerometer (cockpit):. FS 52.0, WL 28.0, BL 14.0
Vertical, lateral, and longitudinal accelerometers:
FS 88.0, WL 24.0, BL -4.0
Attitude gyros: FS 64.0, WL 20.0, BL -15.0
Rate gyros: FS 64.0, WL 26.0, BL-15.0
Horizontal stabilizer angle-of-attack vane:
FS 256.0, WL 50.0, BL 8.0
Horizontal stabilizer strain gages: FS 272.0, WL 50.0, BL 8.0

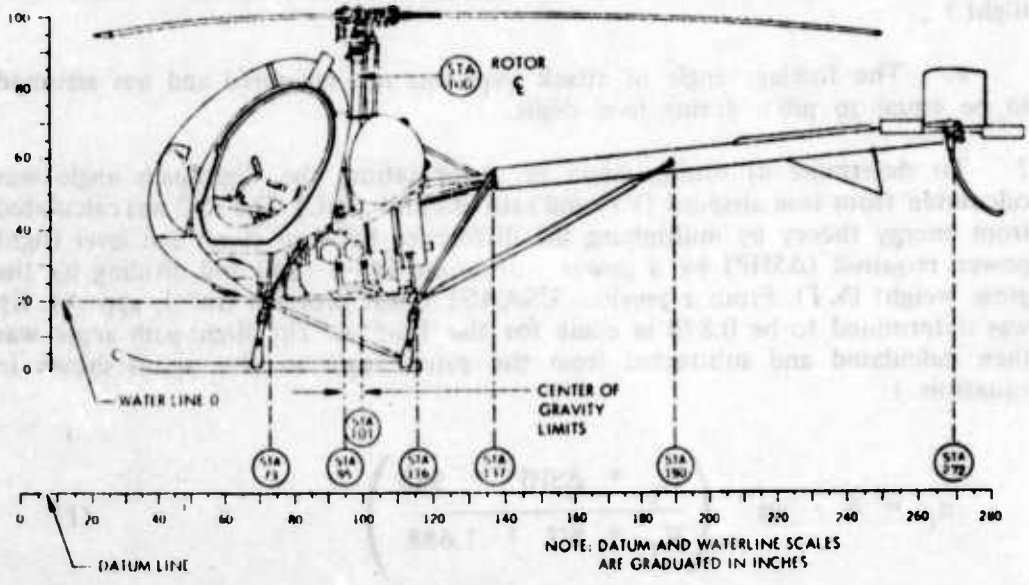

Figure 3. Reference Body Stations for the TH-55A.

APPENDIX C. TEST TECHNIQUES AND DATA ANALYSIS METHODS

WAKE VELOCITY EQUATIONS

1. The TH-55A stabilizer is located in the flow below the aft quarter of the rotor disc, which is very complex and difficult to predict by analytical methods (ref 12, app A). In addition to the basic rotor, the flow acting at the stabilizer could be influenced by the tail rotor inflow and fuselage interference. The stabilizer is mounted at a positive dihedral angle (γ_{hs}) of 35 degrees, which further complicates the spanwise flow conditions. The equations required for calculating the induced velocity and dynamic pressure acting at the horizontal stabilizer from the measured parameters of true airspeed, fuselage pitch, and sideslip are derived below. Since the TH-55A can easily be flown with a significant amount of sideslip, three-dimensional equations were required to define the airflow about the stabilizer. The following simplifying assumptions were required to establish the flow model:

a. Only steady-state forward flight conditions were used in order to omit aircraft rotational velocity terms.

b. Fuselage interference effects on the free airstream were assumed to be negligible at the flow-vane location.

c. The summation of tail rotor induced inflow and main rotor circulation were assumed negligible.

d. The induced velocity (V_I) was parallel to the shaft axis, which assumed that main rotor flapping was negligible. (Calculations indicated that the flapping angle varied 2 degrees at a forward cg to 5 degrees at an aft cg in 50-knot level flight.)

e. The fuselage angle of attack (α_f) was not measured and was assumed to be equal to pitch during level flight.

2. To determine α_f during climb or autorotation, the flight-path angle was calculated from true airspeed (V_T) and rate of climb (R/C). The R/C was calculated from energy theory by multiplying the difference between climb and level flight power required (ΔSHP) by a power correction factor (Kp) and dividing by the gross weight (WT). From a previous USAASTA test program (ref 1, app A), Kp was determined to be 0.878 in climb for the TH-55A. The flight-path angle was then calculated and subtracted from the pitch angle to give α_f, as shown in equation 1:

$$\alpha_f = \theta - \sin^{-1}\left(\frac{K_p * \Delta SHP * 550}{V_T * WT * 1.688}\right) \qquad (1)$$

3. Figure 1 shows a sketch of the basic flow conditions assumed in low-speed level flight which was based on previous NACA flow studies (ref 12, app A). The portion of the flow field which affects the stabilizer is shown by the black arrows. From momentum theory, the airstream encounters the rotor at velocity V_T and is deflected downward by the induced velocity resulting in a final velocity, V'. This analysis is based on uniform disc loading and represents only an average value across the rotor wake. The actual induced velocity and deflection angle are known to vary at any point in the rotor wake. Therefore, a flow vane was used to determine the free stream deflection at the horizontal stabilizer location, and the resultant velocity (V_{hs}) required to cause that deflection was calculated as discussed below.

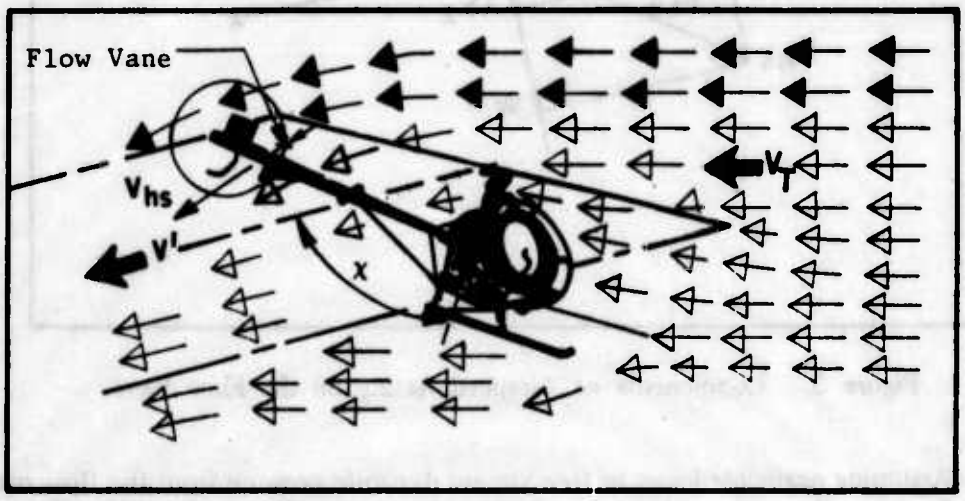

Figure 1. Flow Field Assumed in Level Flight.

4. The airspeed components of the free stream velocity acting along the body axis coordinate system are shown at the flow-vane location in figure 2. Since the TH-55A shaft axis system is essentially aligned with the vertical body axis, the induced velocity is shown parallel to the vertical body axis. Therefore, the local induced velocity (W) may be vectorally summed with the free stream airspeed to obtain the total velocity acting at the horizontal stabilizer (V_{hs}). This also relates the stabilizer angle of attack (α_{hs}) to the induced velocity, as shown in figure 2, and a mathematical relationship was derived.

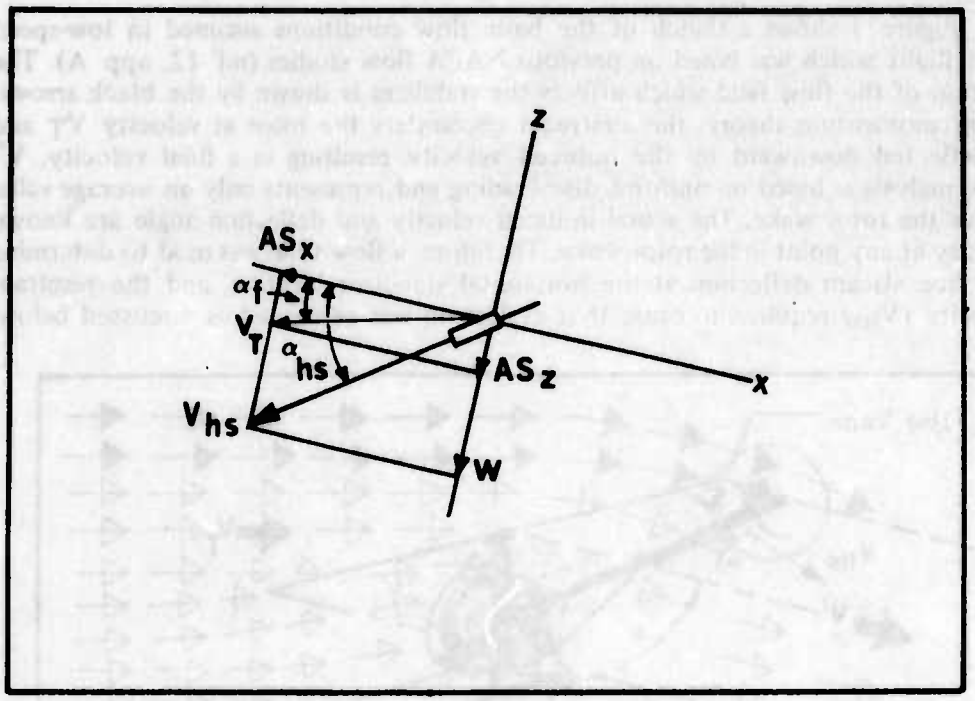

Figure 2. Components of Airspeed Acting on the Flow Vane.

5. Assuming negligible losses in free stream dynamic pressure from the flow over the fuselage, the components of velocity at the stabilizer were defined for steady-state flight by equations 2, 3, 4, and 5 below. Although the aircraft rotational velocity terms are eliminated in this condition, they can be included, if dynamic flight conditions were considered (ref 16, app A). The angle (α'_f) in these equations is the angle between the airspeed vector and the waterline plane of the fuselage and is required since α_f and β_f are defined in the xz and xy planes of the fuselage axis system.

$$\alpha'_f = \tan^{-1}\left(\tan \alpha_f \cos \beta_f\right) \tag{2}$$

$$AS_x = AS_t * \cos \alpha'_f \cos \beta_f \tag{3}$$

$$AS_y = AS_t * \cos \alpha'_f \sin \beta_f \tag{4}$$

$$AS_{z_t} = AS_t * \sin \alpha'_f - W \tag{5}$$

Where: α_f = aircraft angle of attack

β_f = aircraft angle of sideslip

AS_{z_t} = total vertical component of flow

6. In the above equations, the induced wake velocity (W) is unknown. Therefore, W was calculated from the measured value of α_{hs}. Since α_{hs} was measured in the stabilizer axis system, the body axis airspeed components were rotated through α_{hs} into the stabilizer axis system. For simplicity, the stabilizer angle of incidence (α_i) was subtracted from α_{hs} rather than rotating the airspeed components through α_i into the stabilizer axes.

$$AS_{hs_x} = AS_x \tag{6}$$

$$AS_{hs_y} = AS_y * \cos \gamma_{hs} - AS_z * \sin \gamma_{hs} \tag{7}$$

$$AS_{hs_z} = AS_{z_t} * \cos \gamma_{hs} + AS_y * \sin \gamma_{hs} \tag{8}$$

The stabilizer angle of attack (α_{hs}) and angle of sideslip (β_{hs}) were then related to the horizontal stabilizer axes airspeed components by equations 9 and 10. Since α_i is small (4.5 degrees), its effect on AS_{hsx} in equation 10 was assumed to be negligible.

$$\alpha_{hs} - \alpha_i = \tan^{-1}\left(\frac{AS_{hs_z}}{AS_{hs_x}}\right) \tag{9}$$

$$\beta_{hs} = \tan^{-1}\left(\frac{AS_{hs_y}}{AS_{hs_x}}\right) \tag{10}$$

8. By substitution of equations 3, 4, 5, 6, and 8 in equation 9, a solution for W was obtained:

$$W = AS_y * \tan \gamma_{hs} + AS_z - \left(\frac{AS_x * \tan (\alpha_{hs} - \alpha_i)}{\cos \gamma_{hs}}\right) \tag{11}$$

9. Since W was the only unknown term in equation 5, the total velocity acting at the flow vane can be calculated as shown below:

$$V_{hs} = \left(AS_x^2 + AS_y^2 + AS_z^2\right)^{1/2} \tag{12}$$

10. The dynamic pressure acting at the flow vane was then determined by the usual relation (*ie*, $q_{hs} = 1/2\ \rho V_{hs}^2$). The local dynamic pressure ratio was obtained by dividing by the free stream dynamic pressure (q_o), as shown by equation 13:

$$\text{Dynamic pressure ratio} = \frac{q}{q_o} = \frac{V_{hs}^2}{AS_t^2} \tag{13}$$

11. The resultant velocity ratio was determined by dividing the local resultant velocity, V_{hs}, by V', as shown in equation 14:

$$\text{Resultant velocity ratio} = V_{hs}/V' \tag{14}$$

Aerodynamic Loading Equations

12. The aerodynamic loading of the horizontal stabilizer was calculated from data generated by strain gages mounted to measure both flapwise and chordwise bending moments. To generalize the aerodynamic loading data, the bending moments measured in flight were reduced to aerodynamic coefficients of lift and drag. The equations required to calculate these parameters are derived below. Initial reduction of the data indicated that a large error in the analysis was encountered at forward airspeeds below 40 knots. In this speed region, very high angles of attack were generated, and tufting placed on the stabilizer showed that stall was occurring below 25 knots. The values of C_L were very high and resulted in a sharp upturn of the lift curve prior to stall. The reason for this departure was determined from wind tunnel data (ref 8, app A) and is discussed below. The primary assumptions required to obtain lift and drag from the measured bending moments were as follows:

a. The spanwise center-of-pressure (CP) location could be estimated from the dynamic pressure distributions determined from previous NACA wind tunnel tests (ref 12, app A), such as figure 3. The assumption was made that the distributions, but not necessarily the magnitudes, were correct. The chordwise CP location was assumed to be at 25-percent span.

b. The dynamic pressure calculated from a_{hs} represented the mean dynamic pressure when corrected for the spanwise pressure variation shown in the wind tunnel data ($\bar{q}_{hs} = q_{hs} + q_c$).

c. The flow-vane angle represented the mean angle of attack of the horizontal stabilizer.

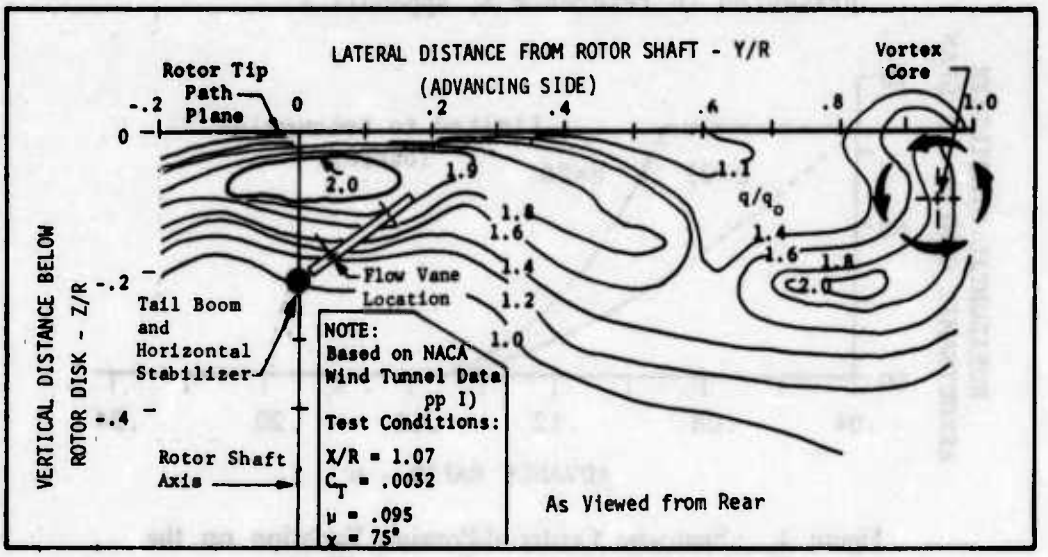

Figure 3. Contours of the Dynamic Pressure Ratio in the Vicinity of the Horizontal Stabilizer in Forward Flight.

13. Using the measured stabilizer bending moments and flow-vane data, the lift (L_{hs}) and drag (D_{hs}) acting on the stabilizer were calculated by first determining the spanwise aerodynamic center. The wind tunnel data show that at the stabilizer location during low-speed forward flight ($\mu < 0.14$), the dynamic pressure is greatest just below the main rotor disc and decreases with distance below the disc. Under these conditions, higher loading would be generated on the outboard sections, effectively moving the aerodynamic center outboard. The spanwise variation of dynamic pressure was determined from these data, and the approximate CP location was assumed to be at the centroid of the resulting distribution. This procedure was used for three advance ratios provided in the NACA data, and the results are shown in figure 4. The pressure distribution was found to be insignificant at advance ratios above 0.14 (approximately 50 knots in the TH-55A). Above this speed, where the stabilizer was located in a nearly uniform dynamic pressure region, the CP was assumed to be at 50-percent span.

NOTE: Data based on pressure contours presented in reference 8, appendix A.

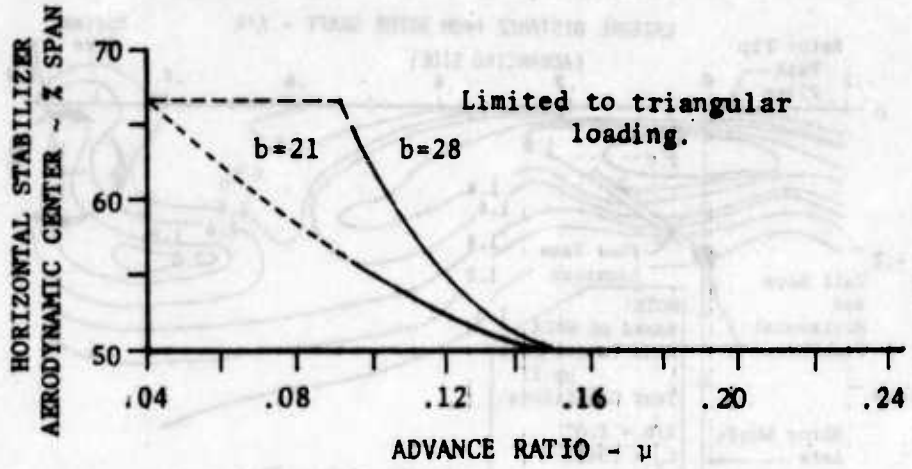

Figure 4. Spanwise Center-of-Pressure Variation on the Horizontal Stabilizer in Forward Flight.

14. The dynamic pressure distribution also implied that the flow vane was not sensing the mean dynamic pressure (q) at advance ratios below 0.14. Since the dynamic pressure variation was known, the dynamic pressure calculated at the flow vane was corrected to the mean dynamic pressure acting at the CP location. This correction factor was also determined as a function of advance ratio from the wind tunnel data (ref 8, app A), and the results are shown in figure 5.

NOTE: Data based on pressure contours presented in reference 8, appendix A.

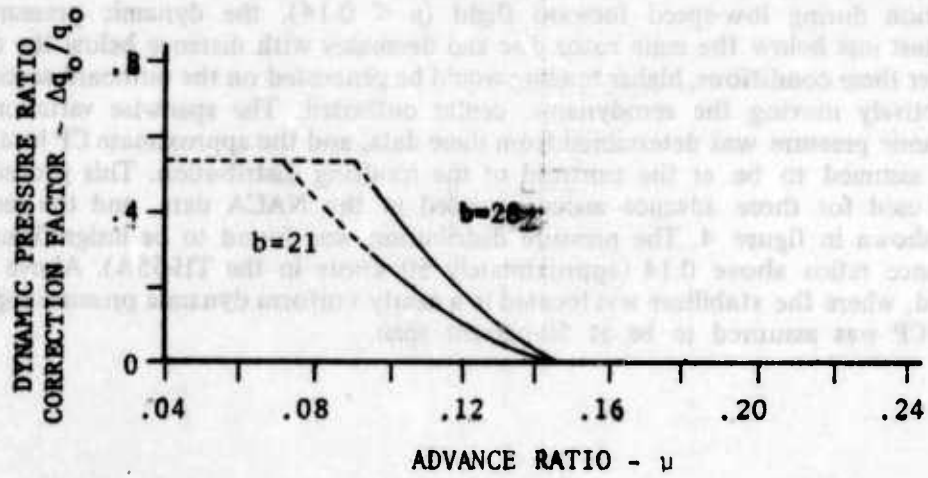

Figure 5. Dynamic Pressure Ratio Correction for the Horizontal Stabilizer in Forward Flight.

15. The equations for calculating lift and drag on the stabilizer were then derived from figure 6. The equations were simplified by solving the force balance in the stabilizer axis system to eliminate spanwise force from the flapwise moment equation. The vertical and longitudinal forces acting on the stabilizer were calculated at the previously determined CP location (L_{cp}) using equations 15 and 16:

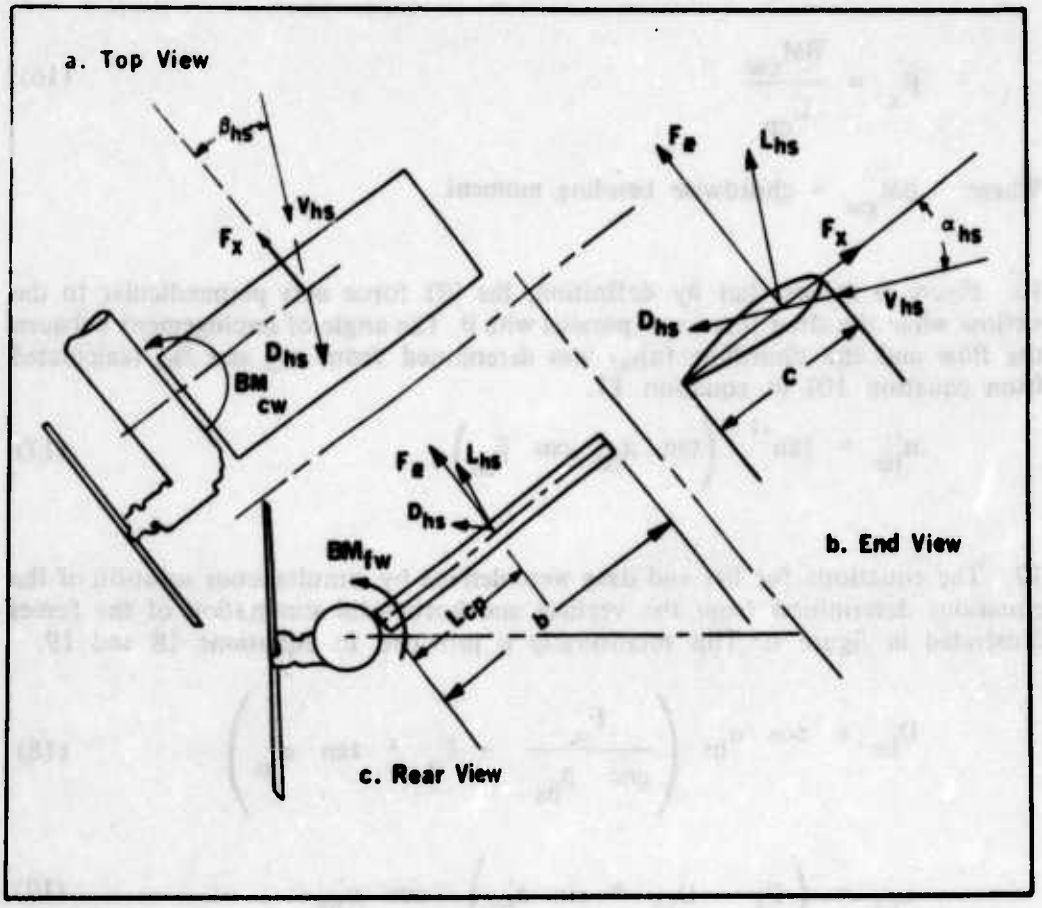

Figure 6. Airloads Acting on the Horizontal Stabilizer in Forward Flight.

$$F_z = \frac{BM_{fw}}{L_{cp}} \tag{15}$$

Where: BM_{fw} = flapwise bending moment

$$F_x = \frac{BM_{cw}}{L_{cp}} \tag{16}$$

Where: BM_{cw} = chordwise bending moment

16. Figure 6 shows that by definition, the lift force acts perpendicular to the airflow while the drag force acts parallel with it. The angle of impingement between the flow and the chordline (α'_{hs}) was determined from α_{hs} and β_{hs} (calculated from equation 10) in equation 17.

$$\alpha'_{hs} = \tan^{-1}\left(\tan \alpha_{hs} \cos \beta_{hs}\right) \tag{17}$$

17. The equations for lift and drag were derived by simultaneous solution of the equations determined from the vertical and horizontal summation of the forces illustrated in figure 6. This relationship is provided in equations 18 and 19.

$$D_{hs} = \cos \alpha'_{hs} \left(\frac{F_x}{\cos \beta_{hs}} + F_z * \tan \alpha'_{hs}\right) \tag{18}$$

$$L_{hs} = \left(F_z - D_{hs} * \sin \alpha'_{hs}\right) / \cos \alpha'_{hs} \tag{19}$$

18. The coefficients of lift and drag were then calculated from equations 18 and 19 as follows:

$$C_L = \frac{L_{hs}}{S\,\bar{q}} \tag{20}$$

$$C_D = \frac{D_{hs}}{S\,\bar{q}} \tag{21}$$

APPENDIX D. TEST DATA

INDEX

FIGURE 1

LONGITUDINAL CONTROL SENSITIVITY AND RESPONSE

XH-59A USA S/N 67-18826

SYMBOL	FLIGHT CONDITION	AVG CG STATION (IN.)	AVG GROSS WEIGHT (LB)	DENSITY ALTITUDE (FT)	ROTOR SPEED (RPM)	CALIB. V/S (KTS)	OAT (°C)
○	Level	96.0 (PRD)	16?0	4000	483	42	7
□	Level	99.35(APT)	1670	5200	485	42	0

NOTE: Standard Stabilizer.

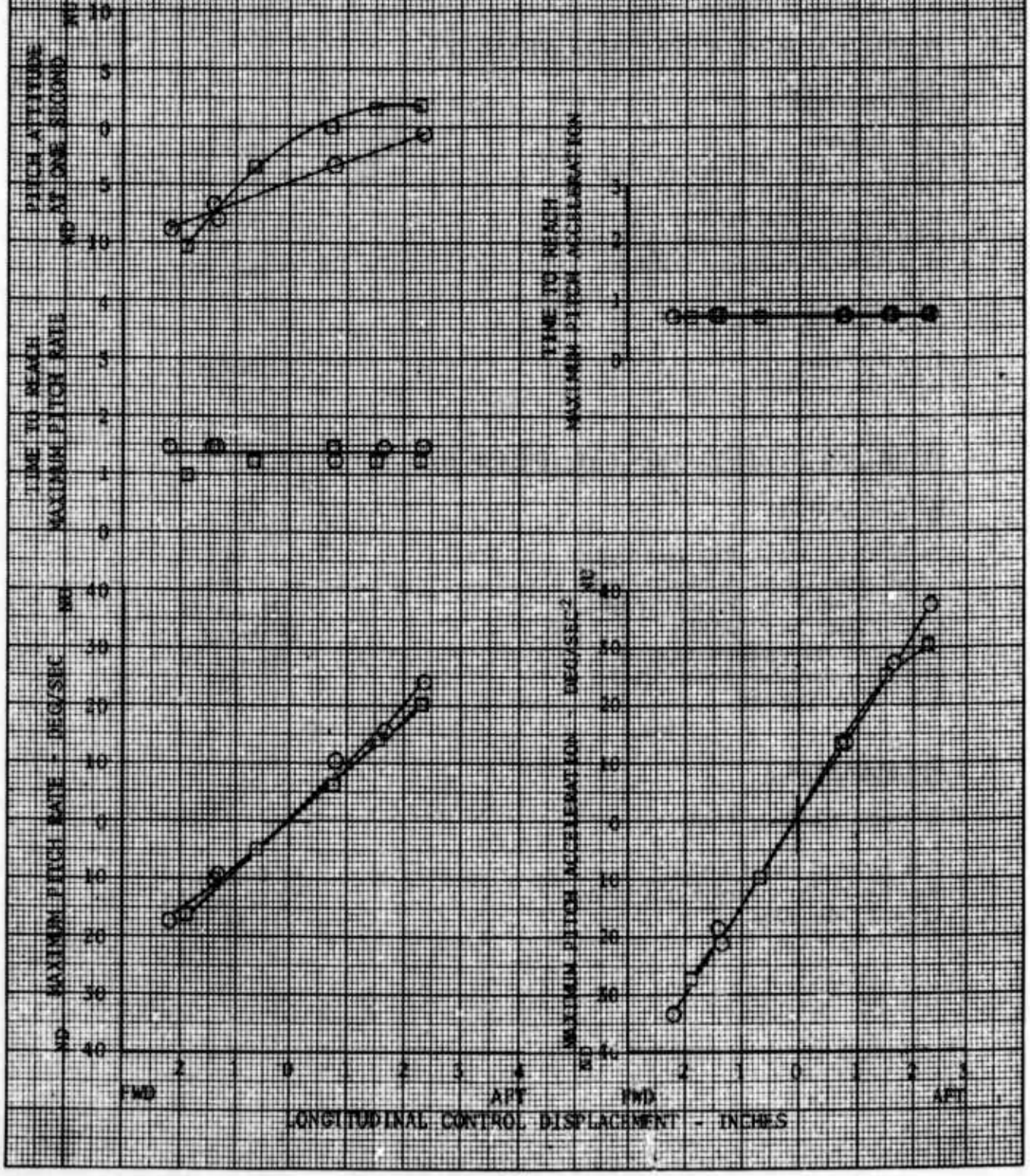

FIGURE 2

LATERAL CONTROL SENSITIVITY AND RESPONSE

TH-55A (USA- 67-16926)

SYMBOL	REMARKS CONDITION	AVG CG STATION (IN.)	AVG GROSS WEIGHT (LB)	DENSITY ALTITUDE (FT)	ROTOR SPEED (RPM)	CAL A AVS (KTS)	OAT (°C)
○	Level	96.0 (RWD)	1670	4000	483	47	7
□	Level	99.35(AFT)	1670	3200	483	47	8

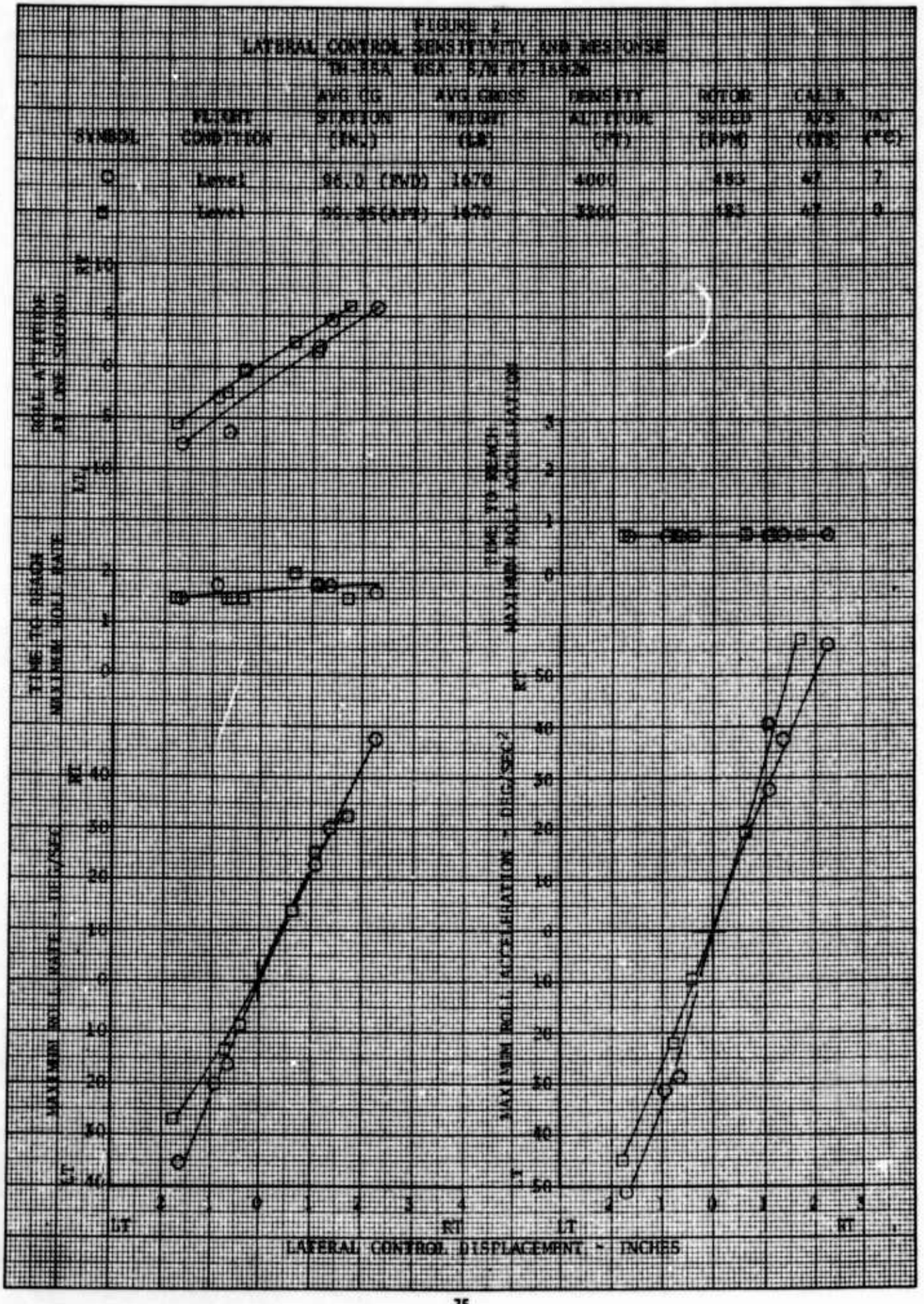

FIGURE 5

DIRECTIONAL CONTROL SENSITIVITY AND RESPONSE

TH-57A BK S/N 67-16928

SYMBOL	FLIGHT CONDITION	AVG CG STATION (IN.)	AVG GROSS WEIGHT (LB.)	DENSITY ALTITUDE (FT.)	ROTOR SPEED (RPM)	CALIB A/S (KIAS)	OAT (°C)
○	Level	96.0 (FWD)	1670	4000	483	62	7
□	Level	99.3 (AFT)	1670	3200	483	62	6

NOTE: Standard Stabilizer

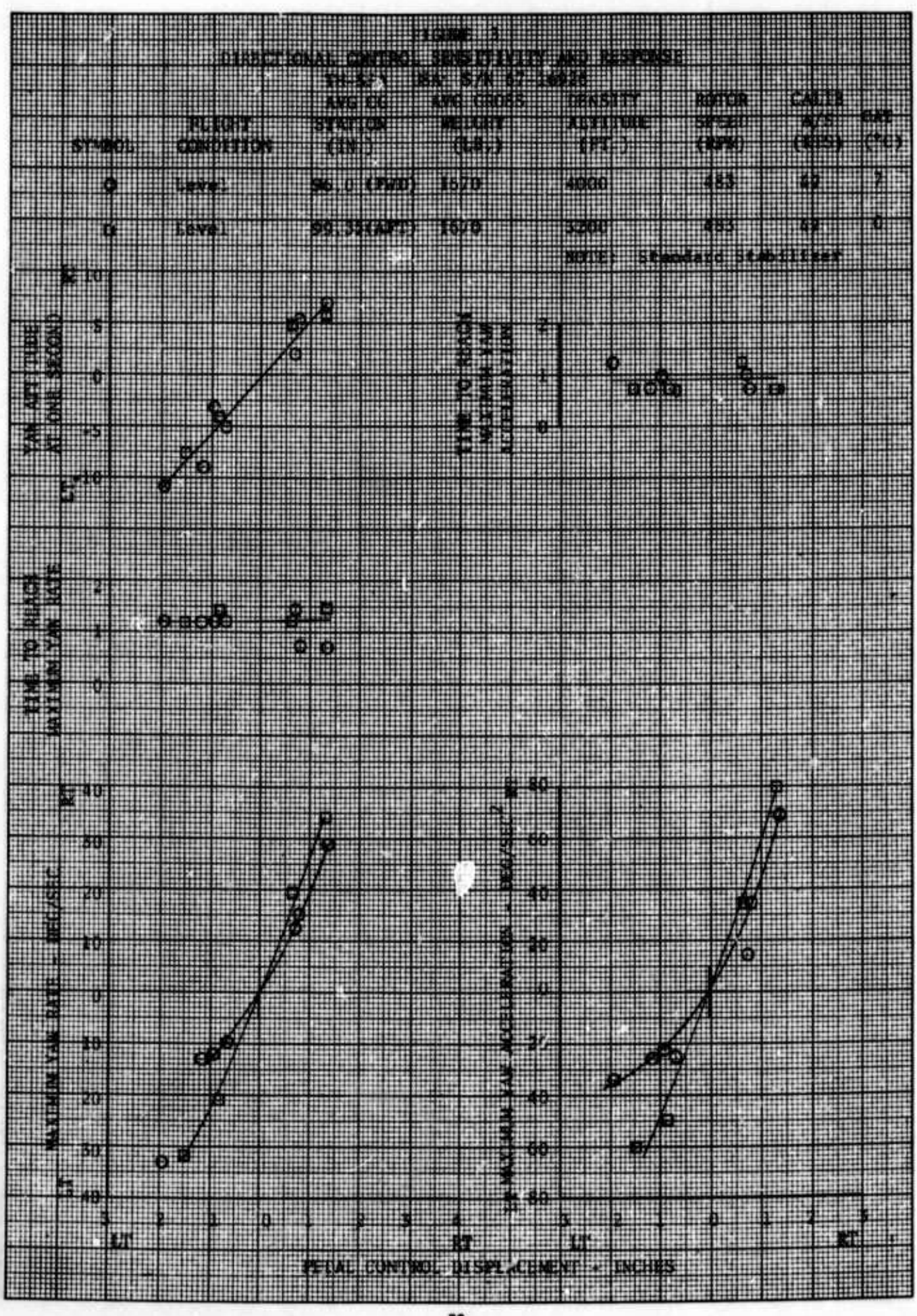

FIGURE 4

CONTROL POSITIONS IN FORWARD FLIGHT

TH-55A USA S/N 67-16926

SYMBOL	FLIGHT CONDITION	AVG. CG STATION (IN.)	AVG. GROSS WEIGHT (LB.)	DENSITY ALTITUDE (FT)	ROTOR SPEED (RPM)	OAT (°C)
○	LEVEL	95.2 (FWD)	1680	4300	485	9
□	LEVEL	95.2 (FWD)	1670	5400	490	10
◇	CLIMB	95.2 (FWD)	1680	5400	485	19
△	AUTO	95.2 (FWD)	1680	5400	485	19

NOTE: Standard Stabilized

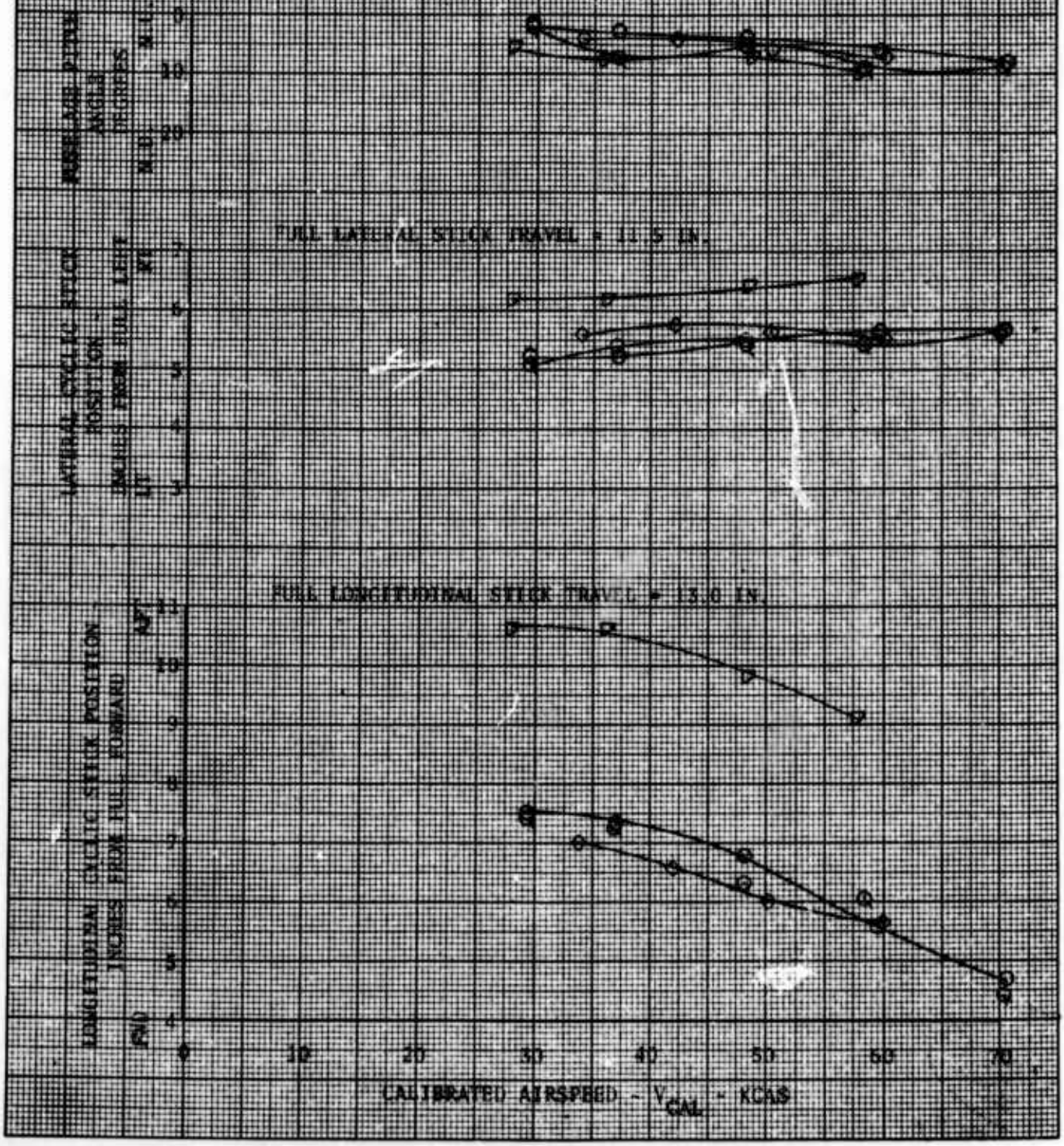

FIGURE 4 (CONCLUDED)
CONTROL POSITIONS IN FORWARD FLIGHT
TH-55A USA S/N 67-18828

SYMBOL	FLIGHT CONDITION	AVG. CG STATION (IN.)	AVG GROSS WEIGHT (LB)	DENSITY ALTITUDE (FT)	ROTOR SPEED (RPM)	OAT (°C)
○	LEVEL	95.8 (FWD)	1680	4300	485	5
□	LEVEL	95.8 (FWD)	1670	5400	480	19
◇	CLIMB	95.8 (FWD)	1680	5400	485	19
▷	AFD	95.8 (FWD)	1680	5400	485	19

NOTE: Standard Stabilizer.

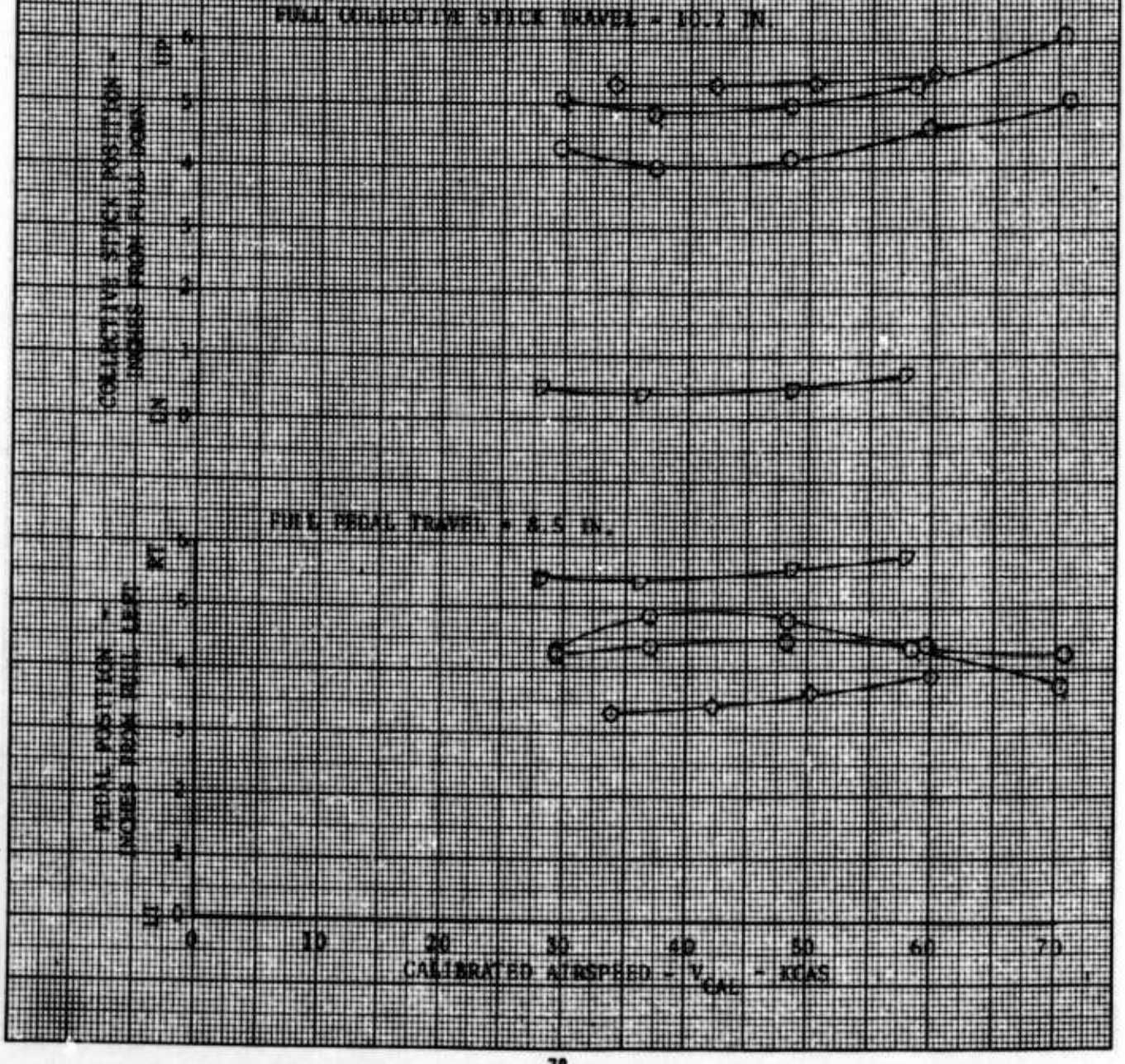

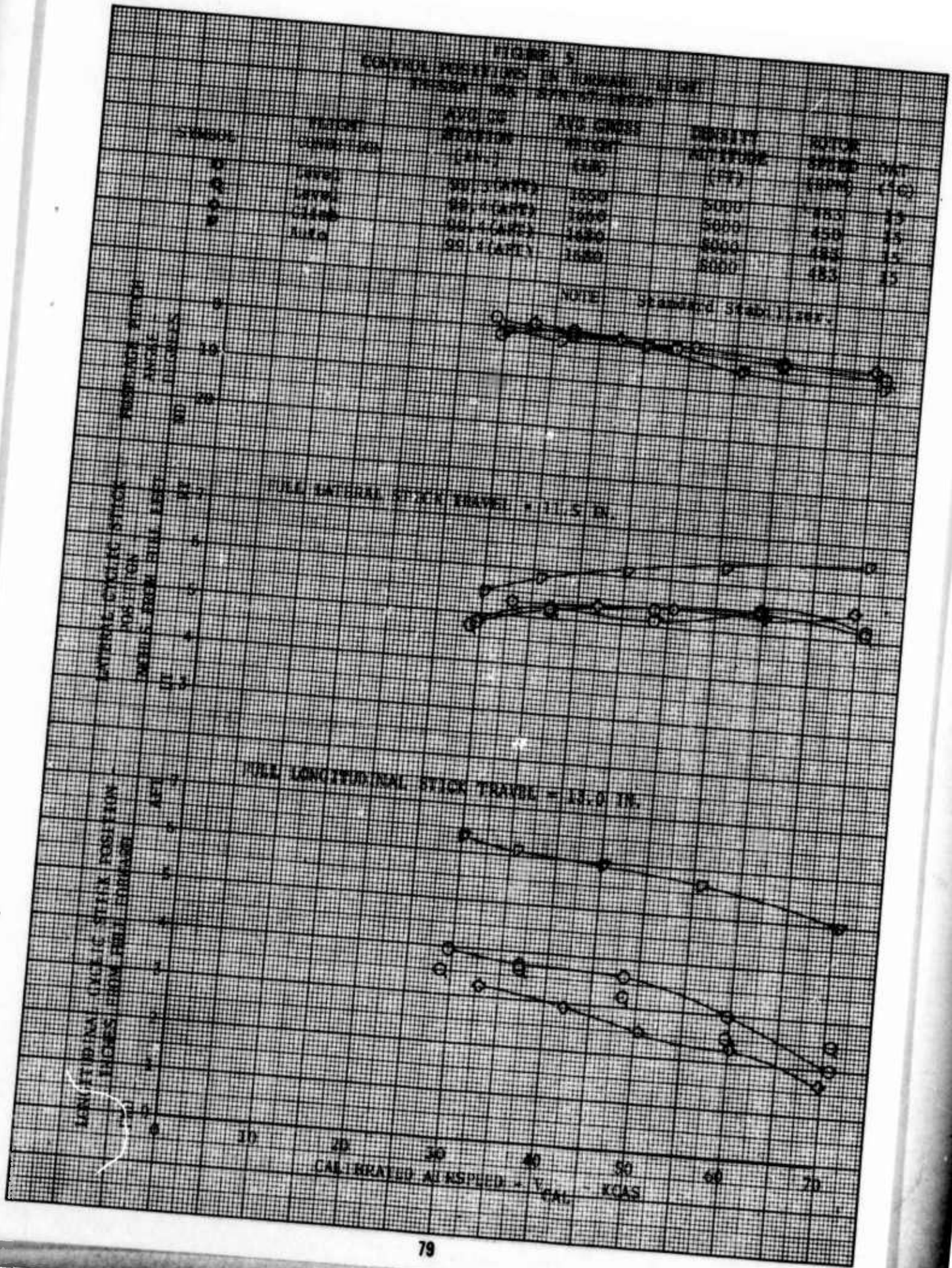
FIGURE 5
CONTROL POSITION VS. CALIBRATED AIRSPEED
TAKEOFF AND APPROACH
SYMBOL
FLAPS
UP
UP
APP
APP
LDG
LDG
AVG CG POSITION (%MAC)
AVG GROSS WEIGHT (LB)
DENSITY ALTITUDE (FT)
ROTOR SPEED (RPM)
OAT (°C)
90
90
90
90
1650
1660
1680
1680
5000
5000
5000
5000
483
450
483
483
15
15
15
15
NOTE: Standard Sea Level Day
FULL LATERAL STICK TRAVEL = 11.5 IN.
FULL LONGITUDINAL STICK TRAVEL = 13.0 IN.
LATERAL CYCLIC STICK POSITION FROM TRIM, IN. RIGHT
LONGITUDINAL CYCLIC STICK POSITION FROM TRIM, IN. AFT
CALIBRATED AIRSPEED - V_{CAL} - KCAS

FIGURE 5 (CONCLUDED)

CONTROL POSITIONS IN FORWARD FLIGHT

TH-55A S/N 570-5425

SYMBOL	FLIGHT CONDITION	STATION (IN.)	GROSS WEIGHT (LB)	DENSITY ALTITUDE (FT)	ROTOR SPEED (RPM)	NOTES
○	Level	99.2 (AFT)	1650	3000	483	1
◇	Level	99.4 (AFT)	1680	3000	480	1
△	Climb	99.4 (AFT)	1680	3000	480	1,2
●	Auto	99.4 (AFT)	1680	3000	483	1,2

NOTES: 1. Standard Stabilizer

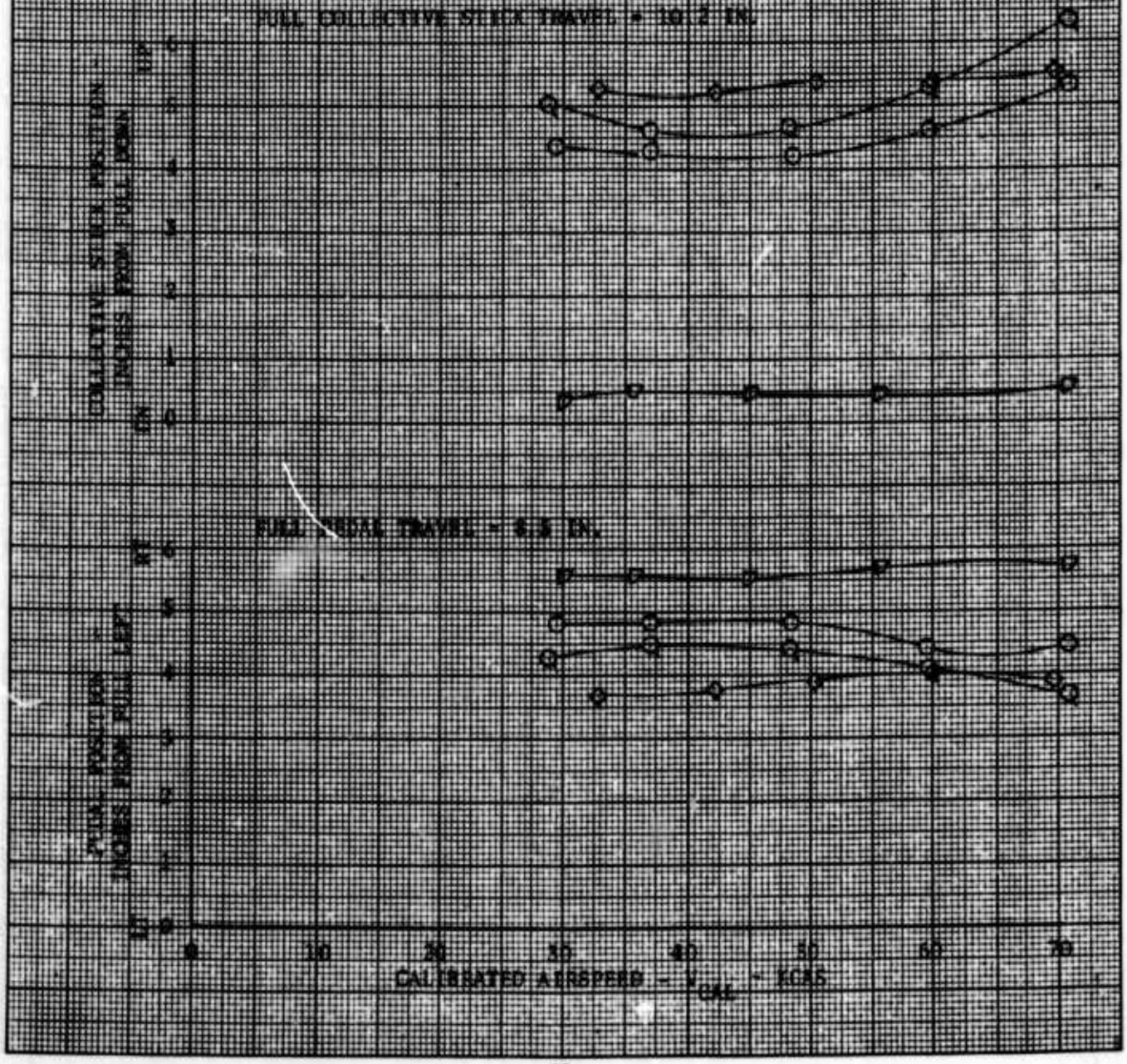

FIGURE 6

CONTROL POSITIONS IN FORWARD FLIGHT

TH-55A OSA S/N 67-16925

SYMBOL	FLIGHT CONDITION	AVG CG STATION (IN.)	AVG GROSS WEIGHT (LB)	DENSITY ALTITUDE (FT)	ROTOR SPEED (RPM)	OAT (°C)
○	Level	99.2 (AFT)	440	4200	485	9
◇	Climb	99.2 (AFT)	440	4200	485	9
△	Auto	99.2 (AFT)	440	4200	485	9

NOTE: Canopy Slat Removed.

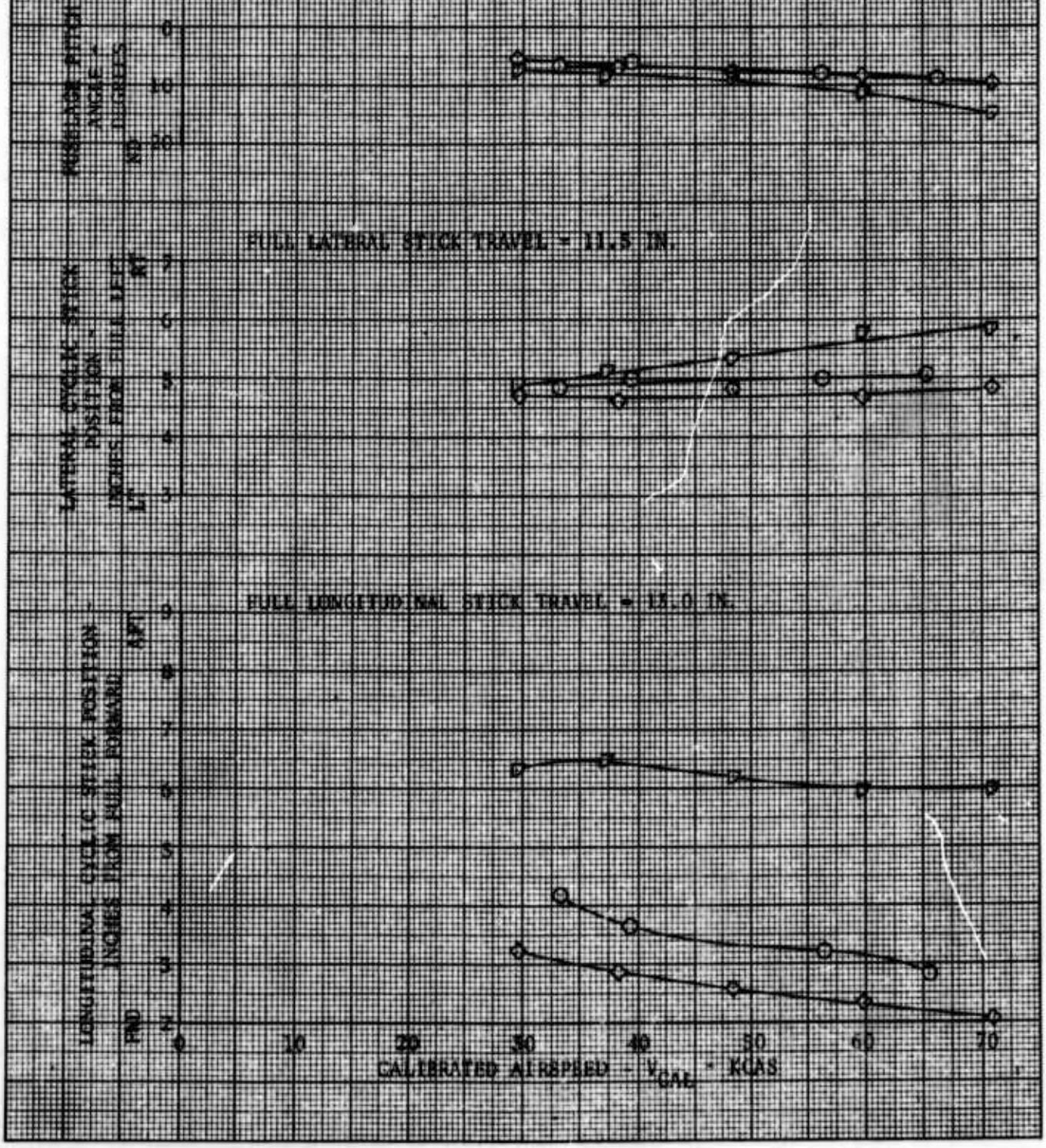

FIGURE 6 (CONCLUDED)
CONTROL POSITIONS IN FORWARD FLIGHT
TH-55A USA S/N 67-16926

SYMBOL	FLIGHT CONDITION	AVG CG STATION (IN.)	AVG GROSS WEIGHT (LB)	DENSITY ALTITUDE (FT)	ROTOR SPEED (RPM)	OAT (°C)
◇	Climb	99.2 (APT)	1640	4200	483	9
◇	Auto	99.2 (APT)	1640	4200	483	9
○	Level	99.2 (APT)	1640	4200	483	9

NOTE: Canopy Slat Removed.

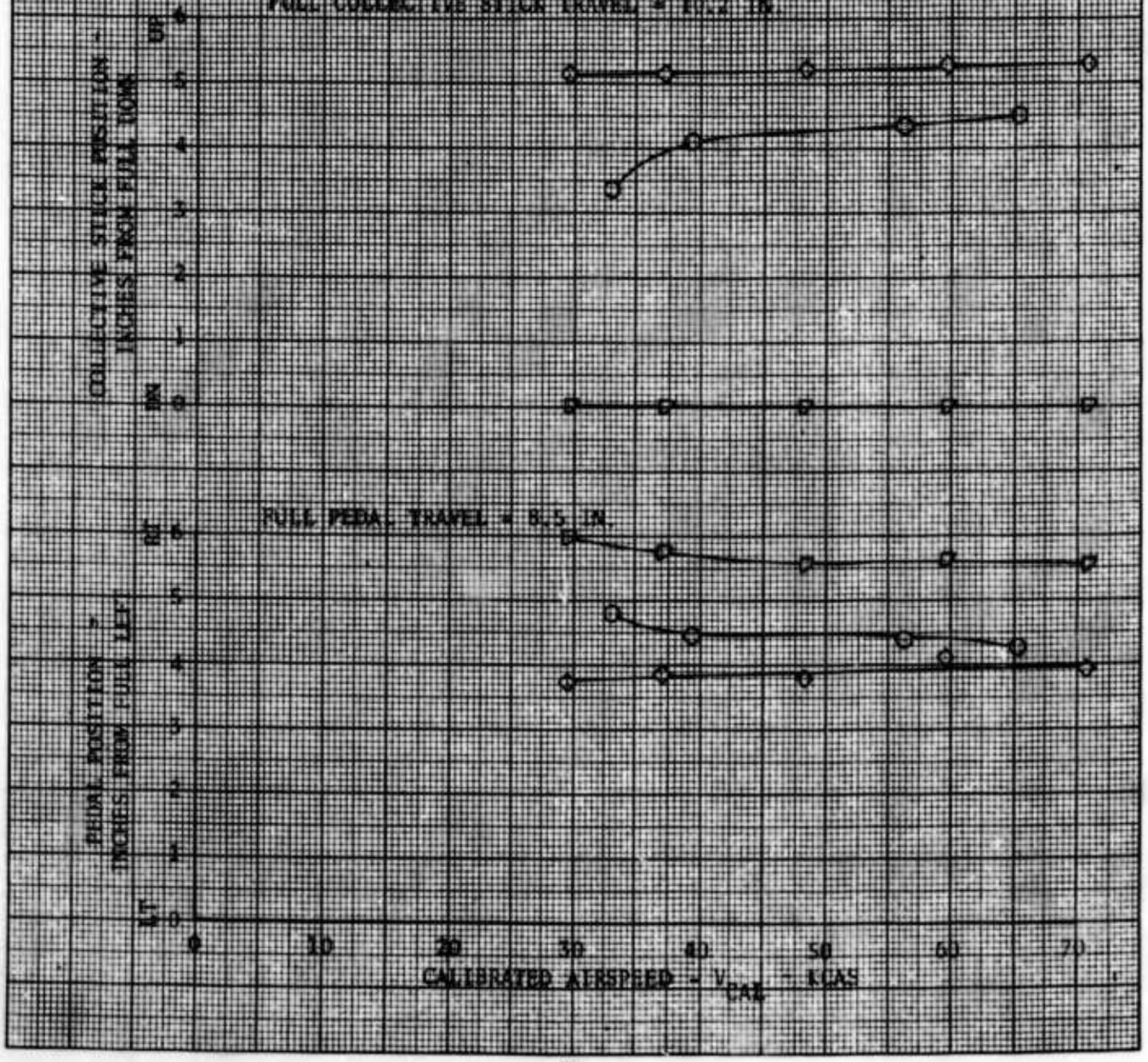

FIGURE 2

CONTROL POSITIONS IN FORWARD FLIGHT

XH-59A (ABC) S/N 72-20936

SYMBOL	FLIGHT CONDITION	AVG CG STATION (IN.)	AVG GROSS WEIGHT (LB)	DENSITY ALTITUDE (FT)	ROTOR SPEED (RPM)	OAT (°C)
○	Level	98.7 (FWD)	16480	4400	483	10
◇	Climb	98.7 (FWD)	16480	4400	483	10
▽	Cruise	98.7 (FWD)	16480	4400	483	10
□	Descent	98.7 (FWD)	16480	4400	483	10

NOTE: Reduced Chord Stabilizer.

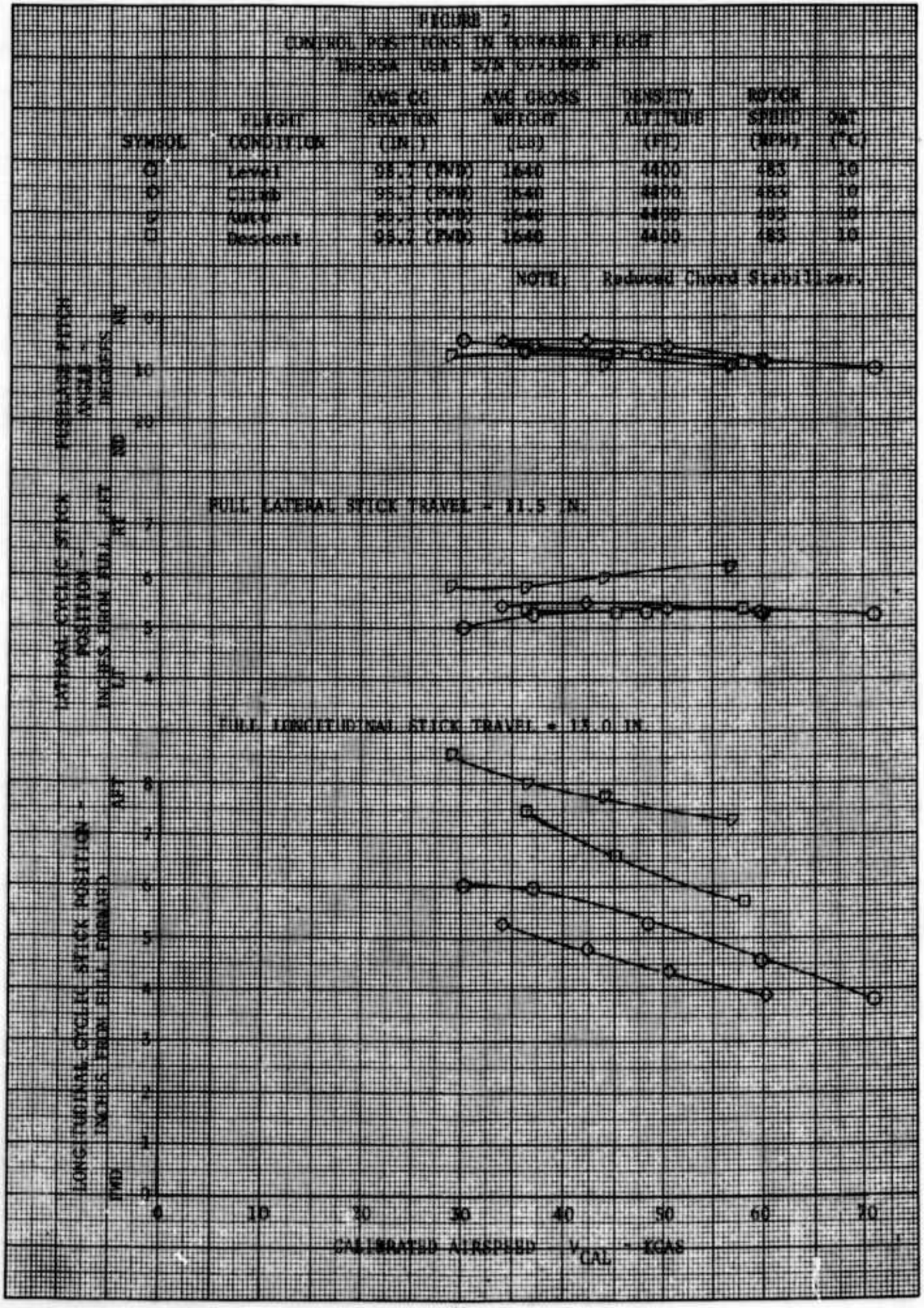

FIGURE 7 (CONCLUDED)

CONTROL POSITIONS IN TORQUE FLIGHT

TESSA USA STA 07-19826

SYMBOL	FLIGHT CONDITION	AVG CG STATION (IN.)	AVG GROSS WEIGHT (LB)	DENSITY ALTITUDE (FT)	ROTOR SPEED (RPM)	OAT (°C)
○	Level	95.7 (FWD)	1640	4400	455	10
◇	Climb	95.7 (FWD)	1640	4400	455	10
△	Turn	95.7 (FWD)	1640	4400	455	10
□	Descent	95.7 (FWD)	1640	4400	455	10

NOTE: Reduced Chord Stabilizer

FULL COLLECTIVE STICK TRAVEL = 10.2 IN.

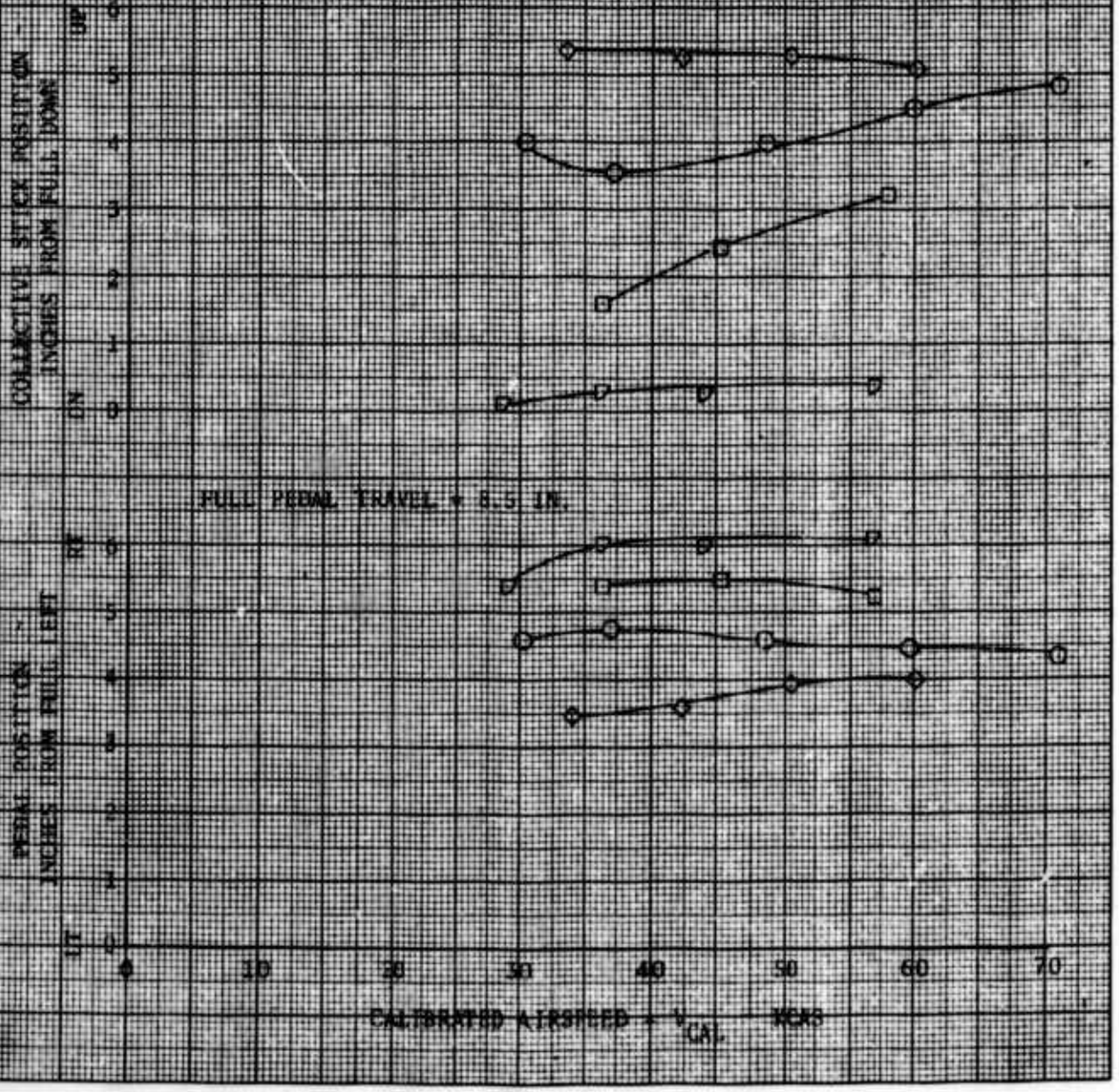

FIGURE 8

CONTROL POSITIONS IN FORWARD FLIGHT

TH-55A USA S/N 67-16926

SYMBOL	FLIGHT CONDITION	AVG. CG STATION (IN.)	AVG. GROSS WEIGHT (LB)	DENSITY ALTITUDE (FT)	ROTOR SPEED (RPM)	OAT (°C)
○	Level	99.5 (AFT)	1580	4400	485	30
◇	Climb	99.5 (AFT)	1580	4400	485	10
□	Hover	99.5 (AFT)	1580	4400	485	10
△	Descent	99.5 (AFT)	1580	4400	485	10

NOTE: Reduced Chord Stabilizer.

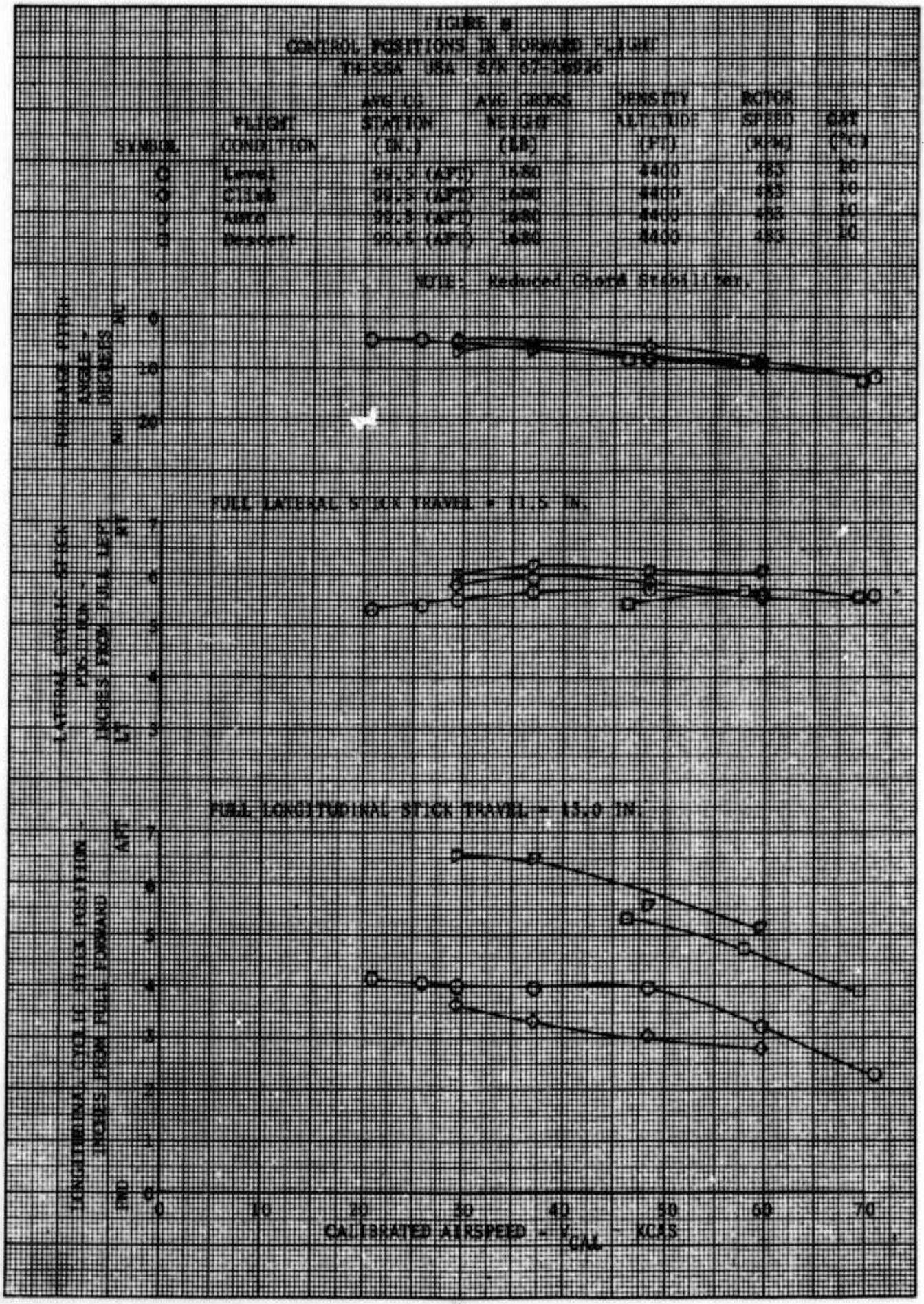

FIGURE 8 (CONCLUDED)

CONTROL POSITIONS IN NOMINAL FLIGHT

YH-60A (USA S/N 77-22926)

SYMBOL	FLIGHT CONDITION	AVG C.G. STATION (IN.)	AVG GROSS WEIGHT (LB)	DENSITY ALTITUDE (FT)	ROTOR SPEED (RPM)	OAT (°C)
○	Level	99.5 (AFT)	16500	4400	483	10
◇	Climb	99.5 (AFT)	16500	4400	483	10
△	Accel	99.5 (AFT)	16500	4400	483	10
□	Descent	99.5 (AFT)	16500	4400	483	10

NOTE: Balanced Chord Stabilizer.

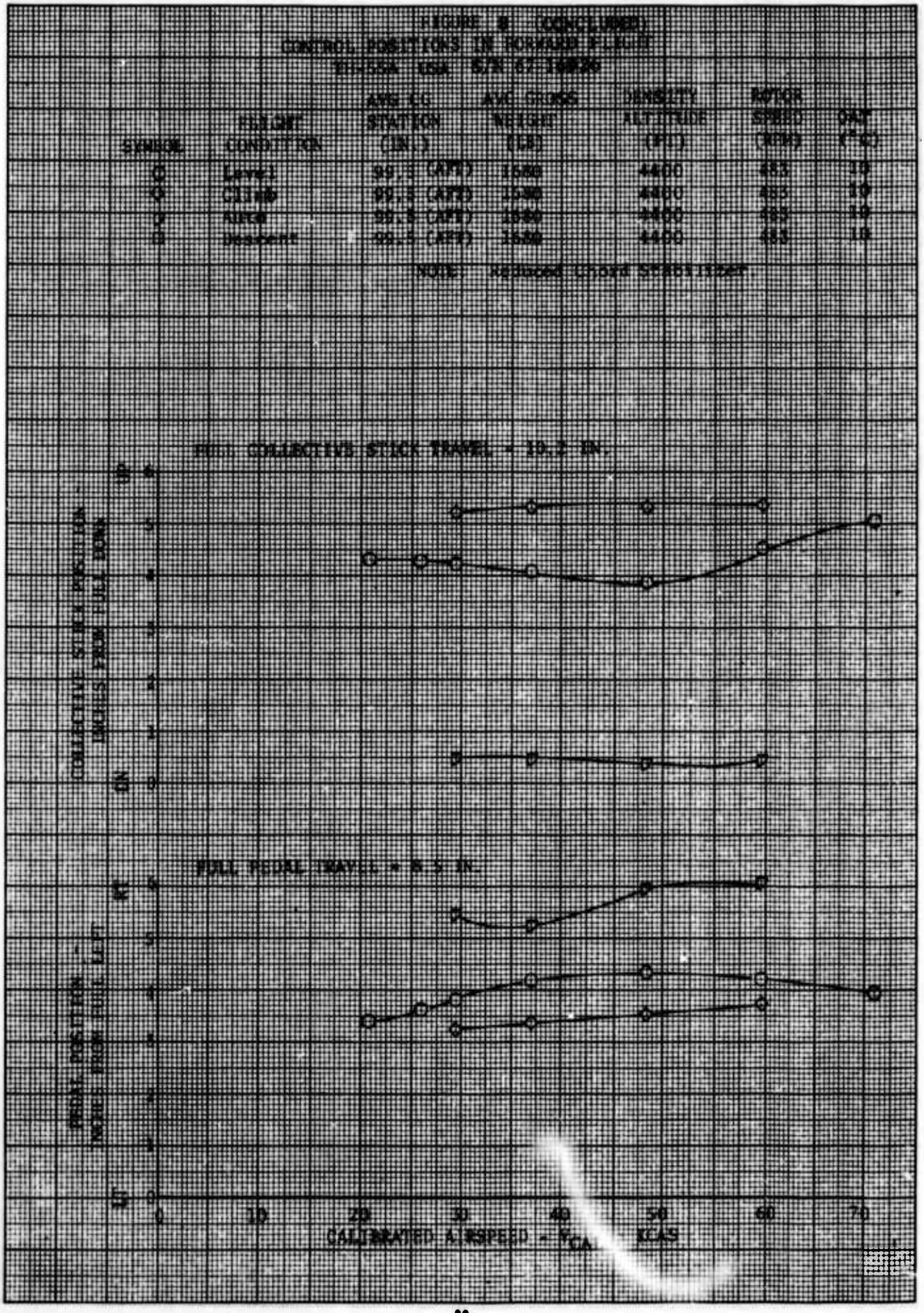

FIGURE 9

STATIC TRIM SHIFT SUMMARY

CLIMBING TO AUTOROTATIONAL FLIGHT

BE-55A USA S/N 67-16826

SYMBOL	CONFIGURATION	AVG CG STATION (IN.)	AVG GROSS WEIGHT (LB)	DENSITY ALTITUDE (FT)	ROTOR SPEED (RPM)	OAT (°C)	DATA OBTAINED FROM FIGURE
———	Standard	95.2	1680	4300	483	9	4
— — —	Reduced Chord	95.7	1648	4400	483	10	7
— · — · —	Final Reduced Span	93.2	1670	4100	483	8	33

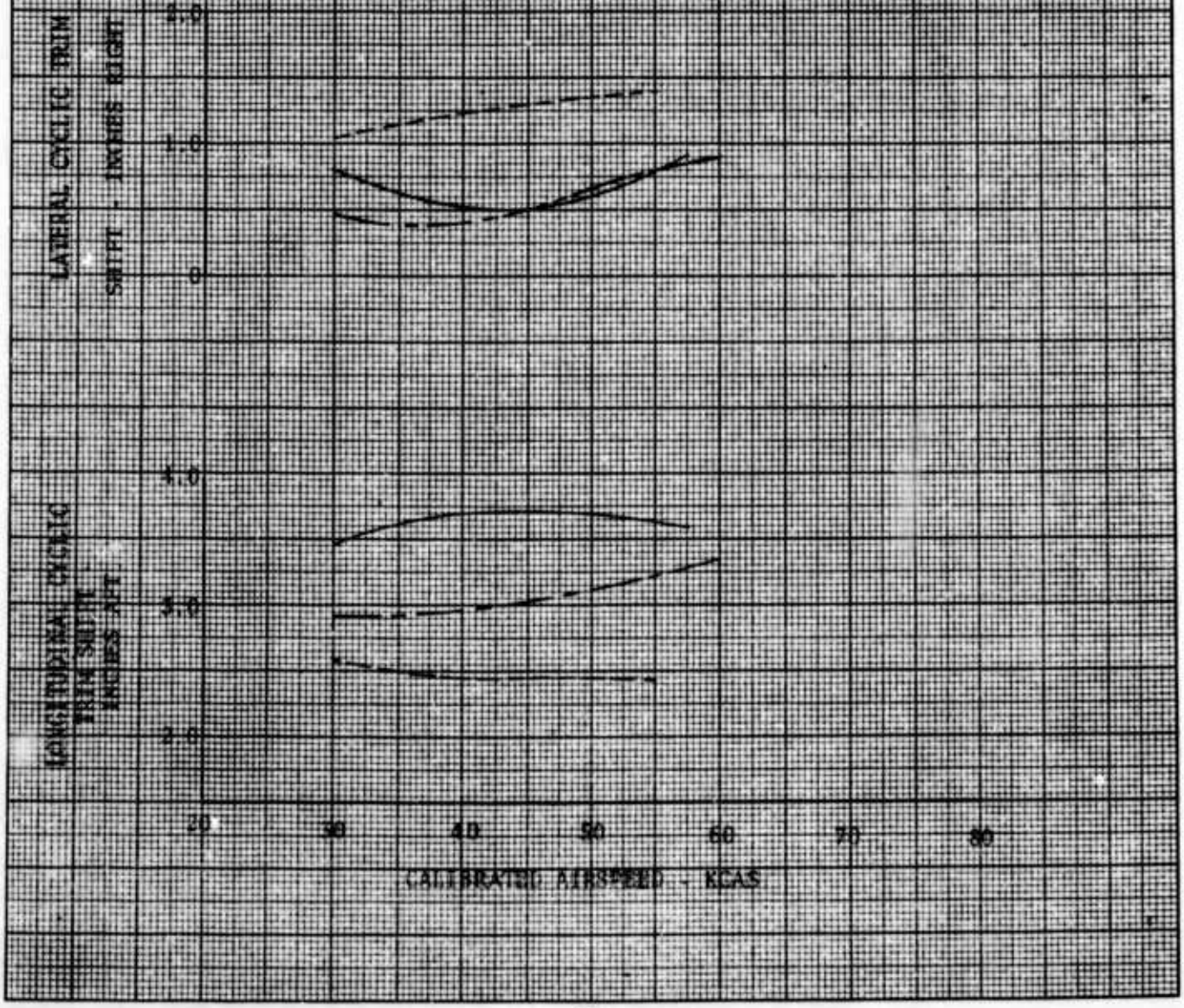

FIGURE 4 (CONTINUED)

STATIC TRIM SHEET SUMMARY

CLIMBING TO AEROBATIONAL FLIGHT

TR-55A USA S/N 67-00026

SYMBOL	CONFIGURATION	AVG CG STATION (IN.)	AVG GROSS WEIGHT (LB)	DENSITY ALTITUDE (FT)	REFER SPEED (KCAS)
———	Standard	85.8 (FWD)	1680	4500	495
– – – –	Reduced Chord	85.7 (FWD)	1640	4400	495
– · – · –	Final Reduced Span	85.2 (FWD)	1670	4700	495

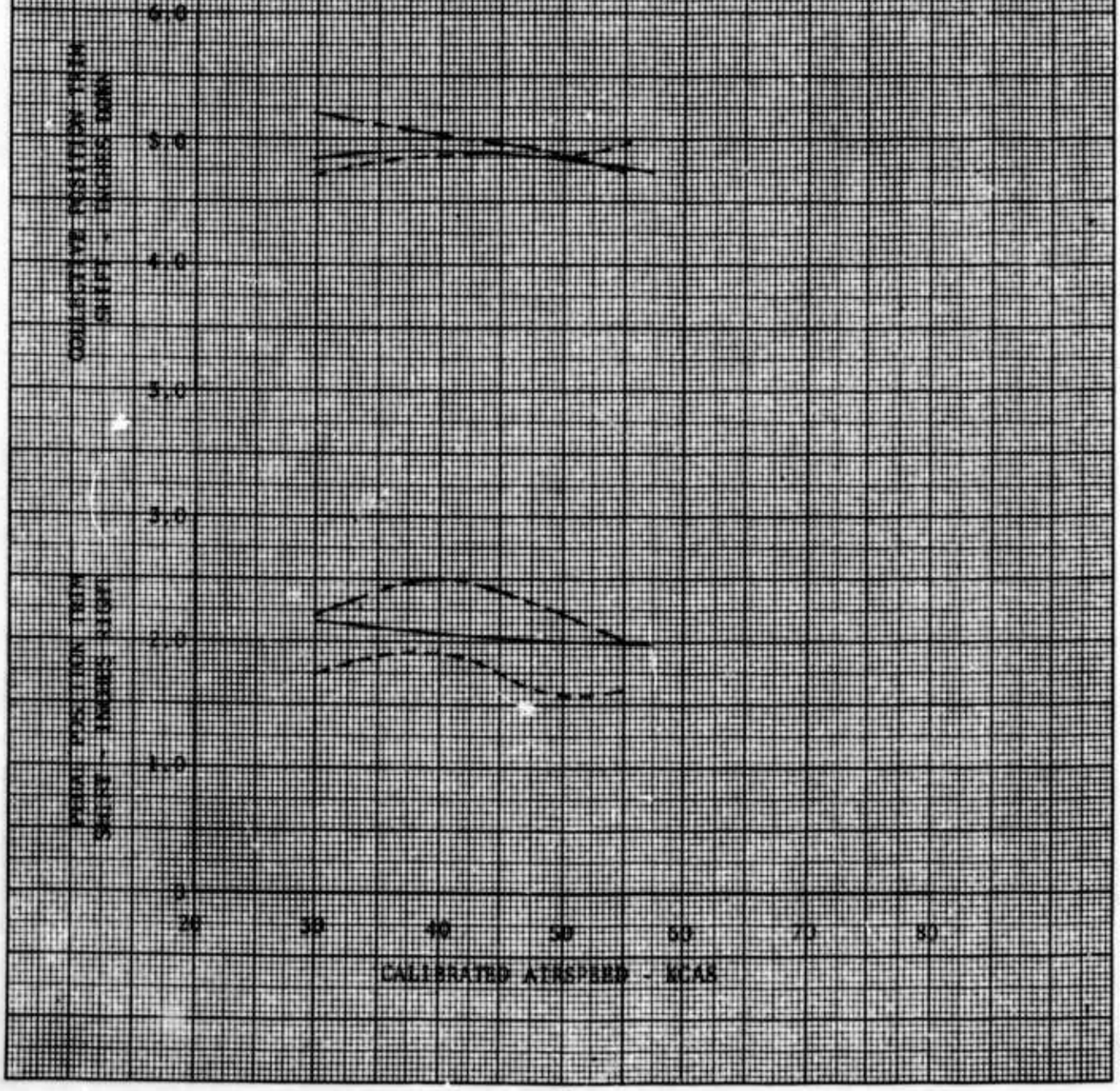

FIGURE 10

STATIC TREK SHIFT SUMMARY

CLIMBING TO AUTOROTATIONAL FLIGHT

YH-55A USA S/N 67-16926

SYMBOL	CONFIGURATION	AVG CG STATION (IN.)	AVG GROSS WEIGHT (LB)	DENSITY ALTITUDE (FT)	ROTOR SPEED (RPM)	OAT (°C)
———	Standard	99.3 (APT)	1650	5000	485	15
— — —	Reduced Chord	99.3 (APT)	1680	4400	485	8
- - - - -	Final Reduced Span	99.3 (APT)	1670	4200	485	9

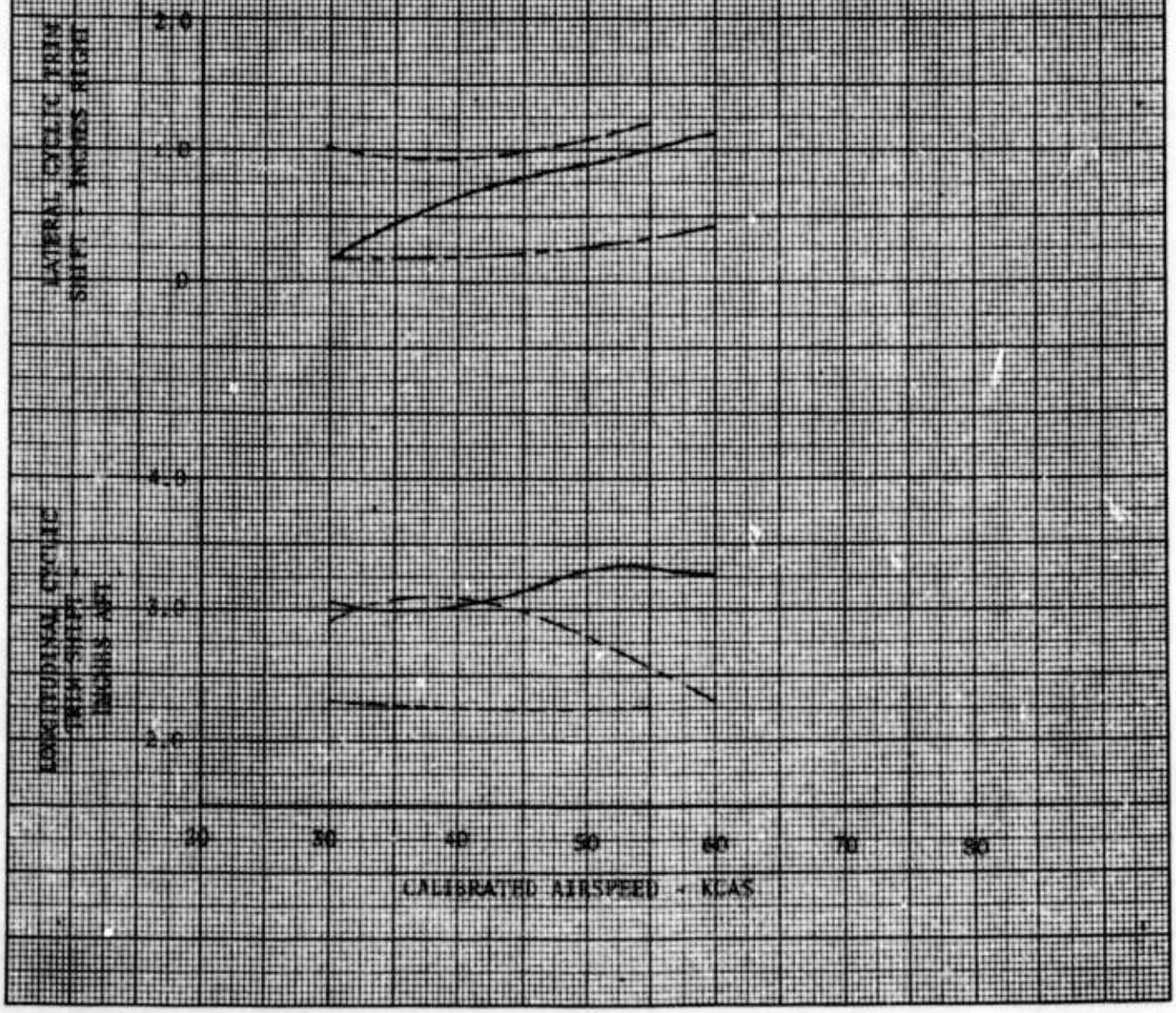

FIGURE 10 (CONTINUED)
STATIC TRIM SURVEY SUMMARY
CLIMBING 70 AUTOROTATIONAL FLIGHT
TH-55A (6A S/N 67-14826

SYMBOL	CONFIGURATION	AVG CG STATION (IN.)	AVG GROSS WEIGHT (LB)	DENSITY ALTITUDE (FT)	ROTOR SPEED (RPM)
———	Standard	99.5(AFT)	1650	5000	485
— - —	Reduced Cloyd	99.5(AFT)	1680	4400	485
— - - -	Final Reduced Spun	99.3(AFT)	1670	4200	485

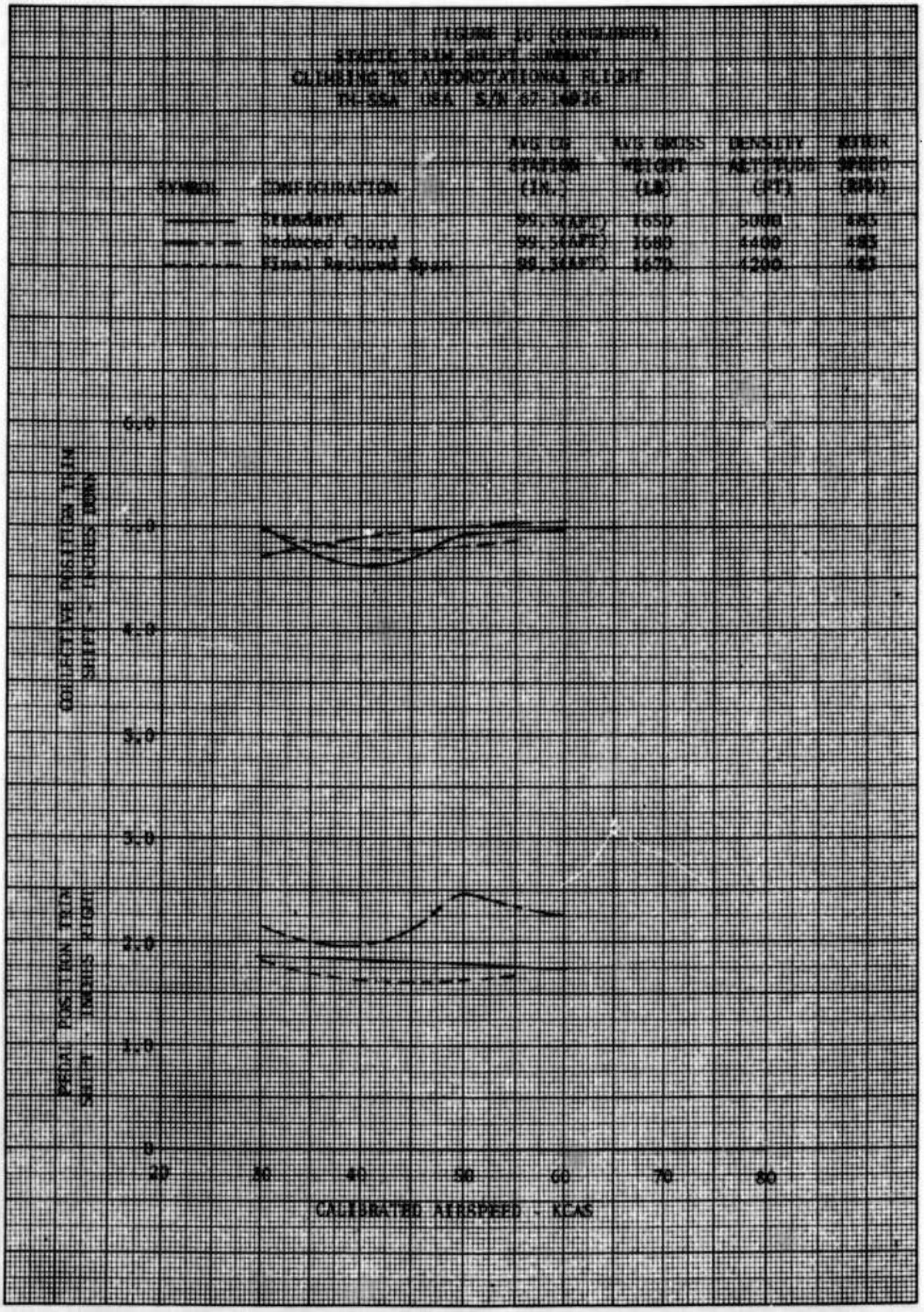

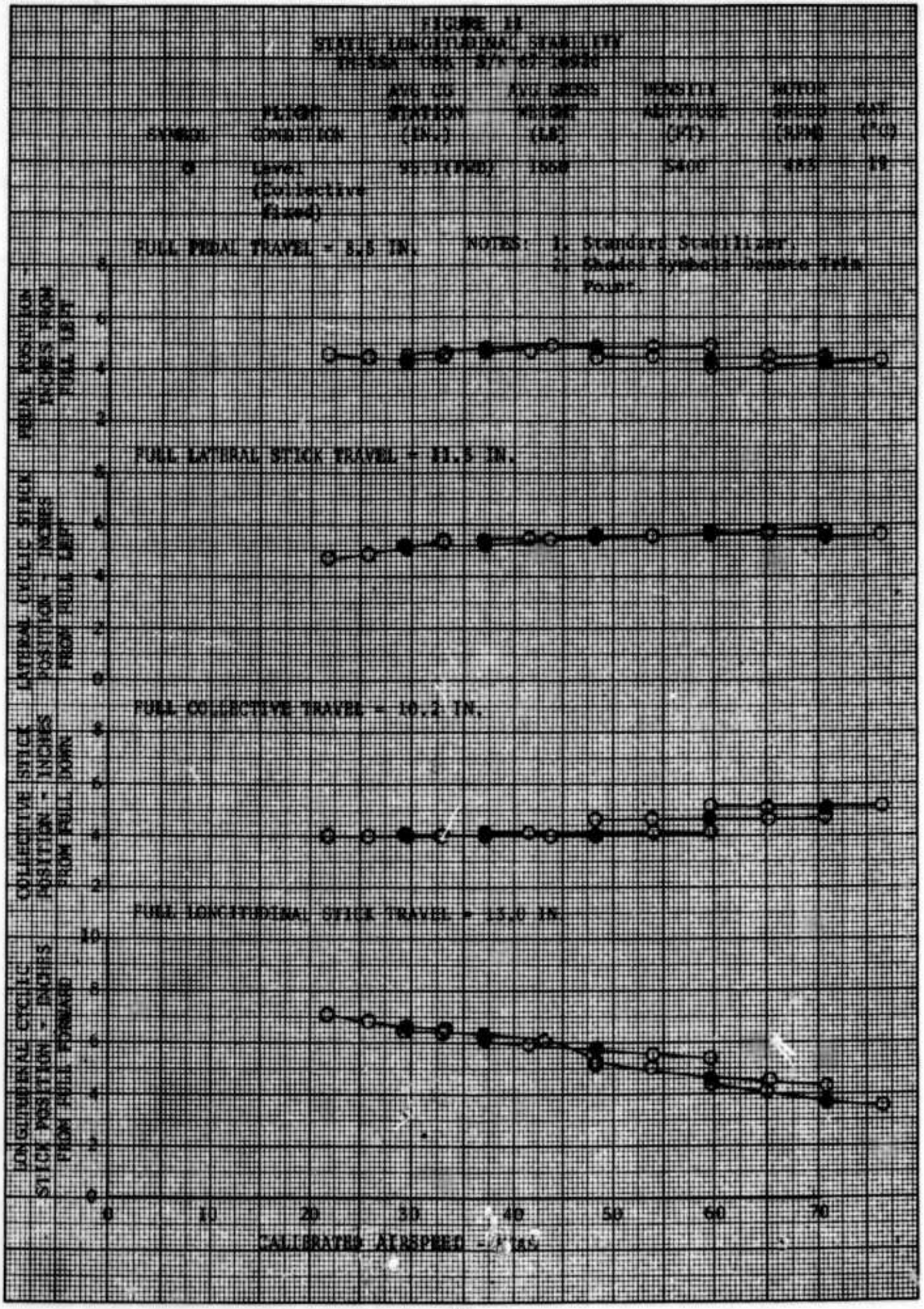
FIGURE 33
STATIC LONGITUDINAL STABILITY
SYMBOL
FLIGHT CONDITION
Level (Collective Fixed)
AVG CG STATION (IN.)
AVG GROSS WEIGHT (LB)
1668
DENSITY ALTITUDE (FT)
5400
ROTOR SPEED (RPM)
GAT (°C)
FULL PEDAL TRAVEL = 5.5 IN.
NOTES: 1. Standard Stabilizer.
2. Shaded Symbols Denote Trim Point.
FULL LATERAL STICK TRAVEL = 11.5 IN.
FULL COLLECTIVE TRAVEL = 10.2 IN.
FULL LONGITUDINAL STICK TRAVEL = 15.0 IN.
LONGITUDINAL STICK POSITION, INCHES FROM TRIM
LATERAL STICK POSITION, INCHES FROM TRIM
PEDAL POSITION, INCHES FROM TRIM
COLLECTIVE STICK POSITION, INCHES FROM TRIM
0
10
20
30
40
50
60
70
CALIBRATED AIRSPEED - KTAS

FIGURE 12
STATIC LONGITUDINAL STABILITY
TH-55A (SN. 570-47-1602)

SYMBOL	FLIGHT CONDITION	AVG CG STATION (IN.)	AVG GROSS WEIGHT (LB)	DENSITY ALTITUDE (FT)	ROTOR SPEED (RPM)	IAS (KIAS)
○	Level (Collective fixed)	99.5(AFT)	1650	5000	438	30

NOTE: 1. Standard Stabilizer.
2. Shaded Symbols Denote Trim Point.

FULL PEDAL TRAVEL = 8.5 IN.

FULL LATERAL STICK TRAVEL = 11.5 IN.

FULL COLLECTIVE TRAVEL = 10.2 IN.

FULL LONGITUDINAL STICK TRAVEL = 13.0 IN.

RIGHT PEDAL POSITION FROM TRIM, INCHES
FOR FULL LEFT

LATERAL CYCLIC STICK POSITION FROM TRIM, INCHES
FOR FULL LEFT

COLLECTIVE STICK POSITION FROM TRIM, INCHES
FOR FULL DOWN

LONGITUDINAL CYCLIC STICK POSITION FROM TRIM, INCHES
FOR FULL FORWARD

CALIBRATED AIRSPEED - KCAS

FIGURE 13

STATIC LONGITUDINAL STABILITY

SYMBOL	FLIGHT CONDITION	AVG CG STATION (IN.)	AVG GROSS WEIGHT (LB)	DENSITY ALTITUDE (FT)	ROTOR SPEED (RPM)	OAT (°C)
○	Level (Collective Fixed)	99.4 (AFT)	1680	4200	483	9

NOTES: 1. Standard Stabilizer with Canopy Slat Removed.
2. Shaded Symbols Denote Trim Point.

FULL PEDAL TRAVEL = 8.5 IN.

FULL LATERAL STICK TRAVEL = 11.5 IN.

FULL COLLECTIVE TRAVEL = 10.2 IN.

FULL LONGITUDINAL STICK TRAVEL = 13.0 IN.

PEDAL POSITION VERSUS CALIBRATED AIRSPEED - INCHES FROM FULL AFT

LATERAL STICK POSITION VERSUS CALIBRATED AIRSPEED - INCHES FROM FULL RIGHT

COLLECTIVE STICK POSITION VERSUS CALIBRATED AIRSPEED - INCHES FROM FULL DOWN

LONGITUDINAL STICK POSITION VERSUS CALIBRATED AIRSPEED - INCHES FROM FULL AFT

0 2 4 6 8

0 10 20 30 40 50 60 70

CALIBRATED AIRSPEED - KCAS

FIGURE 24
STATIC LONGITUDINAL STABILITY
TH-55A OSA S/N 67-16930

SYMBOL	FLIGHT CONDITION	AVG CG POSITION (IN.)	AVG GROSS WEIGHT (LB)	DENSITY ALTITUDE (FT)	ROTOR SPEED (RPM)	OAT (°C)
○	Level	95.6(3KD)	1630	4400	483	10

NOTES: 1. Reduced Chord Stability.
2. Shaded Symbol Denotes Trim Point.

FULL PEDAL TRAVEL = 8.5 IN.

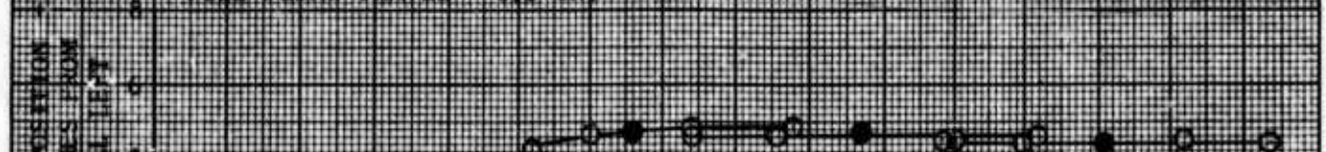

FULL LATERAL STICK TRAVEL = 11.5 IN.

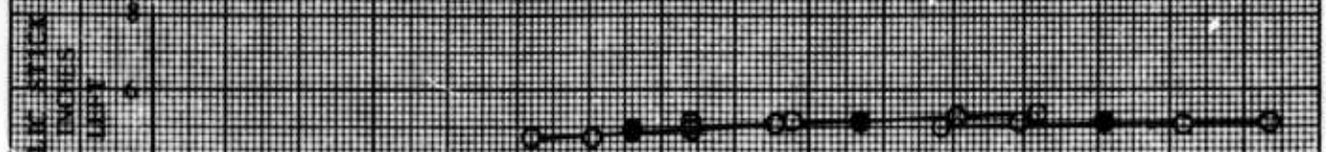

FULL COLLECTIVE TRAVEL = 10.2 IN.

FULL LONGITUDINAL STICK TRAVEL = 13.6 IN.

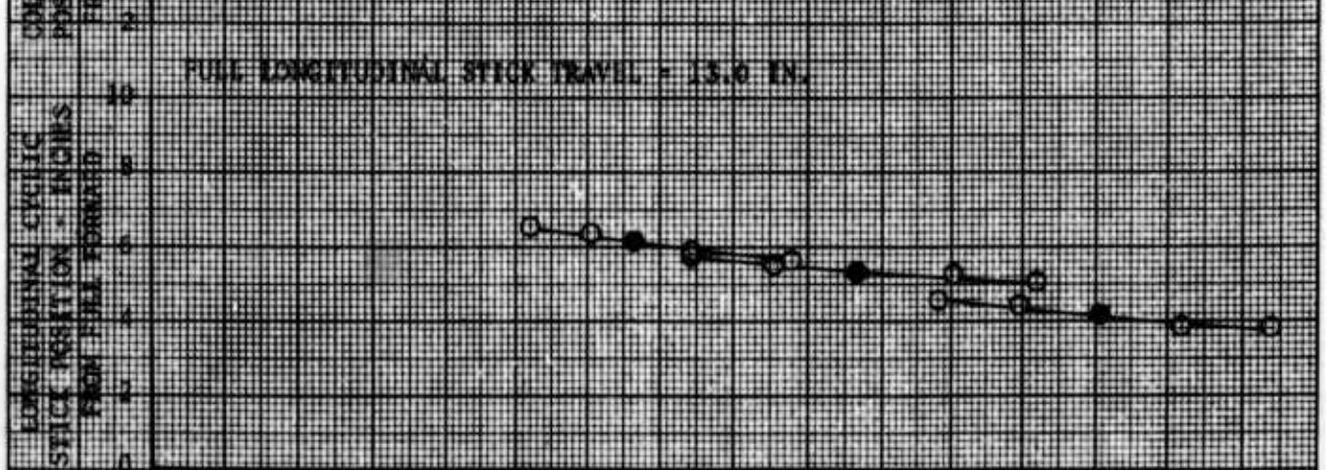

FIGURE 15

STATIC LONGITUDINAL STABILITY

TH-55A USA S/N 67-16026

SYMBOL	FLIGHT CONDITION	AVG CG STATION (IN.)	AVG GROSS WEIGHT (LB)	DENSITY ALTITUDE (FT)	ROTOR SPEED (RPM)	OAT (°C)
○	Level [Collective Fixed]	99.2	1640	4400	483	10

NOTES: 1. Reduced Chord Stabilizer.
2. Shaded Symbol Denotes Trim Point.

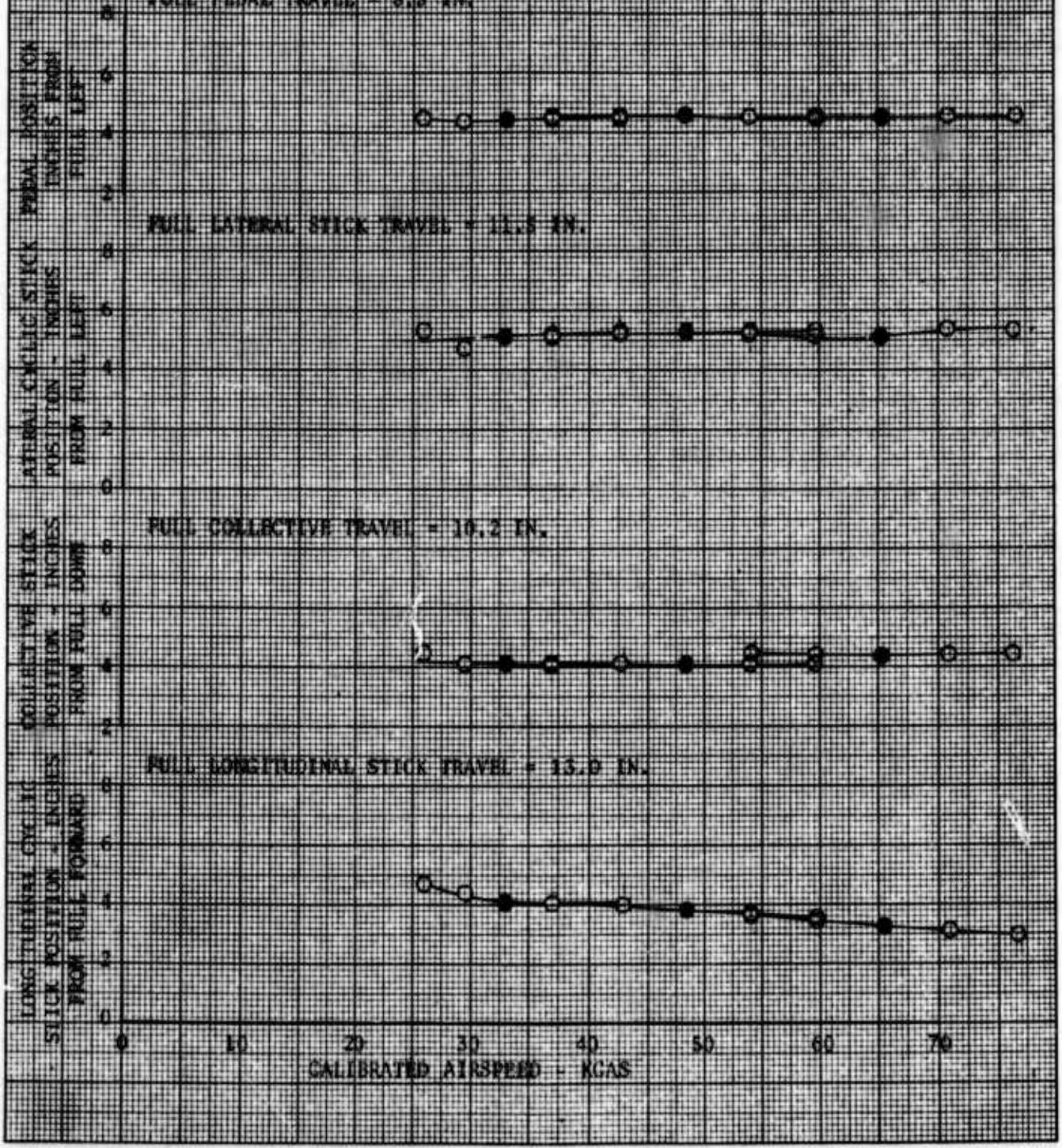

FIGURE 35

STATIC LONGITUDINAL STABILITY SUMMARY

TH-57A USN S/N 67-18826

SYMBOL	CONFIGURATION	AVG CG STATION (INCHES)	AVG GROSS WEIGHT (LBS)	AVG DENSITY ALTITUDE (FEET)	ROTOR SPEED (RPM)	RATING OBTAINED FROM FIGURE
———	STANDARD	95.2 (FWD)	6200	5400	483	11
—— + ——	REDUCED CHORD	95.0 (FWD)	6050	4400	483	24
— — —	FINAL REDUCED SPAN	95.2 (FWD)	6700	4100	483	35
———	STANDARD	98.4 (AFT)	6500	4500	483	12
—— + ——	REDUCED CHORD	98.2 (AFT)	6400	4400	483	13
— — —	FINAL REDUCED SPAN	99.0 (AFT)	6700	4400	483	36
— — — +	STANDARD WITH CANOPY SLAT REMOVED	98.4 (AFT)	6700	4200	483	23

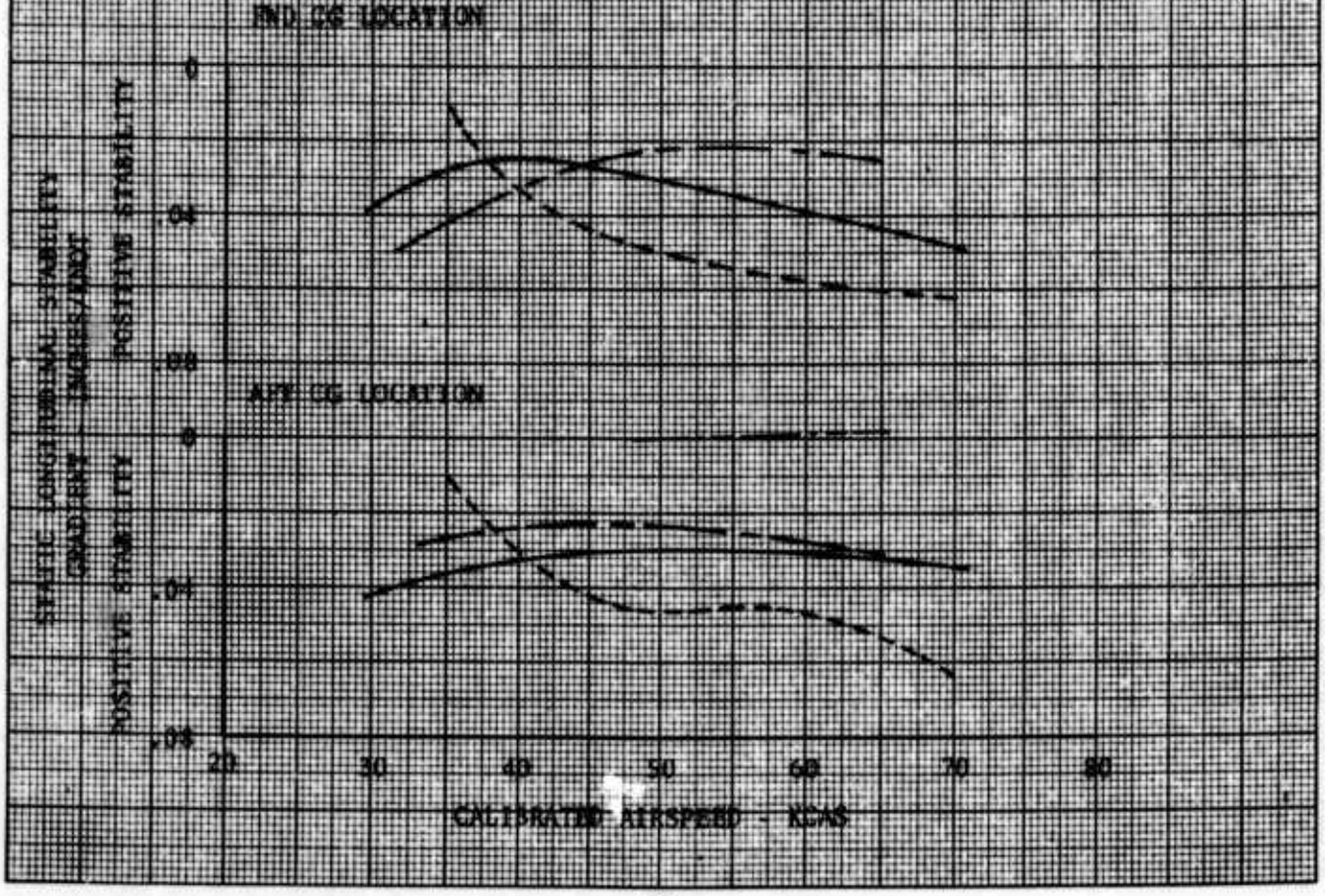

FIGURE 19

STATIC LATERAL DIRECTIONAL STABILITY

BELL SA 365 S/N 67-14006

SYMBOL	FLIGHT CONDITION	AVG CG STATION (IN.)	AVG GROSS WEIGHT (LB)	DENSITY ALTITUDE (FT)	ROTOR SPEED (RPM)	CALIB. A/S (KTS)	OAT (°C)
○	Level	96.3 (FWD)	1590	4000	485	85	7
□	Level	96.3 (FWD)	1580	4000	485	87	7
▽	Level	96.1 (FWD)	1580	4000	485	80	7

NOTES: 1. Standard Stabilizer.
2. Shaded symbols denote trim points.

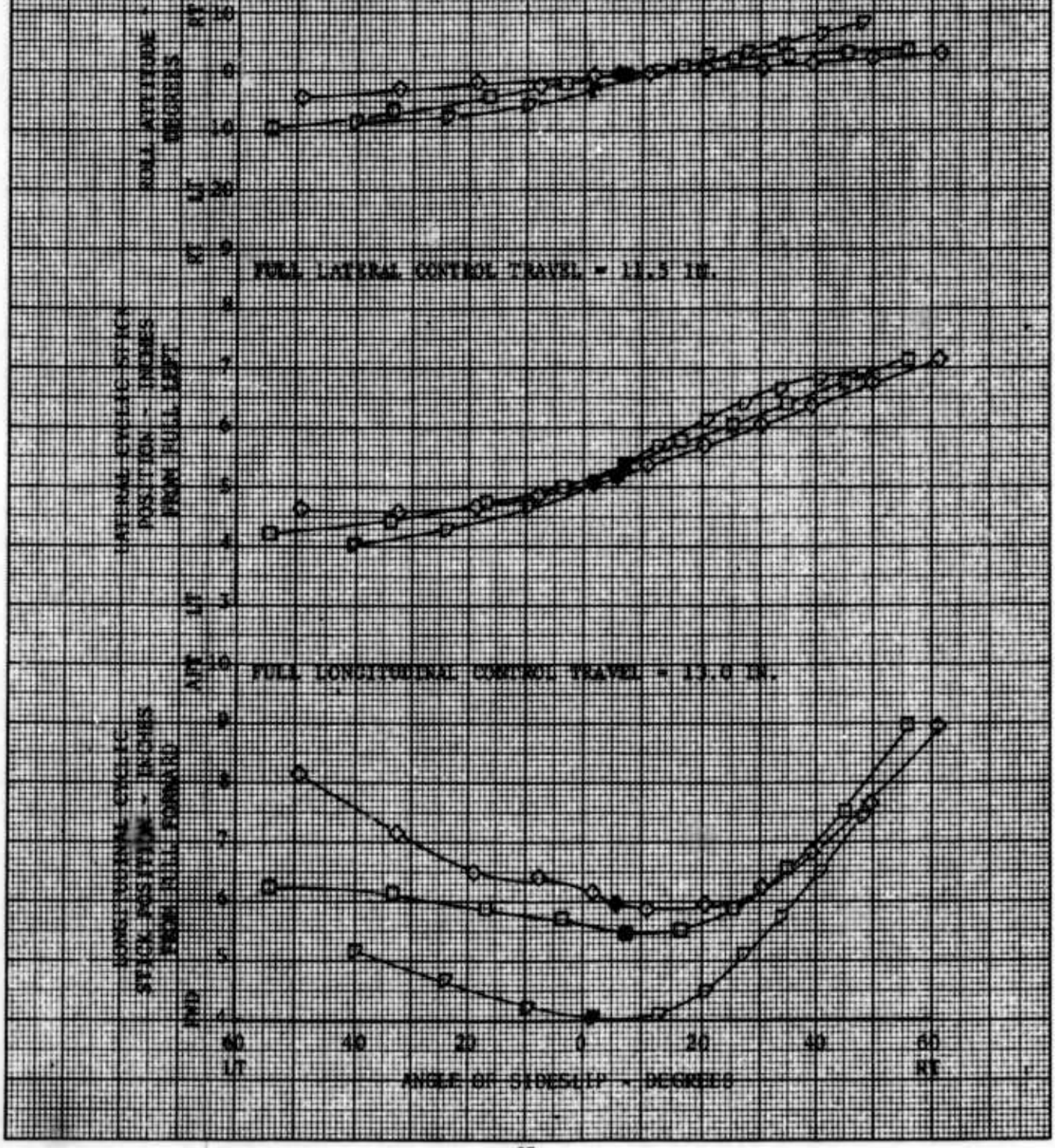

FIGURE 17 (CONCLUDED)

STATIC LATERAL DIRECTIONAL STABILITY

TH-55A USN STF ST-HOVER

SYMBOL	FLIGHT CONDITION	AVG CG STATION (IN.)	AVG GROSS WEIGHT (LB)	DENSITY ALTITUDE (FT)	ROTOR SPEED (RPM)	GATES, KTS	GATES, DEG
○	Level	96.3 (RND)	1696	4000	483	35	7
□	Level	96.3 (RND)	1588	4000	483	47	7
▽	Level	96.3 (RND)	1660	4000	483	60	7

NOTES: 1. Standard Stabilizer.
2. Shaded symbols denote trim points.

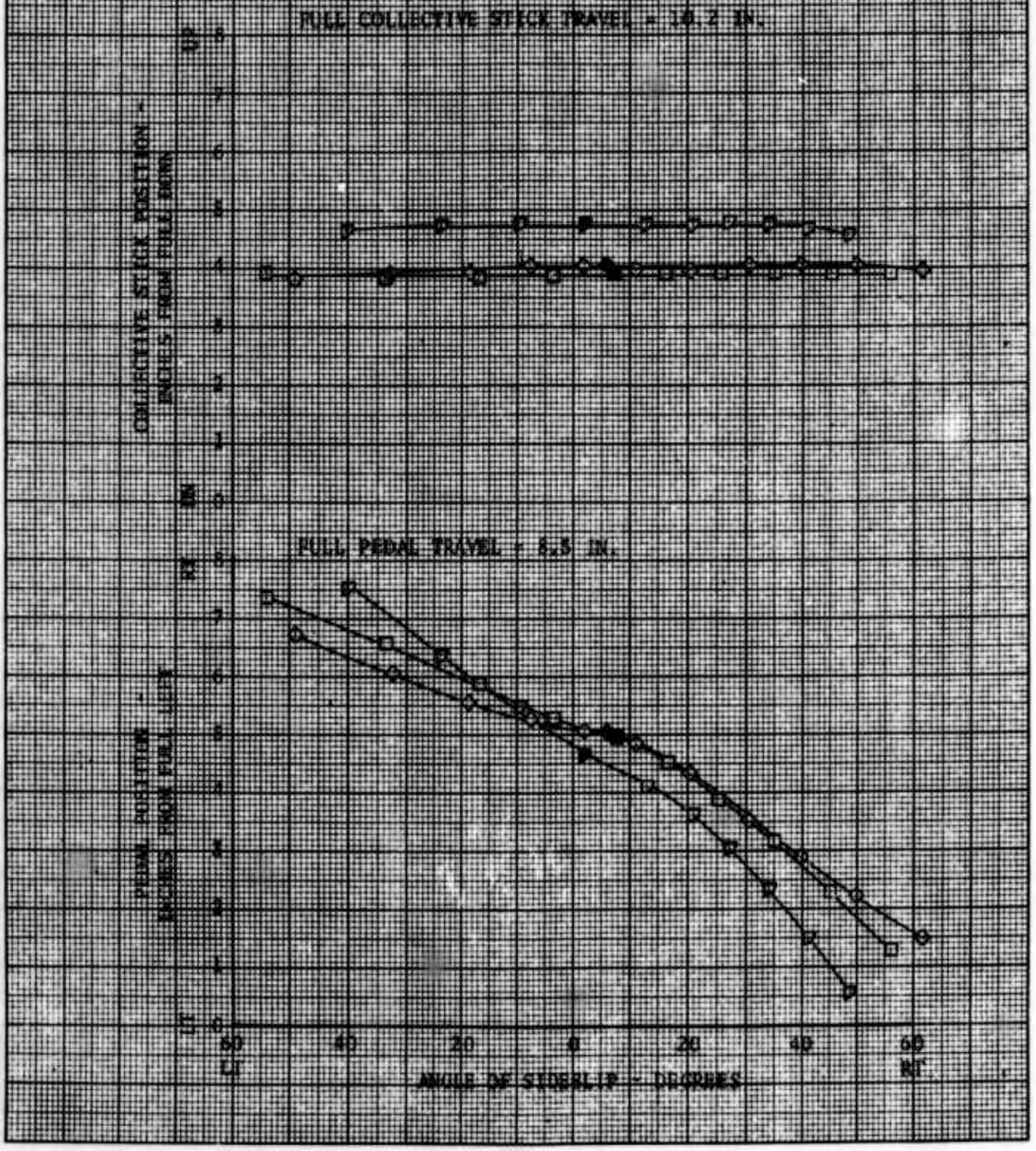

FIGURE 14

STATIC LATERAL DIRECTIONAL STABILITY

SYMBOL	FLIGHT CONDITION	A/C CG STATION (% MAC)	AVG GROSS WT. (LB)	PRESSURE ALTITUDE (FT)	RADIO ALT. (FT)	CALIB. AIRSPEED (KCAS)	GAT (°C)
○	Level	99.3 (AFT)	3041	3200	483	35	0
○	Level	99.0 (AFT)	2640	3200	480	47	0
○	Level	99.1 (AFT)	2060	3200	483	57	0
●	Level	99.2 (AFT)	1670	3200	483	80	0

NOTES: 1. Standard Stabilizer.
2. Shaded symbols denote left turn.

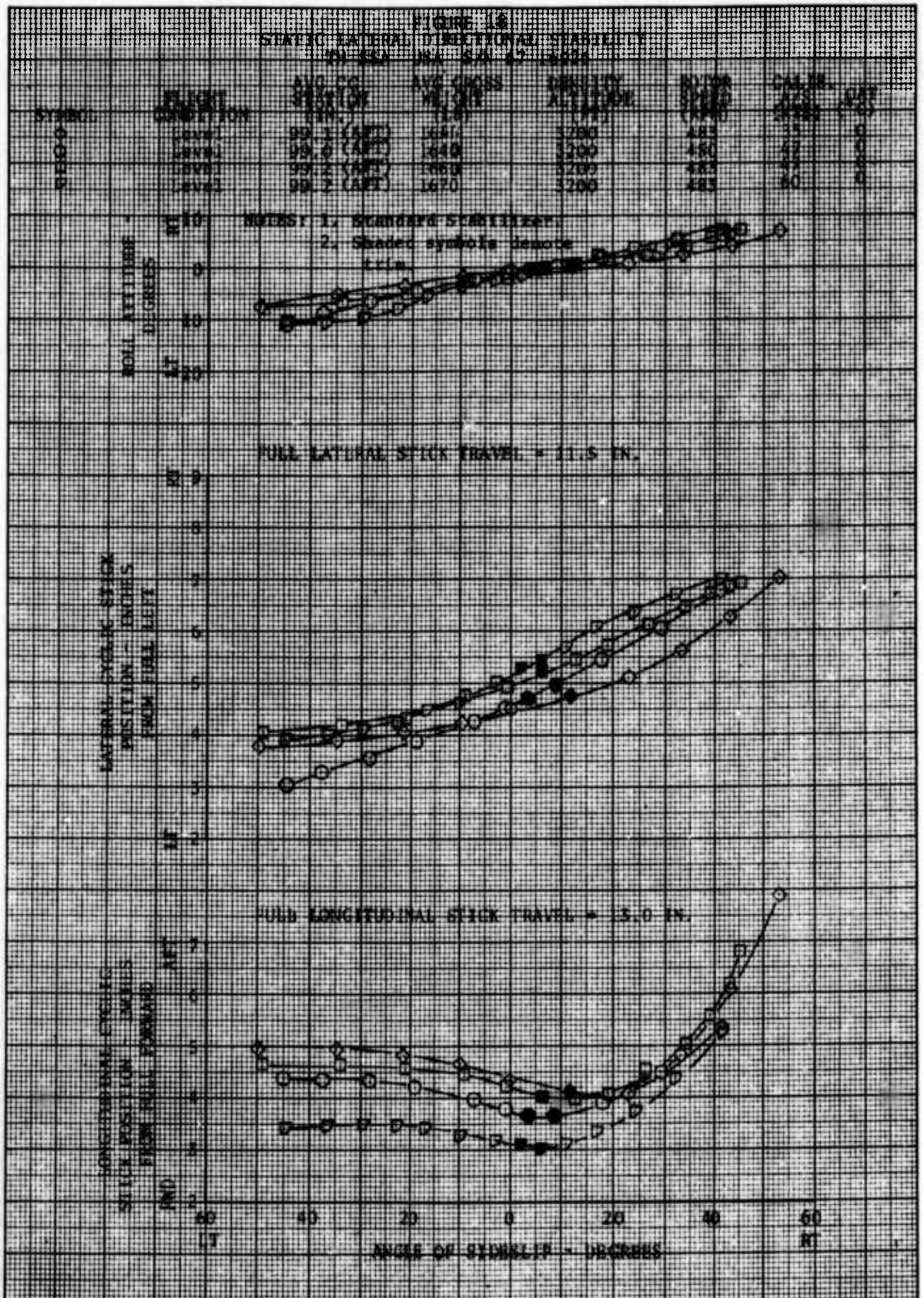

FIGURE 19 (CONCLUDED)

STATIC LATERAL-DIRECTIONAL STABILITY

TH-57A BCA S/N 67-16575

SYMBOL	FLIGHT CONDITION	APP. CG STATION (IN.)	AVG GROSS WEIGHT (LB)	DENSITY ALTITUDE (FT)	ROTOR SPEED (RPM)	CALIB. AIRS (KTAS)	OAT (°C)
◇	LEVEL	98.3 (AFT)	1640	5200	400	70	4
○	LEVEL	99.0 (AFT)	1648	5200	400	70	4
□	LEVEL	99.2 (AFT)	1659	5200	400	70	4
▷	LEVEL	99.2 (AFT)	1679	5200	400	70	4

NOTES: 1. STANDARD CONFIGURATION

2. SHAFT APPROX. PARALLEL TO AIR

FULL COLLECTIVE STICK TRAVEL = 10.2 IN.

CHANGE IN COLLECTIVE STICK POSITION, IN. FROM TRIM

FULL PEDAL TRAVEL = 8.5 IN.

CHANGE IN PEDAL POSITION, IN. FROM TRIM

60 LT 40 20 0 20 40 60 RT

ANGLE OF SIDESLIP, DEGREES

FIGURE 14

STATIC LATERAL DIRECTIONAL STABILITY

TH-55A USA S/N 67-16926

SYMBOL	FLIGHT CONDITION	AVG. CG STATION (IN.)	AVG GROSS WEIGHT (LB)	DENSITY ALTITUDE (FT)	ROTOR SPEED (RPM)	CALIB. A/S (KTS)	CALIB. OAT (°C)
□	Level	99.4 (AFT)	1660	4200	485	67	9

NOTES: 1. Standard Stabilizer with Canopy Skirt Removed.
2. Shaded symbols denote trim.

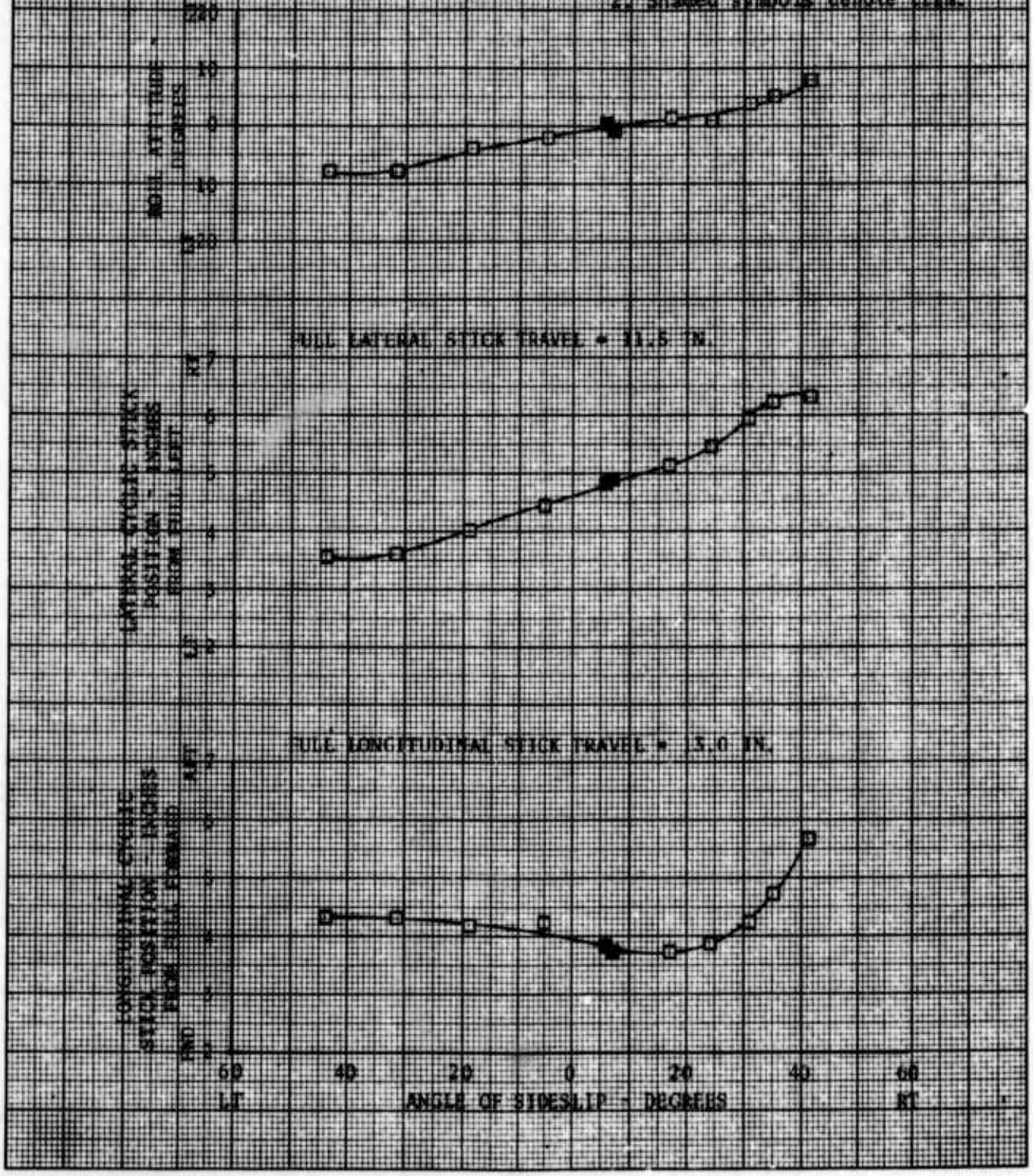

FIGURE 39 (CONCLUDED)

STATIC LATERAL DIRECTIONAL STABILITY

TM 55A USA S/N 67-15829

SYMBOL	FLIGHT CONDITION	AVG. CG STATION (IN.)	AVG GROSS WEIGHT (LB)	DENSITY ALTITUDE (FT)	ROTOR SPEED (RPM)	CYCLIC A/S (KIAS)	OAT (°C)
○	Level	99.4 (AFT)	3660	4200	185	47	9

NOTES: 1. Standard Stabilizer with Canopy Slat Removed.
2. Shaded symbols denote trim.

FULL COLLECTIVE STICK TRAVEL = 10.2 IN.

COLLECTIVE STICK POSITION FROM FULL DOWN, INCHES

FULL PEDAL TRAVEL = 6.5 IN.

PEDAL POSITION FROM FULL LEFT, INCHES

LT ANGLE OF SIDESLIP - DEGREES RT

FIGURE 28

STATIC LATERAL DIRECTIONAL STABILITY

YF-5SA USA S/N 67-18926

SYMBOL	FLIGHT CONDITION	AVG CG STATION (IN.)	AVG GROSS WEIGHT (LB)	DENSITY ALTITUDE (FT)	ROTOR SPEED (RPM)	CALIB. A/S (KTS)	OAT (°C)
	Level	96.2 (PND)	1690	4080	483	92	7

NOTE: 1. Reduced Chord Stabilizer.
2. Shaded Symbol Denote Trim Point.

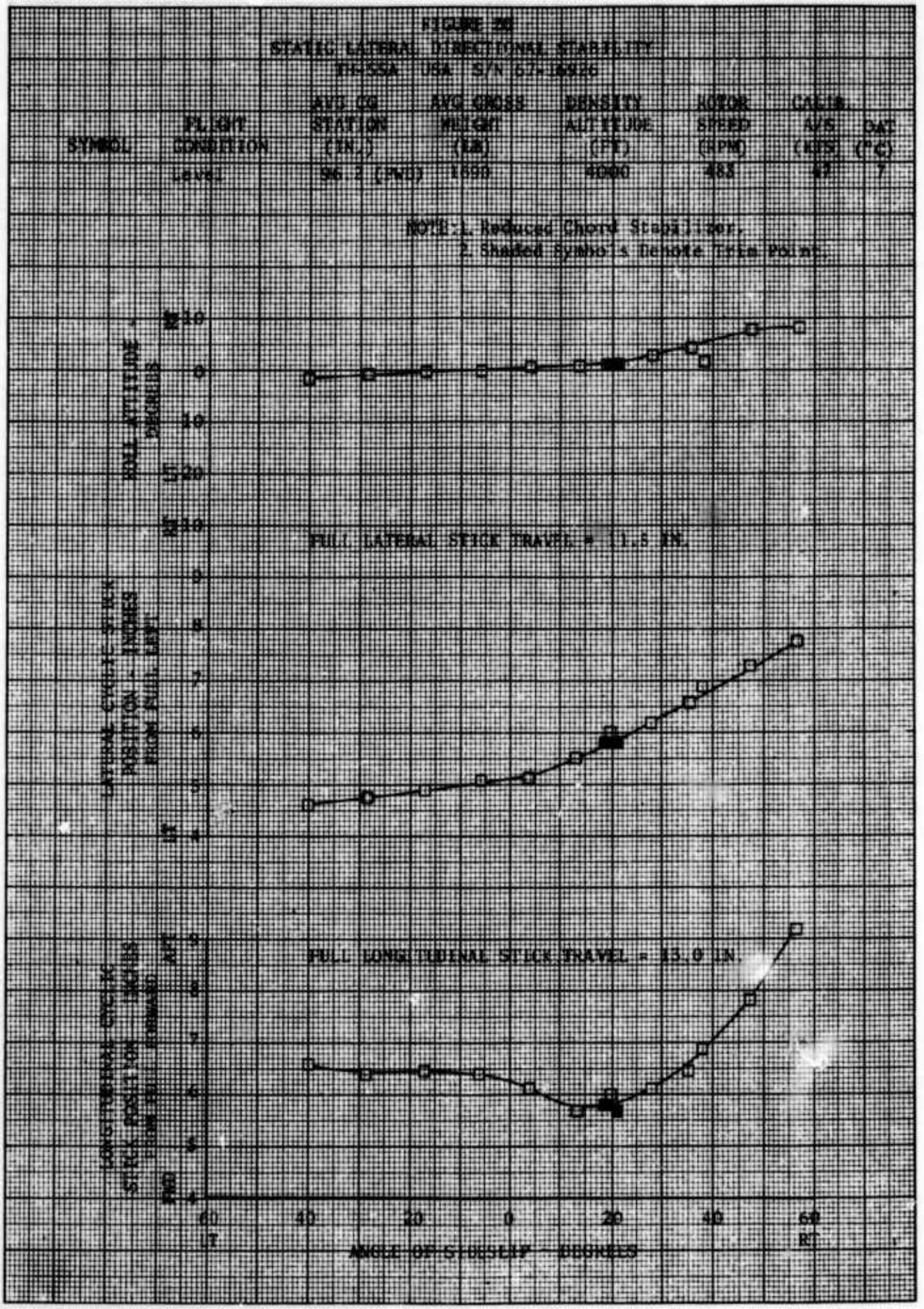

FIGURE 20 (CONCLUDED)

STATIC LATERAL-DIRECTIONAL STABILITY

TH-55A (USA S/N 67-18925)

SYMBOL	FLIGHT CONDITION	AVG. CG STATION (IN.)	AVG GROSS WEIGHT (LB)	DENSITY ALTITUDE (FT)	ROTOR SPEED (RPM)	CALIB. AIRSPEED KCAS	CALIB. AIRSPEED KTAS
□	Level	96.2 (FWD)	1593	4000	485	47	49

NOTE: 1. Reduced Chord Stabilizer
2. Shaded Symbols Denote Trim Point.

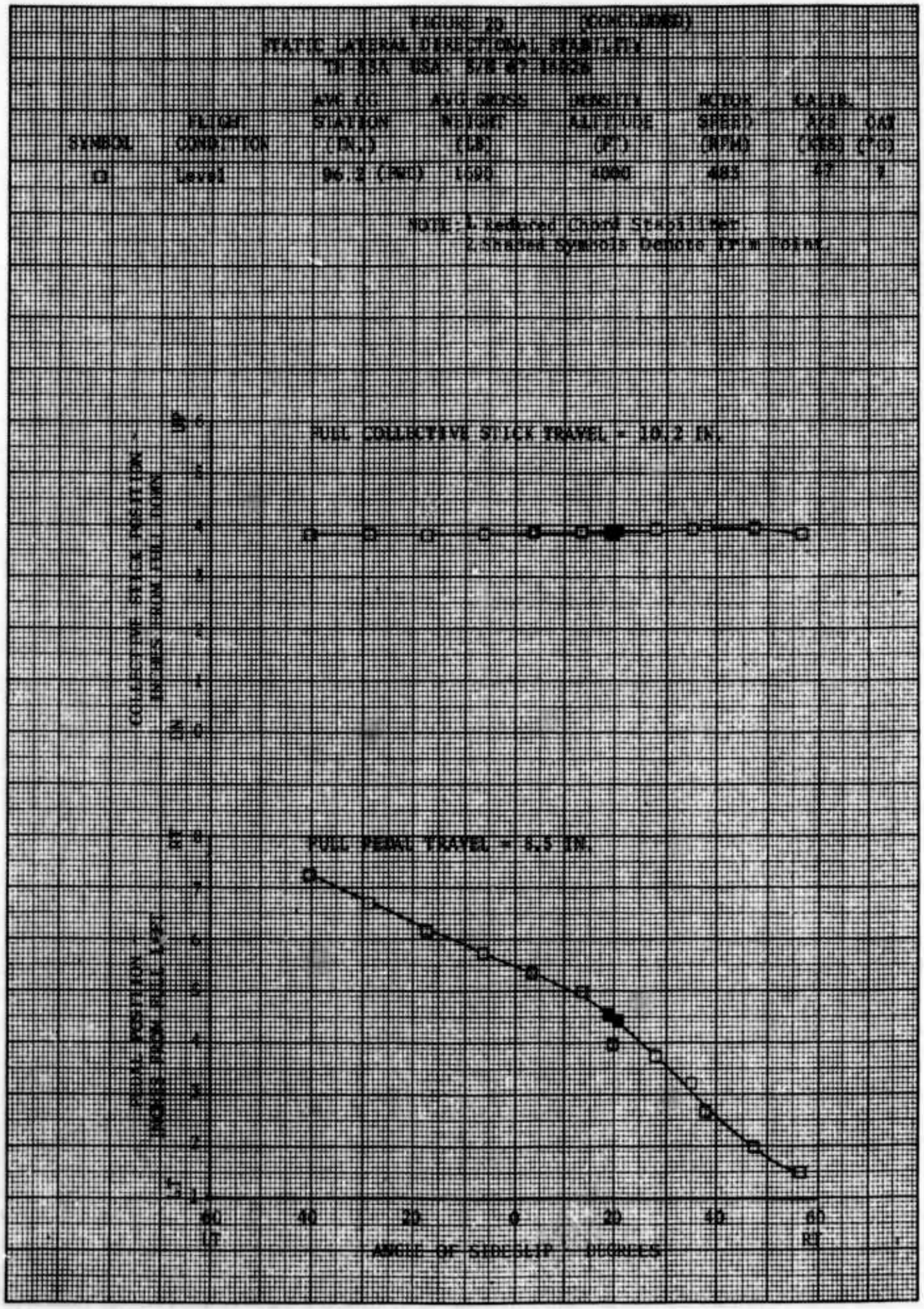

FIGURE 21

STATIC LATERAL DIRECTIONAL STABILITY

SYMBOL	FLIGHT CONDITION	XTR-ESA AVG CG STATION (IN.)	ESA AVG GROSS WEIGHT (LB)	DENSITY ALTITUDE (FT)	ROTOR SPEED (RPM)	CALIB. A/S (KTS)	OAT (°C)
○	Level	99.4 (ARP)	4000	+4490	485	47	10

NOTES: 1. Reduced Chord Stabilizer.
2. Shaded Symbols Denote Trim Point.

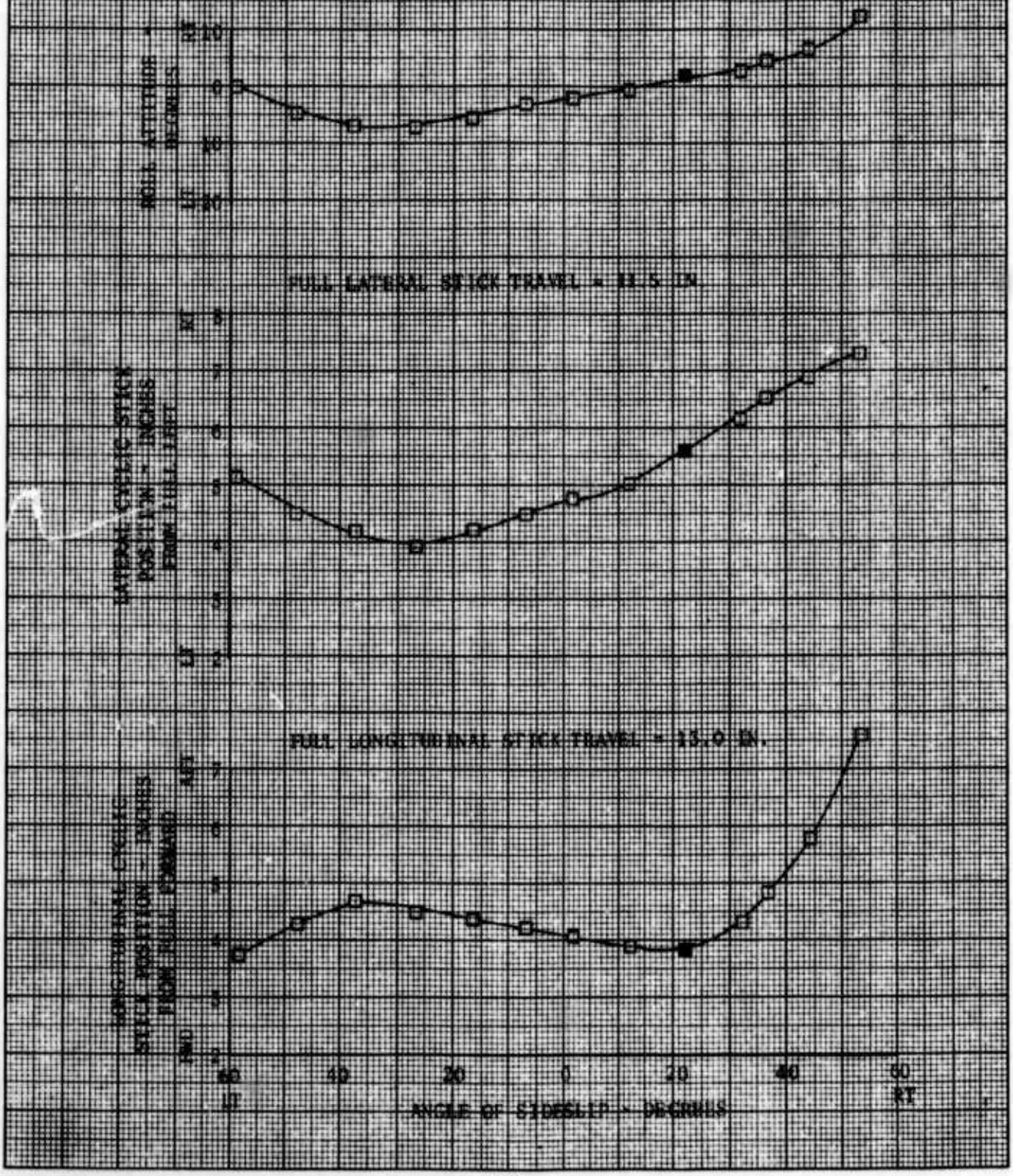

FIGURE 24 (CONCLUDED)

STATIC LATERAL DIRECTIONAL STABILITY

SENSOR USE S/N 67-19976

SYMBOL	FLIGHT CONDITION	AVG CG STATION (IN.)	AVG GROSS WEIGHT (LB)	DENSITY ALTITUDE (FT)	ROTOR SPEED (RPM)	CAL AS A/S (KTS)	OAT (°C)
□	Level	90.4 (AFC)	1560	4400	485	47	10

NOTES: 1. Reduced Chord Stabilizer.
2. Shaded Symbols Denote Trim Point.

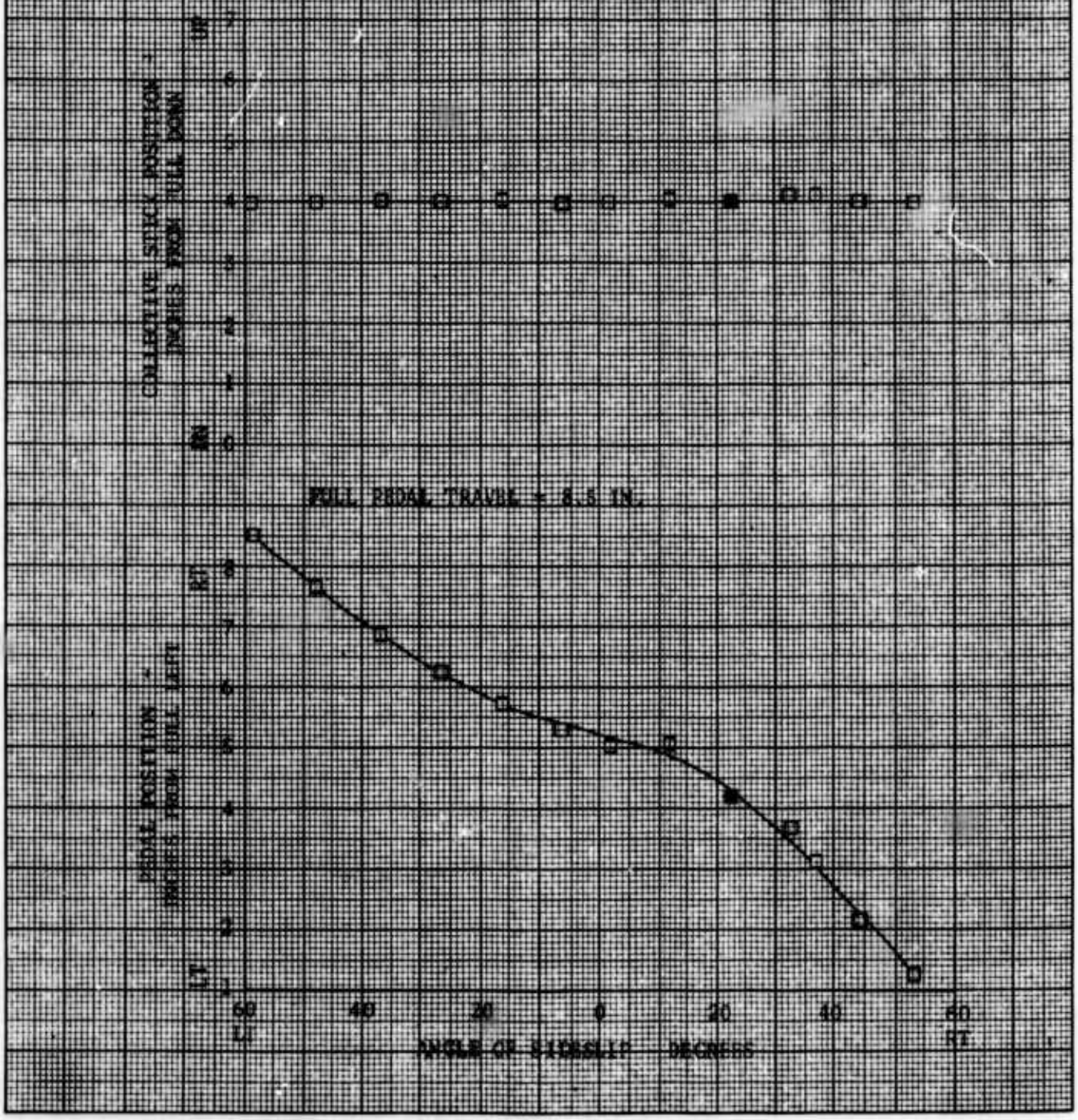

FIGURE 22
AUTOROTATIONAL ENTRY CHARACTERISTICS
TH-55A USA S/N 67-16826

SYMBOL	STABILIZER CONFIGURATION	ENTRY AIRSPEED (KCAS)	FLIGHT CONDITION	DENSITY ALTITUDE (FT)	GROSS WEIGHT (LB)	AVG CG LOCATION (IN.)	OAT (°C)
———	STANDARD	47	LEVEL	4100	1670	95.9 (FWD)	6
- - - -	FINAL REDUCED SPAR	47	LEVEL	5900	1610	96.0 (FWD)	23

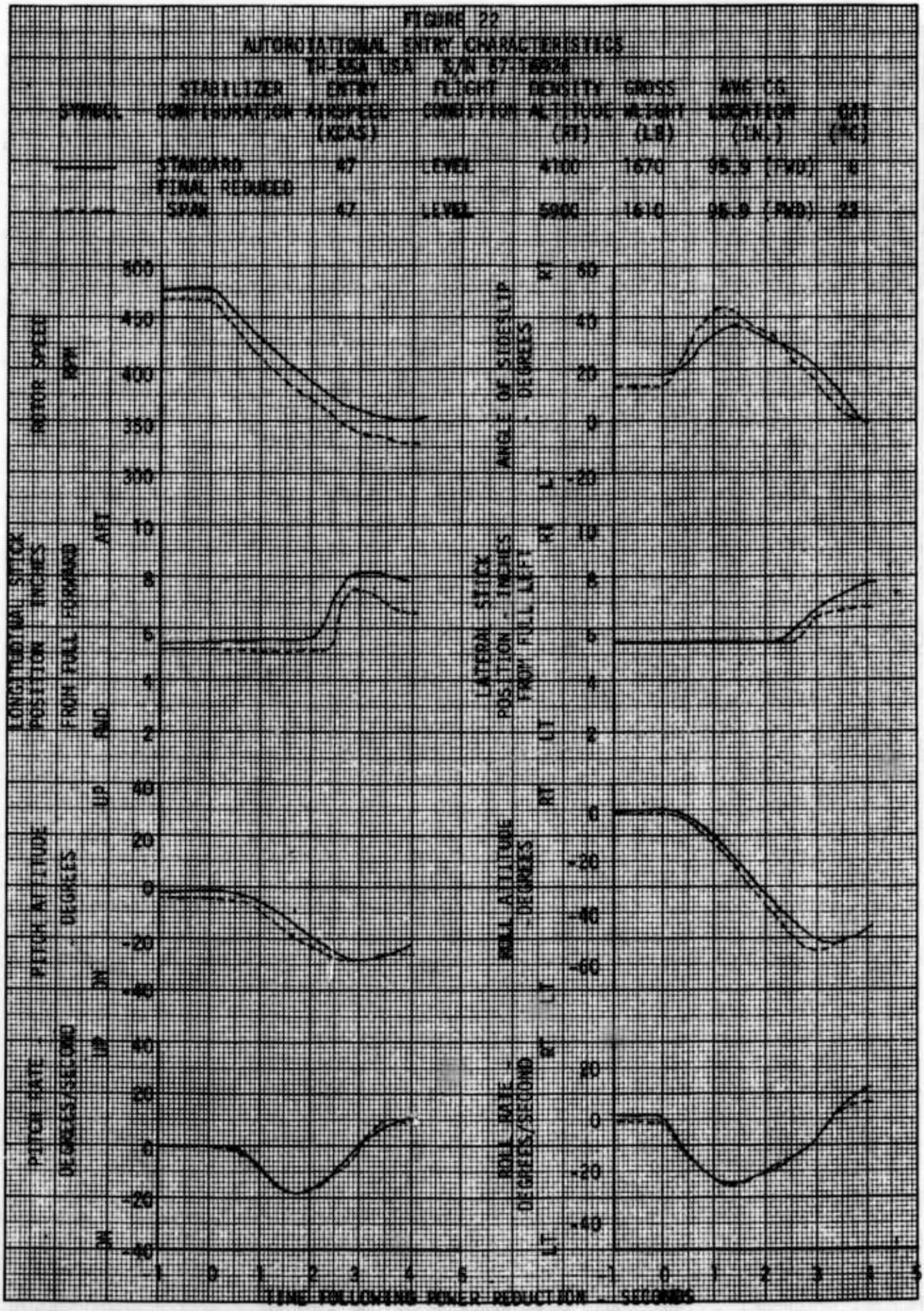

FIGURE 23

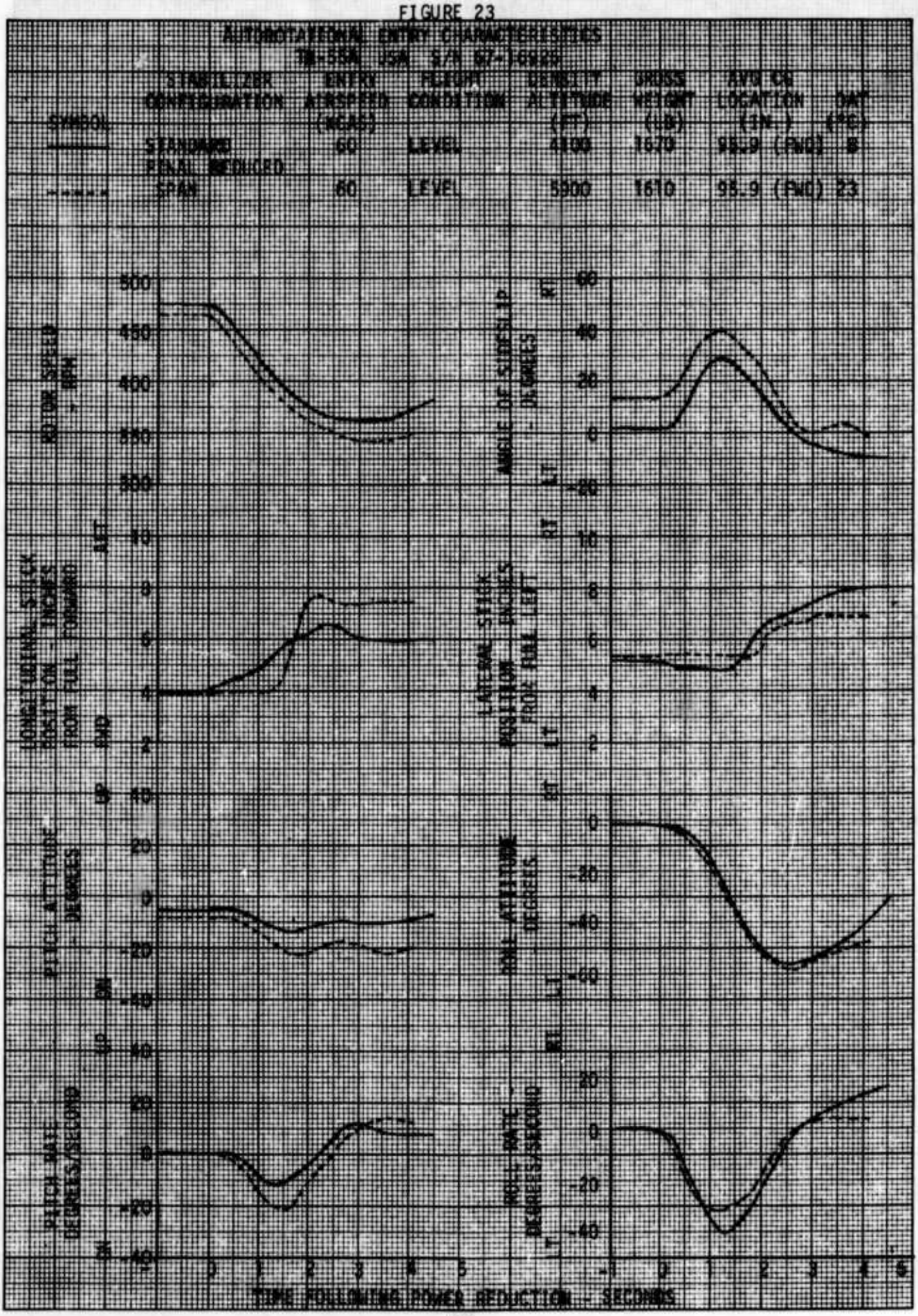
AUTOROTATIONAL ENTRY CHARACTERISTICS
TH-55A USA S/N 67-16563
SYMBOL
STABILIZER CONFIGURATION
ENTRY AIRSPEED (KCAS)
FLIGHT CONDITION
DENSITY ALTITUDE (FT)
GROSS WEIGHT (LB)
CG LOCATION (IN.)
OAT (°C)
STANDARD FINAL REDUCED
SPAN
60
LEVEL
4100
1620
98.9 (FWD)
8
60
LEVEL
5900
1610
98.9 (FWD)
23
ROTOR SPEED RPM
AIRSPEED KNOTS
ANGLE OF SIDESLIP DEGREES
LONGITUDINAL STICK POSITION FROM FULL FORWARD INCHES
LATERAL STICK POSITION FROM FULL LEFT INCHES
PEDAL POSITION FROM FULL LEFT INCHES
PITCH ATTITUDE DEGREES
ROLL ATTITUDE DEGREES
PITCH RATE DEGREES/SECOND
ROLL RATE DEGREES/SECOND
TIME FOLLOWING POWER REDUCTION - SECONDS

FIGURE 24
AUTOROTATIONAL ENTRY CHARACTERISTICS
TM-55A USN S/N 67-16026

SYMBOL	STABILIZER CONFIGURATION	ENTRY AIRSPEED (KCAS)	FLIGHT CONDITION	DENSITY ALTITUDE (FT)	GROSS WEIGHT (LB)	AVG CG LOCATION (IN.)	OAT (°C)
———	STANDARD	50	CLIMB	4100	1670	95.9 (FWD)	8
- - - - -	FINAL REDUCED SPAN	50	CLIMB	5900	1810	95.9 (FWD)	23

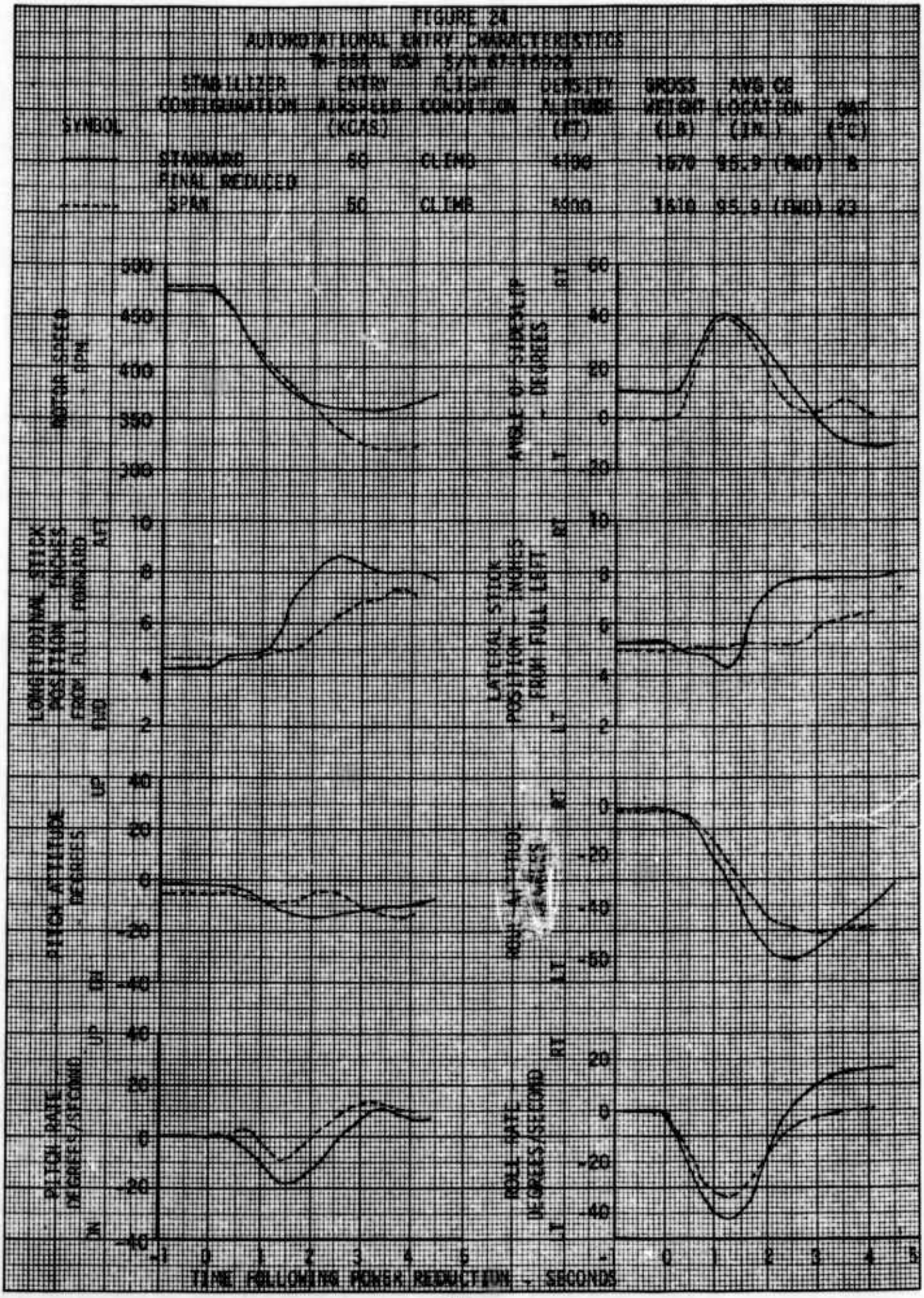

FIGURE 25
AUTOROTATIONAL ENTRY CHARACTERISTICS
TH-55A USA S/N 57-1692[illegible]

SYMBOL	STABILIZER CONFIGURATION	ENTRY AIRSPEED (KCAS)	FLIGHT CONDITION	DENSITY ALTITUDE (FT)	GROSS WEIGHT (LB)	A/C CG LOCATION (IN.)	OAT (°C)
———	STANDARD	47	LEVEL	4500	1670	99.3(AFT)	11
- - - -	FINAL REDUCED SPAN	47	LEVEL	3800	1670	99.3(AFT)	5

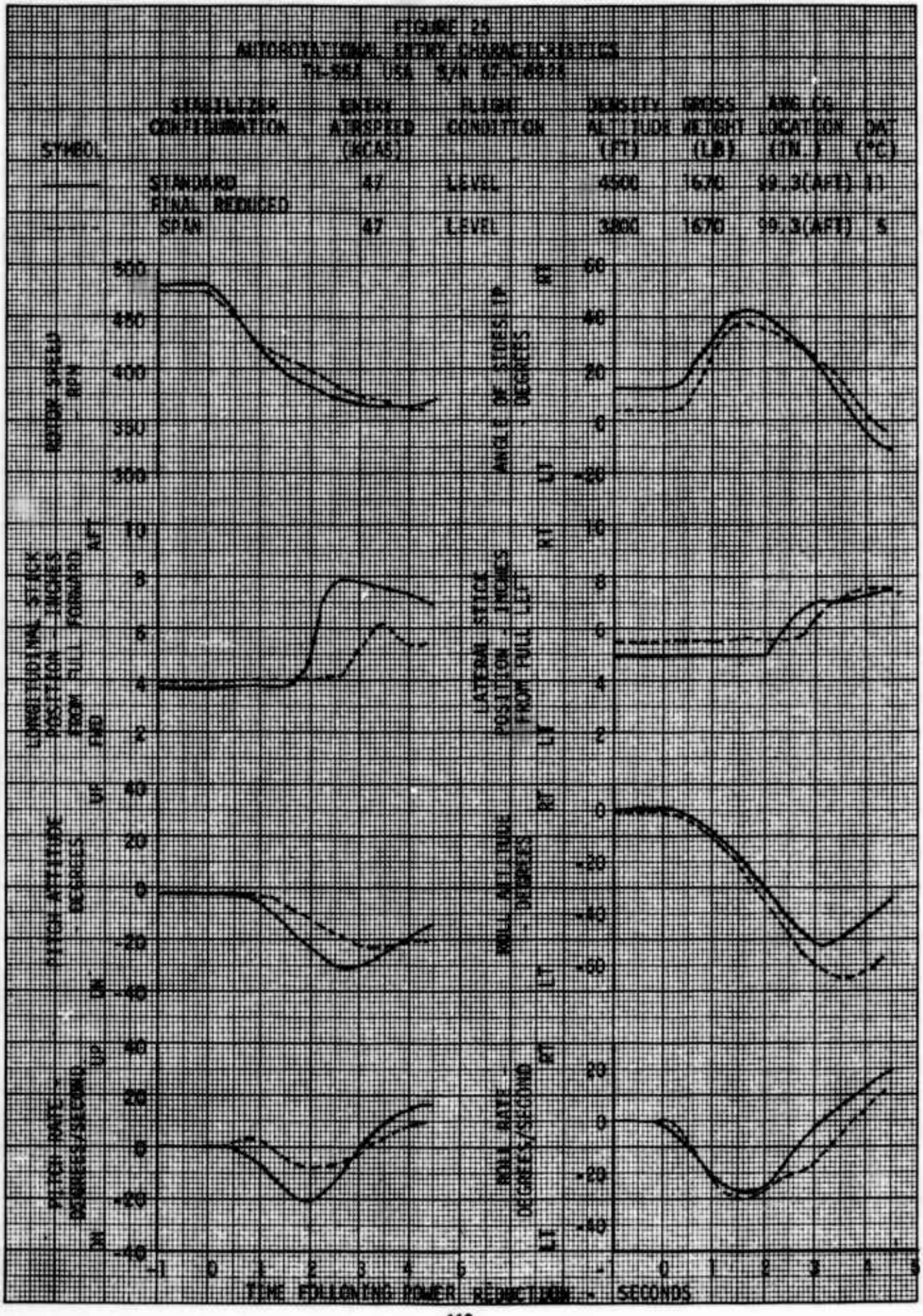

FIGURE 26

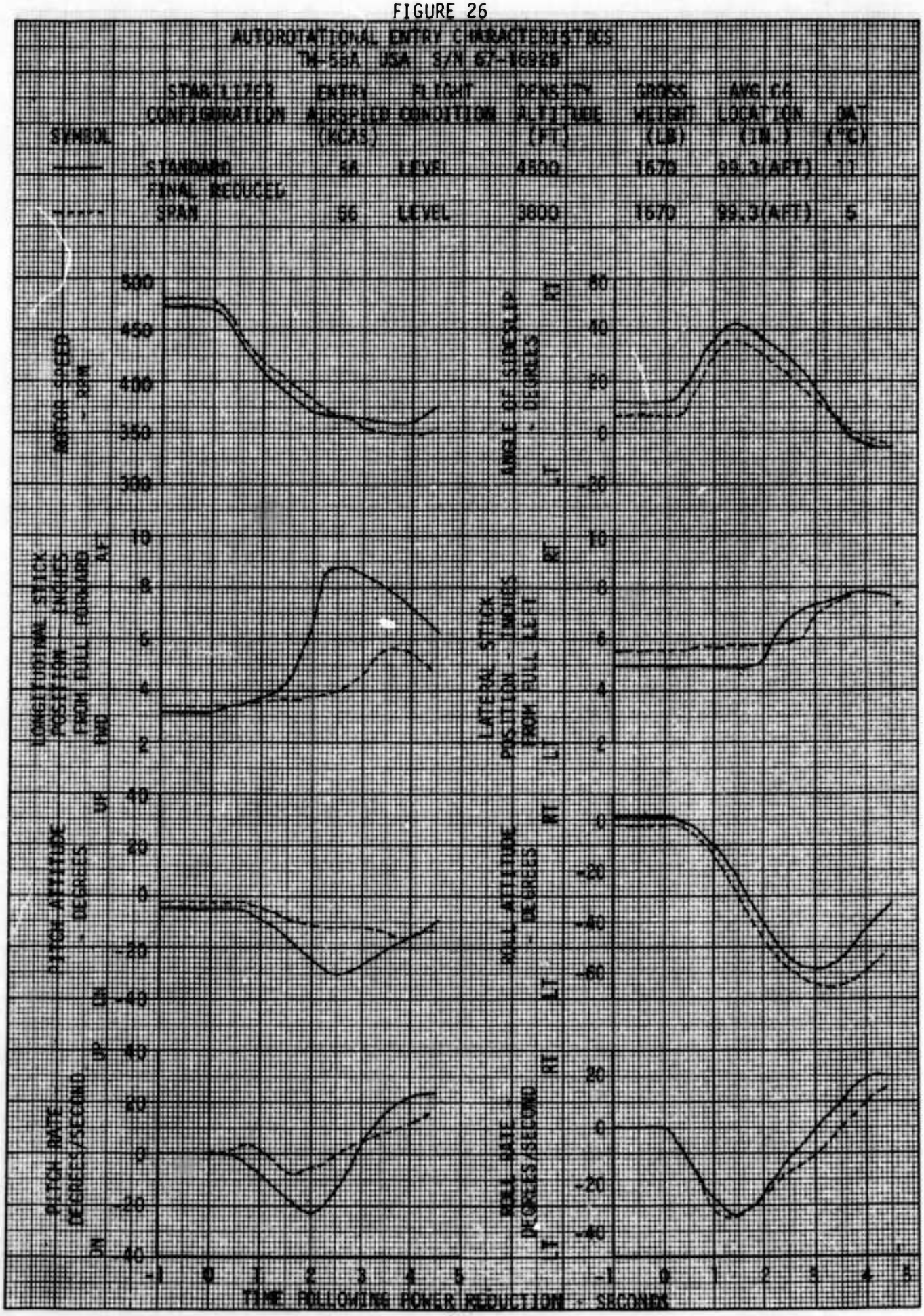
AUTOROTATIONAL ENTRY CHARACTERISTICS
TH-55A USA S/N 67-16926
SYMBOL
STABILIZER CONFIGURATION
ENTRY AIRSPEED (KCAS)
FLIGHT CONDITION
DENSITY ALTITUDE (FT.)
GROSS WEIGHT (LB)
AVG C.G. LOCATION (IN.)
OAT (°C)
STANDARD
55
LEVEL
4800
1670
99.3(AFT)
11
FINAL REDUCED SPAN
55
LEVEL
3800
1670
99.3(AFT)
5
AIRSPEED KCAS
ROTOR RPM
MAIN ROTOR SPEED
LONGITUDINAL STICK POSITION INCHES FROM FULL FORWARD
AFT
FWD
PITCH ATTITUDE DEGREES
NOSE UP
NOSE DOWN
PITCH RATE DEGREES/SECOND
NOSE UP
NOSE DOWN
LATERAL STICK POSITION INCHES FROM FULL LEFT
RT
LT
ROLL ATTITUDE DEGREES
RT
LT
ROLL RATE DEGREES/SECOND
RT
LT
TIME FOLLOWING POWER REDUCTION - SECONDS

FIGURE 27

AUTOROTATIONAL ENTRY CHARACTERISTICS

TH-55A USA S/N 67-16926

SYMBOL	STABILIZER CONFIGURATION	ENTRY AIRSPEED (KCAS)	FLIGHT CONDITION	DENSITY ALTITUDE (FT)	GROSS WEIGHT (LB)	AVG CG LOCATION (IN.)	OAT (°C)
———	STANDARD	60	LEVEL	4500	1670	99.3(AFT)	11
- - - - - -	FINAL REDUCED SPAN	60	LEVEL	3800	1670	99.3(AFT)	5

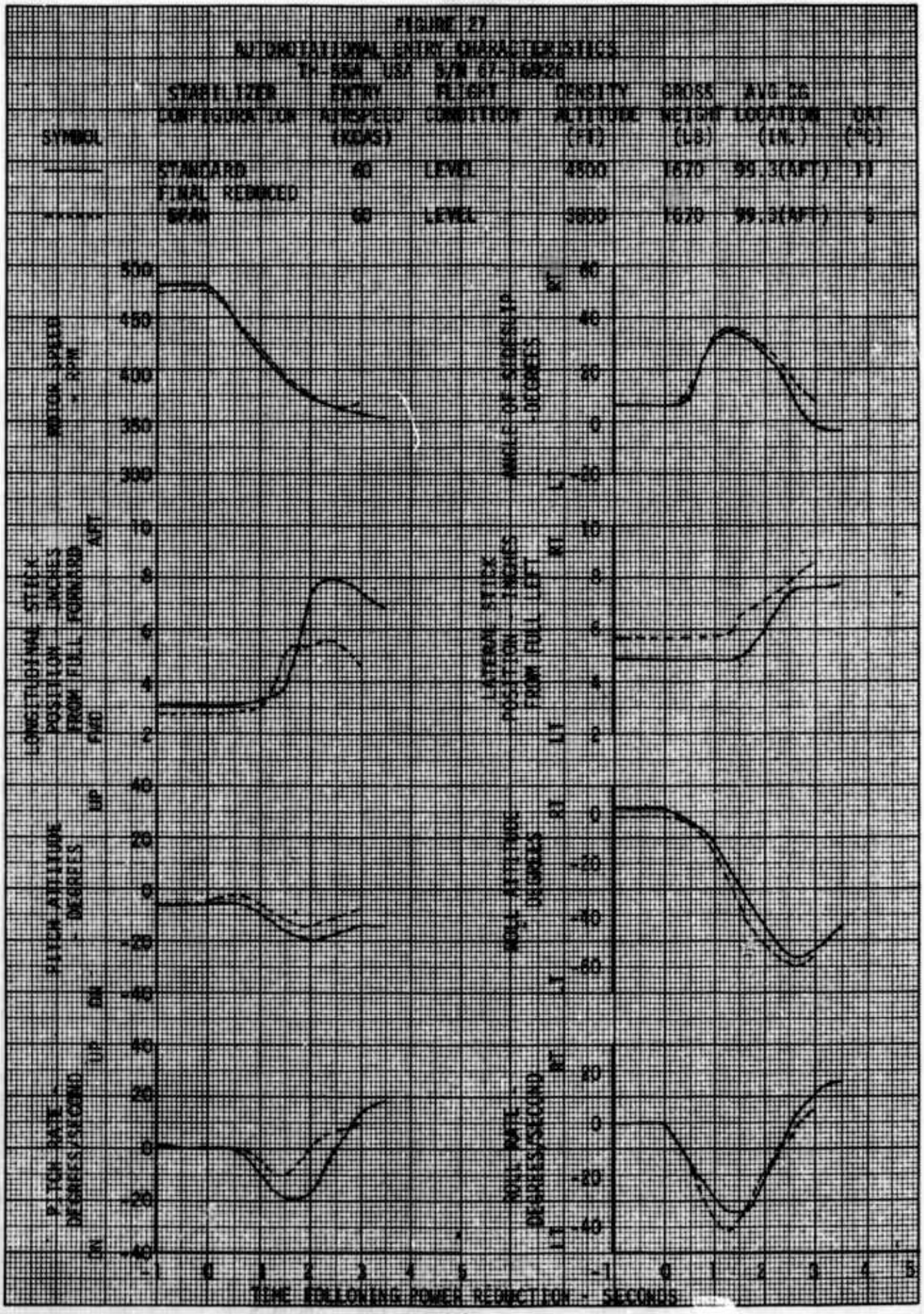

FIGURE 28

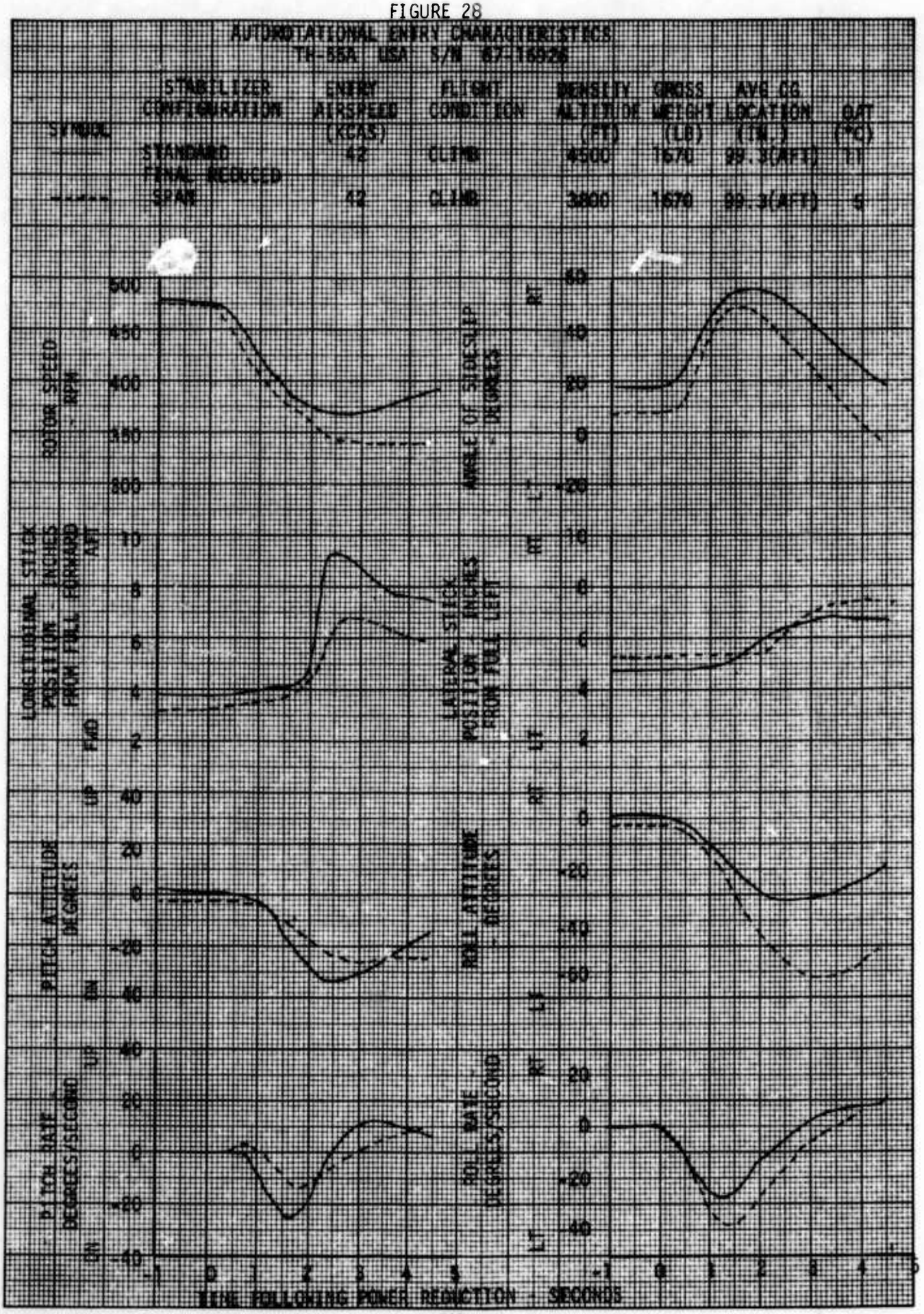
AUTOROTATIONAL ENERY CHARACTERISTICS
TH-55A USA S/N 67-16926
SYMBOL
STABILIZER CONFIGURATION
ENERY AIRSPEED (KCAS)
FLIGHT CONDITION
DENSITY ALTITUDE (FT)
GROSS WEIGHT (LB)
AVG CG LOCATION (IN.)
OAT (°C)
STANDARD
FINAL REDUCED SPAN
42
CLIMB
4500
1670
99.3(AFT)
11
42
CLIMB
3800
1670
99.3(AFT)
5
ROTOR SPEED RPM
LONGITUDINAL STICK POSITION INCHES FROM FULL FORWARD
PITCH ATTITUDE DEGREES
PITCH RATE DEGREES/SECOND
ANGLE OF SIDESLIP DEGREES
LATERAL STICK POSITION INCHES FROM FULL LEFT
ROLL ATTITUDE DEGREES
ROLL RATE DEGREES/SECOND
TIME FOLLOWING POWER REDUCTION - SECONDS

FIGURE 29
AUTOROTATIONAL ENTRY CHARACTERISTICS
TH-55A USN S/N 67-16826

SYMBOL	STABILIZER CONFIGURATION	ENTRY AIRSPEED (KCAS)	FLIGHT CONDITION	DENSITY ALTITUDE (FT)	GROSS WEIGHT (LB)	AVG CG LOCATION (IN.)	OAT (°C)
	STANDARD	50	CLIMB	4600	1670	99.3(AFT)	11
	FINAL REDUCED SPAR	50	CLIMB	3800	1670	99.3(AFT)	6

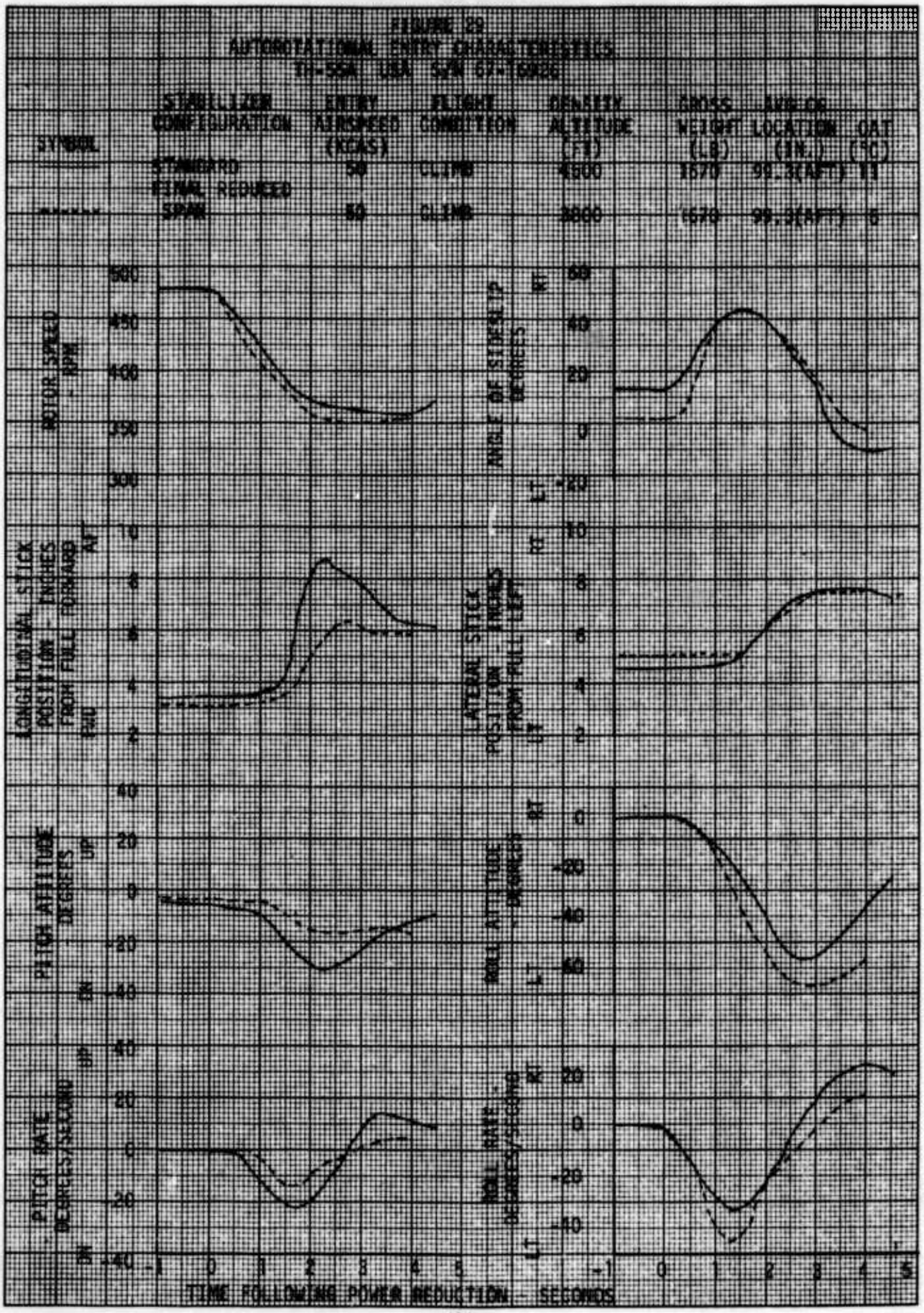

FIGURE 80

ROTOR SPEED DECAY DURING AUTOROTATIONAL ENTRIES

TH-55A OSH S/N 67-16626

SYMBOL	FLIGHT CONDITION	CALIBRATED AIRSPEED (KNOTS)
▽	Hover	0
○	Level	47
□	Level	68
◇	Level	80
▯	Climb	42
△	Climb	50
○	Climb	60
▯	Descent	47

NOTES:

1. Open symbols denote initial rotor speed of 483 RPM.
2. Shaded symbols denote initial rotor speed of 450 RPM.
3. The decay rate is average over the first second.
4. The data is representative of all autorotational entries flown. The average gross weight was 1670 lb and the average density altitude was 4400 ft. The controls were held fixed.

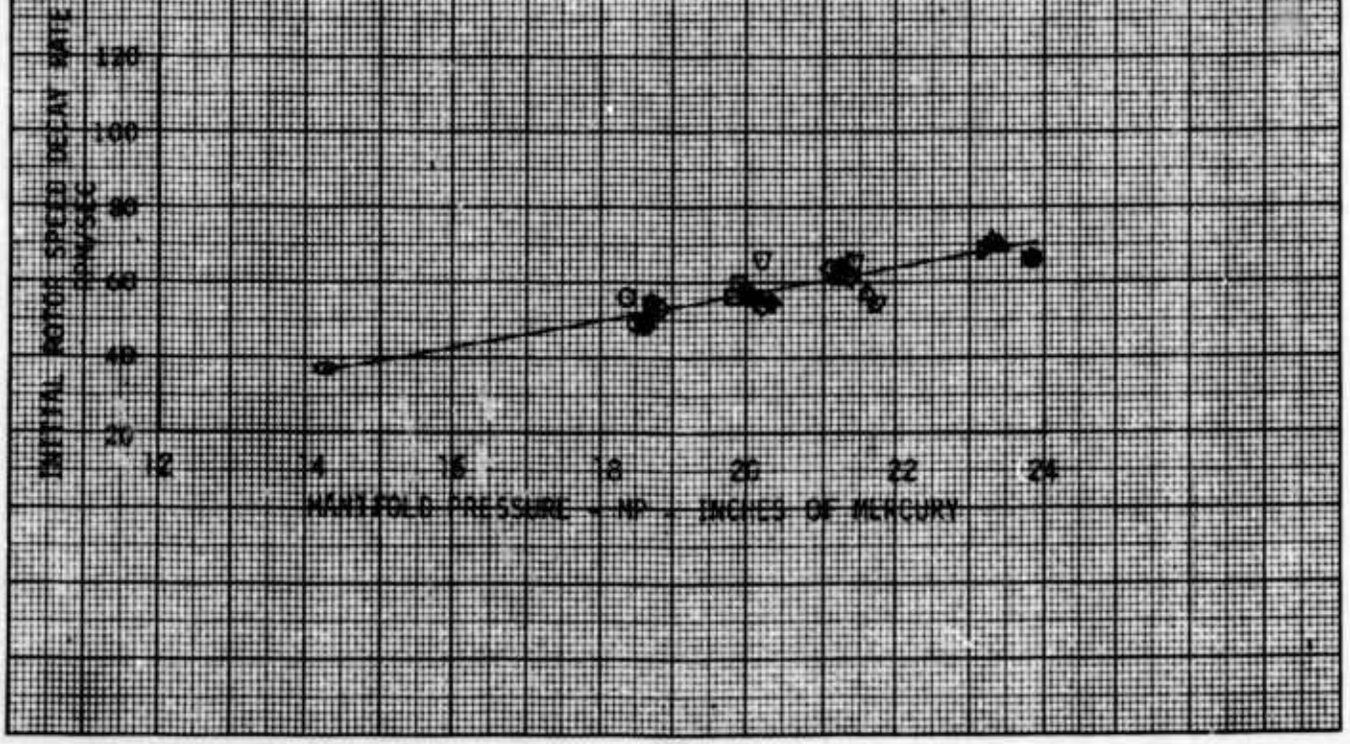

FIGURE 34

CONTROL POSITIONS IN REARWARD AND LOW SPEED FLIGHT

XV-15A USA S/N 72-1082A

SYMBOL	AVG CG STATION (IN.)	AVG GROSS WEIGHT (LB)	DENSITY ALTITUDE (FT)	ROTOR SPEED (RPM)	AVG SKID HEIGHT (FT)	OAT (°C)
○	95.2(IND)	1670	2,400	485	10	14
△	90.0(APP)	1610	2,400	485	10	14

NOTE: Fixed Reduced Span Stabilizer

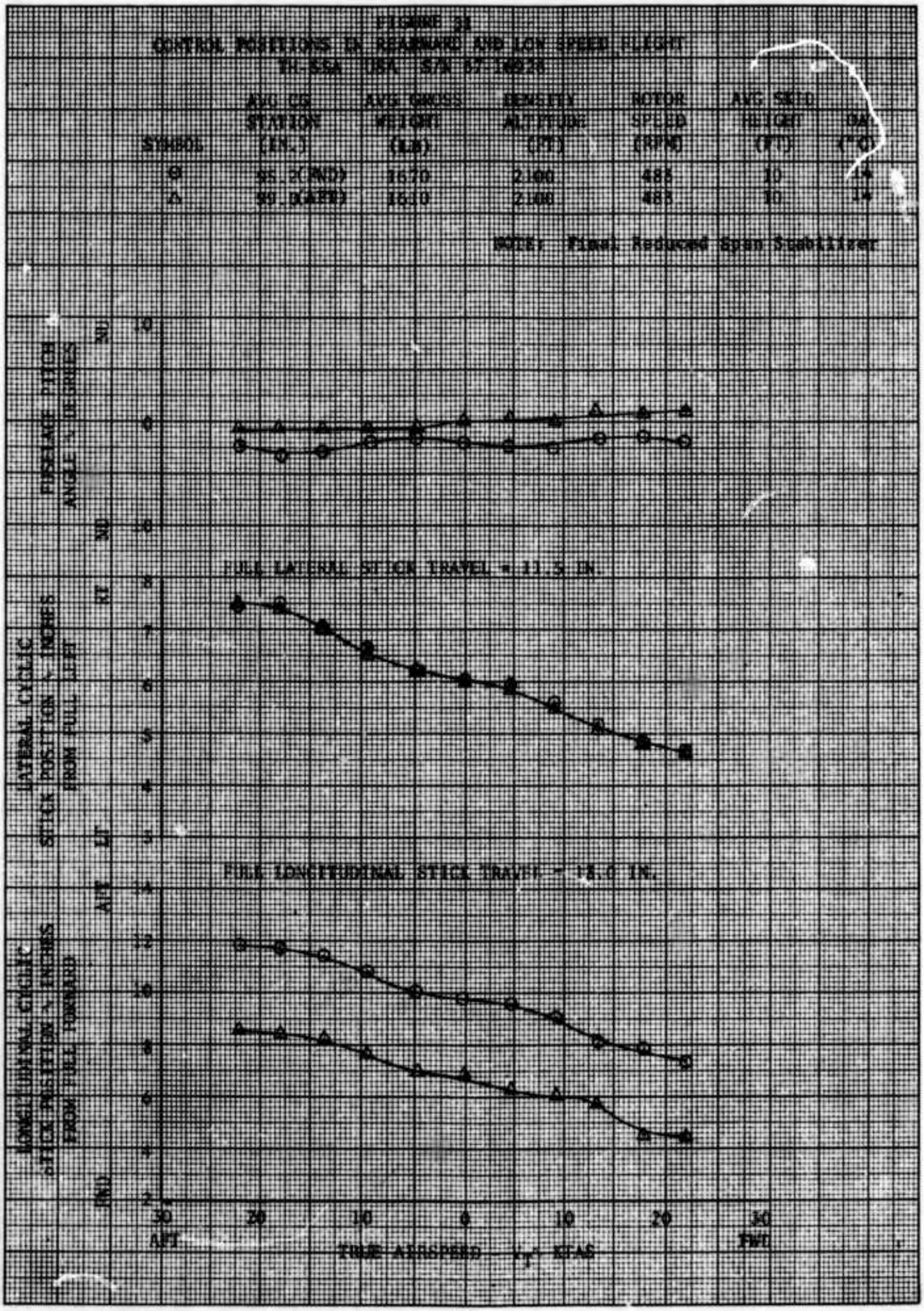

FIGURE 33(CONTINUED)

CONTROL POSITIONS IN REARWARD AND LOW SPEED FLIGHT

TH-55A, ARMY S/N 67-16576

SYMBOL	AVG CG STATION (IN.)	AVG GROSS WEIGHT (LBS)	DENSITY ALTITUDE (FT)	ROTOR SPEED (RPM)	AVG SKID HEIGHT (FT)	OAT (°C)
○	95.2(FWD)	1670	2100	483	10	14
△	99.0(AFT)	1610	2100	483	10	14

NOTE: Final Reduced Swan Stabilizer

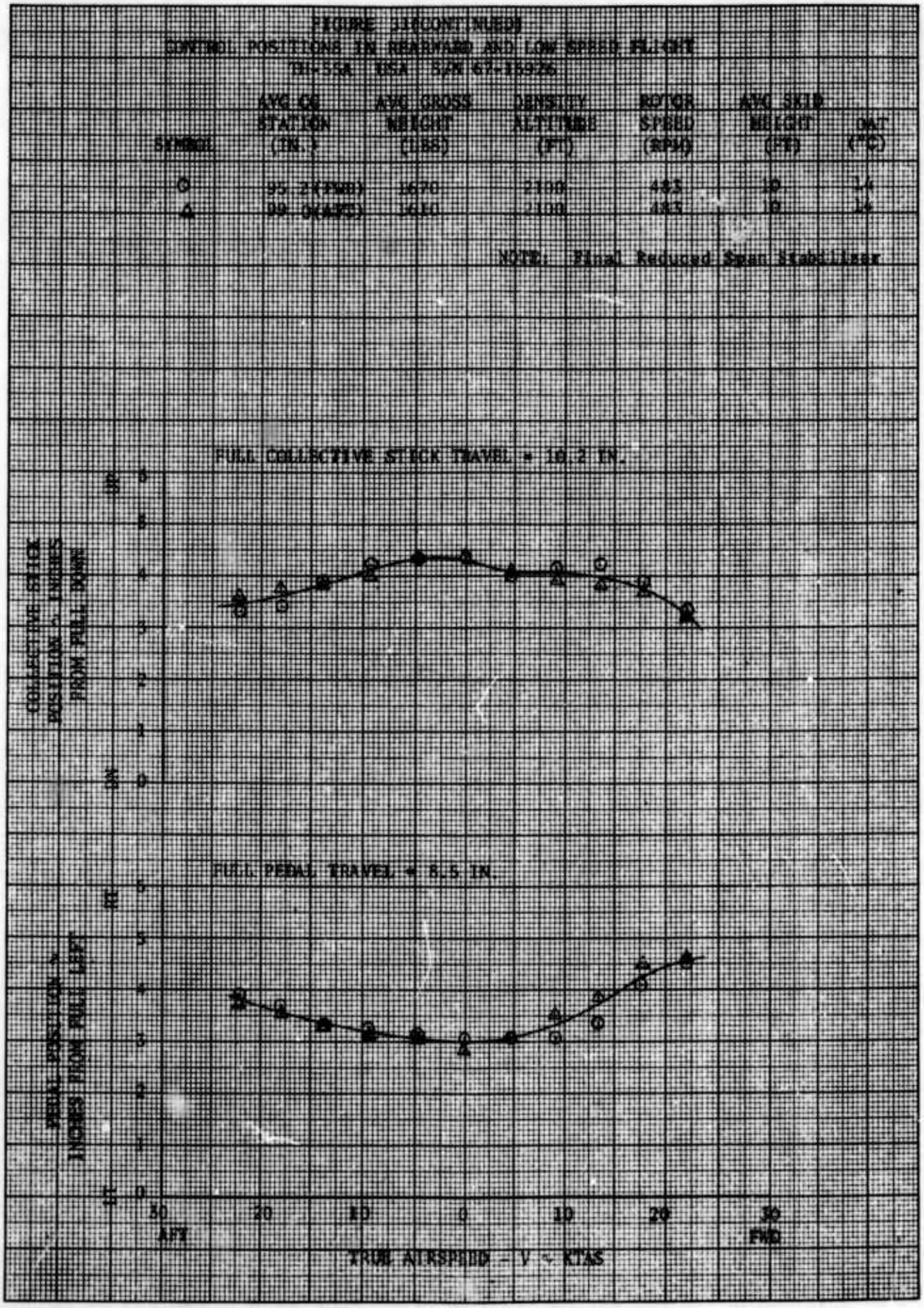

FIGURE 32

CONTROL POSITIONS IN SIDEWARD FLIGHT

TH-55A OSA S/N 67-16926

SYMBOL	AVG CG STATION (IN.)	AVG GROSS WEIGHT (LBS)	DENSITY ALTITUDE (FT)	ROTOR SPEED (RPM)	AVG SKID HEIGHT (FT)	OAT (°C)
○	95.2 (FWD)	1670	2300	483	10	14
△	99 (AFT)	1610	2300	483	10	14

NOTE: Final Reduced Span Stabilizer

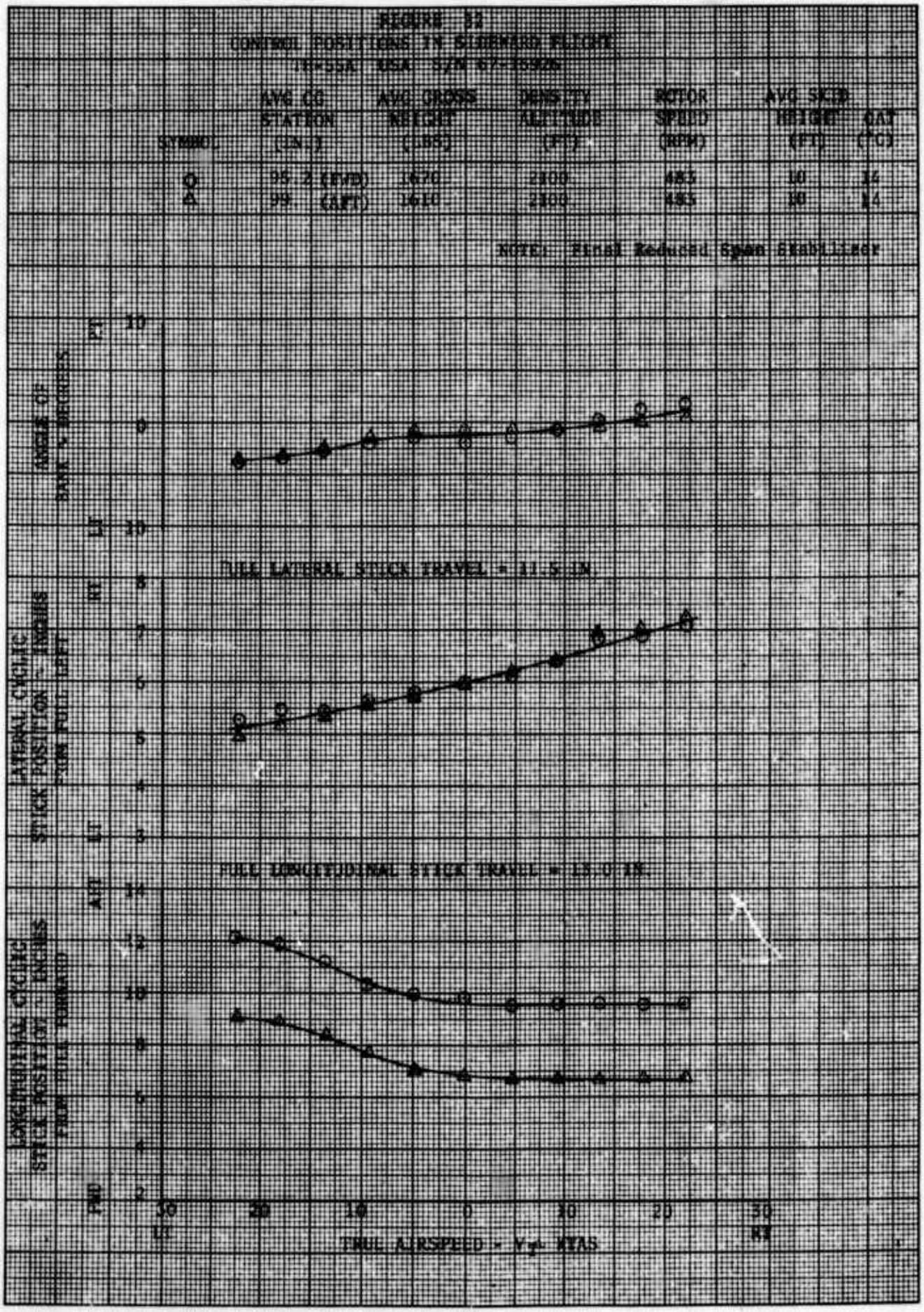

FIGURE 32(CONTINUED)
CONTROL POSITIONS IN SIDEWARD FLIGHT
TH-55A (BSA SN 67-16526)

SYMBOL	AVG CG STATION (IN.)	AVG GROSS WEIGHT (LBS)	DENSITY ALTITUDE (FT)	ROTOR SPEED (RPM)	AVG SKID HEIGHT (FT)	OAT (°C)
○	95.2(FWD)	1670	2,000	483	10	16
△	99.0(AFT)	1610	2,000	483	10	14

NOTE: Final Reduced Span Stabilizer

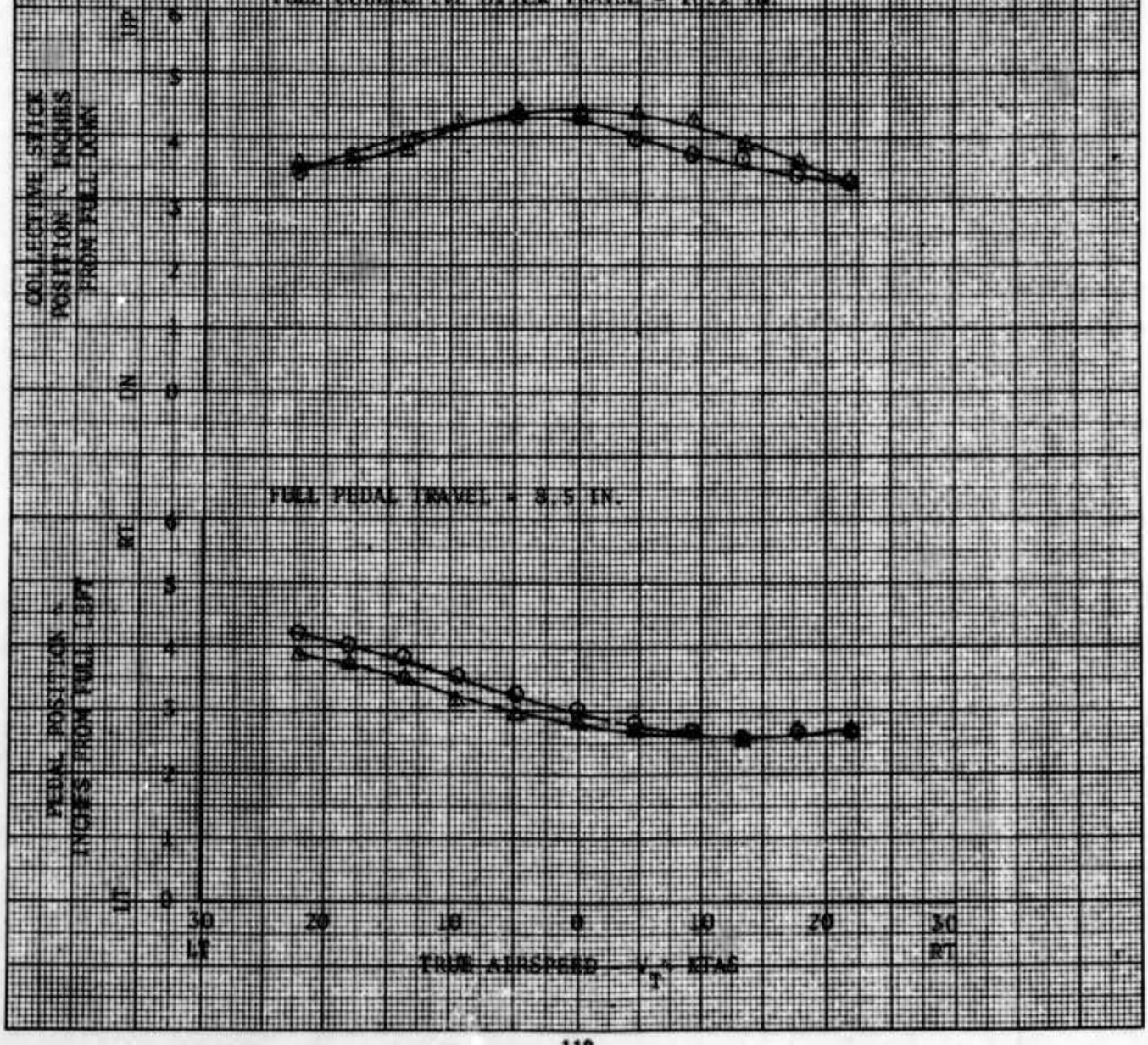

FIGURE 33
CONTROL POSITIONS IN FORWARD FLIGHT
TH-55A (BSA 67-16626)

SYMBOL	FLIGHT CONDITION	AFD CG STATION (IN.)	AVG GROSS WEIGHT (LB)	DENSITY ALTITUDE (FT)	ROTOR SPEED (RPM)	OAT (°C)
○	LEVEL	95.2 (FWD)	1670	4100	483	8
◇	CLIMB	95.2 (FWD)	1670	4100	483	8
▽	AUTO	95.2 (FWD)	1670	4100	483	8

NOTE: Pedal Required Spot Stabilized

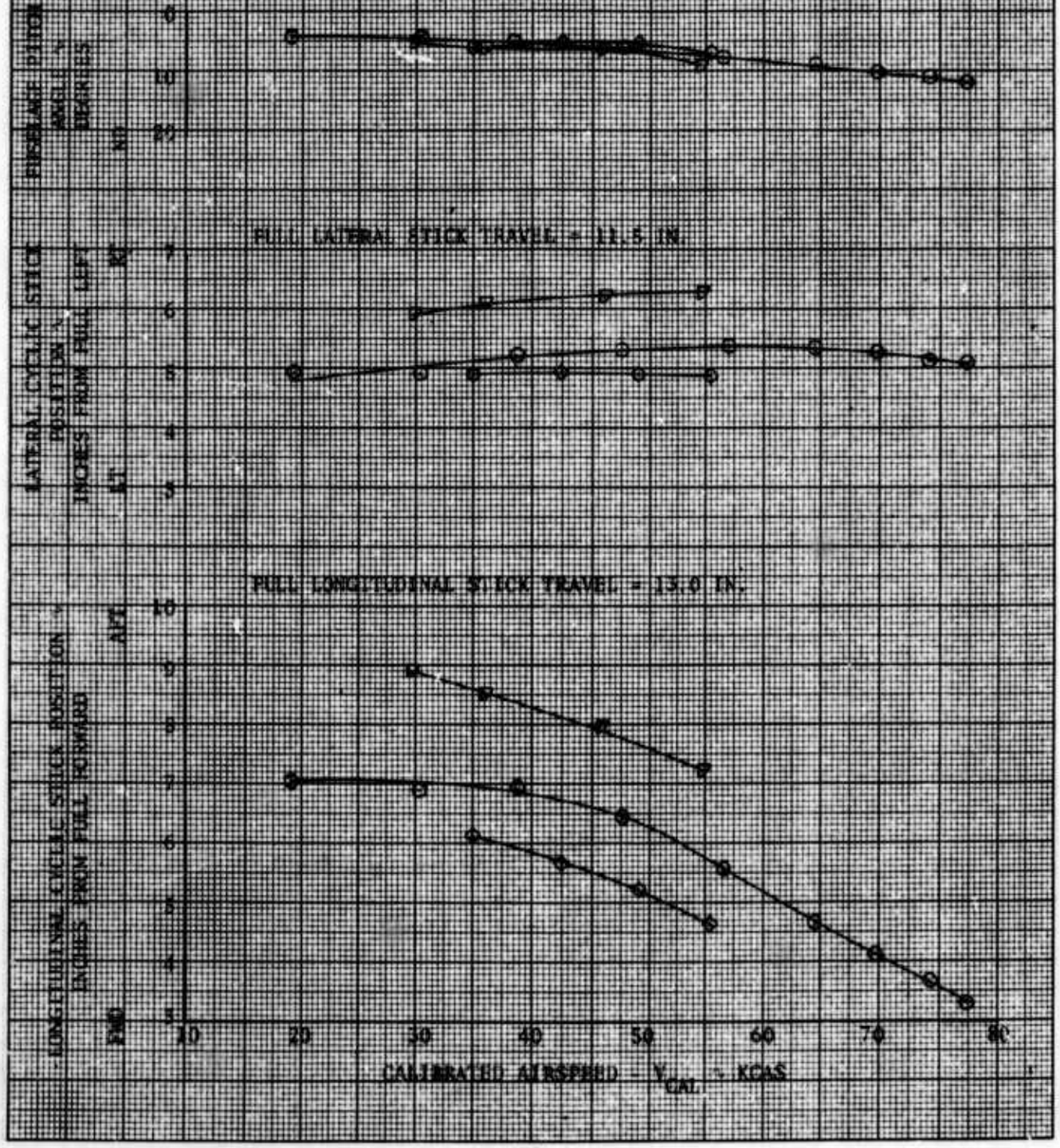

FIGURE 33(CONCLUDED)

CONTROL POSITIONS IN FORWARD FLIGHT

YH-55A USA S/N 67-15826

SYMBOL	FLIGHT CONDITION	AVG CG STATION (IN.)	AVG GROSS WEIGHT (LB)	DENSITY ALTITUDE (FT)	ROTOR SPEED (RPM)	OAT (°C)
○	LEVEL	95.2 (FWD)	1670	4100	483	8
◇	CLIMB	95.2 (FWD)	1670	4100	483	8
▽	AUTO	95.2 (FWD)	1670	4100	483	8

NOTE: Final Recorded Span Stabilizer

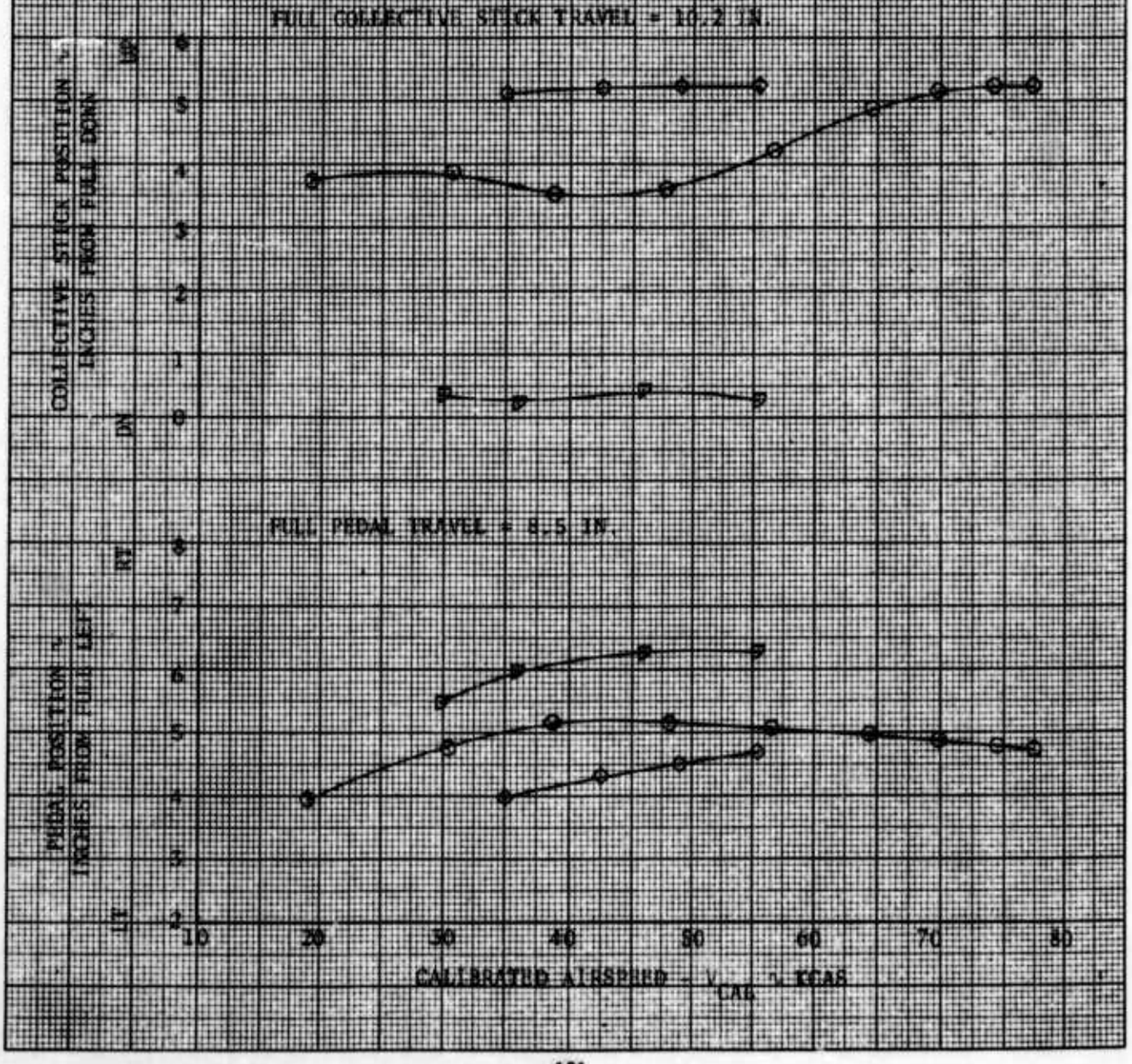

FIGURE 36
CONTROL POSITIONS IN FORWARD FLIGHT
TH-55A USA SN# 67-16566

SYMBOL	FLIGHT CONDITION	AVG CG STATION (IN.)	AVG GROSS WEIGHT (LB)	DENSITY ALTITUDE (FT)	ROTOR SPEED (RPM)	OAT (°C)
○	LEVEL	99.3 (AFT)	1670	4200	485	9
◇	CLIMB	99.3 (AFT)	1670	4200	485	9
▽	AUTO	99.3 (AFT)	1670	4200	485	9

NOTE: Pivot Reduced Span Shaft Utilized

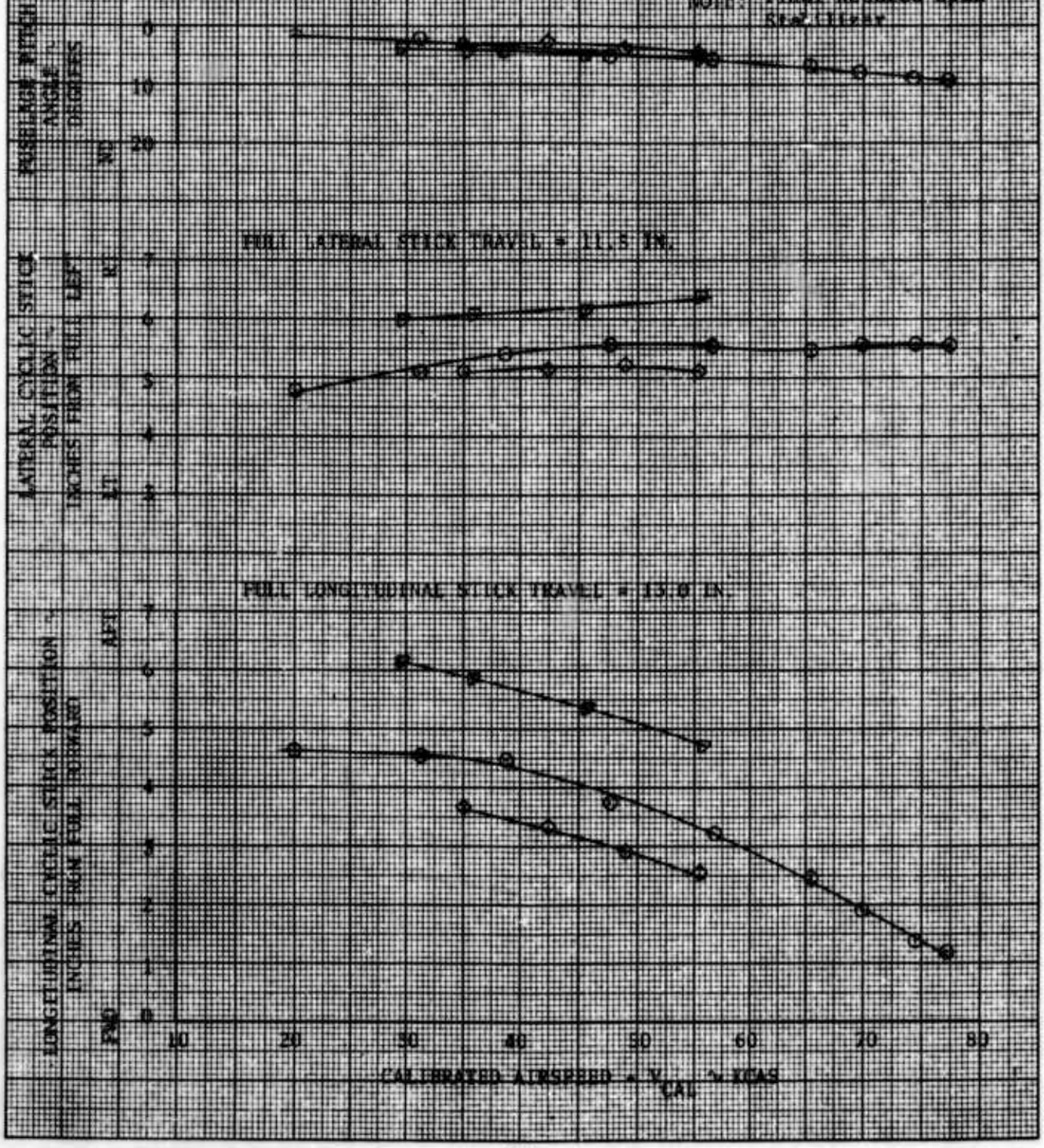

FIGURE 9a (CONCLUDED)

CONTROL POSITIONS IN NORMAL FLIGHT

TH-55A, MSA S/N 67-16526

SYMBOL	FLIGHT CONDITION	AVG CG STATION (IN.)	AVG GROSS WEIGHT (LB)	DENSITY ALTITUDE (FT)	ROTOR SPEED (RPM)	OAT (°C)
○	LEVEL	96.3 (FWD)	1671	4200	485	8
◇	CLIMB	99.3 (FWD)	1670	4200	485	8
△	AUTO	99.3 (FWD)	1670	4200	485	8

NOTE: Steal Reduced Spen Stabilizer

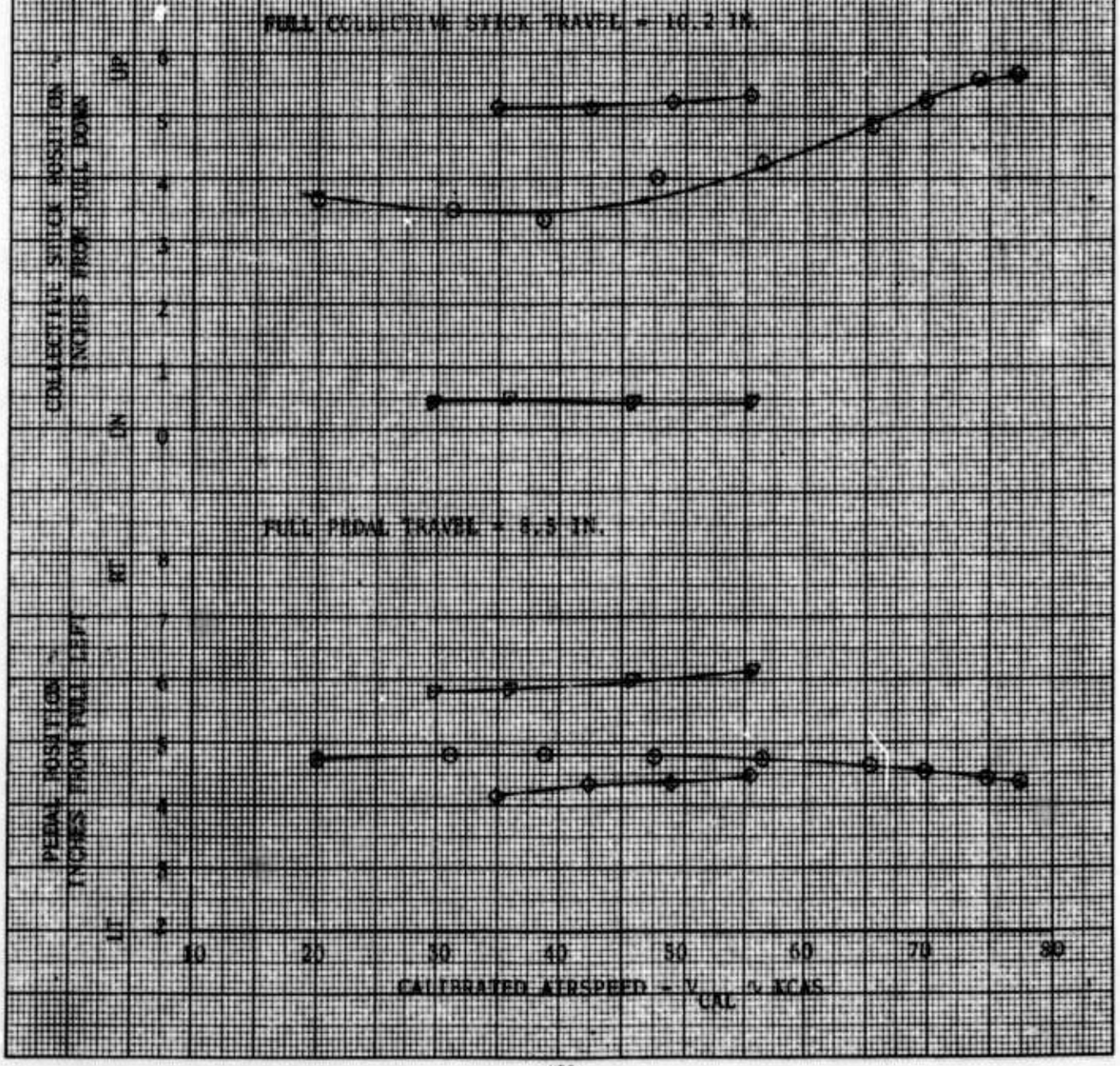

FIGURE 35

STATIC LONGITUDINAL STABILITY

TH-55A, USA S/N 67-16026

SYMBOL	FLIGHT CONDITION	AVG. CG LOCATION (IN.)	AVG. GROSS WEIGHT (LB)	DENSITY ALTITUDE (FT)	ROTOR SPEED (RPM)	OAT (°C)
○	LEVEL	95.2 (AND)	1670	4100	483	8
◇	CLIMB	95.0 (AND)	1620	4100	483	8
△	AUTO	98.0 (AND)	1620	4100	483	8
▽	LEVEL	96.2 (FWD)	1670	5900	483	29

NOTES: 1. Reduced Span Stabilizer
2. Shaded symbol denotes (TRIM)

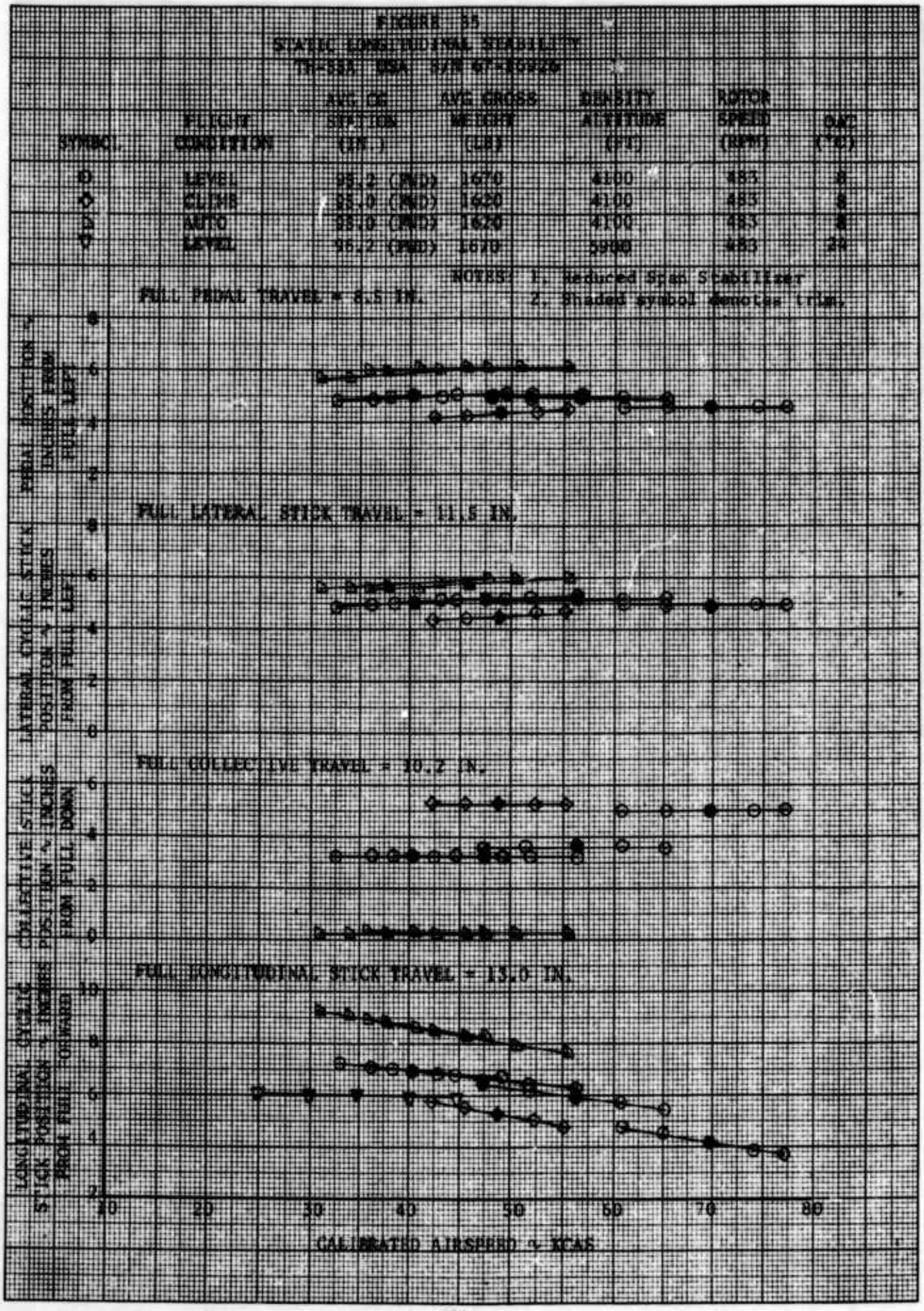

FIGURE 36

STATIC LONGITUDINAL STABILITY

TH-55A USA S/N 67-16826

SYMBOL	FLIGHT CONDITION	AVG CG STATION (IN.)	AVG GROSS WEIGHT (LB)	DENSITY ALTITUDE (FT)	ROTOR SPEED (RPM)	OAT (°C)
○	LEVEL	99.0 (AFT)	1570	4490	483	10
▽	LEVEL	99.2 (AFT)	1670	5900	483	04

NOTES: 1. Reduced Span Stabilizer
2. Shaded symbol denotes trim.

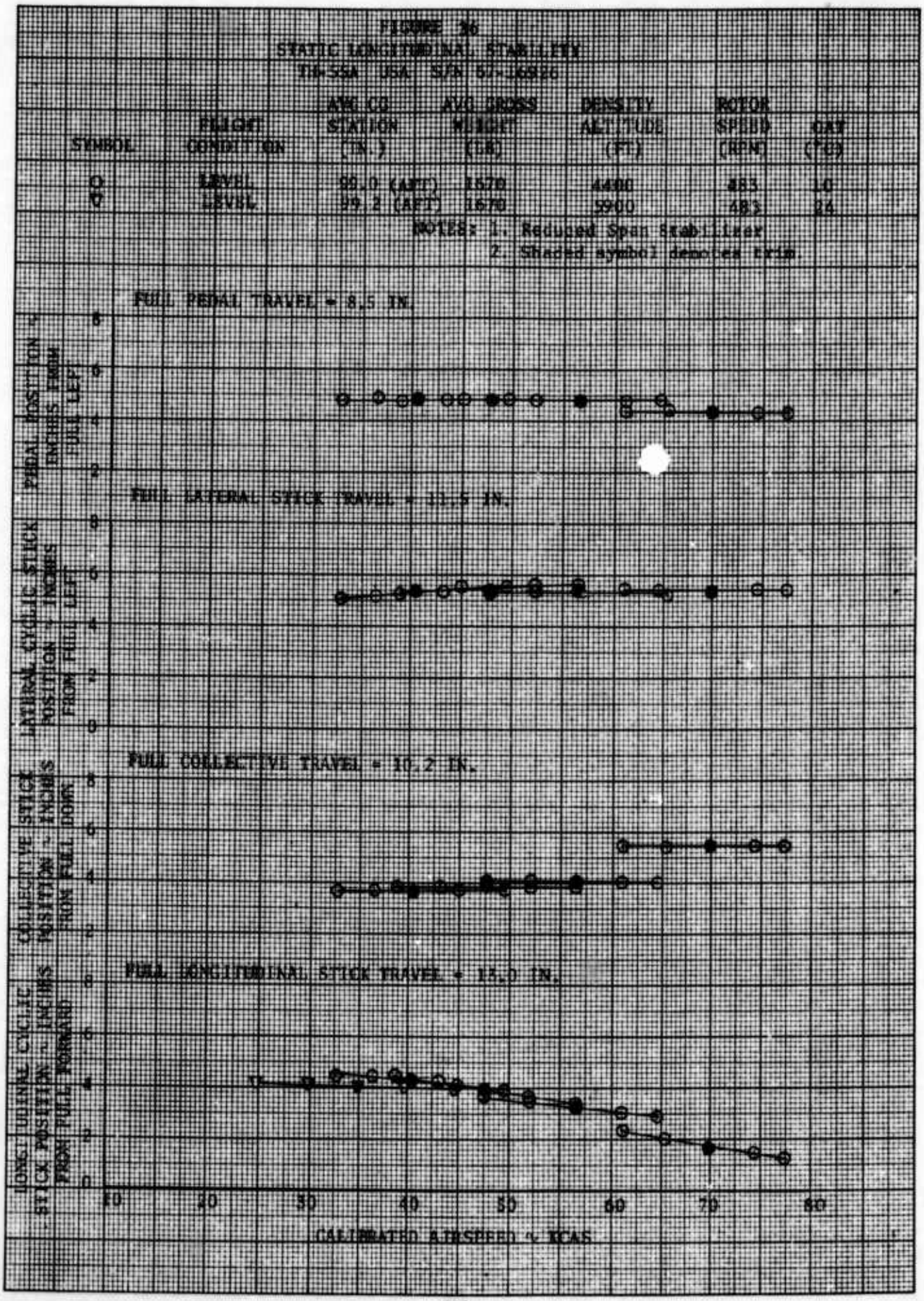

FIGURE 37

STATIC LONGITUDINAL STABILITY

TH-55A (REF. SER 670-0001)

SYMBOL	FLIGHT CONDITION	AVG. CG STATION (IN.)	AVG. GROSS WEIGHT (LB)	DENSITY ALTITUDE (FT)	ROTOR SPEED (RPM)	OAT (°C)
○	CLIMB	99.0 (AFT)	1620	4400	485	10
●	AUTO	99.0 (AFT)	1620	4400	485	10

NOTES: 1. Boost Servos Span Stabilizer
2. Shaded symbol denotes trim.

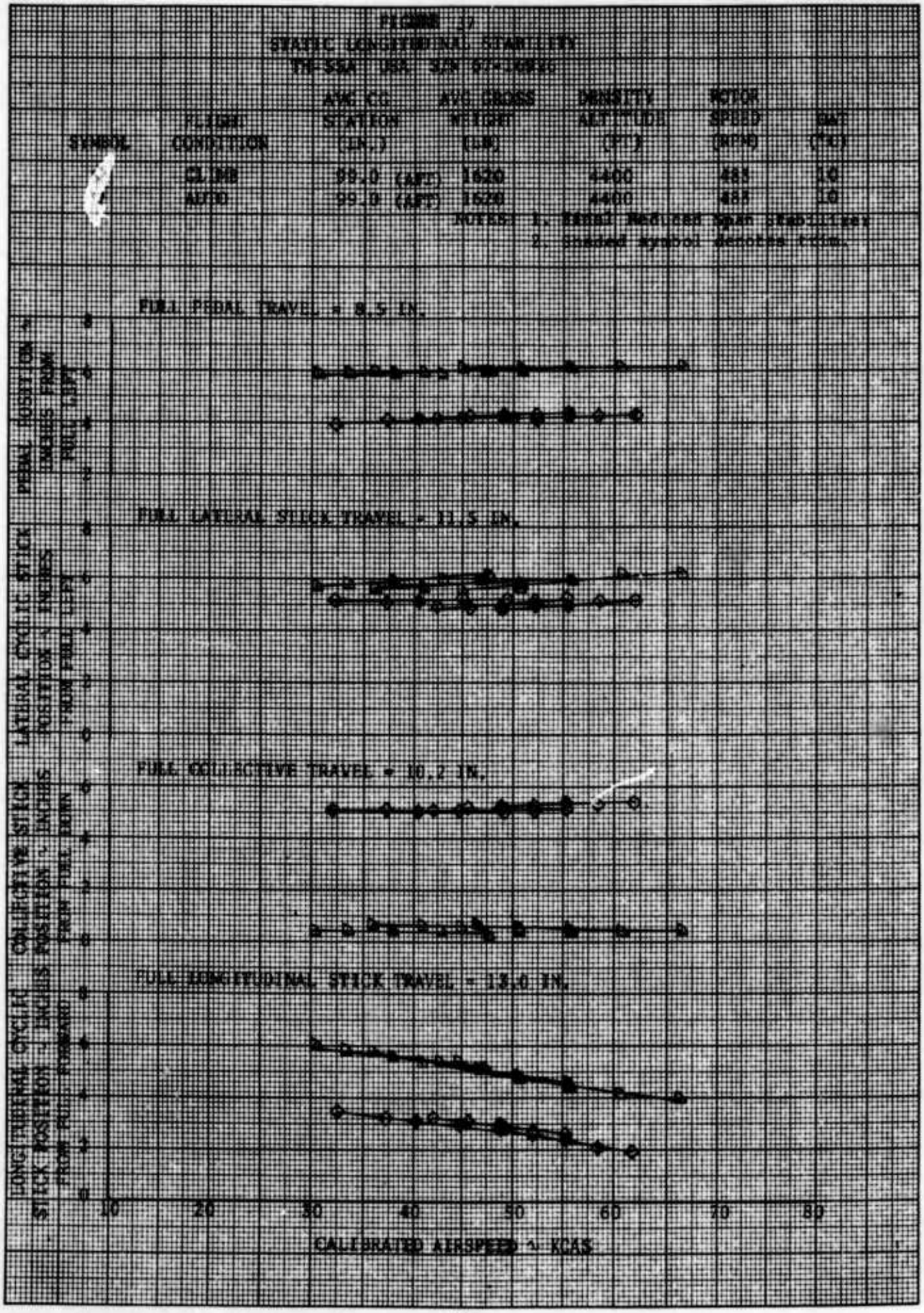

FIGURE 38

STATIC LATERAL DIRECTIONAL STABILITY

XH-55A USA S/N 62-12926

SYMBOL	FLIGHT CONDITION	AVG CG STATION (IN.)	AVG GROSS WEIGHT (LB)	DENSITY ALTITUDE (FT)	ROTOR SPEED (RPM)	CALIB. A/S (KCAS)	OAT (°C)
○	LEVEL	95.2 (FNDY)	1670.	4150	483	40	8
◐	LEVEL	95.2 (FNDY)	1670.	4150	483	47	8
●	LEVEL	95.2 (FNDY)	1670.	4150	483	56	8

NOTES: 1. Fixed Reduced Span Stabilizer
2. Shaded symbol denotes trim.

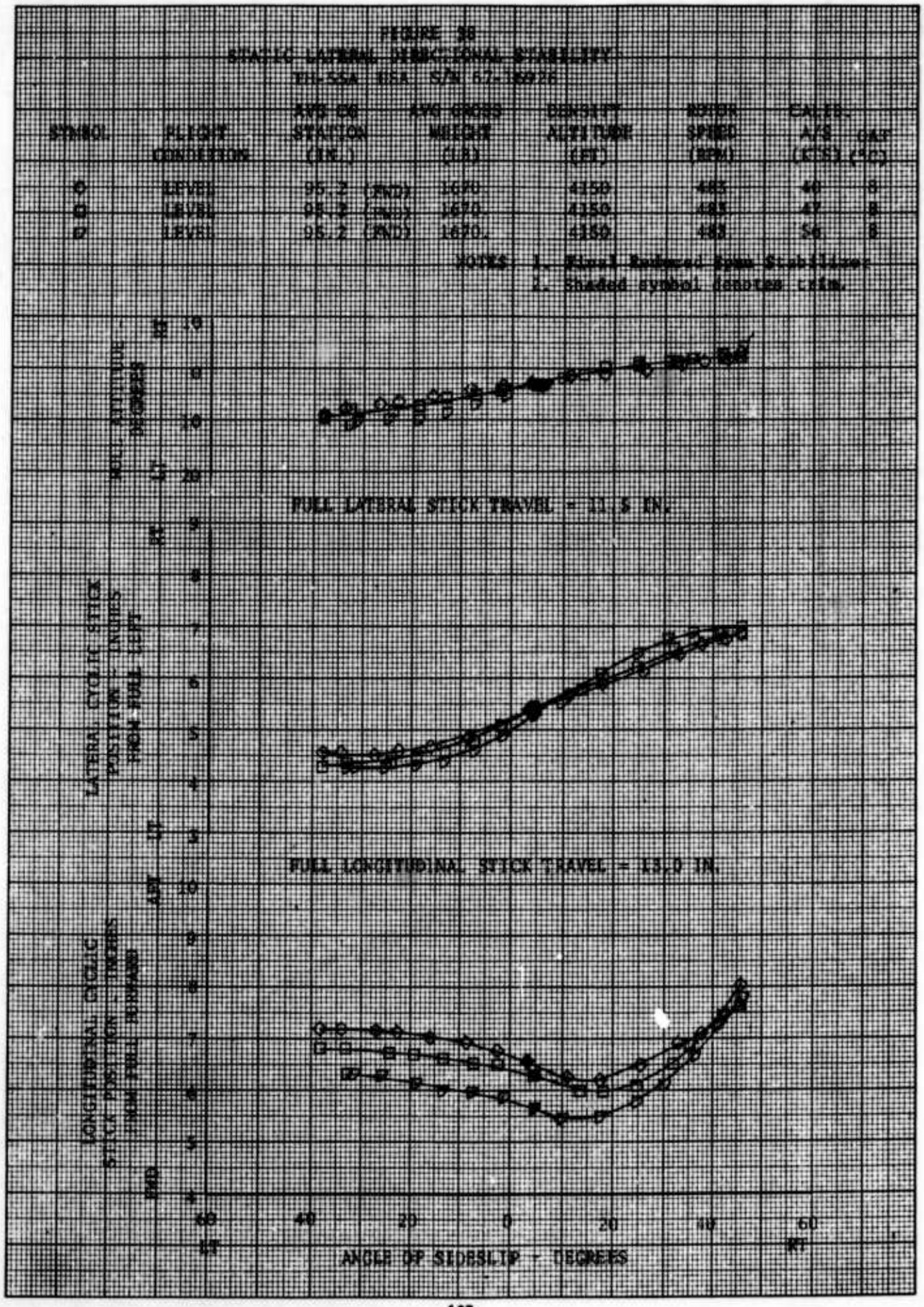

FIGURE 38(CONCLUDED)

STATIC LATERAL DIRECTIONAL STABILITY

TH-55A ESA SN 67-22026

SYMBOL	FLIGHT CONDITION	AVG CG STATION (IN.)	AVG GROSS WEIGHT (LB)	DENSITY ALTITUDE (FT)	ROTOR SPEED (RPM)	CAL IAS x/8 (KTS)	OAT (°C)
○	LEVEL	95.2 (FWD)	1670	4150	485	40	8
□	LEVEL	95.2 (FWD)	1670	4150	485	47	8
▽	LEVEL	95.2 (FWD)	1670	4150	485	56	8

NOTES: 1. Reduced Span Stabilizer

2. Shaded symbol denotes left

FULL COLLECTIVE STICK TRAVEL = 10.2 IN.

DEFLECTION OF LONGITUDINAL STICK POSITION, INCHES FROM FULL AFT

FULL PEDAL TRAVEL = 8.5 IN.

PEDAL POSITION, INCHES FROM FULL LEFT

60 LT 40 20 0 20 40 60 RT

ANGLE OF SIDESLIP, DEGREES

FIGURE 39

STATIC LATERAL DIRECTIONAL STABILITY

TH-55A (SN 67-15820)

SYMBOL	FLIGHT CONDITION	AVG CG STATION (IN.)	AVG GROSS WEIGHT (LB)	DENSITY ALTITUDE (FT)	ROTOR SPEED (RPM)	CAL A/S (KTS)	OAT (°C)
◇	LEVEL	99.0 (AFT)	1650.	4200.	485.	40.	9
□	LEVEL	99.0 (AFT)	1650.	4200.	485.	47.	9
▽	LEVEL	99.0 (AFT)	1650.	4200.	485.	56.	9
	AUTO	99.0 (AFT)	1650.	3200.	485.	56.	0

NOTES: 1. Final Reduced Span Stabilizer
2. Shaded symbol denotes trim.

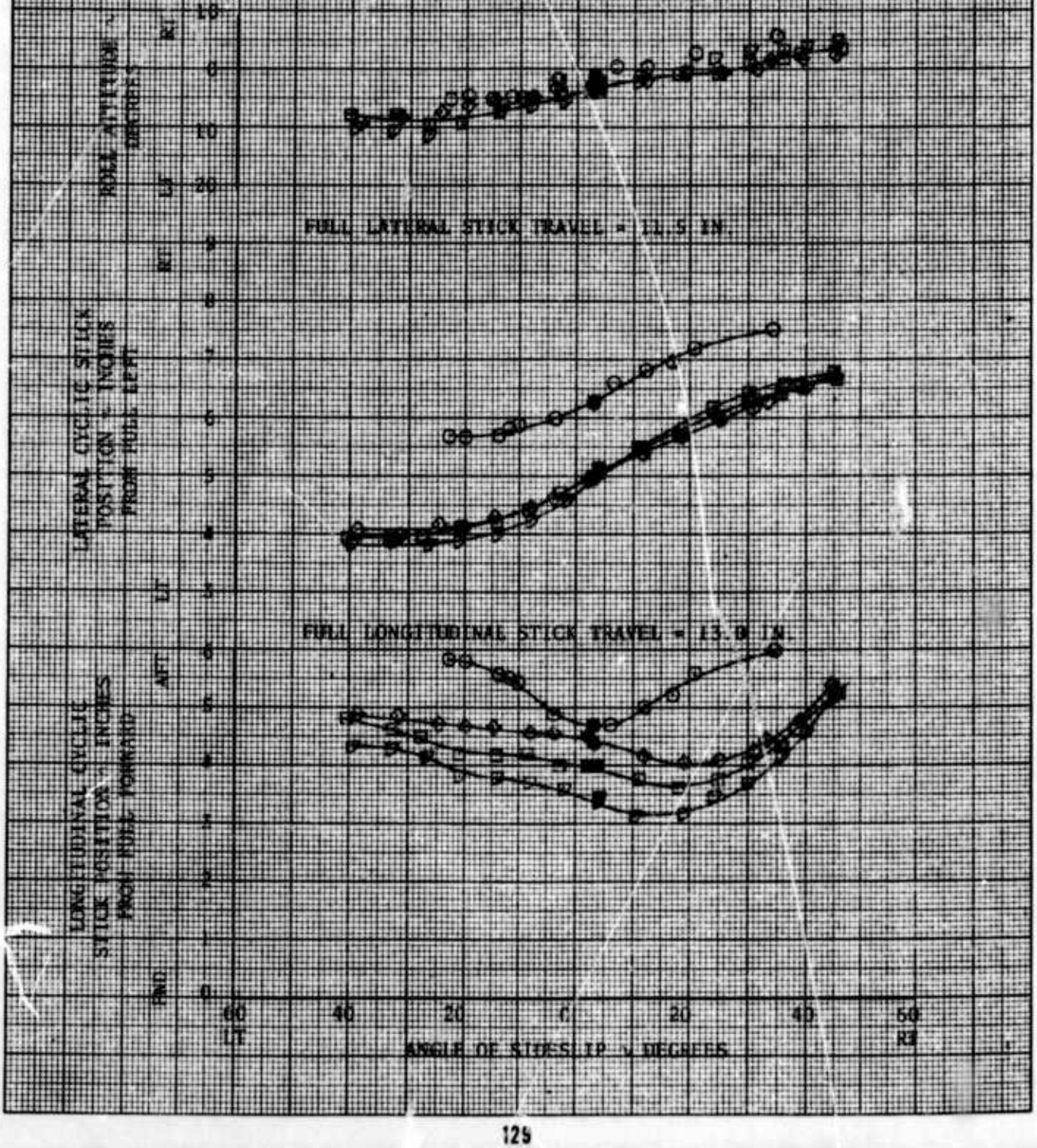

FIGURE 39(CONCLUDED)

STATIC LATERAL DIRECTIONAL STABILITY

TH-55A USA S/N 67-00026

SYMBOL	FLIGHT CONDITION	AVG. GC STATION (IN.)	AVG. GROSS WEIGHT (LB)	DENSITY ALTITUDE (FT)	ROTOR SPEED (RPM)	CAL. I.A.S. (KTS)	OAT (°C)
◇	LEVEL	99.0 (AFT)	1650	4200	483	40	9
□	LEVEL	99.0 (AFT)	1650	4200	483	47	9
▽	LEVEL	99.0 (AFT)	1650	4200	483	55	9
	AUTO	99.0 (AFT)	1500	4200	483	56	0

FULL COLLECTIVE STICK TRAVEL = 10.2 IN.

NOTES: 1. Reduced Span Stabilizer
2. Shaded Symbol Denotes Trim

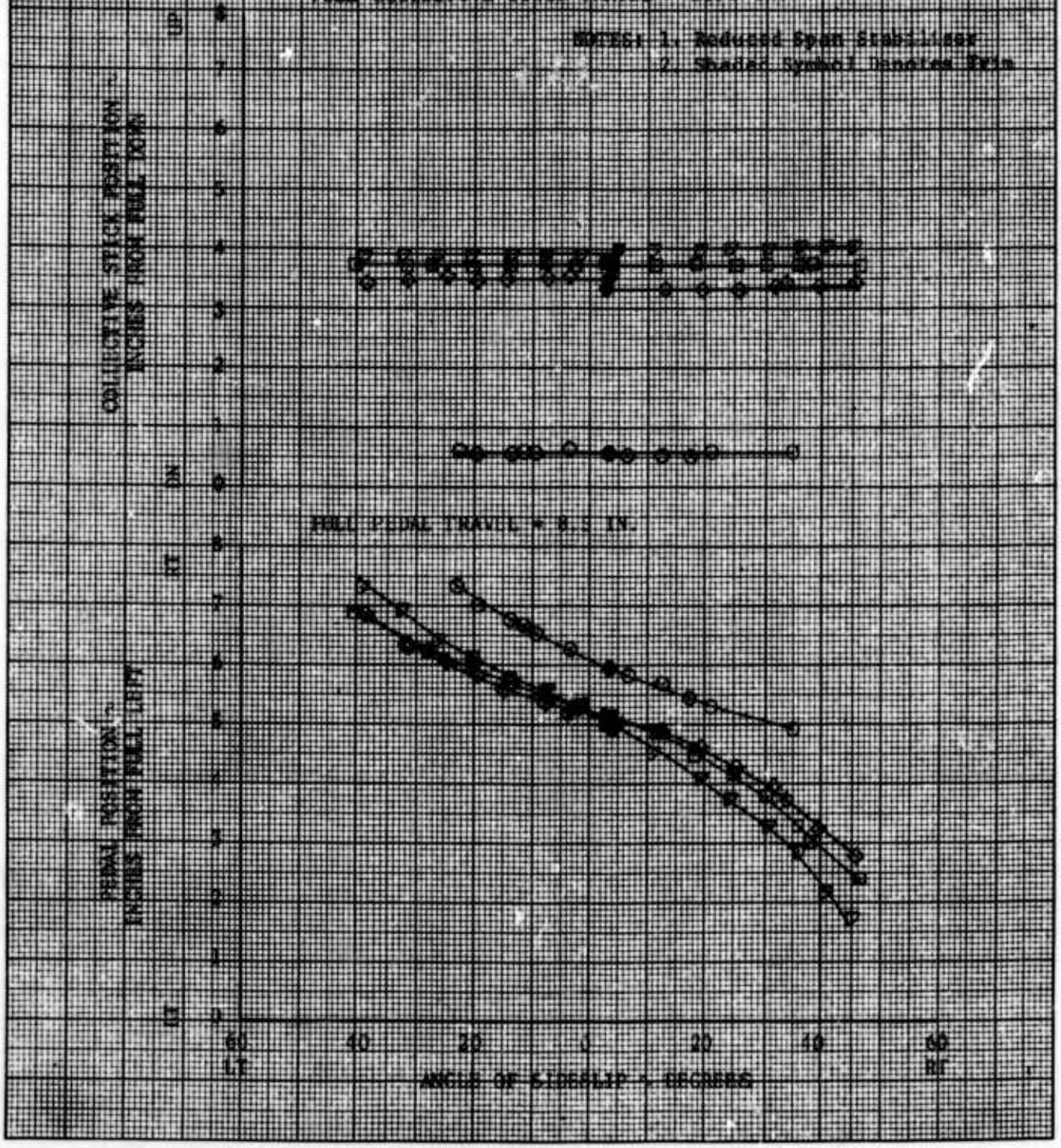

FIGURE 40
AIRCRAFT RESPONSE FOLLOWING A LEFT LATERAL PULSE NOTE: Final Reduced Span Stabilizer
TH-55A USA S/N 67-16926

LIGHT CONDITION	AVG CG STATION (INCHES)	AVG GROSS WEIGHT (LBS)	DENSITY ALTITUDE (FEET)	ROTOR SPEED (RPM)	CALIBRATED AIRSPEED (KCAS)	OAT (°C)
LEVEL	99.	1670.	3800.	483.	47.	5

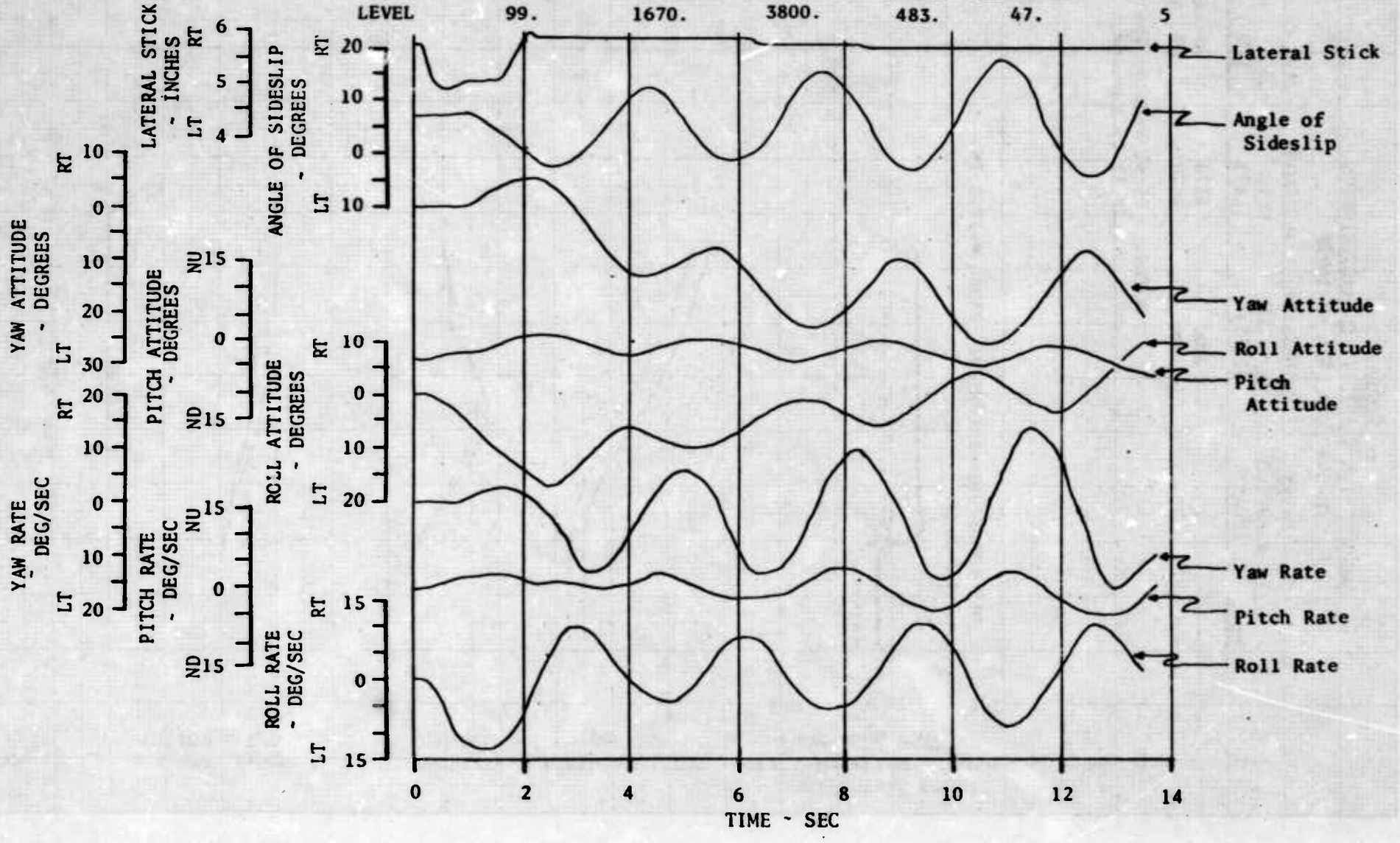

FIGURE A1

MANEUVERING STABILITY CHARACTERISTICS

EH-55A USA S/N 67-16026

SYMBOL	ENTRY AIRSPEED (KCAS)	AVG DENSITY ALTITUDE (FEET)	AVG GROSS WEIGHT (LBS)	AVG CG LOCATION (IN.)	OAT (°C)
———	80	3000	4670	99 (AFT)	5
- - - -	70	3000	4670	99 (AFT)	5

NOTES: 1. Pitot Balanced Span Stabilizer

2. Full Up Hardware

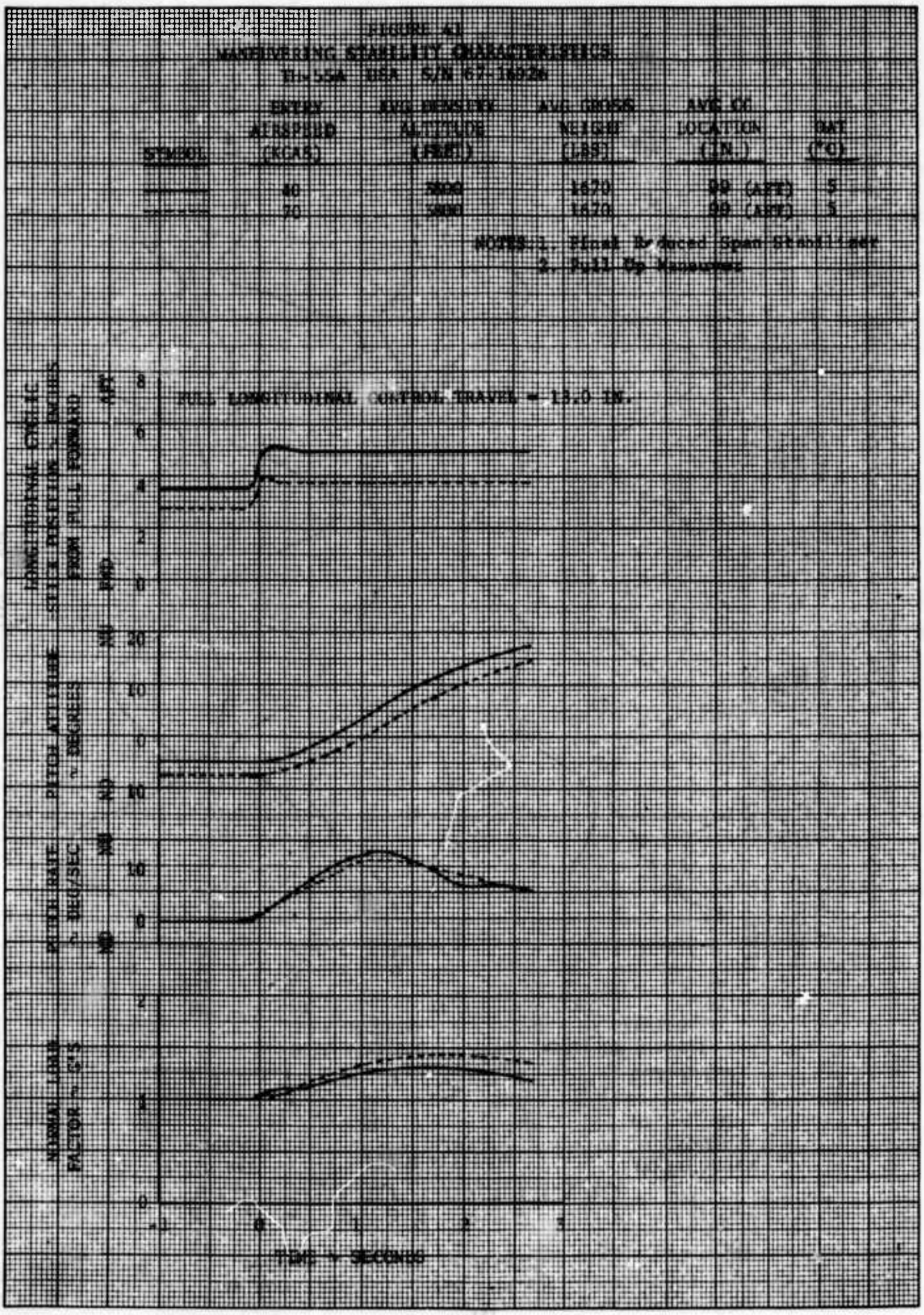

FIGURE A2

HORIZONTAL STABILIZER LOADS IN STEADY FORWARD FLIGHT

TH-55A USA S/N 67-16926

SYMBOL	FLIGHT CONDITION	AVG CG STATION* (IN.)	AVG GROSS WEIGHT (LB)	DENSITY ALTITUDE (FT)	ROTOR SPEED (RPM)	OAT (°C)
○	Level	95.3 (FWD)	1668	5400	483	19
□	Level	95.2 (FWD)	1670	5400	480	19
◇	Climb	95.2 (FWD)	1680	5400	483	19
▽	Auto	95.2 (FWD)	1680	5400	483	19

NOTE: Standard Stabilizer

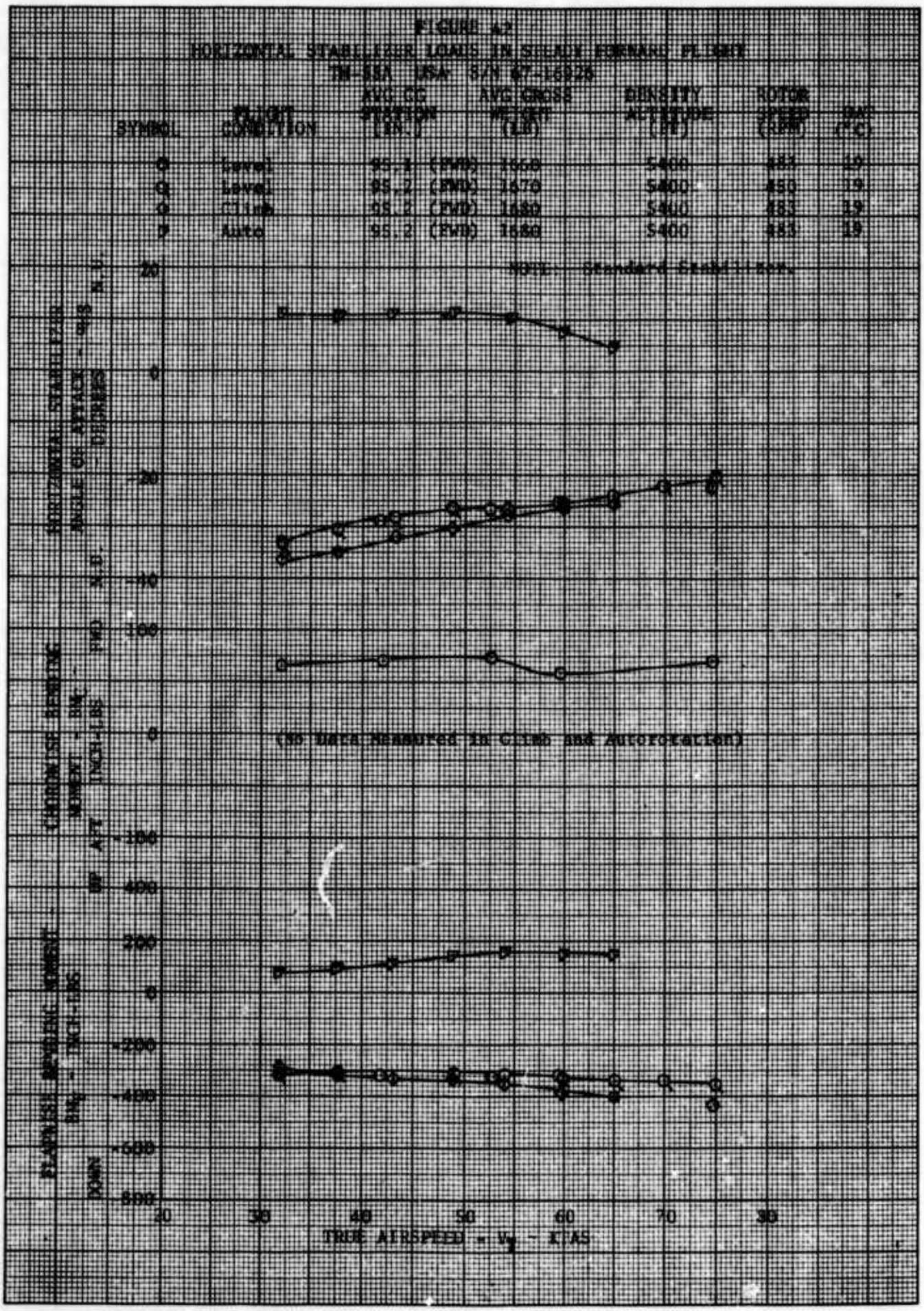

FIGURE 43

HORIZONTAL STABILIZER LOADS IN STEADY FORWARD FLIGHT

TH-55A HSR, S/N 67-16525

SYMBOL	FLIGHT CONDITION	AVG. GW STATION (IN.)	AVG. GROSS WEIGHT (LB)	DENSITY ALTITUDE (FT)	ROTOR SPEED (RPM)	OAT (°C)
○	Level	99.3 (APT)	1650	5000	485	15
□	Level	99.4 (APT)	1650	5000	490	15
◇	Climb	99.4 (APT)	1650	5000	485	15
△	Auto	99.4 (APT)	1650	5000	485	15

NOTE: Standard Stabilizer.

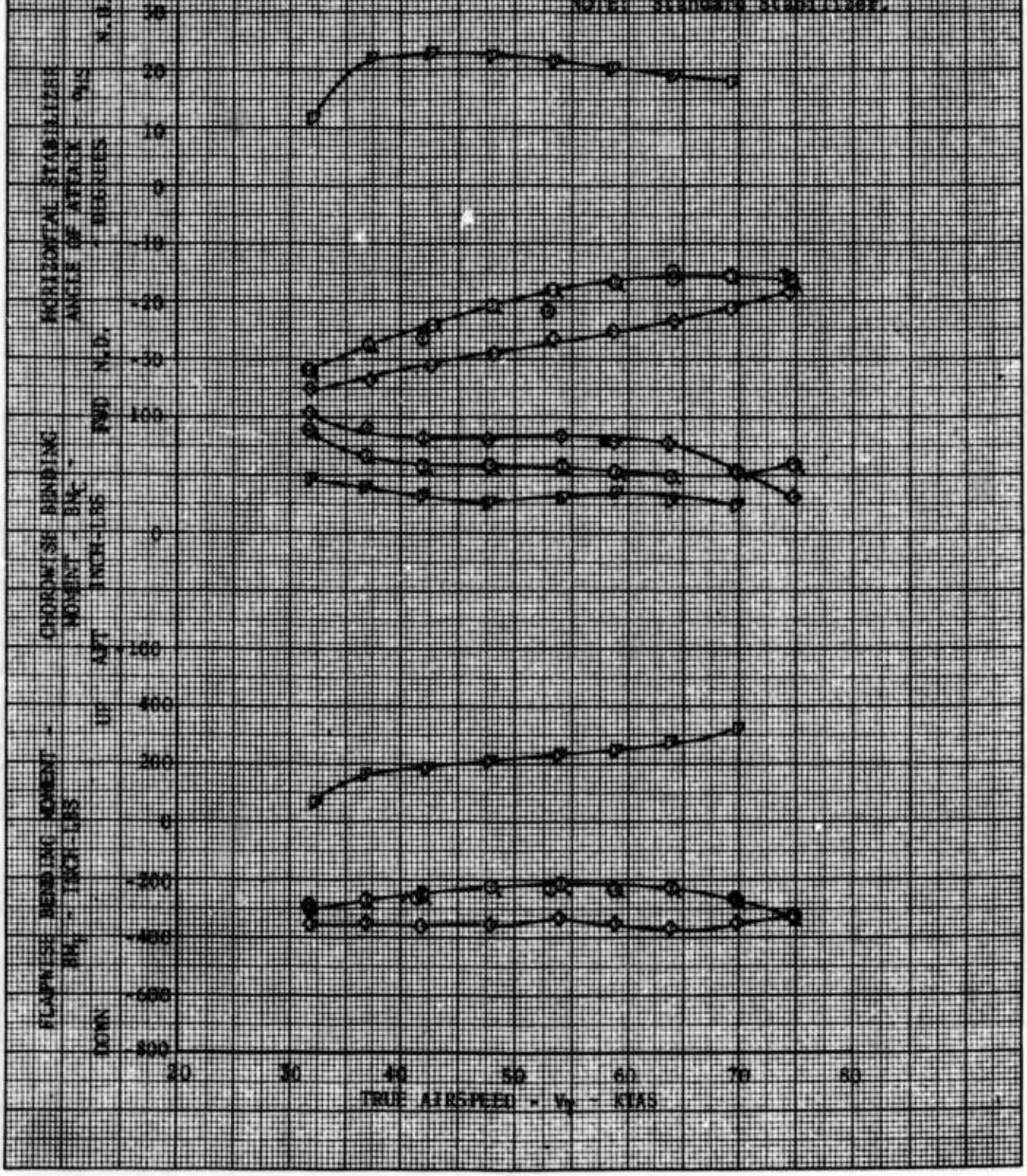

FIGURE AA

HORIZONTAL STABILIZER LOADS IN STEADY FORWARD FLIGHT

TH-55A SN/AF 67-16205

SYMBOL	PILOT CONDITION	AVG CG STATION (IN.)	AVG GROSS WEIGHT (LB)	DENSITY ALTITUDE (FT)	ROTOR SPEED (RPM)	OAT (°C)
○	Level	96.2 (FWD)	1690	4900	485	15
◇	Climb	96.2 (FWD)	1690	4900	485	15
□	Auto	96.2 (FWD)	1690	4900	485	15

NOTE: Standard Stabilizer with Upper Spoiler.

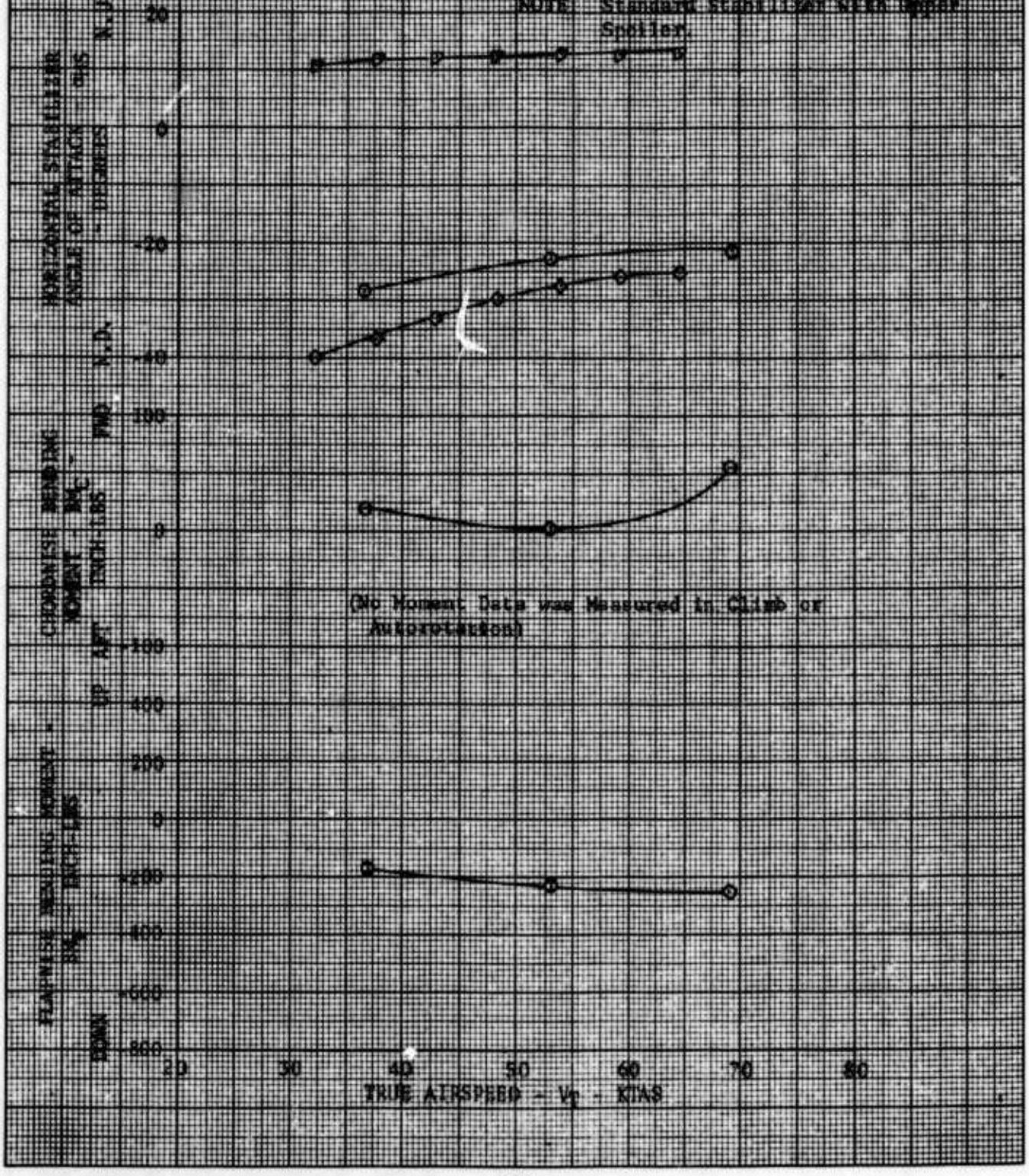

FIGURE 45

HORIZONTAL STABILIZER LOADS IN STEADY FORWARD FLIGHT

TH-55A USA S/N (7-16826

SYMBOL	FLIGHT CONDITION	AVG CG STATION (IN.)	AVG GROSS WEIGHT (LBS)	DENSITY ALTITUDE (FT)	ROTOR SPEED (RPM)	OAT (°C)
◇	Level	95.7 (FWD)	1640	4400	485	10
◇	Climb	95.7 (FWD)	1640	4400	485	10
▽	Auto	95.7 (FWD)	1640	4400	485	10
▽	Descent	95.7 (FWD)	1640	4400	485	10

NOTE: 1. Reduced Chord Stabilizer.
2. Descent was made with 4 inches less manifold pressure than required for Level Flight.

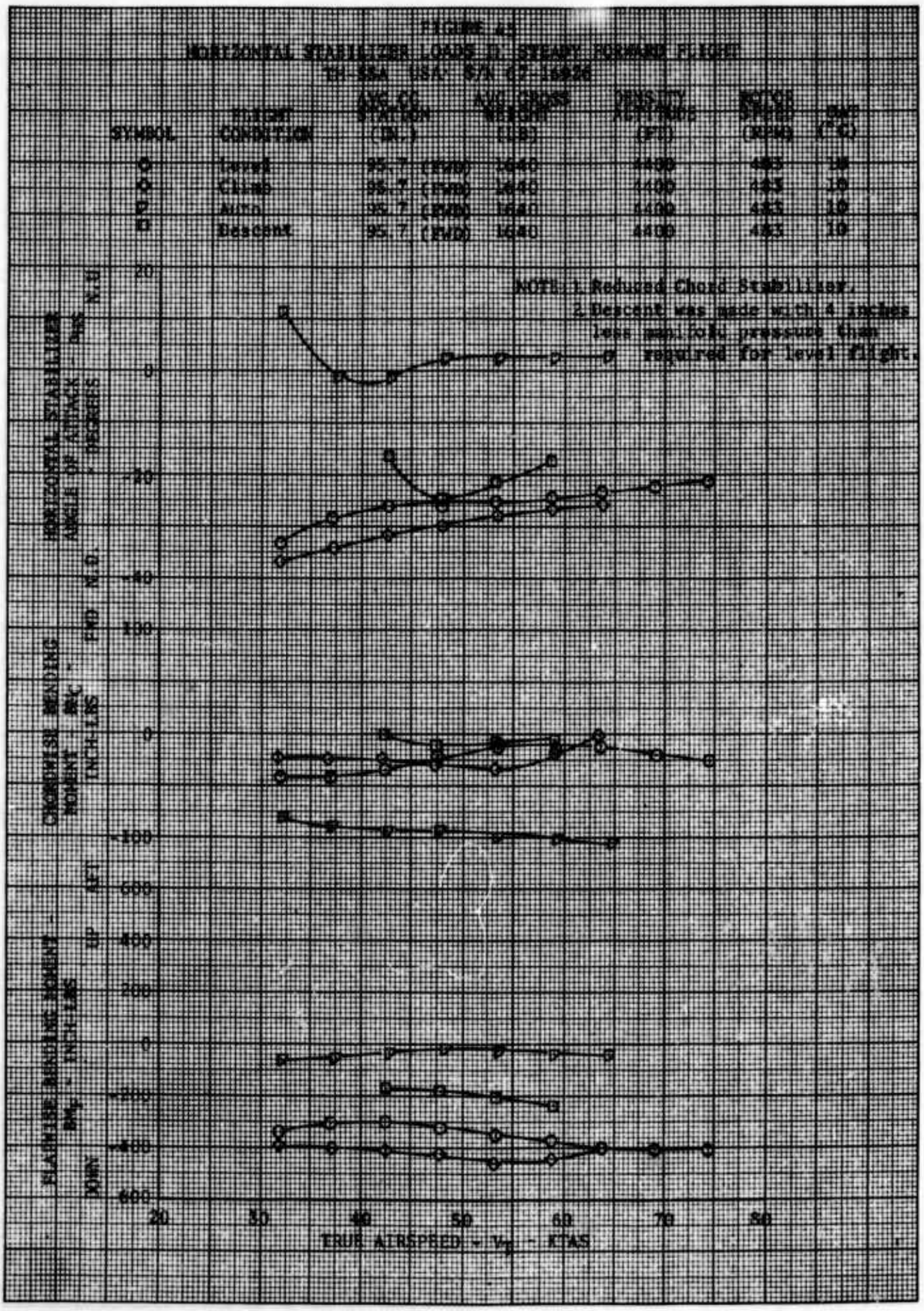

FIGURE 44

HORIZONTAL STABILIZER LOADS IN STEADY FORWARD FLIGHT

TH-55A HSA- S/N 67-16626

SYMBOL	FLIGHT CONDITION	AVG CG STATION (INCH)	AVG GROSS WEIGHT (LB)	DENSITY ALTITUDE (FT)	ROTOR SPEED (RPM)	OAT (°C)
○	Level	99.5 (APT)	1680	4400	485	10
△	Climb	99.5 (APT)	1680	4400	485	10
□	Auto	99.5 (APT)	1680	4400	485	10
▽	Descent	99.5 (APT)	1680	4400	485	10

NOTE: 1. Reduced Chord Stabilizer.
2. Descent was made with 3 inches less manifold pressure than required for level flight.

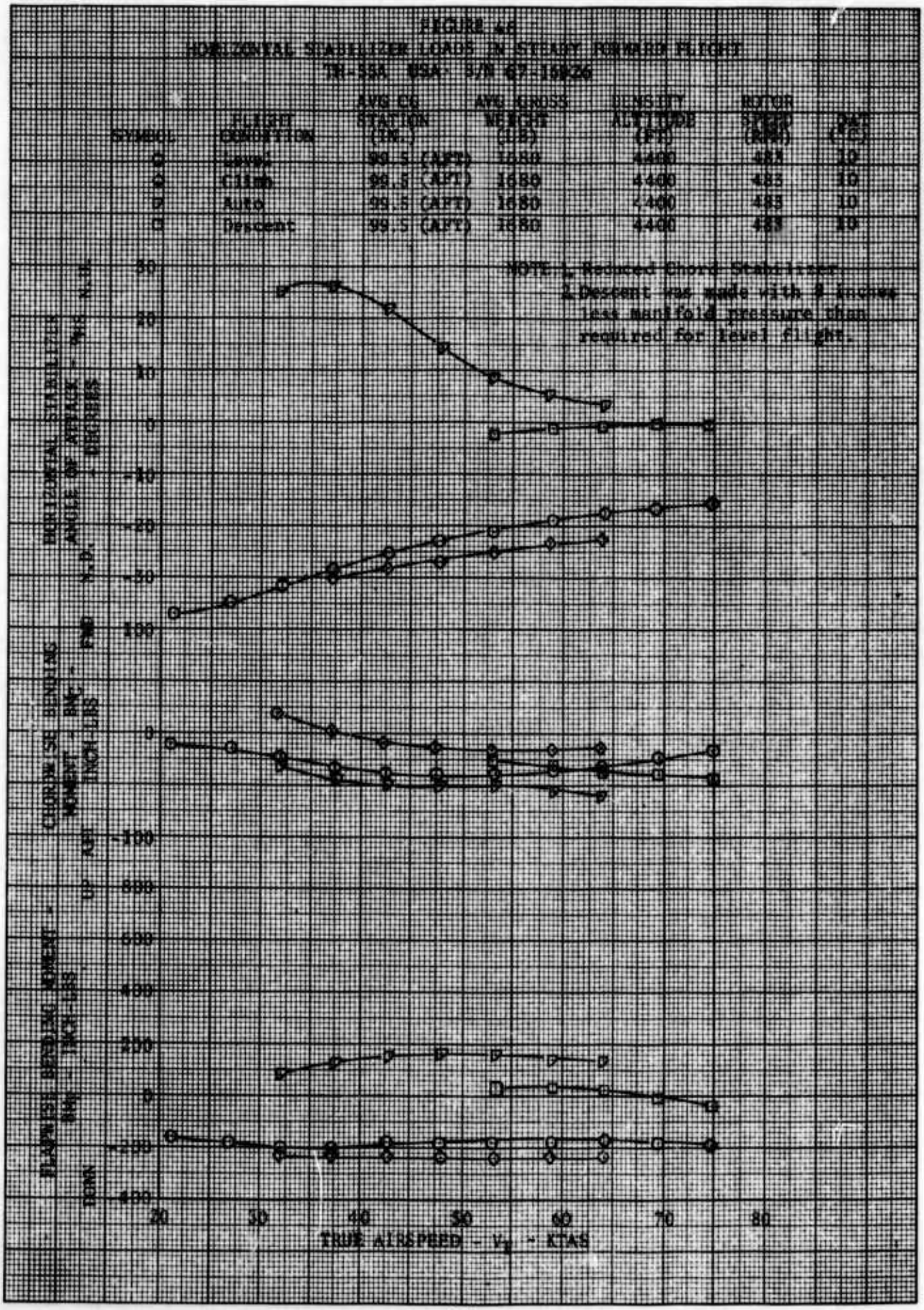

FIGURE 47

HORIZONTAL STABILIZER LOADS IN STEADY ROLLING FLIGHT

TH-55A (SN, S/N 82-[illegible])

SYMBOL	FLIGHT CONDITION	A/C CG STA (IN.)	A/C GROSS WEIGHT (LB)	DENSITY ALTITUDE (FT)	ROTOR SPEED (RPM)	OAT (°C)
○	Level	96.2 (FWD)	1650	5300	483	1.8
◇	Climb	96.2 (FWD)	1650	5300	483	1.8
▽	Auto	96.2 (FWD)	1650	5300	483	1.8

NOTE: Reduced Chord Stabilizer with Gap Spoiler.

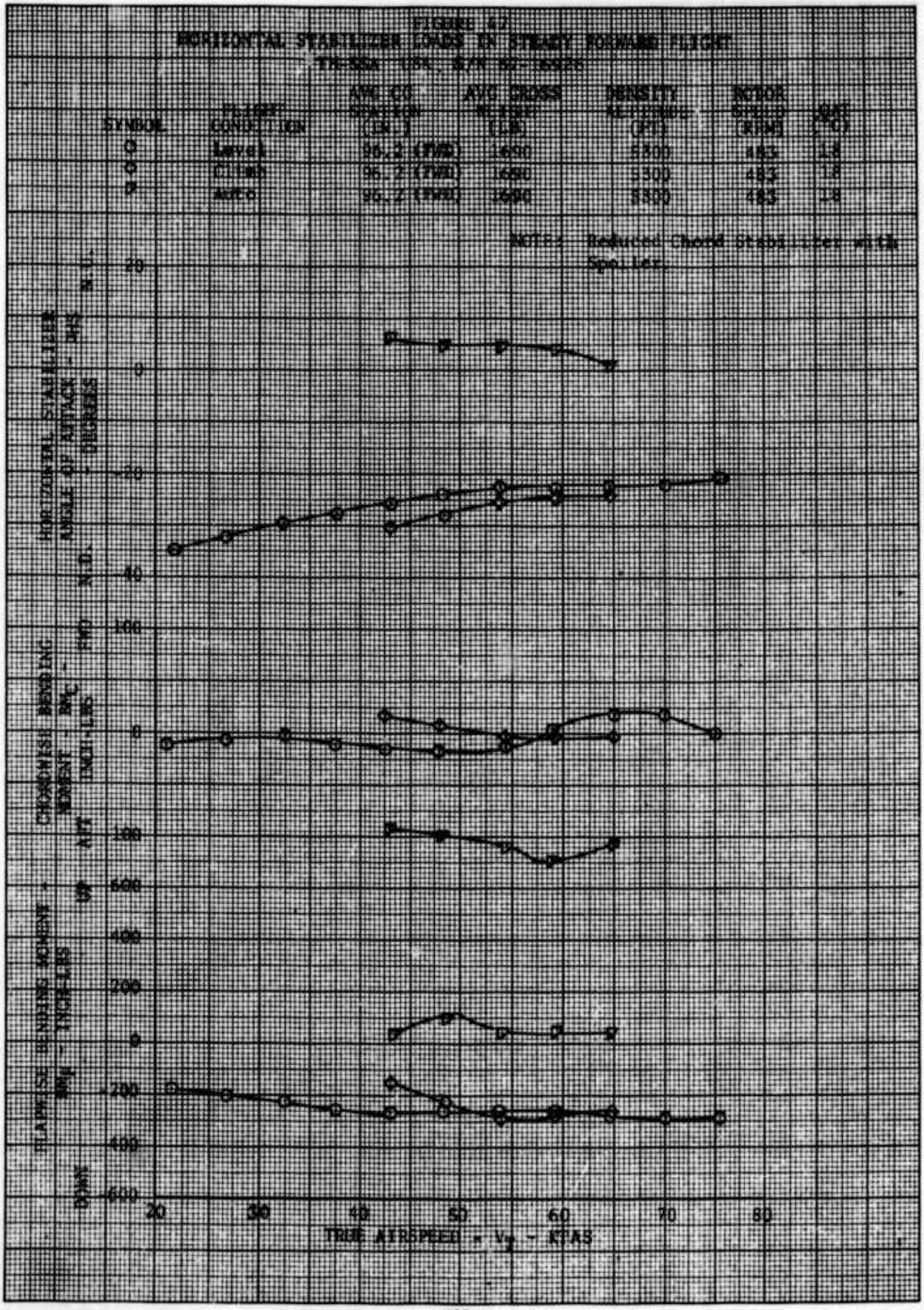

FIGURE 48

HORIZONTAL STABILIZER LOADS IN STEADY FORWARD FLIGHT

YF-16A USA S/N 72-1567

SYMBOL	FLIGHT CONDITION	AVG CG STATION (PERCENT)	AVG GROSS WEIGHT (LBS)	DENSITY ALTITUDE (FT)	INDICATED SPEED (KNOTS)	KEAS (PSF)
○	LEVEL	35.2 (FWD)	16700	4100	485	0
▽	CLIMB	35.2 (FWD)	16700	4100	485	0
◇	AUTO	35.2 (FWD)	16700	4100	485	0

NOTE: FINAL REDUCED SPAN STABILIZER

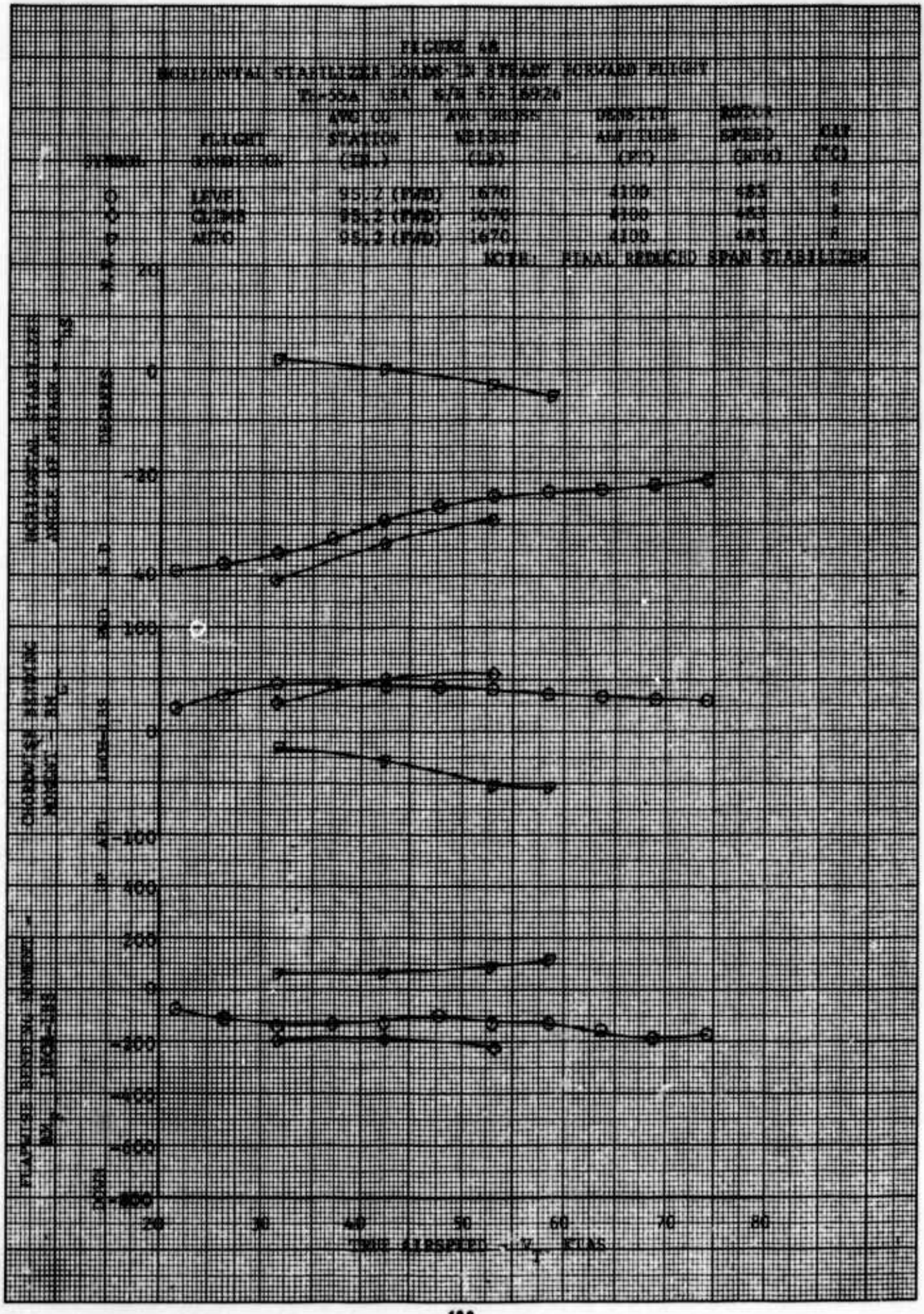

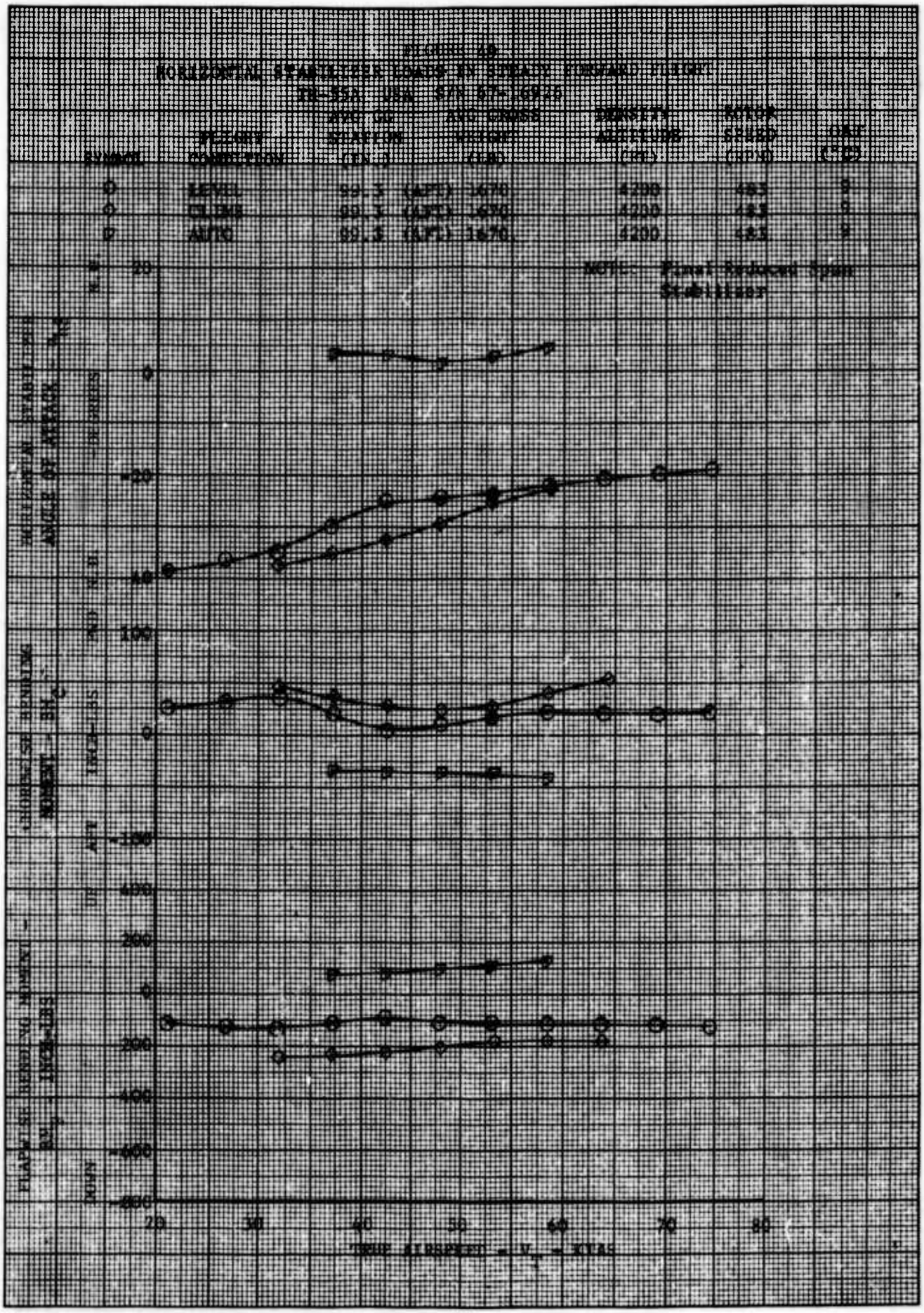
HORIZONTAL STABILIZER LOADS IN STEADY FORWARD FLIGHT
SYMBOL
FLIGHT CONDITION
AVG. GW AT TEST (LB)
AVG CG LOCATION (%MAC)
DENSITY ALTITUDE (FT)
ROTOR SPEED (RPM)
OAT (°C)
LEVEL
CRUISE
AUTO
Flight Reduced Span Stabilizer
TRUE AIRSPEED - V_T - KNOTS
FLAP-WISE BENDING MOMENT, IN-LBS
CHORD-WISE BENDING MOMENT, IN-LBS
TORSIONAL MOMENT, IN-LBS

FIGURE 50

VERTICAL AND HORIZONTAL STABILIZER LOADS IN STEADY

LATERAL DIRECTIONAL FLIGHT

TH-55A USA S/N 67-16926

SYMBOL	FLIGHT CONDITION	AVG CG STATION (IN.)	AVG GROSS WEIGHT (LB)	DENSITY ALTITUDE (FT)	ROTOR SPEED (RPM)	CALIB. A/S (KTS)	OAT °F (°C)
◇	Level	98.1 (AFT)	1640	3200	483	33	0
□	Level	99.2 (AFT)	1660	3200	483	47	0
▽	Level	99.2 (AFT)	1670	3200	483	54	0

NOTES: 1. Standard Stabilizer.
2. Shaded symbol denotes yaw.

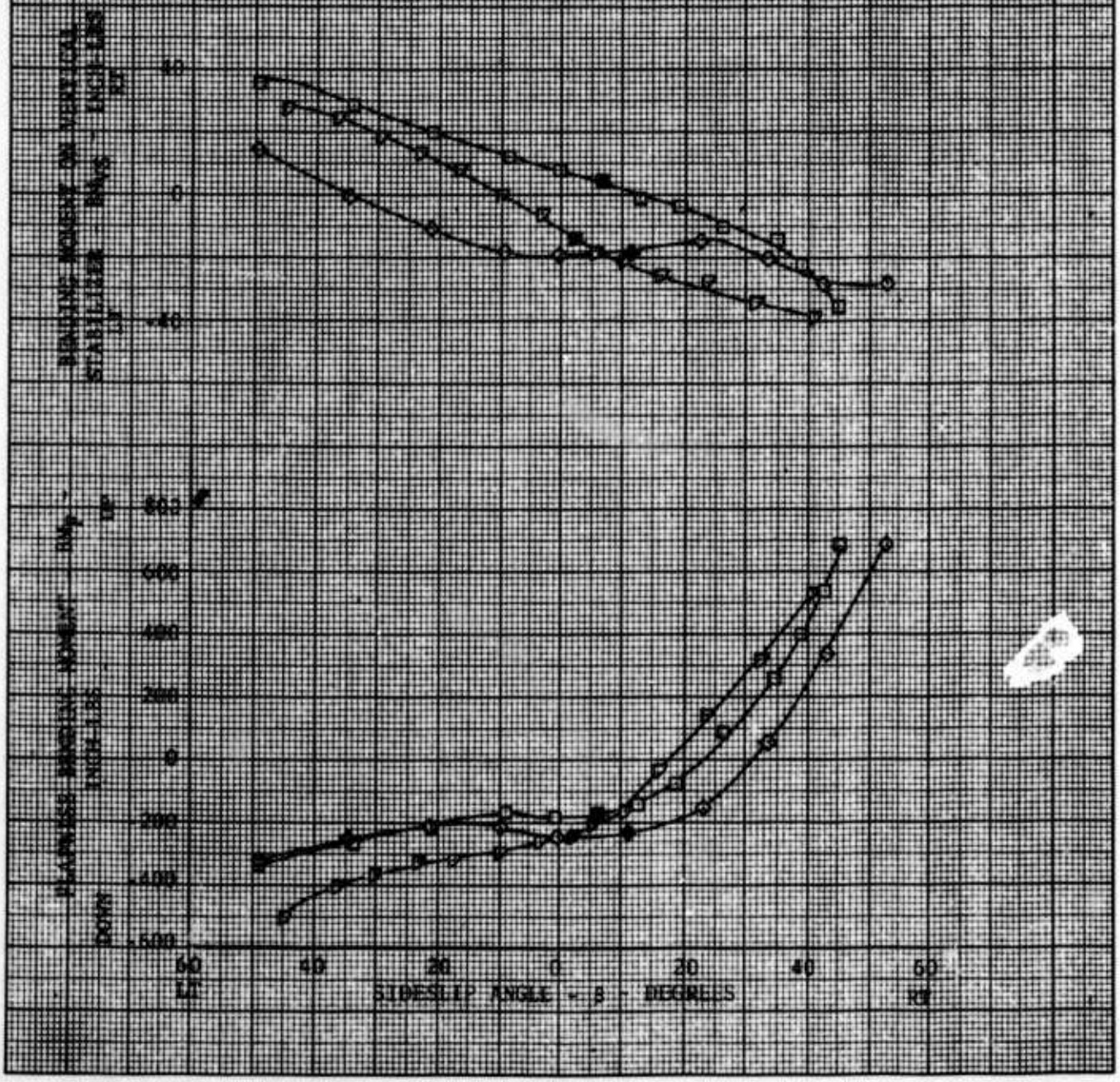

FIGURE 8

HORIZONTAL STABILIZER LOADS IN STEADY PITCHING STRAIGHT-CHAR. FLIGHT

TR-1535 USA - 2/3 SCALE MODEL

SYMBOL	FLIGHT CONDITION	AVG C.G. STATION (Sta.)	AVG GROSS WEIGHT (LB)	DENSITY ALTITUDE (FT)	ROTOR SPEED (RPM)	CAL. AS AIS (KTAS)	CAL. MAT (°C)
○	Level	96.3 (FWD)	1690	4000	483	57	7
⊕	Level	96.3 (FWD)	1690	4000	483	47	7
⊗	Level	96.2 (AFT)	1690	4000	483	64	7
△	Auto	96.2 (FWD)	1690	4000	483	47	10

NOTES: 1. Standard Stabilizer.
2. Shaded symbols denote trim.

(No Angle of Attack or Chordwise Bending Moment Data was Measured)

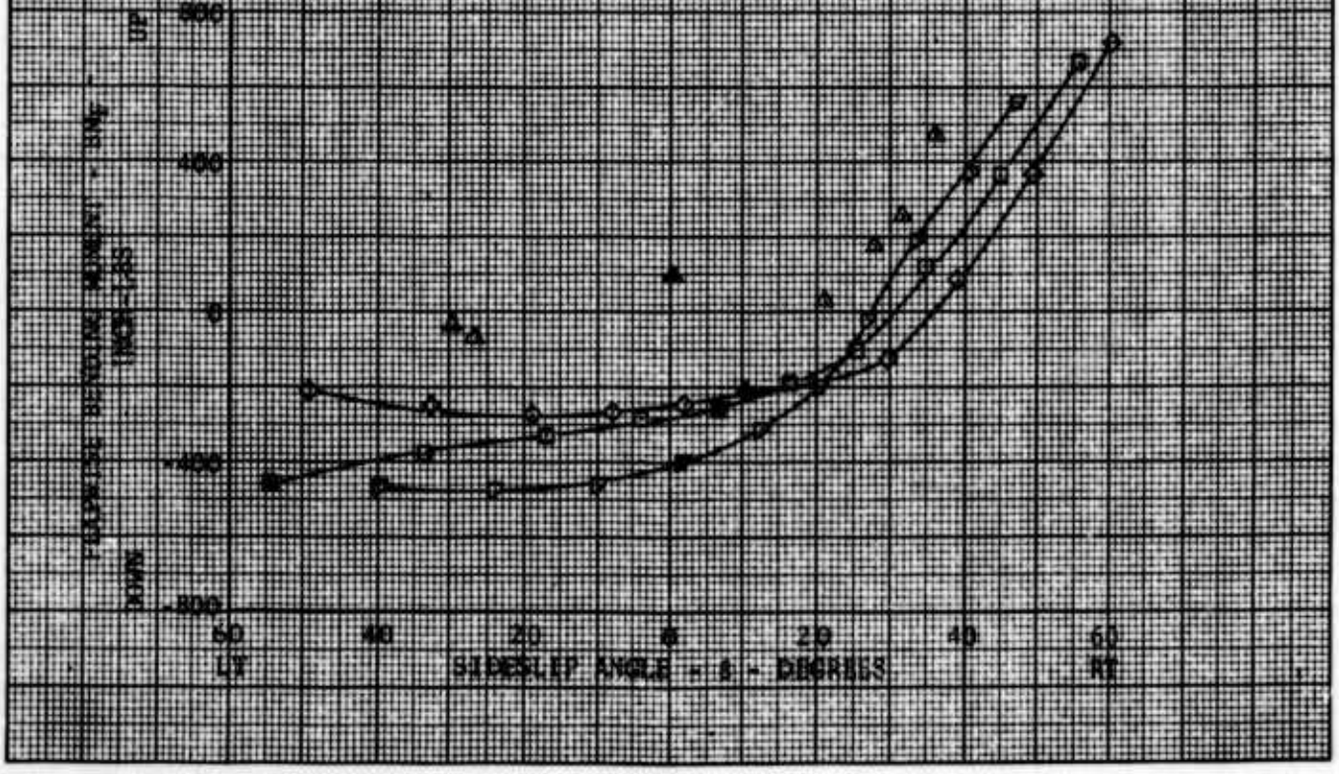

FIGURE 52
HORIZONTAL STABILIZER LOADS IN STEADY LATERAL DIRECTIONAL FLIGHT
TH-55A USA S/N 67-16920

SYMBOL	FLIGHT CONDITION	AVG CG STATION (IN.)	AVG GROSS WEIGHT (LB)	DENSITY ALTITUDE (FT)	ROTOR SPEED (RPM)	CALIB. A/S (KTS)	OAT (°C)
◻	Level	99.4 (AFT)	1660	4400	485	47	10

NOTES: 1. Reduced Chord Stabilizer.
2. Shaded symbols denote trim.

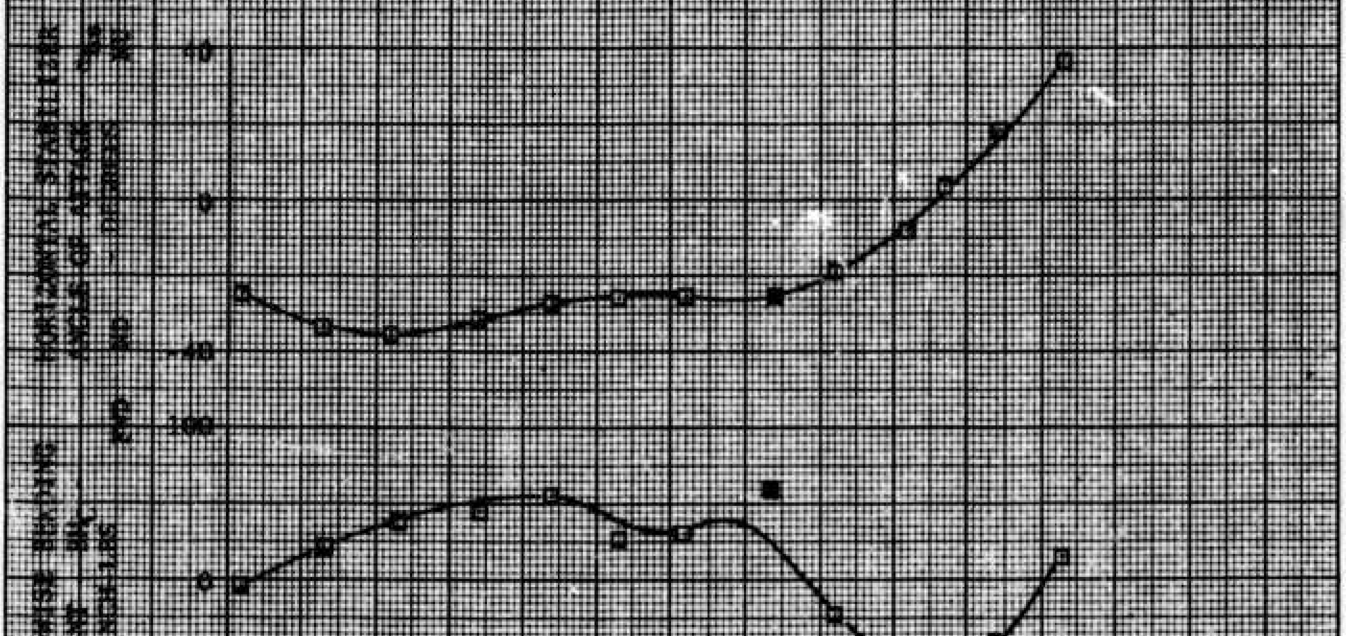

FIGURE 53

HORIZONTAL STABILIZER LOADS IN STEADY LATERAL DIRECTIONAL FLIGHT

YEL-58A (REA) S/N 67-16926

SYMBOL	FLIGHT CONDITION	AVG CG STATION (IN.)	AVG GROSS WEIGHT (LB)	DENSITY ALTITUDE (FT)	ROTOR SPEED (RPM)	CALIB. A/S (KTS)	OAT (°C)
⊕	Level	95.2 (FWD)	3690	4000	485	47	7

NOTES: 1. Reduced Chord Stabilizer.
2. Shaded symbols denote trim.

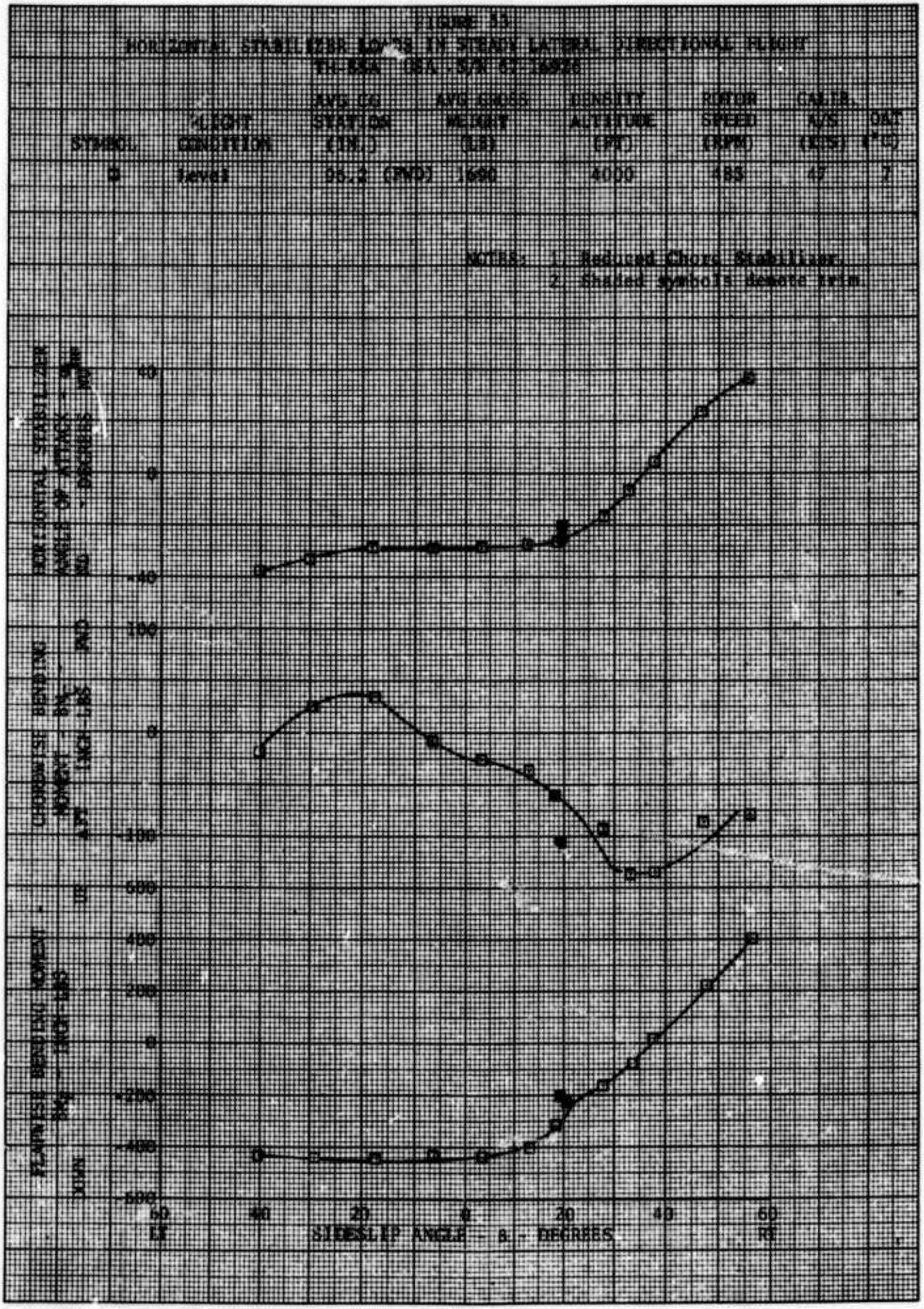

FIGURE 56

HORIZONTAL STABILIZER LOADS IN STEADY LATERAL DIRECTIONAL FLIGHT

TH-55A USA S/N 57-16925

SYMBOL	FLIGHT CONDITION	AVG CG STATION (IN.)	AVG GROSS WEIGHT (LB)	DENSITY ALTITUDE (FT)	ROTOR SPEED (RPM)	CAL'B. A/S (KTS)	OAT (°C)
○	LEVEL	95.2 (FWD)	1670	4150.	483.	40.	8
□	LEVEL	95.2 (FWD)	1670	4150.	483.	47.	8
△	LEVEL	95.2 (FWD)	1670	4150.	483.	56.	8

NOTE: FINAL REDUCED SPAN STABILIZER

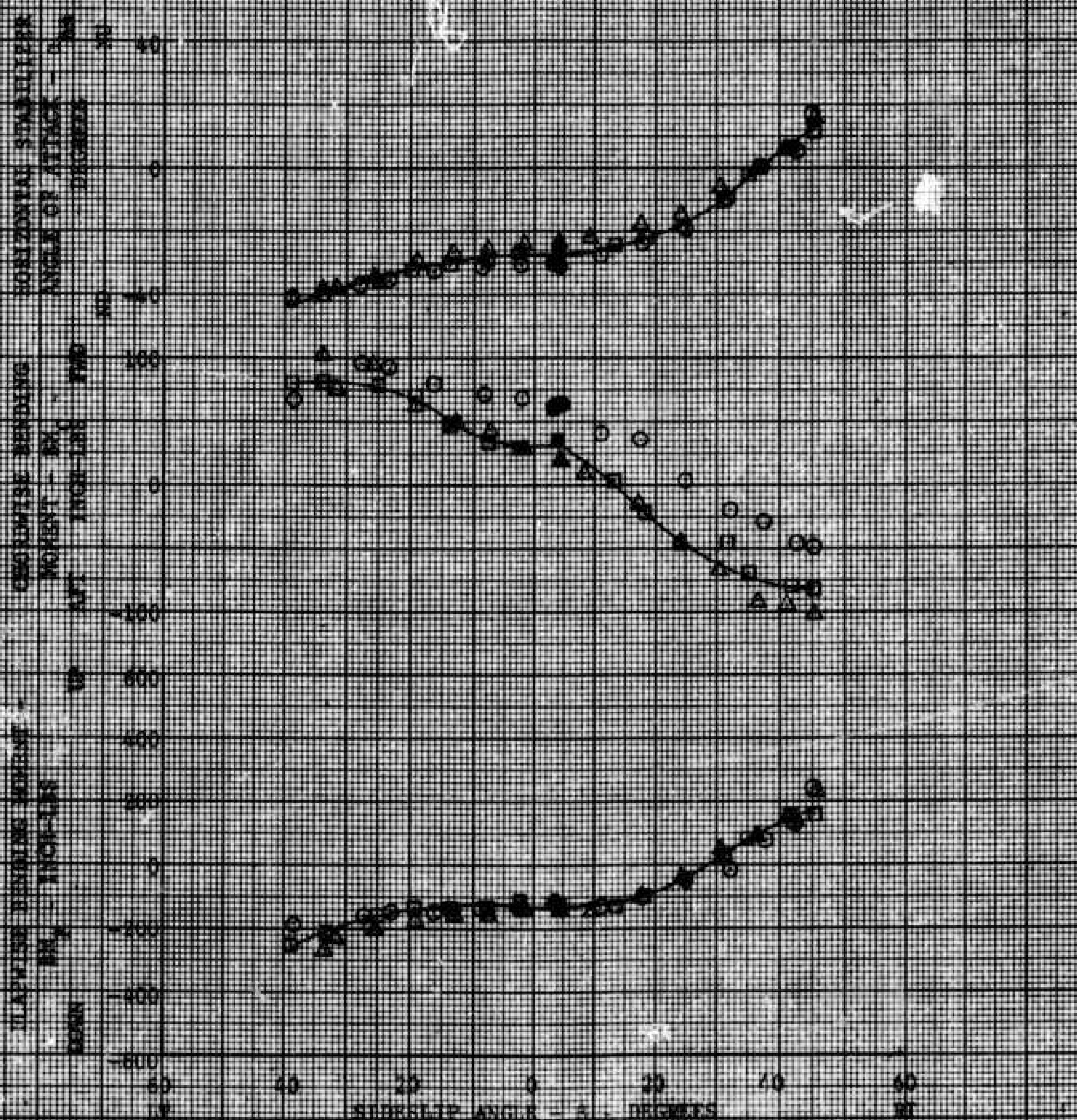

FIGURE 24

HORIZONTAL STABILIZER LOADS IN STEADY LATERAL DIRECTIONAL FLIGHT

TU-554 USA(S/N 63-16926)

SYMBOL	FLIGHT CONDITION	AVG STATION (IN.)	AVG GROSS WEIGHT (LB)	DENSITY ALTITUDE (FT)	ROTOR SPEED (RPM)	CALIB. A/S (KTS)	CALIB. OAT (°C)
○	LEVEL	99.0 (AFT)	16530	4200	485	40	8
□	LEVEL	99.0 (AFT)	16530	4200	485	47	8
△	LEVEL	99.0 (AFT)	16530	4200	485	56	8

NOTE: FINAL REDUCED SPAN STABILIZER

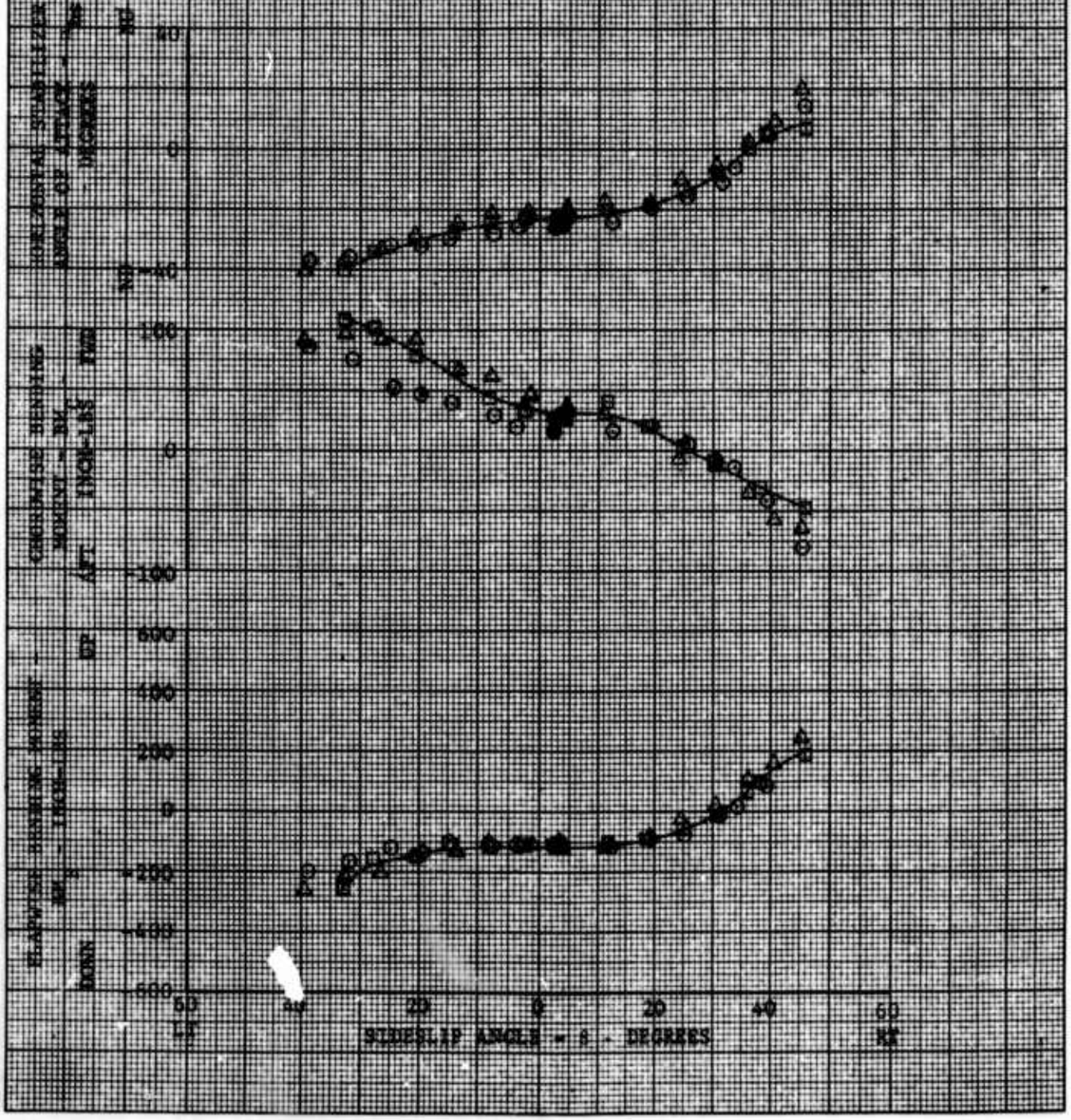

FIGURE 56
AIRSPEED CALIBRATION
TH-55A USA S/N 67-16026

SYMBOL	DENSITY ALTITUDE (FT)	GROSS WEIGHT (LB)	CG LOCATION (IN.)	FLIGHT CONDITION	OAT (°C)
◇	2400	1670	98.0 (AFT)	LEVEL	+4
□	4100	1670	96.2 (FWD)	AUTO	+0
△	4400	1670	96.2 (FWD)	CLIMB	+0

SEUP PITOT STATIC SYSTEM WITH A SENSITIVE AIRSPEED INDICATOR

METHOD: PACE AIRCRAFT WITH A GPS

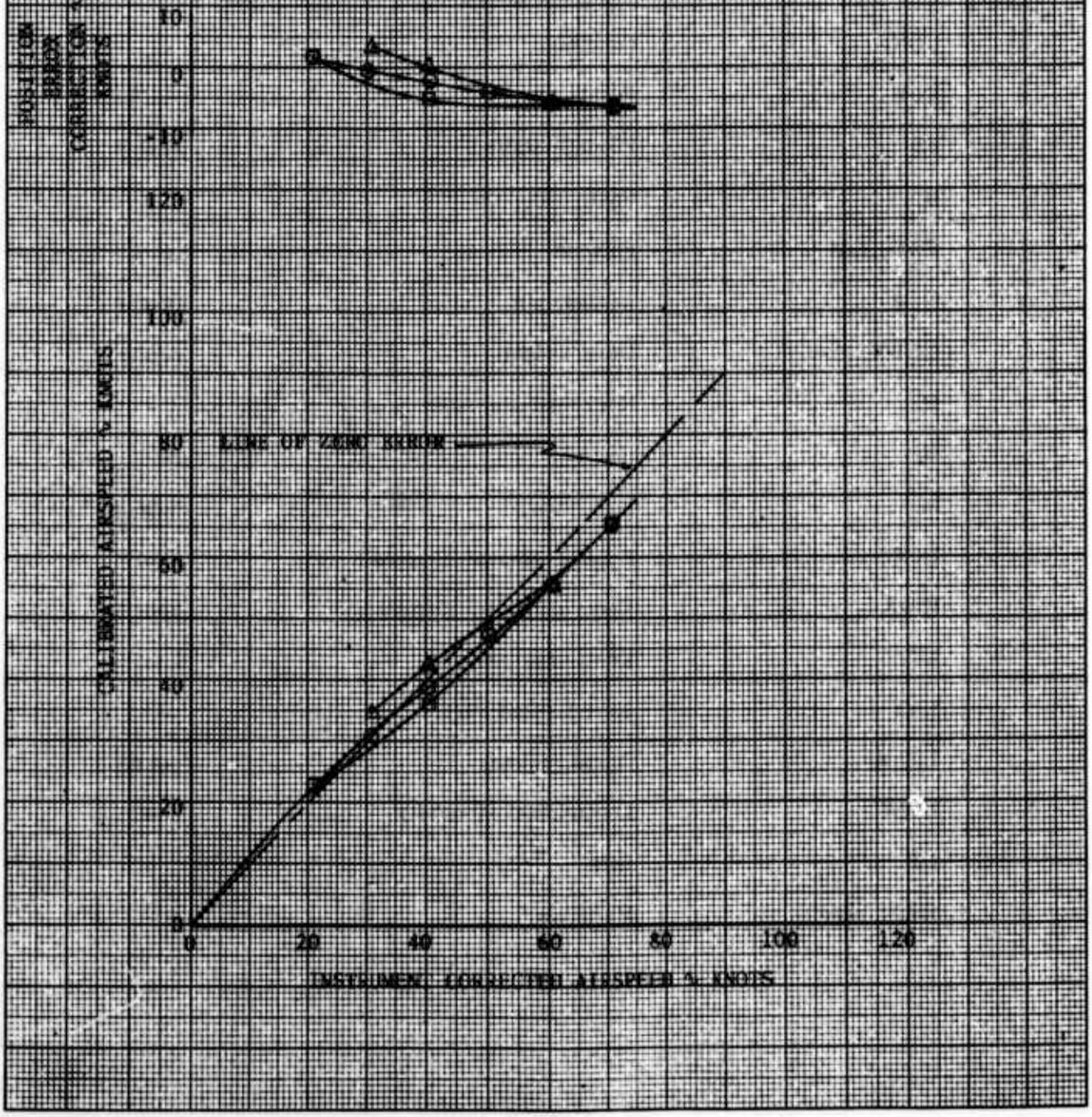

APPENDIX E. SYMBOLS AND ABBREVIATIONS

Abbreviation	Definition	Unit
ALT	Altitude	foot
AVG	Average	–
BL	Buttline	inch
CG, cg	Center of gravity	–
COND	Condition	–
FLT	Flight	–
FS	Fuselage station	inch
ft	Foot, feet	foot
FWD, fwd	Forward	–
G, g	Acceleration	ft/sec^2
GRWT, grwt	Gross weight	pound
HS	Horizontal stabilizer	–
Hz	Hertz	Hz
in.	Inch, inches	inch
KCAS	Knots calibrated airspeed	knot
KIAS	Knots indicated airspeed	knot
KTAS	Knots true airspeed	knot
LAT	Lateral (right/left)	–
LB, lb	Pound, pounds	pound
LONG.	Longitudinal (fore/aft)	–
LT	Left	–
MAX, max	Maximum	–

MIN, min	Minimum	–
MP	Manifold pressure	in./mg
NL	Nose left	–
NU	Nose up	–
OGE	Out of ground effect	–
R/C	Rate of climb	ft/min
R/D	Rate of descent	ft/min
Ref	Reference	–
RPM	Revolutions per minute	–
RT	Right	–
SEC, sec	Second	–
SL	Sea level	–
S/N	Serial number	–
STD, std	Standard	–
SYM	Symbol	–
VERT	Vertical (up/down)	–
WL	Water line	inch

Symbol	Definition	Unit
AR	Aspect ratio of horizontal stabilizer = b/c	–
AS_t	True airspeed vector	ft/sec
AS_x	Component of AS_t along aircraft longitudinal axis (positive aft)	ft/sec
AS_y	Component of AS_t along aircraft lateral axis (positive left)	ft/sec

AS_z	Component of AS_t along aircraft vertical axis (positive up)	ft/sec
AS_{zt}	Total vertical component of airspeed at the flow vane	ft/sec
AS_{hs_x}	Component of AS_t along horizontal stabilizer chordwise axis (positive aft)	ft/sec
AS_{hs_y}	Component of AS_t along horizontal stabilizer spanwise axis (positive left)	ft/sec
AS_{hs_z}	Component of AS_t along horizontal stabilizer vertical axis (positive up)	ft/sec
b	Span of horizontal stabilizer	in.
BM_{cw}	Chordwise bending moment about the horizontal stabilizer root (positive aft)	in.-lb
BM_{fw}	Flapwise bending moment about the horizontal stabilizer root (positive up)	in.-lb
c	Chord of horizontal stabilizer	inch
C_D	Coefficient of drag of horizontal stabilizer	-
C_{L_a}	Lift curve slope	/deg
C_P	Center of pressure or aerodynamic center	% span
C_T	Rotor thrust coefficient = $T/(\rho(\Omega R)^2 \pi R^2$	-
D_{hs}	Drag force on horizontal stabilizer (positive aft)	lb
F_x	Chordwise force acting on horizontal stabilizer CP (positive aft)	lb
F_z	Flapwise force acting on horizontal stabilizer CP (positive up)	lb
H_D	Density altitude	ft

H_P	Pressure altitude	ft
K_P	Power correction factor	–
L_{cp}	Length of stabilizer to CP	in.
L_{hs}	Lift force on horizontal stabilizer (positive up)	lb
q	Dynamic pressure at flow vane location = $1/2\rho V_{hs}^2$	lb/ft^2
$\overline{q}$	Mean dynamic pressure on horizontal stabilizer = $1/2\rho \overline{V}_{hs}^2$	lb/ft^2
q_c	Dynamic pressure correction required to go from flow vane to center of pressure = $\overline{q} - q$	lb/ft^2
q_o	Free stream dynamic pressure = $1/2\rho AS_t^2$	lb/ft^2
R	Rotor radius	ft
S	Planform area of horizontal stabilizer = b x c/144	ft^2
V'	Resultant rotor wake velocity = $\Omega R\sqrt{\mu^2 + \lambda^2}$	ft/sce
V_{cal}	Calibrated airspeed	knot
V_{hs}	Flow velocity at the flow vane location	ft/sec
$\overline{V}_{hs}$	Mean flow velocity at the horizontal stabilizer center of pressure	ft/sec
V_H	Maximum airspeed for level flight	knot
V_I	Mean induced velocity of main rotor ~ $\Omega RC_T/2\sqrt{\lambda^2 + \mu^2}$	ft/sec
V_{max}	Maximum-possible airspeed in level flight	knot
$V_{max\ R/C}$	Airspeed for maximum rate of climb	knot

$V_{min\ R/D}$	Airspeed for minimum autorotational rate of descent	knot
V_{NE}	Never-exceed airspeed	knot
V_T	True airspeed	knot
W	Vertical induced velocity at the flow vane (positive down)	ft/sec
X/R	Nondimensional distance parallel to rotor longitudinal axis (positive rearward from rotor shaft)	–
Y/R	Nondimensional distance parallel to rotor lateral axis (positive to right of rotor shaft)	–
Z/R	Nondimensional distance parallel to rotor shaft (positive up from rotor hub)	–
a_f	Aircraft angle of attack (positive NU)	deg
a'_f	Angle between AS_t vector and horizontal plane of aircraft (positive NU)	deg
a_{hs}	Horizontal stabilizer angle of attack (positive NU)	deg
a'_{hs}	Angle between AS_t vector and horizontal plane of stabilizer (positive NU)	deg
a_i	Incidence angle between longitudinal axis and chordline of the stabilizer (positive NU)	deg
β_f	Sideslip angle of aircraft (positive NL)	deg
β_{hs}	Sideslip angle of horizontal stabilizer (positive NL)	deg
γ	Dihedral angle of horizontal stabilizer	deg
θ	Pitch attitude of aircraft (positive NU)	deg
$\dot{\theta}$	Pitch rate of aircraft (positive NU)	deg/sec

λ	Inflow ratio = $(AS_t \sin a_f - V_I)/\Omega R$	–
μ	Tip speed ratio = $AS_t \cos a_f/\Omega R$	–
ρ	Atmospheric density	$slug/ft^3$
Φ	Roll attitude of aircraft	deg

UNCLASSIFIED
Security Classification

DOCUMENT CONTROL DATA - R & D

(Security classification of title, body of abstract and indexing annotation must be entered when the overall report is classified)

1. ORIGINATING ACTIVITY *(Corporate author)*

US ARMY AVIATION SYSTEMS TEST ACTIVITY
EDWARDS AIR FORCE BASE, CALIFORNIA 93523

2a. REPORT SECURITY CLASSIFICATION

UNCLASSIFIED

2b. GROUP

3. REPORT TITLE

AUTOROTATIONAL ENTRY IMPROVEMENT PROGRAM
TH-55A HELICOPTER

4. DESCRIPTIVE NOTES *(Type of report and inclusive dates)*

FINAL REPORT 8 October 1970 through 26 May 1972

5. AUTHOR(S) *(First name, middle initial, last name)*

BARCLAY H. BOIRUN, Project Officer/Engineer
WILLIAM R. BENOIT, LTC, TC, US Army, Project Pilot

6. REPORT DATE	7a. TOTAL NO. OF PAGES	7b. NO. OF REFS
DECEMBER 1972	159	16

8a. CONTRACT OR GRANT NO.	9a. ORIGINATOR'S REPORT NUMBER(S)
b. PROJECT NO. AVSCOM PROJECT NO. 70-24	USAASTA PROJECT NO. 70-24
c.	9b. OTHER REPORT NO(S) *(Any other numbers that may be assigned this report)*
d.	NA

10. DISTRIBUTION STATEMENT Distribution limited to United States Government agencies only; test and evaluation, December 1972. Other requests for this document must be referred to the Commander, United States Army Aviation Systems Command, Attention: AMSAV-EF, Post Office Box 209, St. Louis, Missouri 63166.

11. SUPPLEMENTARY NOTES	12. SPONSORING MILITARY ACTIVITY
	US ARMY AVIATION SYSTEMS COMMAND ATTN: AMSAV-EF PO BOX 209, ST. LOUIS, MISSOURI 63166

13. ABSTRACT

The TH-55A helicopter was tested by the United States Army Aviation Systems Test Activity from October 1970 to May 1972 as part of a development program to improve the autorotational entry characteristics. Previous United States Army Aviation Systems Test Activity tests and operational experience at the United States Army Primary Helicopter School, Fort Wolters, Texas, indicated that the TH-55A exhibited excessive nose-down pitching and left rolling motions following simulated power failures. The United States Army Aviation Systems Command directed the United States Army Aviation Systems Test Activity to investigate the autorotational entry characteristics of the standard helicopter and to evaluate the characteristics with a reduced-chord horizontal stabilizer configuration developed by the Hughes Tool Company. The data from these tests indicated that other minor stabilizer configuration changes could also improve the autorotational entry characteristics. An experimental development program was conducted to determine an optimum stabilizer configuration. This program resulted in the development of a reduced-span stabilizer with an upper-leading-edge spoiler which improved the nose-down pitching characteristics without seriously degrading other handling qualities. A second phase of the test program was conducted to verify the structural adequacy and basic airworthiness of the new stabilizer for the entire flight envelope contained in the 1967 Hughes TH-55A owner's manual. Testing was successfully concluded, but a reduction of dynamic directional stability of the helicopter was observed. However, the decrease in dynamic directional stability was significantly outweighed by the improvement that was achieved in the autorotational entry characteristics and other flying qualities. As a result of this test program, the active fleet of TH-55A helicopters was converted to the horizontal stabilizer configuration developed by the United States Army Aviation Systems Test Activity.

DD FORM 1 NOV 65 1473

UNCLASSIFIED
Security Classification

14. KEY WORDS	LINK A		LINK B		LINK C	
	ROLE	WT	ROLE	WT	ROLE	WT
TH-55A helicopter						
Autorotational entry improvement program						
Nose-down pitching and left rolling motion following simulated power failure						
Reduced-chord horizontal stabilizer configuration						
Optimum stabilizer configuration						
Reduced-span stabilizer with an upper-leading-edge spoiler						
Stabilizer structural adequacy and basic airworthiness						
Dynamic directional stability						
Flying qualities						